PROTEIN ENGINEERING STUDIES OF STREPTOKINASE

THESIS SUBMITTED TO

THE JAWAHARLAL NEHRU UNIVERSITY

NEW DELHI, INDIA

FOR THE AWARD OF THE DEGREE OF

DOCTOR OF PHILOSOPHY

JAYEETA DHAR
INSTITUTE OF MICROBIAL TECHNOLOGY
CHANDIGARH
INDIA
2003

Dedicated to
Ma and Baba

सूक्ष्मजीव प्रौद्योगिकी संस्थान
सैक्टर 39-ए, चण्डीगढ़. 160 036 (भारत)
INSTITUTE OF MICROBIAL TECHNOLOGY
(A CONSTITUENT ESTABLISHMENT OF CSIR)
Sector 39-A, Chandigarh-160 036 (INDIA)

इमटैक
IMTECH

CERTIFICATE

The research work embodied in this thesis entitled 'Protein Engineering studies of Streptokinase' has been carried out at the Institute of Microbial Technology, Sector 39A, Chandigarh, India. "This thesis is an original work and has not been submitted, in whole or in part, for a degree at this or any other university, nor does it contain, to the best of my knowledge and belief, any material published or written by another person, except as acknowledged in the context."

Girish Sahni
Dr. Girish Sahni
Supervisor

Jayeeta Dhar.
Jayeeta Dhar
Research Fellow
24.11.2003.

दूरभाष Phones : 695215 / 216 / 219 / 225 / 226 / 227, 690004, 690025, 690138, 690173, 690713, 690908, 692737
फैक्स Fax : 0091-172-690585, 0091-172-690632
एस. टी. डी. कोड : STD CODE : 0172
तार : Gram : IMTECH
E-mail : system@imtech.res.in
Web : http://www.imtech.res.in

CONTENTS

Acknowledgements

During this short but significant period of my life, I have been fortunate enough to meet, interact and know several people, without whose timely advice and help, this treatise would not have been brought to fruition. I take this opportunity to thank all of them.

First and foremost, I am deeply indebted to my mentor, Dr. Girish Sahni, for patiently teaching me the nuances of doing bench work and critically analyzing data, for spending quality-time in stimulating discussions and for channeling my efforts towards completion of this study and also building my self-confidence. I thank him for his excellent guidance, whole-hearted encouragement and independence offered to me in my work. His positive attitude and commitment to science have been and shall always remain a great source of inspiration for me.

I am deeply grateful to Dr. Amit Ghosh, Director, IMTech, for giving me the opportunity to work in this institute and for providing excellent laboratory facilities, all under a single roof.

I owe my sincere gratitude to Drs. Ganesan, Jagmohan Singh, Alok Mondal and Dibyendu Sarkar for their immense help in automated DNA sequencing.

I am thankful to Dr. S.C. Mande for helping me in the computer modeling required for this study.

I am grateful to Dr. R. P. Roy, for allowing me to use the CD facilities at NII, New Delhi.

I express my heartfelt thanks to my colleagues and labmates, Mrs. Paramjit Kaur, Mr. Rajagopal, Dr. S. S. Komath, Dr. A. H. Pande, Vasudha, Jagpreet, Suman, Kishore and Shekhar for their whole-hearted cooperation. I shall always remember my senior, Vasudha, for everything she did for me. I am very grateful to Jagpreet for providing me the proteins necessary for completion of this work and for all his timely help. I thank Dr. A. H. Pande for helping me in the Resonant Mirror studies and Mr. Rajagopal for providing the plasmid construct required during the course of my study. A big thanks is owed to Suman for always being ready to help and for keeping the atmosphere cheerful. I greatly appreciate the expert and efficient technical assistance of Mrs. Paramjit Kaur, who has been a great help on numerous occasions and has stood by me at all times. I also thank Mrs. Sheela Devi for her cooperation. I am grateful to Suman, Shekhar, Kishore, Meghna and Anuradha for proofreading the manuscript.

I am extremely grateful to Dr. G. P. S Raghava for always helping me whenever I faced problems in computer software and handling. I thank Dr. B. Singh for his kind help. I am indebted to Amit, Mahendra, Rajeev, Jitin and rest of the BIC staff. Special thanks are due to Manoj and Sudipto for their timely help.

I thank Dr. R.M. Vohra, Dr. Anand Bachhawat, Dr. P. Chakraborty, Dr. N. Kumar, Dr. P. Guptasarma, Dr. T. Charaborty, Dr. P. Aggarwal, Dr. M. Raje and Dr. K. V. Radhakishan for the constant encouragement, during the entire research period.

I thank Mr. Kamlesh Sharma and Dr. Sabita Basu of the Department of Haematology and the Blood Bank at the Government Medical College Hospital, Chandigarh, for providing human plasma, whenever required.

The cooperation provided by the entire IMTech staff - Library, Instrumentation, Administration, Store and Purchase is truly acknowledged. Special thanks are due to the Mess workers for everything that they did for me.

I shall always cherish the good times I had spent with my seniors, Vasudha, K. K. Pandey and Maneesh, and I deeply appreciate the help rendered by them at times of need. I thank Ashishda, Sudipda, Kislay, Gautam, Sankar, Bhupesh, Vinod, Vishal, Ranjana, Jyoti and Kakolidi for all their valuable suggestions.

I shall always remember the cheerful support of my batchmates, Radha, Rachna, Puja, Purva, Vibha, Chitranshu, Naresh, Souvik and Vishal, not only during the pre-Ph.D coursework, but the successive years.

I thank Srikanth, Rekha, Vikas, Harpreet, Debarati, Pratima, Monica, Sangeeta, Jasdeep, Sumit, Vandana, Sourabh, Amita, Vijaya, Amrita, Pradipto, Saurav, Arvind, Swati, Meghna, Sudesh, Sukhwinder, Shubbir and Ajit for their whole-hearted encouragement.

Words fail to justify the love and affection showered over me by my friends, Biju, Lakshmipathi, Dwaipayan, Sanjoy and Naresh. I shall cherish the moments spent with them. I thank Rajeshwari and Rani for their warmth and hospitality.

I thank my roommate, Anuradha for her warmth and affection, for being there at the end of the day to share my feelings and for all her help in the final phase.

The silent yet untiring support of my friend, Souvik has been a big emotional help during the entire period.

I owe my sincere gratitude to the Ball family in building my zeal and enthusiasm to pursue research as my career. I shall always remember Mashi for her constant encouragement and timely advice. Annie and Moutushi deserve a special mention for 'being there'.

Lastly, but immensely, I am profoundly indebted to my parents, who have spared no time and effort in making me stand where I am today. Their ineffable love, unstinted support and prayers have helped me sail through the difficult moments in life. They have been the driving forces behind completion of this treatise.

The financial assistance provided by CSIR is duly acknowledged.

Jayeeta Sharma

ABBREVIATIONS

Weights and measures

bp	base pair
cm, mm, μm, nm	centimeter, millimeter, micrometer, nanometer
°C	degree Celsius
g, mg, μg, ng	gram, milligram, microgram, nanogram
h, min, sec	hour, minute, second
I.U.	international standard units for SK
kDa	kilo Dalton
kv, v	kilovolt, volt
L, ml, μl	liter, milliliter, microliter
mmol, nmol, pmol	millimoles, nanomoles, picomoles
M, mM, μM, nM	molar, millimolar, micromolar, nanomolar
MW	molecular weight
M_r	relative molecular weight
OD	optical density
%	percentage
rpm	revolutions per minute
v/v	volume by volume
w/v	weight by volume

Symbols

α	alpha
~	approximately
β	beta
=	equal to
γ	gamma
>	greater than

Techniques

ELISA	enzyme linked immuno sorbent assay
CD	circular dichroism
DEAE	diethyl amino ethyl
DSC	differential scanning calorimetry
HIC	hydrophobic ion chromatography
IMAC	immobilized metal affinity chromatography
NMR	nuclear magnetic resonance
PCR	polymerase chain reaction
SDS-PAGE	sodium dodecyl sulphate-polyacrylamide gel electrophoresis

Chemicals/Reagents

Amp	ampicillin
APS	ammonium persulphate
BSA	bovine serum albumin

Dnase	deoxyribonuclease
dNTP	deoxy nucleotide triphosphate
EACA	epsilon amino caproic acid
EDTA	ethylene diamine tetra acetic acid
FN	fibrin
HEPES	N-(2-hydroxyethyl)piperazine-N′-(2-ethanesulphonic acid)
HBS	HEPES-buffered saline
HPG	human plasminogen
HPN	human plasmin
IPTG	iso-propyl-1-thio-β-D-galactopyranoside
K1-5	kringles 1 through 5
LB	Luria Bertani medium
μPG, μPN	microplasminogen, microplasmin
mPG	miniplasminogen
NaCl	sodium chloride
NPGB	p-nitrophenyl p-guanidinobenzoate
PBS	phosphate buffer saline
PG	plasminogen (either human or bovine)
PN	plasmin (either human or bovine)
RE	restriction endonuclease
SAK	staphylokinase
SDS	sodium dodecyl sulphate
SK	streptokinase
STE	sodium tris.EDTA buffer
SUPA	*Streptococcus uberis* plasminogen activator
TAME	alpha-N-p-tosyl-L-arginine methyl ester
TEMED	N, N, N′, N′ -tetramethylethylenediamine
t-PA	tissue-plasminogen activator
UK	urokinase

Amino acids

Ala	A	alanine
Arg	R	arginine
Asn	N	asparagine
Asp	D	aspartate
Cys	C	cysteine
Glu	E	glutamate
Gln	Q	glutamine
Gly	G	glycine
His	H	histidine
Ile	I	isoleucine
Leu	L	leucine
Lys	K	lysine
Met	M	methionine
Phe	F	phenylalanine
Pro	P	proline
Ser	S	serine
Thr	T	threonine
Trp	W	tryptophan
Tyr	Y	tyrosine
Val	V	valine

Miscellaneous

Abs	absorbance
C	carboxy
DNA	deoxyribonucleic acid
IBs	inclusion bodies
IC_{50}	concentration at which inhibition is 50 %
K_M	Michaelis constant
k_a	association rate constant
k_d	dissociation rate constant
K_D	equilibrium dissociation constant
LBS	lysine binding sites
N	amino
RNA	ribonucleic acid
RT	room temperature
UV	ultraviolet
V_{max}	maximum velocity

A part of the work embodied in this dissertation has been accepted for publication and is as follows :

Dhar J, Pande AH, Sundram V, Nanda JS, Mande SC, Sahni G (2002). Involvement of a nine-residue loop of streptokinase in the generation of macromolecular substrate specificity by the activator complex through interaction with substrate kringle domains. *J Biol Chem* **277,** 13257-13267.

List of figures

List of tables

CHAPTER I

INTRODUCTION

One of the predominant causes of death in modern times has been circulatory disorders that have assumed alarming proportions worldwide, due to a combination of several 'modern' factors, besides genetic predisposition, such as stressful urban lifestyles and unhealthy food habits. What was previously a scourge of developed societies is now wrecking havoc in developing countries as well. This has resulted in an explosion of cardiac maladies across the globe, partially as nations shed their poverty and move into greater prosperity. In India alone, it is believed that nearly *2 % of the population* suffers from various cardiac maladies. The current rate of deaths due to coronary diseases (nearly 200 per 100,000 population) is increasing at an appalling rate in our country. Thus, there is a desperate need for newer, improved thrombolytic drugs to bring the situation under control.

The application of thrombolytic agents like tissue-plasminogen activator (t-PA), urokinase (UK) and streptokinase (SK) has transformed the clinical management of various circulatory diseases, for example, myocardial infarction, deep-vein thrombosis and pulmonary embolism (Collen *et al.*, 1988). These thrombolytic agents exert their fibrinolytic effect through activation of plasminogen (PG) in circulation, by cleavage of the scissile peptide bond between residues Arg561 and Val562 in PG. Consequently, the inactive zymogen PG is converted to its active form, plasmin (PN) that then acts on fibrin and degrades it into soluble degradation products. What is fascinating is that PN, by itself, is not capable of activating PG into PN but requires an activator such as t-PA and UK to catalyze this reaction. Unlike t-PA and UK, which directly act on PG, SK is enzymatically inert and first forms an equimolar complex with PG (the SK.PG complex) that then activates other PG molecules into PN (reviewed by Castellino, 1981).

The clinical choice of the clot-dissolver drug during therapy is dictated by several factors like fibrin-selectivity, immunological reactivity, appearance of side effects and their severity, and circulatory clearance rates. Of the thrombolytic agents approved clinically, SK is the drug of choice, especially in the developing countries, mainly because of its markedly low cost (nearly 10-fold lower) when compared to t-PA and UK. In addition to being economical, the SK.PG complex is a highly potent activator enzyme, and possesses longer plasma half-life than its counterparts *viz.* t-PA and UK. On the other hand, the relative disadvantages with SK are its comparitively

low fibrin specificity, and high immunogenicity due to its heterologous origin. Thus, one of the principal aims of the current investigation was to design a smaller analogue or derivative of SK so that its immunogenicity is reduced compared to the full-length native protein. However, the development of such analogues or derivatives with improved properties requires a comprehensive understanding of the mechanistic and structure-function aspects of SK, which is not presently available.

Considerable efforts have been made in the last two decades to acquire deeper mechanistic insights into one of the most challenging issues associated with SK action *viz.* the molecular basis of its highly specific and targeted action of SK on its substrate, PG. With a view to obtain fundamental insights into the regions of SK involved in imparting substrate specificity to the 'partner' PN in the SK.PN complex, as well as decipher regions involved in formation of the strong 1:1 interaction, 'Peptide-Walking' studies in our laboratory involving limited proteolysis and fragment analysis have been carried out (Nihalani *et al.*, 1997; Nihalani *et al.*, 1998). By this approach, two 'hotspots' in SK, one in the α domain (encompassing residues 16-51) and another in the β domain (spanning residues 230-290) were identified to be involved in PG interacting functions. While residues 37-51 in the α domain of SK and two short segments in the β domain spanning residues 230-250 and 270-290, were thought to be involved in formation of the high affinity 1:1 interaction between SK and PG, residues 16-36 in SK α and residues 250-270 in SK β were proposed to be involved in the docking of substrate PG to the activator complex.

The crystal structure of SK with microplasmin (μPN), the catalytic domain of PN (Wang *et al.*, 1998) has been recently solved. Although it does provide a high-resolution picture of selected inter-molecular interactions amongst the three domains of SK (namely α, β and γ) with μPN, it fails to reveal the intimate role of the β domain of SK, postulated earlier by our group (Nihalani and Sahni, 1995; Nihalani *et al.*, 1997; Chaudhary *et al.*, 1999) as well as by others (Rodriguez *et al.*, 1995 and Conejero-Lara *et al.*, 1998) that have clearly indicated that the β domain plays a crucial role not only in engendering affinity with partner PG, but with substrate PG as well. This lacuna between the structural data, on one hand, and biochemical results, on the other, needed to be actually addressed in order to gain a truthful glimpse into the mechanism of action of SK.

In contrast to the three-domain structure of SK, staphylokinase (SAK), another functionally similar, 'indirect' PG activator protein, but one that has a single domain only, also operates by docking substrate HPG into the active center of its binary complex with plasmin(ogen) (Parry *et al.*, 1998). Although SAK displays little sequence similarity with SK, its single domain bears remarkable structural homology with the α domain of SK, and all the three domains of SK in general, which, in turn, are structurally homologous to each other (Parry *et al.*, 2000). A crucial question that can be posed in the above context is whether the isolated α domain of SK also possesses, like the single domain of SAK, the ability to bind with PG in both 'substrate' and 'partner' modes and, if the answer is affirmative, whether this binding is functionally translated into a capability, even if highly compromised compared to native SK, to switch the non-specific substrate preference of partner PN to that of a PG activator enzyme. A recent study (Loy *et al.*, 2001) could elegantly demonstrate the presence of only, barely detectable levels of PG activator activity in the α domain of SK. However, this report did open the question of finding ways, chiefly by protein engineering, to enhance and/or amplify this 'nascent' activity in the isolated α domain. Accordingly, here we have explored various strategies to enhance the catalytic efficiency of isolated SK α and then gone on to generate SAK-like catalytic efficiency in the hitherto nearly inactive domain.

In brief, we embarked on this treatise with the following objectives in mind.

- To identify critical epitope(s)/microstructure(s) within the known 'hotspot' in the β domain of SK, *viz.* spanning residues 250-270, which is/are crucial for substrate PG activation. This involved computer modeling studies to identify structure/s that might be involved in interaction with PG, construction of the desired mutant, followed by detailed analysis of the kinetic and binding parameters of the mutant.
- To examine whether the α domain of SK possesses any detectable activity or not, when isolated after expression by recombinant DNA methods.
- To make a rational and systematic attempt to engineer derivatives of α that possess significant cofactor activity. This would involve identification of epitope/s that play a crucial role in substrate recognition, present in the

structurally homologous SAK, followed by the transposition of the motif/s into an equivalent position in the α domain and its physico-chemical and kinetic characterization. In addition, 'hotspot' saturation mutagenesis and subsequently screening of a repertoire of mutants would be carried out to select those with superior functional properties. The kinetics of PG activation and binding properties of the selected mutants would then be studied.

CHAPTER II

REVIEW OF LITERATURE

Humans have evolved a well-regulated and finely balanced hemostatic system. Hemostasis is a balance of the physiological processes, which on one hand prevent excessive bleeding after vessel injury, and on the other hand, maintain viable circulation by keeping the blood in an uncoagulated state (maintain blood in a fluid state). Hemostasis can be divided into four components, vessel function, platelet function, coagulation and fibrinolysis.

2.1 Vessel Function

The normal vascular endothelium produces inhibitors of blood coagulation (heparan sulphate and thrombomodulin) and platelet aggregation. It modulates fibrinolysis by synthesizing and secreting t-PA and inhibitors of HPG activators. It also separates blood cells and plasma factors from highly reactive elements like collagen, von Willebrand factor that stimulate platelet adhesion, and tissue factor that trigger coagulation of blood.

Vascular spasm occurs when the smooth muscles that line the walls of blood vessels contract after injury. It is mediated by serotonin and thromboxane A2 released from platelets and is the beginning of primary hemostasis that leads to the formation of a reversible platelet plug within minutes of the injury.

2.2 Platelets

Platelets play a fundamental role in hemostasis. They adhere to the surface of injured blood vessels that provide sites for binding to von Willebrand factor (via the receptor GP-Ib, a glycoprotein found on the platelet cell surface, in a complex formation with Factor IX); and fibrinogen and fibronectin through integrin receptors (Pytela *et al.*, 1986). Fibrinogen, due to its divalent structure enables formation of a bridge between platelets, thereby mediating aggregation of platelets. These adherent platelets spread on the exposed sub-endothelial surface, and further form large aggregates.

Different agents like thrombin, adenosine diphosphate and epinephrine that bind to the platelet membrane, via specific receptors, can stimulate platelets (reviewed

by Nemerson and Nossel, 1982). The aggregation response of platelets to these stimuli is modulated by several regulatory substances, of which the most important is cyclic 3′, 5′-adenosine monophosphate (Haslam *et al.*, 1978; Grant and Colman, 1988). A strong stimulus increasing platelet cyclic 3′, 5′-adenosine monophosphate levels and thereby inhibiting aggregation is prostacyclin, produced by vascular endothelial cells.

Platelets contain different classes of granules ('dense bodies', alpha granules and lysosomes). The contents of dense granules are small molecules and include adenosine monophosphate, calcium and serotonin. Alpha granules contain large molecules like fibronectin, the von Willebrand protein, fibrinogen, platelet-derived growth factor, platelet factor 4 and β-thromboglobulin. Secondary platelet aggregation is accompanied by, and may be mediated by platelet release reaction in which the contents of platelet alpha and dense granules are discharged into the ambient fluid (Nemerson and Nossel, 1982).

2.3 Coagulation

The coagulation system is a proteolytic cascade that involves several serine proteases and cofactors and consists of a series of highly coordinated events that finally lead to the formation of thrombin, which can convert soluble fibrinogen to fibrin that forms a clot (reviewed in Jackson and Nemerson, 1980). Each enzyme of the pathway is present in the plasma as a zymogen, in other words, in the inactive form, which on activation undergoes proteolytic cleavage to release the active factor of the precursor molecule.

Conceptually, coagulation came to be viewed as consisting of two pathways (intrinsic pathway and extrinsic pathway), functioning independently for the generation of factor X, and finally converging in the common pathway that leads to thrombin formation. Intrinsic pathway is termed so because coagulation is initiated by the components of the vascular system, whereas the extrinsic system involves components of both the blood and vascular system.

2.4 Fibrinolysis

After the primary phase of platelet aggregation, the second phase in hemostasis involves the formation of fibrin strands. The precursor of fibrin (FN) is fibrinogen, a glycoprotein of M_r 340,000. The fibrinogen molecule is a dimeric molecule (Doolittle, 1984) consisting of three pairs of disulphide-bonded polypeptide chains (Hoeprich and Doolittle, 1983). It is present in plasma as well as platelet granules.

The process of FN formation first involves the binding of the enzyme, thrombin to fibrinogen and liberation of fibrinopeptides, resulting in monomer and polymer formation (Blomback and Blomback, 1972). This is followed by the non-covalent FN assembly that entails the progressive longitudinal and lateral elongation of polymer chains to form FN strands (Hermans and McDonagh, 1982). Finally, FN gets covalently stabilized by Factor XIIIa-catalyzed cross-linking (Schwartz *et al.*, 1973; Folk and Finlayson, 1977; Pisano *et al.*, 1968) rendering the FN clot mechanically more robust (Shen *et al.*, 1975) and more resistant to chemical and enzymatic lysis (Shen *et al.*, 1977).

Wiman and Collen (1978a) proposed that under physiological conditions, the dissolution of FN clots involves the binding of the circulating zymogen PG to the clot, conversion of PG to the active protease PN, lysis of the clot and inactivation of PN by the circulating α_2-antiplasmin. A cardinal feature of both physiological fibrinolysis and that achieved by therapeutic administration of PG activators is targeted generation of PN activity at the surface of the clot (FN selectivity) (Marder and Sherry, 1988). Thus, there is a complex interplay between different pathways to maintain normal hemostasis and a delicate balance has to be maintained to allow a rapid and efficient hemostatic response to bleeding, but that can avoid a thrombogenic response away from the site of injury (see Figure 2.1).

The key components of the fibrinolytic pathway include PG, PG activators and inhibitors of PG activators and PN.

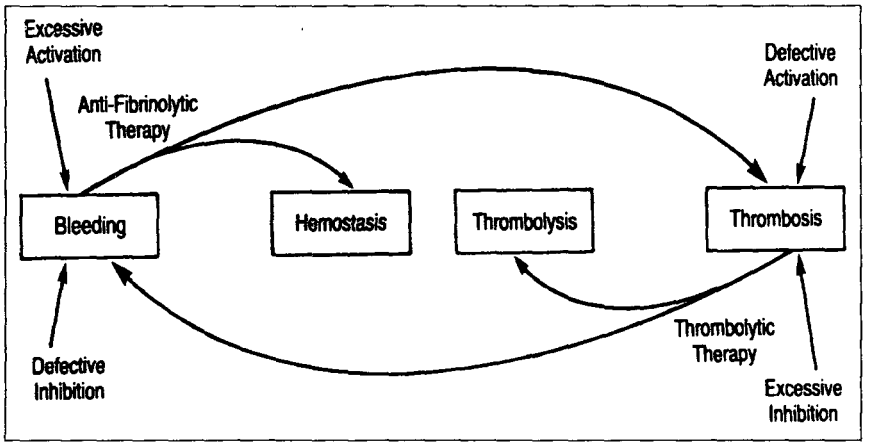

Figure 2.1 Disruption of the balance between the opposing forces of fibrinolysis and antifibrinolysis, leading to bleeding or thrombotic manifestations. Bleeding may result from defective inhibition of excessive activation of fibrinolysis. Conversely, defective activation or excess inhibition of fibrinolysis may result in thrombosis. Therapy with fibrinolytic agents may dissolve a thrombus, but bleeding may complicate the clinical management. Bleeding due to excess fibrinolysis may be improved by antifibrinolytic therapy or result in thrombotic complication. Successful therapy involves restoration of effective hemostasis or achievement of thrombolysis without complications (adapted from Francis and Marder, 1994).

2.4.1 Plasminogen

Human plasminogen (HPG) is a single-chain glycoprotein of M_r 92,000-94,000 (De Renzo *et al.*, 1967) consisting of 791 amino acids and contains 22 disulphide bonds. It is the inactive precursor of the general plasma serine protease called PN. Majority of the HPG is synthesized in the liver. However, it is also present in other cells and in the extravascular spaces of many tissues, a few of which might be capable of producing it such as red blood cells and the kidney (Raum *et al.*, 1980; Saito *et al.*, 1980; Highsmith and Kline, 1971). The N-terminal amino acid residue of HPG is Glu (Wallen and Wiman, 1972) and the C-terminal amino acid is Asn (Robbins *et al.*, 1967).

The human Glu-PG exists in two forms, which differ from each other in their glycosylation (Castellino, 1984). Variant I contains the carbohydrate groups at Asn289 and Thr346 (Hayes and Castellino, 1979a, 1979b, 1979c). Variant II that constitutes half of the PG molecules, contains only the carbohydrate group at Thr346. Recently, a site for O-linked glycosylation was discovered in variant II at Ser248 (Pirie-Shepherd *et al.*, 1997). Recombinant PG, expressed in *Escherichia coli* is non-glycosylated (Gonzalez-Gronow *et al.*, 1990), and cannot be activated into PN by PG activators and when injected into mice, was much more rapidly cleared from circulation than the glycosylated forms.

Three truncated forms of HPG have been illustrated.

i) Cleavage by human plasmin (HPN) at residue 77 leads to the removal of N-terminal domain and yields a shorter form of HPG commonly called Lys-PG. This HPN-catalyzed conversion to Lys-PG is accompanied by a large conformational change to an extended conformation that has different functional properties than Glu-PG (Violand and Castellino, 1976; Ponting *et al.*, 1992a; Horrevoets *et al.*, 1995).

ii) Cleavage by elastase leads to the formation of miniplasminogen (mPG) that is composed of the catalytic domain with kringle 5.

iii) The isolated catalytic domain devoid of all the kringle domains is known as microplasminogen (μPG) (Shi and Wu, 1988). Both mPG and μPG are

capable of being activated by HPG activators (Christensen *et al.*, 1979; Shi and Wu, 1988).

In human adult, the concentration of HPG in the plasma is 2 μM (200 mg per L). The half-life of human Glu-PG is 2.2 days whereas Lys-PG has a shorter half-life of 0.8 days (Collen and Maeyer, 1975).

Plasminogen contains seven structural domains: an N-terminal peptide (Glu1-Lys77), five kringle domains, K1 through K5, respectively (K1-5) and a C-terminal serine protease catalytic domain (amino acids 544-791) (Sottrup-Jensen *et al.*, 1978; Ponting *et al.*, 1992b). Figure 2.2 shows the schematic diagram of the domain structure of HPG.

Kringles are independently folding domains that are composed of three-disulphide, triple-loop structures consisting of approximately 80 amino acids each (Sottrup-Jensen *et al.*, 1978). Comparison of the cDNA sequences of HPG with those of monkey, mouse, bovine and porcine PG reveals 76-85 % identity of the kringle domains (Degen *et al.*, 1990; Schaller and Rickli, 1988). The PG kringles contain lysine-binding sites (LBS) (Lerch *et al.*, 1980; Castellino and Powell, 1981; Motta *et al.*, 1987; Sehl and Castellino, 1990; Thewes *et al.*, 1990; Menhart *et al.*, 1991) that confer on the kringles the unique ability to interact with lysine residues of other proteins including fibrin (Sottrup-Jensen *et al.*, 1978; Wiman *et al.*, 1979; Wiman and Wallen, 1977; Wu *et al.*, 1990) and lysine analogues, such as epsilon-amino caproic acid (EACA) (Lerch *et al.*, 1980). The HPG kringles possess different affinities and specificities for omega-amino acid ligands. Equilibrium dialysis, microcalorimetry and nuclear magnetic resonance (NMR) studies on isolated kringles have been done that show that the strongest binding site for EACA is provided by kringle 1 (Lerch *et al.*, 1980; Menhart *et al.*, 1991) followed by kringle 4 (Lerch *et al.*, 1980; Sehl and Castellino, 1990; McCance *et al.*, 1994) and kringle 5 (McCance *et al.*, 1994; Novokhatny *et al.*, 1989). Kringle 3 does not interact with EACA to a measurable extent, whereas kringle 2 displays a very weak interaction with EACA (Marti *et al.*, 1994).

The crystal structure of the entire HPG molecule has not been determined as yet. However, the structures of a number of domains of PG have been established, for

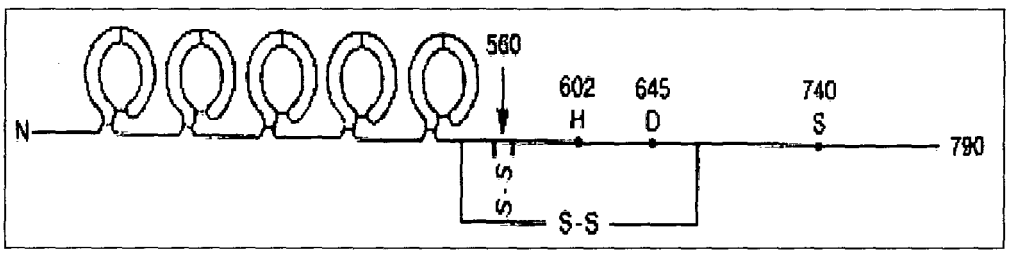

Figure 2.2 Schematic diagram of the domain structure of HPG. Plasminogen is a protein composed of 791 amino acid residues. It is composed of the N-terminal peptide, five kringle domains of 80 amino acid residues each, and the C-terminal catalytic domain (μPG). The arrow indicates the activation (scissile) peptide bond (Arg561-Val562), the cleavage of which activates HPG. The amino acid residues constituting the catalytic triad (His602, Asp645 and Ser740) are also indicated.

example, the structures of kringle 1 (Mathews *et al.*, 1996; Rejante and Llinas, 1994a; Rejante and Llinas, 1994b), kringle 4 (Atkinson and Williams, 1990; Mulichak *et al.*, 1991) and kringle 5 (Chang *et al.*, 1998) with various ligands bound have been determined by NMR and X-ray crystallography. There have been reports of structures of human μPG alone (Peisach *et al.*, 1999; Wang *et al.*, 2000a) and those of microplasmin (μPN) complexed with SAK (Parry *et al.*, 1998) and SK (Wang *et al.*, 1998).

The structure of the pro-enzyme domain of HPG was solved to 2.0 Å resolution by Peisach and coworkers (1999). The catalytic domain is made of 230 amino acids, whose overall architecture is very similar to other chymotrypsin-like serine proteases, is made up of two β-sheet barrels connected by loops (Shotton and Watson, 1970). The structure presents an inactive protease characterized by Asp740 (chymotrypsin 194) hydrogen-bonded to His586 (chymotrypsin 40), preventing proper formation of the oxyanion hole and S1 specificity pocket. In addition, the residues constituting the catalytic triad are oriented relative to the active conformation adopted by serine proteases in the chymotrypsin family.

The X-ray crystal structure of the complexes of the recombinant kringle 1 domain of HPG with ligands, EACA and AMCHA (trans-4-(aminomethyl) cyclohexane-1-carboxylic acid) have been determined at 2.1 Å (Mathews *et al.*, 1996). In the crystal structure, the anionic center of kringle 1 is composed of Asp54 and Asp55, while the cationic center that contributes to the stability of binding of the carboxylate moiety of the ligands, is composed of Arg70 and possibly Arg34. The binding pocket is characterized by the presence of two polar surfaces separated by the hydrophobic trough formed by the indole ring of Trp61 and the phenolic ring of Tyr71. The methylene groups of the ligand are stabilized in the binding pocket by van der Waals contacts with the side-chain atoms of Trp61 and Tyr71.

Crystallization of kringle 4 has revealed that the kringle 4 structure is well stabilized by an internal hydrophobic core and extensive hydrogen-bonding network (Mulichak *et al.*, 1991). The LBS on the surface of kringle 4 is a relatively shallow and elongated trough formed by hydrophobic amino acids Trp62, Phe64 and Trp72, surrounded by positively charged Lys35 and Arg71 on one side, and negatively

charged side-chains of Asp55 and Asp57, at a distance of 7 Å (Mulichak *et al.*, 1991; Wu *et al.*, 1991). This structure provides for ideal docking of zwitterions such as lysine and EACA, whose opposite charges are also 7 Å apart.

The structure of recombinant kringle 5 domain of HPG has been solved at 1.7 Å resolution (Chang *et al.*, 1998). The LBS is defined by the region His33-Thr37, Pro54-Val58, Pro61-Tyr64, Leu71-Tyr74, that together form an elongated depression on the kringle surface lined with water molecules. An unusual feature of the LBS of apo-kringle 5 of HPG is the absence of cationic center formed by Arg34-Arg70 and Lys35-Arg71 pairs of kringle 1 (Mathews *et al.*, 1996) and kringle 4 (Wu *et al.*, 1991) respectively. Since this locus is responsible for binding of negatively charged groups of ligands, the interaction between apo-kringle 5 and omega-amino acid ligands is restricted to positively charged groups of ligands and anionic center of LBS along with hydrophobic contacts in the binding pocket. While wild-type recombinant kringle 5 interacted weakly with these types of ligands, replacement by site-directed mutagenesis of Leu71 by Arg led to substantially increased affinity of the ligands for the LBS of kringle 5.

2.4.2 Plasmin

Plasmin, the active form of the zymogen PG, is a serine protease that has broad specificity, but cannot directly catalyze the proteolytic activation of HPG (Robbins *et al.*, 1967; Summaria *et al.*, 1967). It is formed by the cleavage of the scissile peptide bond in PG that is mediated by PG activators. The three forms of PN are Glu-PN form, that is the intact molecule with only Arg561-Val562 bond cleaved; Lys77 form that lacks the N-terminal 76 residue activation peptide and the Val442 form that contains an intact light chain but only one kringle structure and lacks all of the lysine binding sites (Christensen *et al.*, 1979). These different forms of PN are capable of hydrolyzing susceptible Arg and Lys bonds in proteins at neutral pH and act on most synthetic substances and proteins susceptible to trypsin (Weinstein and Doolittle, 1972).

The interactions of PN with the inhibitors play a crucial role in regulation of fibrinolysis. Two chief inhibitors of PN in blood are α_2-antiplasmin and α_2-macroglobulin.

2.4.3 Fibrinolytic system inhibitors

The inhibitors of the fibrinolytic system include inhibitors of PN as well as of the HPG activators (reviewed by Akoi and Harpel, 1984). These are briefly discussed below.

2.4.3.1 α_2-antiplasmin inhibitor

α_2-antiplasmin inhibitor is a single-chain molecule of M_r ~ 70,000 and contains about 13 % carbohydrates. It is synthesized in the liver and its half-life is about 3 days. The primary structure of human α_2-antiplasmin inhibitor has been reported by Holmes and coworkers (1987) and the organization of the gene has been determined in 1988 by Hirosawa and co-workers. In plasma, α_2-antiplasmin inhibitor (present at a concentration of 1 μM) swiftly reacts with PN, causing its irreversible inhibition through generation of a stable 1:1 stoichiometric complex with Ser at the active site of PN (Moroi and Aoki, 1976; Wiman and Collen, 1977; Wiman and Collen, 1978b; Wiman and Collen, 1979; Collen, 1976; Aoki and Harpel, 1984). The reaction between PN and the inhibitor is extremely rapid and the bimolecular complex is stable and devoid of enzymatic activity (Wiman and Collen, 1979; Christensen and Clemmensen, 1977). The α_2-antiplasmin inhibitor has specific binding sites for PN and FN. The C-terminal Lys residue (Lys 452) is a major site of interaction with PN (Hortin *et al.*, 1988) while the N-terminal Gln2 is covalently cross-linked to a C-terminal Lys residue in the α chain of FN by Factor XIIIa.

Deficiency of α_2-antiplasmin inhibitor (that is, during fibrinolytic activation, the amount of PN generated exceeds the neutralizing capacity of inhibitors), results in proteolysis of plasma proteins, a patho-physiological condition termed hyperfibrino(geno)lysis.

α_2-antiplasmin inhibitor is the most important PN inhibitor, but other inhibitors such as α_2-macroglobulin and plasminogen-activator inhibitor-I also exert their action, though in a restricted manner.

2.4.3.2 α_2-macroglobulin

α_2-macroglobulin is a glycoprotein of M_r 725,000, consisting of four identical chains each of M_r 160,000. It is present in plasma at concentrations ranging from 2 to 5 μM. The complete amino acid sequence of α_2-macroglobulin has been determined (Sottrup-Jensen *et al.*, 1984). The half-life of native α_2-macroglobulin in humans is about 5-6 days. It has broad specificity for different types of proteases. The mechanism of action involves an initial limited proteolysis of the 'bait region' that offers substrate specificity to many different proteases (Travis and Salvesen, 1983; Barrett and Starkey, 1973; Harpel, 1973; Mortensen *et al.*, 1981). The cleavage of different peptide bonds leads to a conformational change in the α_2-macroglobulin molecule that traps the proteinase inside the inhibitor (Barrett, 1981; Barrett and Starkey, 1973; Gonias *et al.*, 1982a).

α_2-macroglobulin appears to be the 'back-up' or 'second-line' inhibitor which becomes the major anti-PN inhibitor when the levels of α_2-antiplasmin are depleted by extensive generation of PN, for example during SK infusion (Gonias *et al.*, 1982b).

2.4.3.3 Plasminogen-activator inhibitor-1

Plasminogen-activator inhibitor-1 is a glycoprotein of M_r 52,000 that is chiefly produced by endothelial cells. It inhibits t-PA and two-chain urokinase plasminogen activator, but not single-chain urokinase plasminogen activator. Different forms of plasminogen-activator inhibitor-1 have been identified (Loskutoff and Schleef, 1988). One of these forms is active and makes an equimolar complex with t-PA and two-chain urokinase plasminogen activator, leading to loss in activity. The second form is inactive, while the third form is latent but can be activated by urea and SDS.

Plasminogen-activator inhibitor-1, being in molar excess of t-PA, serves to minimize surplus fibrinolytic activity in the systemic circulation. The levels of the inhibitor are highly regulated; its high incidence has been reported in several diseased states (Kruithof *et al.*, 1988).

2.4.4 Plasminogen activators

The activation of HPG is the central event in the fibrinolytic cascade. The HPN generated from this event hydrolyzes FN and dissolves blood clots. Plasminogen activators can be broadly divided into two categories.

Direct PG activators, produced by vertebrate cells, are highly specific limited proteases that cleave a single Arg561-Val562 bond at the activation site to yield PN. These include t-PA and UK.

Indirect PG activators, SK and SAK are of bacterial origin and do not possess enzymatic activity. These form complexes with PG and/or PN and these complexes act as PG activators.

2.4.4.1 Tissue-plasminogen activator

Tissue-type plasminogen activator is a chymotrypsin family serine proteinase central to fibrinolysis (reviewed by Madison, 1994; Collen and Lijnen, 1995). The principal physiological source of t-PA are vascular endothelial cells, where it is synthesized as single-chain glycoprotein, however, it is also isolated from other tissues (Booyse *et al.*, 1981; Levin and Loskutoff, 1982; Cole and Bachmann, 1977). *In vivo*, t-PA activation of HPG occurs preferentially on clots, as both t-PA as well as substrate HPG are adsorbed to fibrin surface sites, which leads to increased HPN generation, while preventing systemic activation of HPG.

The mature protein contains 527 amino acids and is organized by sixteen disulphide bonds into five distinct structural domains. It contains a finger domain (Ser1-His44), an epidermal growth factor-like domain (Ser50-Asp87), two kringle domains (Cys92-Cys173 and Cys180-Cys261) and the C-terminal catalytic domain (Ser262-Pro527) (Pennica *et al.*, 1983). This latter catalytic domain shares homology

with other chymotrypsin-like enzymes and contains a typical catalytic triad (Asp371, His322 and Ser478).

Various methods including differential scanning calorimetry (DSC) (Novokhatny *et al.*, 1991) and ^{1}H-NMR spectroscopy (Hu *et al.*, 1994) have been used to show that the five domains of human single chain-t-PA can fold and function autonomously. The binding of t-PA and fibrin has been localized to kringle 2 and the finger domain (van Zonneveld *et al.*, 1986; Verheijen *et al.*, 1986; Gething *et al.*, 1988). Upon cleavage of the Arg275-Ile276 peptide bond by PN, or during fibrinolysis (Ranby *et al.*, 1982; Ichinose *et al.*, 1984), single chain-t-PA is converted to two chain-t-PA, consisting of 275 residue heavy (A) chain and 252 residue light (B) chain, both disulphide connected by Cys264-Cys395. Tissue-type plasminogen activator displays greater enzymatic activity in presence of fibrin (Hoylaerts *et al.*, 1982). The crystal structure of single chain human t-PA (Renatus *et al.*, 1997) and the catalytic domain of recombinant two chain human t-PA (Lamba *et al.*, 1996) have given deep insight that would help in furthering the understanding of this complex protein and in development of new therapeutic activators.

2.4.4.2 Urokinase

Urokinase, also termed two-chain urokinase plasminogen activator, is responsible for the fibrinolytic activity of urine. It has been isolated from urine and from cultures of embryonic kidney cells (Barlow, 1976). It is found to exist in two forms of M_r, 31,300 and 54,700 (White *et al.*, 1966), the smaller one being the proteolytic product of the larger form (Soberano *et al.*, 1976; Barlow *et al.*, 1981). The complete primary amino acid sequence was determined in 1982 (Günzler *et al.*, 1982; Steffens *et al.*, 1982). Urokinase has a four-domain structure including an epidermal growth factor domain, a kringle domain, a connecting peptide and the protease domain in which His204, Asp255and Ser356 form a catalytic triad.

A single chain form of UK has been isolated from urine, plasma and human cell cultures (Husain *et al.*, 1983; Stump *et al.*, 1986a; Stump *et al.*, 1986b). There is a lot of controversy regarding its intrinsic catalytic activity (Pannell and Gurewich, 1987; Petersen *et al.*, 1988; Urano *et al.*, 1988; Husain, 1991). The Lys158-Ile159

bond in single-chain urokinase plasminogen activator is cleaved by PN resulting in the formation of two-chain urokinase plasminogen activator, while the Arg156-Phe157 bond is cleaved by thrombin, converting it into an inactive two-chain derivative (Ichinose *et al.*, 1986; Gurewich and Pannell, 1987; Zamarron *et al.*, 1984).

Several groups have studied the molecular mechanism of activation of PG by UK (Wiman and Wallen, 1973; Rickli and Otavsky, 1973; Violand and Castellino, 1976). Broadly, it involves firstly the cleavage of the scissile peptide bond in Glu-PG (Arg561-Val562), forming Glu-PN, which then autocatalytically cleaves the Lys76-Lys77 peptide bond in Glu-PN heavy chain, yielding Lys77-PN. The formation of Lys77-PN is influenced by the pH, temperature and buffer conditions (Violand and Castellino, 1976).

2.4.4.3 Streptokinase (SK)

Streptokinase (SK) is an extracellular protein produced by a variety of hemolytic streptococci that indirectly cause the activation of PG into its active form, PN (Tillet and Garner, 1933). SK has been used in the clinical treatment of acute myocardial infarction following coronary thrombosis (ISIS-3, 1992) and has served as a thrombolytic agent for more than three decades. The basic mechanism of action of SK has been discussed in detail later in this review.

2.4.4.4 *Streptococcus uberis* plasminogen activator (SUPA)

Streptococcus uberis plasminogen activator (SUPA) was isolated from *Streptococcus uberis*, a species of *Streptococcus* causing bovine mastitis (Leigh, 1993; Rosey *et al.*, 1999; Johnsen *et al.*, 1999). *Streptococcus uberis* was able to acquire surface-localized PN activity by the action of its specific PG activator (Leigh and Lincoln, 1997) which would facilitate the degradation of extracellular matrix proteins and subsequent colonization and also help in availability and utilization of essential amino acids from PN-derived casein peptides, liberated as a result of hydrolysis of milk proteins (Kitt and Leigh, 1997).

Streptococcus uberis plasminogen activator has a putative two-domain structure (having M_r ~ 29,000) intermediate between the one-domain structure of

SAK (having M_r ~ 16,000) and the three-domain structure of SK (having M_r ~ 47,000) (Sazonova *et al.*, 2001). Kinetic data have revealed that SUPA is capable of induction of virgin enzyme activity in bovine PG (in absence of γ-equivalent domain) (Johnsen *et al.*, 2000). Also, the C-terminal β domain of SUPA could not activate PG but formed an activator complex with PN (Johnsen *et al.*, 2000). Thus SUPA showed activation kinetics similar to SK, but exhibits SAK-like susceptibility to α_2-antiplasmin (Johnsen *et al.*, 2000), and thus its mechanism of action is also intermediate between SK and SAK (Sazonova *et al.*, 2001).

2.4.4.5 Staphylokinase

Staphylokinase (SAK), a protein of M_r 15,500 produced by *Staphylococcus aureus*, (Lack, 1948) was shown to have pro-fibrinolytic properties more than four decades ago (Christie and Wilson, 1941; Lewis and Ferguson, 1951). The fibrinolysis was later shown to be due to activation of HPG rather than the direct action of SAK itself (Lack, 1948). Thus like SK, SAK is not an enzyme as it does not show any proteolytic activity by itself; rather it forms a 1:1 complex with HPN, which in turn activates other HPG molecules. In circulating plasma, in absence of fibrin, the HPN.SAK complex gets rapidly neutralized by α_2-antiplasmin, thus preventing systemic HPG activation. In presence of fibrin, the lysine-binding sites of the complex are occupied and inhibition by α_2-antiplasmin is retarded, thereby enabling preferential HPG activation at the fibrin surface (Lijnen *et al.*, 1991). Thus SAK is able to induce lysis in a plasma milieu without causing systemic HPG activation and marked fibrinogen breakdown (Hauptmann and Glusa, 1995), thereby decreasing the risk of severe bleeding. Thus, in contrast to SK, it is a more fibrin-specific fibrinolytic agent in human plasma *in vitro* (Matsuo *et al.*, 1990).

The gene coding for the bacterial protein has been cloned and expressed in *Escherichia coli* (Sako *et al.*, 1983; Sako, 1985) and *Bacillus subtilis* (Behnke and Gerlach, 1987). The nucleotide sequence of SAK gene and the deduced amino acid sequence have been described and are not related to those of SK (Sako and Tsuchida, 1983; Malke *et al.*, 1985; Jackson and Tang, 1982).

The structure of SAK has been analyzed by solution X-ray scattering, dynamic light scattering, ultra-centrifugation and ultra-violet circular dichroism (UV-CD) spectroscopy (Damaschun *et al.*, 1993). The three-dimensional structures of SAK and SAK.HPN complex have been elucidated by X-ray diffraction studies (Rabijns *et al.*, 1997; Parry *et al.*, 1998). In the heterotrimer complex, comprising of two μPN molecules and one SAK molecule, SAK binds one μPN molecule in the proximity of its active site (Parry *et al.*, 1998). Formation of this bi-molecular complex presents a slightly complex surface onto which the second molecule of μPN docks in a substrate-like manner.

Apart from those mentioned above, other PG activators are currently available that have been claimed to possess greater fibrin-specificity, longer half-lives and a potential for increased thrombolytic potency (Weitz *et al.*, 1999; Ross, 1999; Verstraete, 2000).

2.4.4.6 Anisoylated plasminogen streptokinase activator complex

Anisoylated plasminogen streptokinase activator complex consists of SK in complex with anisoylated Lys-PG (Smith *et al.*, 1981; Summaria *et al.*, 1979). It has higher affinity for fibrin than Glu-PG and it would remain inactive until deacylation occurs allowing the formation of the activator. Anisoylated plasminogen streptokinase activator complex has a half-life of 70 min. It is easier to administer since it permits intravenous bolus administration. However, it is more expensive and therefore not widely used.

2.4.4.7 Vampire bat plasminogen activator

Vampire bat PG activator was isolated from the saliva of the vampire bat, *Desmodus rotundus* (Gardell and Friedman, 1993). It is structurally homologous to human t-PA, consisting of a finger domain, an epidermal growth factor domain and a single kringle domain, but lacks the second kringle domain, and the PN cleavage site essential for conversion to a two-chain form of PG activator (Gardell *et al.*, 1989). It shows more fibrin-specificity than t-PA *in vitro* (Gardell *et al.*, 1990) and in laboratory animals (Gardell *et al.*, 1991). However, until trials with this molecule are

complete and reported, it would be uncertain whether it has a selective advantage over the native t-PA molecule.

2.4.4.8 Reteplase

Reteplase is a deletion mutant of t-PA, consisting of kringle 2 and the protease domain of t-PA, but the finger, epidermal growth factor and the kringle 1 regions of the native t-PA have been deleted (Kohnert *et al.*, 1992). It also lacks carbohydrate side chains (Smalling, 1997). These mutations endow a prolonged half-life (about 15 min), thereby allowing its administration as two intravenous boluses, given 30 min apart (Smalling *et al.*, 1995). Like SK, reteplase has an efficacy and safety profile, similar to that of t-PA (GUSTO III, 1997).

2.4.4.9 TNK tissue-type plasminogen activator

TNK tissue-type plasminogen activator, another variant of t-PA, has been specifically bioengineered to retain full fibrinolytic activity of wild-type t-PA, while significantly improve upon some features like prolonged half-life, resistance to PAI-1 and greater fibrin-specificity than t-PA (Keyt *et al.*, 1994; Refino *et al.*, 1993; Cannon *et al.*, 1998). With a half-life of about 20 min, TNK-t-PA can be administered as a single intravenous bolus (Cannon *et al.*, 1997). Large phase III trails are required to determine whether the enhanced fibrin-specificity of TNK-t-PA renders greater safety than t-PA or not.

2.4.4.10 Lanoteplase

Lanoteplase is a t-PA deletion mutant in which the finger and the epidermal growth factor domains have been removed and the glycosylation site in kringle 1 domain has been modified (by replacing Asn117 with Gln) (Larsen *et al.*, 1991). It is produced in Chinese hamster ovary cells. The half-life of approximately 30 min permits its administration via a single intravenous bolus (Ogata *et al.*, 1996; den Heijer *et al.*, 1998). It also shows improved lytic activity (with respect to t-PA) in animal models and reduced fibrin affinity.

Although a multitude of new plasminogen activators have been engineered and many are in the process of being developed, clear-cut evidence that these have advantages of greater efficacy and safety over those currently in use is lacking.

2.5 Streptokinase

Streptokinase is an extracellular protein produced by β-hemolytic streptococci that is not intrinsically an enzyme, but requires the presence of PG for its action. In the streptococcal cells that produce SK, it has been projected to play a role in pathogenesis by virtue of its ability to activate PG into PN, a protease of broad specificity that can result in massive tissue damage and bacterial invasiveness into secondary infection sites within the host body (Lähteenmäki *et al.*, 2001; Esmon and Mather, 1998).

2.5.1 Nucleotide sequence and amino acid sequence of SK

The complete amino acid sequence of SK was determined by sequential Edman's degradation analysis of SK fragments produced by cyanogen bromide and enzymatic methods (Jackson and Tang, 1982). The nucleotide sequence was reported by Malke and co-workers, in 1985. The amino acid sequence derived from the nucleotide sequence of SK (Malke *et al.*, 1985) has been shown in Figure 2.3.

2.5.2 Genetics, expression and production of SK

Streptokinase is naturally produced and secreted by various strains of hemolytic streptococci, best studied of them is *Streptococcus equisimilis*. The gene was cloned from *Streptococcus equisimilis* H46A and expressed in *Escherichia coli* (Malke and Ferretti, 1984). Alternative host systems for expression of SK have also been studied. Streptokinase has been expressed in various Gram-negative and Gram-positive bacteria including *Proteus mirabilis* (Laplace *et al.*, 1989), *Streptococcus sanguis* Challis strain (Malke *et al.*, 1984; Jackson *et al.*, 1986), *Streptococcus lactis* (Laplace *et al.*, 1989) and *Bacillus subtilis* (Klessen and Malke, 1986; Wong *et al.*, 1994). Expression of SK has also been studied in *Pichia pastoris* (Hagenson *et al.*, 1989).

```
  I   A   G   P   E   W   L     L   D   R     P   S   V     N   N   S   Q     L   V   V
ATTGCTGGAC CTGAGTGGCT GCTAGACCGT CCATCTGTCA ACAACAGCCA ATTAGTTGTT 60
  S   V   A   G   T   V   E     G   T   N     Q   D   I     S   L   K   F     F   E   I
AGCGTTGCTG GTACTGTTGA GGGGACGAAT CAAGACATTA GTCTTAAATT TTTTGAAATC 120
  D   L   T   S   R   P   A     H   G   G     K   T   E     Q   G   L   S     P   K   S
GATCTAACAT CACGACCTGC TCATGGAGGA AAGACAGAGC AAGGCTTAAG TCCAAAATCA 180
  K   P   F   A   T   D   S     G   A   M     S   H   K     L   E   K   A     D   L   L
AAACCATTTG CTACTGATAG TGGCGCGATG TCACATAAAC TTGAGAAAGC TGACTTACTA 240
  K   A   I   Q   E   Q   L     I   A   N     V   H   S     N   D   D   Y     F   E   V
AAGGCTATTC AAGAACAATT GATCGCTAAC GTCCACAGTA ACGACGACTA CTTTGAGGTC 300
  I   D   F   A   S   D   A     T   I   T     D   R   N     G   K   V   Y     F   A   D
ATTGATTTTG CAAGCGATGC AACCATTACT GATCGAAACG GCAAGGTCTA CTTTGCTGAC 360
  K   D   G   S   V   T   L     P   T   Q     P   V   Q     E   F   L   L     S   G   H
AAAGATGGTT CGGTAACCTT GCCGACCCAA CCTGTCCAAG AATTTTTGCT AAGCGGACAT 420
  V   R   V   R   P   Y   K     E   K   P     I   Q   N     Q   A   K   S     V   D   V
GTGCGCGTTA GACCATATAA AGAAAAACCA ATACAAAACC AAGCGAAATC TGTTGATGTG 480
  E   Y   T   V   Q   F   T     P   L   N     P   D   D     D   F   R   P     G   L   K
GAATATACTG TACAGTTTAC TCCCTTAAAC CCTGATGACG ATTTCAGACC AGGTCTCAAA 540
  D   T   K   L   L   K   T     L   A   I     G   D   T     I   T   S   Q     E   L   L
GATACTAAGC TATTGAAAAC ACTAGCTATC GGTGACACCA TCACATCTCA AGAATTACTA 600
  A   Q   A   Q   S   I   L     N   K   N     H   P   G     Y   T   I   Y     E   R   D
GCTCAAGCAC AAAGCATTTT AAACAAAAAC CACCCAGGCT ATACGATTTA TGAACGTGAC 660
  S   S   I   V   T   H   D     N   D   I     F   R   T     I   L   P   M     D   Q   E
TCCTCAATCG TCACTCATGA CAATGACATT TTCCGTACGA TTTTACCAAT GGATCAAGAG 720
  F   T   Y   R   V   K   N     R   E   Q     A   Y   R     I   N   K   K     S   G   L
TTTACTTACC GTGTTAAAAA TCGGGAACAA GCTTATAGGA TCAATAAAAA ATCTGGTCTG 780
  N   E   E   I   N   N   T     D   L   I     S   E   K     Y   Y   V   L     K   K   G
AATGAAGAAA TAAACAACAC TGACCTGATC TCTGAGAAAT ATTACGTCCT TAAAAAAGGG 840
  E   K   P   Y   D   P   F     D   R   S     H   L   K     L   F   T   I     K   Y   V
GAAAAGCCGT ATGATCCCTT TGATCGCAGT CACTTGAAAC TGTTCACCAT CAAATACGTT 900
  D   V   D   T   N   E   L     L   K   S     E   Q   L     L   T   A   S     E   R   N
GATGTCGATA CCAACGAATT GCTAAAAAGT GAGCAGCTCT TAACAGCTAG CGAACGTAAC 960
  L   D   F   R   D   L   Y     D   P   R     D   K   A     K   L   L   Y     N   N   L
TTAGACTTCA GAGATTTATA CGATCCTCGT GATAAGGCTA AACTACTCTA CAACAATCTC 1020
  D   A   F   G   I   M   D     Y   T   L     T   G   K     V   E   D   N     H   D   D
GATGCTTTTG GTATTATGGA CTATACCTTA ACTGGAAAAG TAGAGGATAA TCACGATGAC 1080
  T   N   R   I   I   T   V     Y   M   G     K   R   P     E   G   E   N     A   S   Y
ACCAACCGTA TCATAACCGT TTATATGGGC AAGCGACCCG AAGGAGAGAA TGCTAGCTAT 1140
  H   L   A   Y   D   K   D     R   Y   T     E   E   E     R   E   V   Y     S   Y   L
CATTTAGCCT ATGATAAAGA TCGTTATACC GAAGAAGAAC GAGAAGTTTA CAGCTACCTG 1200
  R   Y   T   G   T   P   I     P   D   N     P   N   D     K TER
CGTTATACAG GGACACCTAT ACCTGATAAC CCTAACGACA AATAA
```

Figure 2.3 Nucleotide and amino acid sequences of SK from *Streptococcus equisimilis* H46A.

2.5.3 Purification of SK

It becomes pertinent to obtain highly purified preparations of SK both for therapeutic purposes and for biochemical studies to study the mechanism of its interaction with HPG. Over the years, several purification procedures for obtaining highly purified preparations of SK have been reported including chromatography on DEAE-cellulose followed by density gradient electrophoresis (De Renzo *et al.*, 1967), a combination of ion-exchange chromatography and gel filtration (Taylor and Botts, 1968) and a series of procedures including ammonium sulphate based fractionation, gel filtration and chromatography using DEAE-cellulose (Einarrson *et al.*, 1979). For single-step purification of SK, Castellino and co-workers in 1976 reported the use of affinity chromatography on insolubilized diisopropyl fluorophosphate-PN. Rodriguez and coworkers (1992) described the purification of SK by affinity chromatography on acylated PG or PN with p-nitrophenyl p′-guanidinobenzoate (NPGB), which yields purified SK with high specific activity.

In our laboratory, Nihalani (1997) described a combination of two different purification procedures *viz.* hydrophobic interaction chromatography (HIC) and ion-exchange chromatographies, which could purify extracellular SK from *Streptococcus equisimilis* H46A culture broth to apparent homogeneity with very high specific activities (~ 200,000 IU/mg) with overall yields ranging from 65-70 %.

2.5.4 Physico-chemical properties of SK

The molecular weight of SK was determined to be 47,600 by equilibrium sedimentation (De Renzo *et al.*, 1967). The isoelectric point was estimated to be about pH 4.7 (De Renzo *et al.*, 1967). Carbohydrates and lipids were found to be absent from highly purified preparations of SK (reviewed in Castellino, 1981). Amino acid analysis showed that SK is also free of cystines and cysteines (De Renzo *et al.*, 1967).

No synthetic substrates for SK have been found till date. SK forms an equimolar complex with HPG that catalyzes activation of HPG from plasma of different mammalian species like human, monkey, baboon, chimpanzee, cat, dog and rabbit (Sodetz *et al.*, 1972; Wulf and Mertz, 1969).

2.5.5 Secondary structure analysis

Data analyses of circular dichroism (CD) (Brockway and Castellino, 1974) and optical rotation (Taylor and Botts, 1968) indicate that the helical content of SK is of the order of 10-12 %. The conformational properties of SK have been investigated by Radek and Castellino (1989). Streptokinase was tested for its ability to renature from a chemically induced unfolding of its native conformation. Streptokinase was fully capable of renaturing from urea-unfolded state into a conformation that gave thermal and kinetic patterns similar to the native protein. Thermal and guanidinium deuterochloride-induced unfolding studies of SK using ^{1}H-NMR spectroscopy established several distinct unfolding transitions and the existence of a number of partially folded states of the protein (Teuten *et al.*, 1993).

Streptokinase was analyzed by DSC in a series of buffer conditions and different pH values in order to determine the stability of the conformation of the protein. In the acidic range, SK was stable down to pH of 4.4 and in the alkaline range, it was marginally stable up to pH 10.4. Further increase in pH led to the unfolding of the molecule.

The far-UV CD spectra were also analyzed to determine the tertiary structure class (Levitt and Chothia, 1976) to which SK belongs. Streptokinase is classified as an $\alpha+\beta$ protein based on the predictions of Johnson (Johnson, 1986) who observed that $\alpha+\beta$ proteins display a more intense band at 208 nm than as compared to 222 nm, with the inverse being true for α/β proteins. Secondary structural characteristics were estimated *viz.* ~ 17 % α-helix, 28 % β-sheet, 21 % β-turn and 34 % random coil. Similar secondary structural characteristics were also revealed from analysis of CD, Infra-Red and Fourier Transform Infra-Red and Raman spectral studies (Welfe *et al.*, 1992; Fabian *et al.*, 1992). A comparative picture of the secondary structural data from various sources has been presented in Table 2A. A prediction of the secondary structural elements from the amino acid sequence yielded results similar to those of experimental techniques (Radek and Castellino, 1989).

Table 2A Comparative data of the secondary structure elements in SK

Type of spectral study	Subject of study	% α-helix	% β-sheet	% β-turns	% others	Reference
CD	Native SK	17	28	21	34	Radek and Castellino, 1989
Fourier Transform-Infra-red	Native SK	12-13	30-37	25-26	15-16	Fabian *et al.*, 1992
Infra-Red	Native SK	16	40	26	19	Fabian *et al.*, 1992
CD	Native SK	14-23	38-46	10-30	12-23	Welfle *et al.*, 1992
CD	Native SK	32.1	33.8	0.4	33.8	Parrado *et al.*, 1996
ProMotif Program (Hutchinson and Thornton, 1996)	Crystal structure of SK.μPN	10.7	36.9	18	34.4	Wang *et al.*, 1998

2.5.6 Immunobiology of SK

Antibodies against SK can be detected in most humans since humans are exposed frequently to streptococcal infections. High titres of anti-SK immunoglobulins are rapidly generated after SK administration; these antibodies have been shown to persist in patients for up to 54 months (Lee *et al.*, 1993). These antibodies neutralize SK upon administration (Jalihal and Morris, 1990) or cause a range of allergic reactions (McGrath and Patterson, 1984; McGrath *et al.*, 1985; Schweitzer *et al.*, 1991), thereby preventing future therapy with SK.

Therefore, in order to facilitate design of less immunogenic and thereby improved SK derivatives, a thorough understanding of the interaction of SK and its antibodies is essential. Several groups have tried to map the segments of immunodominance (Reed *et al.*, 1993; Parhami-Seren *et al.*, 1996; Bruserud *et al.*, 1992; Parhami-Seren *et al.*, 1997; Torréns *et al.*, 1999a). Different approaches based on competitive binding studies with native and truncated SK fragments, random peptide libraries, affinity-derived mass spectroscopic techniques were utilized to define the antigenic regions of SK (Coffey *et al.*, 2001; Parhami-Seren *et al.*, 1996; Parhami-Seren *et al.*, 1997).

Efforts to develop SK molecules with improved clinical efficacy have been reported. To reduce antigenicity, SK has been modified *in vitro* with polyethylene-glycol (Rajagopalan *et al.*, 1985). A mutant lacking the C-terminal 42 amino acids has been found to be less immunogenic (Torrens *et al.*, 1999b; Torrens *et al.*, 1999c).

2.5.7 Mechanism of action

Several biochemical studies have been carried out for more than three decades that have provided deep insights into the mechanism of activation of HPG, mediated by SK. Since SK is neither a protease nor an esterase (De Renzo *et al.*, 1967; Buck *et al.*, 1968; McClintock and Bell, 1971), much interest has been evoked as to the manner in which SK activates HPG.

SK can form a HPG activator by two pathways.

Pathway 1 - SK forms a stoichiometric 1:1 complex with HPG (Wohl *et al.*, 1978; Castellino, 1979) resulting in the formation of SK.HPG. As a result of this interaction,

a conformational transition occurs in the complex yielding SK.HPG′, possessing an active site as was established by the use of active center-specific reagent, NPGB and analysis of these complexes by starch gel electrophoresis (McClintock and Bell, 1971) and SDS-PAGE (Reddy and Markus, 1972). The SK.HPG′ is not stable and is rapidly altered to SK*.HPN. This is accomplished by intra-molecular cleavage (Kosow, 1975; Bajaj and Castellino, 1977) of Arg561-Val562 peptide bond in SK.HPG′, catalyzed by the active site in HPG moiety of the complex. It appears that the major activator of HPG is a complex of SK*.HPN, consisting of a proteolytically altered SK* (Reddy and Markus, 1972; Taylor and Beisswenger, 1973).

This process of zymogen activation is similar among the enzymes of the trypsin family (Neurath, 1989). As described earlier, HPG activation involves the proteolytic cleavage of the Arg561-Val562 bond. The amino group of Val562 forms a salt-bridge with Asp740, which triggers a conformational change producing the active protease, HPN (Wang *et al.*, 2000b). However, in SK.HPG′, which is functionally active despite the intact Arg561-Val562 bond, another residue is likely to provide a counter-ion for Asp740.

Two hypotheses have been proposed to explain the non-proteolytic zymogen activation of HPG by SK.

Bode and Huber (1976) proposed that the N-terminus of SK forms a salt-bridge with Asp740 of HPG, inducing a structural change in a manner analogous to the N-terminal Val562 of HPN (molecular sexuality hypothesis). Jackson and Tang (1978) reported a similar mechanism that was termed as the N-terminal insertion hypothesis. Wang and coworkers (1999a) provided experimental evidence of this hypothesis where the deletion of the N-terminal residue of SK (Ile) abolished HPG activation by SK under conditions where the conversion of SK.HPG to SK.HPG′ is rate-limiting (at 4°C).

An alternative hypothesis proposes that a residue of HPG itself might form a salt-bridge and the most likely residue is Lys698 (Renatus *et al.*, 1997; Wang *et al.*, 1998). This is based on the observation that the analogous residue, Lys156, provides the counter-ion in zymogen of t-PA (Nienaber *et al.*, 1992; Lamba *et al.*, 1996).

Support for this hypothesis has also been gauged from the crystal structure of SK with μPN, where the γ domain of SK contacts HPG near to Lys698. This region of HPG corresponds to the activation domain of trypsinogen (Esmon and Mather, 1998) and is predicted to structurally position Lys698 for the formation of the critical salt-bridge. Reports of the SK molecule with non-native terminus being as active as the native molecule (Lee *et al.*, 1997; Fay and Bokka, 1998) along with mutational analysis of the γ domain (Wu *et al.*, 2001), which confirm the involvement of the γ domain in zymogen activation, give credibility to this theory.

Pathway 2 - Alternatively, SK can complex directly with HPN, thereby forming a HPG activator (Wang *et al.*, 2000b). Trace amounts of HPN are always present in HPG preparations and HPN appears to have a higher affinity for SK (Gonzalez-Gronow *et al.*, 1978; Boxrud *et al.*, 2000), thereby resulting in the initiation of Pathway 2.

The final step in PG activation involves the activation of 'substrate' HPG by the activator complex. The events that take place are schematically represented in Figure 2.4. Plasmin, a broad-spectrum protease having specificity for Arg and Lys residues, by itself is a very poor activator of HPG (Castellino *et al.*, 1976). However the binding of SK to HPN modulates the specificity of the active protease such that it becomes highly specific for 'substrate' HPG molecules. Markus and Werkheiser (1964) elegantly demonstrated this 'specificity switch' in HPN molecule bound to SK. In this experiment, the activation of HPG to HPN by catalytic amounts of SK was monitored. The activity of free HPN generated was followed using three kinds of substrate- the esterolytic, proteolytic and specific PG activation activities were followed using TAME (alpha-N-tosyl-L-arginine methyl ester), azocasein and bovine PG as substrates, respectively.

The HPN generated was able to catalyze the general protease activity, as well as the esterolytic activity, but was unable to activate bovine PG. However, with increasing concentration of SK, while the esterase activity of HPN remained unaffected, the general trypsin like proteolytic activity of HPN, as observed by azocasein digestion decreased linearly as a function of increasing SK concentration,

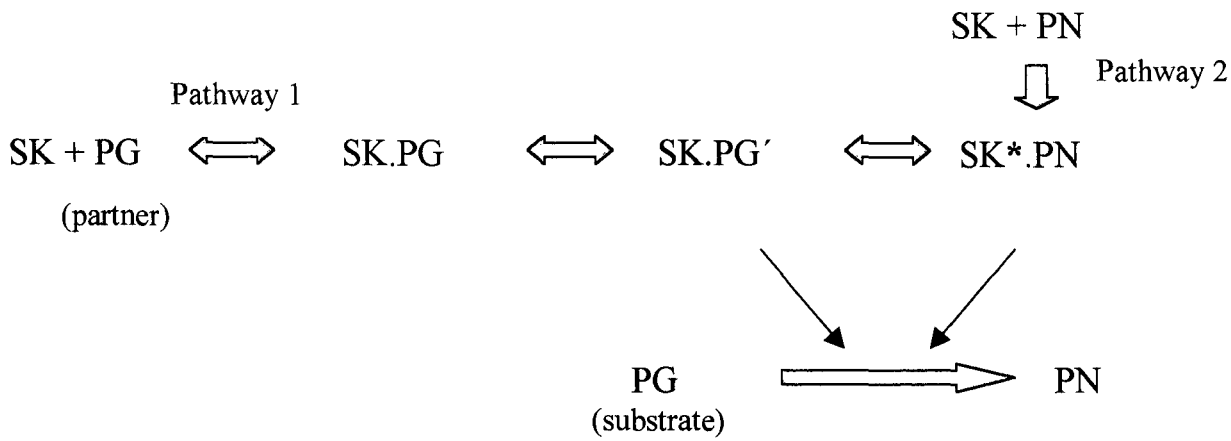

Figure 2.4 Schematic representation of the steps involved in the activation of PG by SK. SK forms a high-affinity complex with PG (Pathway 1) that leads to the generation of an active center in the complex (SK.PG′) prior to scissile peptide bond cleavage in the 'partner' PG. This 'virgin complex' then gets converted to SK^*.PN, which can also be formed by the direct complexation of preformed PN with SK (Pathway 2). The activator complex then catalytically acts on 'substrate' PG molecules and converts them into PN.

reaching a minimum at equimolar concentration of SK with regard to HPG/HPN (Figure 2.5). Strikingly, concomitant with the decrease in the general protease activity, the ability of PN to activate bovine PG increased with increasing amounts of SK.

2.5.8 Regions of SK interacting with HPG

Before the crystal structure of SK was solved in 1998, only low-resolution NMR data were available (Misselwitz *et al.*, 1992; Welfe *et al.*, 1992; Fabian *et al.*, 1992; Teuten *et al.*, 1993). These studies revealed that SK is a multi-domain protein possessing upward of two (Radek and Castellino, 1989), three (Teuten *et al.*, 1993) or four (Damaschun *et al.*, 1992) domains. Different modified (fragmented) forms have been obtained using chemical (Misselwitz *et al.*, 1992) and biochemical (Nakashima *et al.*, 1990; Misselwitz *et al.*, 1992; Rodriguez *et al.*, 1994; Shi *et al.*, 1994) methods or upon expression of SK in *Streptococcus sanguis* (Jackson *et al.*, 1986) and in *Escherichia coli* (Reed *et al.*, 1995; Rodriguez *et al.*, 1995). A series of proteolytic fragments were generated whose molecular weights ranged from 8 kDa to 44 kDa, some of which partially retained the PG activation function of intact SK (Brockway and Castellino, 1974; Summaria *et al.*, 1974; Markus *et al.*, 1976; Nakashima *et al.*, 1990; Rodriguez *et al.*, 1994; Shi *et al.*, 1994). Further meaningful insight into the domain-organization of SK was gleaned through limited proteolysis and other biophysical techniques (Conejero-Lara *et al.*, 1996; Parrado *et al.*, 1996).

In order to decipher the sub-regions of SK which are involved in either 1:1 high affinity binding with HPG and those that selectively interact with substrate HPG, a synthetic peptide approach was employed in our laboratory, in which the overlapping synthetic peptides encompassing the central domain and the N-terminal domain of SK were synthesized and their HPG activation abilities were systematically analyzed. Results suggested that regions encompassing residues 250-270, in the core region of the β domain impart an ability to the SK.HPN complex to bind to substrate HPG during the activation process, whereas flanking segments spanning residues 230-250 and 270-290 of β domain of SK bind close to the active center of HPN, and are involved in 1:1 binding with partner HPG (Nihalani *et al.*, 1997). Similarly, in the N-

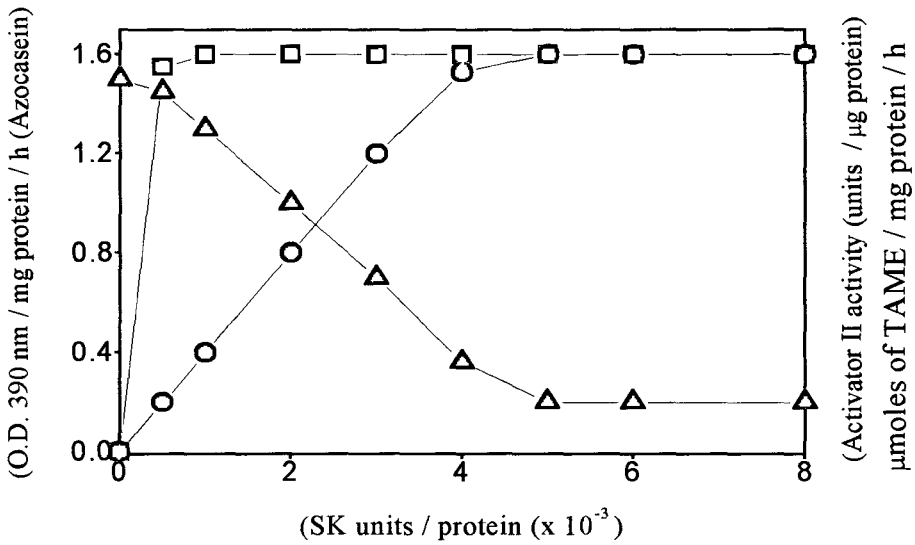

Figure 2.5 Alteration of substrate specificity of HPN upon binding with SK. Activation of HPG by the addition of catalytic amounts of SK generates HPN that displays azocasein hydrolysis (triangles) and esterase activities (µmoles of TAME/mg protein/h) (squares). However, it is unable to catalyze the conversion of bovine PG to its PN form (activator II activity) (circles). When the amount of SK used in the reaction is gradually increased, the generalized proteolytic activity of HPN on azocaesin decreases linearly with SK concentration and reaches a low of about 25 % of the maximum activity. Concomitantly, its activator activity increases linearly with increasing concentrations of SK and reaches a maximum at equimolar concentrations of SK and HPG/HPN (adapted from Markus and Werkheiser, 1964).

terminal region of SK, site located between residues 16 and 36 of SK contain epitopes involved in substrate interactions, whereas there is a strong 1:1 affinity region in the locus composed of residues 37-51 (Nihalani *et al.*, 1998). The linear map of the regions in SK interacting with HPG has been illustrated in Figure 2.6.

2.5.9 Mutagenesis studies of SK

In order to find out the residues in SK that are involved in binding to partner HPG or activating substrate HPG, site-directed mutagenesis was carried out in different regions of SK. Mutagenesis studies in the α domain of SK have indicated that Gly24 (Lee *et al.*, 1989), Val19 (Lee *et al.*, 1997), Leu42 (Liu *et al.*, 2000), and residues Asp41-His48 (Kim *et al.*, 2000) are involved in substrate HPG activation. Recent mutational studies in the α domain have shown that residues 1-59 in the α domain of SK play a role in regulation of active-site induction in bound HPG, resistance to inhibition of the SK.HPN complex to α_2-antiplasmin and control of fibrin-independent HPG activation (Mundada *et al.*, 2003). Studies on deletions at the N-terminal region (Lee *et al.*, 1997; Fay and Bokka, 1998) and the C-terminal region (Fay and Bokka, 1998; Kim *et al.*, 1996) indicated that deletion of upto 16 residues from the N-terminus and 41-residue deletion from the C-terminus did not have any effect on the PG activator activity. Deletions of certain loop regions, for example residues 48-59 of the α domain of SK have shown the importance of these surface-exposed regions in substrate recognition and PG activation (Wakeham *et al.*, 2002).

Mutagenesis of the lysine residues in the region 244-352 (Lin *et al.*, 1996) has revealed the crucial role played by the lysine residues in SK.HPG interaction. The importance of the β domain of SK substrate docking and processing was validated by mutational studies on charged residues in the central domain of SK (Chaudhary *et al.*, 1999).

Similar studies on the C-terminal domain (Wu *et al.*, 2001) have provided deep insight regarding the involvement of charged residues in the coiled coil region of SK γ in non-proteolytic activation of partner HPG and stabilization of the activator complex. The γ domain of SK has also been proposed to contribute, along with the β

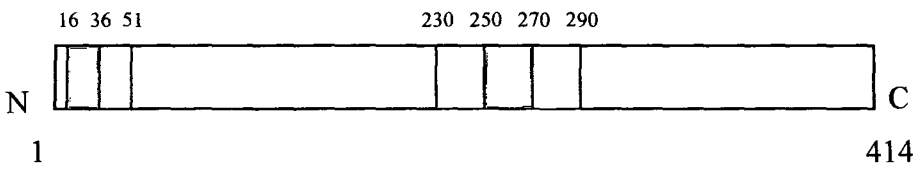

Figure 2.6 Functional map of the regions in SK that interact with HPG. Both the α domain (residues 1-143) and the β domain (residues 143-293) of SK contain loci that are bi-functional, that is, they interact with HPG in 'partner' as well as 'substrate' modes. While residues 36-51 in the α domain and residues 230-250 and 270-290 in the β domain have been proposed to be involved in the formation of high affinity complex with HPG (shaded grey); residues 16-51 in SK α and residues 250-270 in SK β (shaded red) were involved in the binding and docking of 'substrate' HPG to the activator complex between SK and HPG (Nihalani *et al.*, 1997; Nihalani *et al.*, 1998). 'N' and 'C' represent the N-terminus and the C-terminus of the 414 amino acid long SK protein, respectively.

domain, to the species specificity of SK, upon forming a PG-activator complex (Kim *et al.*, 2002; Gladysheva *et al.*, 2002). Recently, the C-terminal flexible peptide in the γ domain of SK encompassing residues 375-414, has been shown to play a functional role in active site formation and substrate recognition in HPG activation (Zhai *et al.*, 2003).

Fusion proteins have also been constructed where domains of one protein have been swapped with those of other related proteins; these give interesting clues viz. the basic functionalities of SK domains (Kim *et al.*, 2002; Gladysheva *et al.*, 2002).

2.5.10 X-ray diffraction studies of SK

The crystal structure of SK complexed with the catalytic domain of HPN, described at 2.9 Å by Wang and coworkers (1998) was one of the major achievements in this field in the last decade (Figure 2.7). Streptokinase was shown to be composed of three domains (α, β and γ) separated by two coiled coils. Both the α and β domains contain a major β-sheet of five mixed β-strands and an α-helix, a structure that is characteristic of the β-grasp folding class (Murzin *et al.*, 1995). The γ domain, on the other hand, lacks an α-helix; consists of four β-strands and a coiled coil. There are some disordered segments in the crystal structure that include the N-terminal fifteen residues of SK, the C-terminal thirty two residues (Jackson *et al.*, 1986; Young *et al.*, 1995), residues 46-70 in the α domain of SK, and residues 170-182 and residues 251-264 in the β domain of SK. The diffraction studies also reveal that all the three domains of SK interact with μPN, with the maximum interaction being with α, followed by γ and then β. The α domain (β_1 and β_2 strands) interact with the loop regions of μPN (residues 713-721), whereby Arg719 of μPN (Dawson *et al.*, 1994) forms a salt-bridge with Glu39 and Glu134 and also has Van der Waal's contact with Val19 (Lee *et al.*, 1997). The SK α domain has also been shown to network with HPG near the residues constituting the catalytic triad (His603 and Asp646). The crystal structure also revealed that the coiled coil region and the β_1 and β_2 strands of the SK γ domain bind to μPN *viz.* the calcium-binding loop spanning residues 622-628 and the

Figure 2.7 Crystal structure of SK in complex with the catalytic domain of HPN, solved at 2.9 Å. The structure indicates that SK is composed of three structurally homologous domains, α (shaded light green), β (shaded dark green) and γ (shaded violet), which are connected by coiled coils. The three domains of SK surround μPN (shaded blue), the catalytic domain of HPN, forming a 'valley', that is proposed to be optimum for docking of 'substrate' HPG via its catalytic domain (adapted from Wang *et al.*, 1998). However, the role of kringle domains, if any, of either 'partner' HPG or the macromolecular substrate, is not explained by this structure.

autolysis loop covering residues 692-695, which lead to extensive charged and hydrophobic interactions.

The crystal structure also elucidates how the three domains of SK surround the μPN active site in the form of a 'valley' with the active center at the base and SK forming the rim. Thus the activator complex seems to be optimally positioned for the stereo-chemical 'docking' of the substrate HPG molecule. Computer simulations studies on the docking of a model of μPG substrate show that there are extensive interactions with the substrate and the SK domains, maximally with the α domain of SK.

Though several biochemical studies have unequivocally shown the involvement of the β domain of SK in HPG binding and activation (Lin *et al.*, 1996; Chaudhary *et al.*, 1999), the interaction of the central domain with μPN in the structure proposed by Wang and coworkers (1998) is quite ambiguous, probably due to large thermal factors and absence of the kringle domains of the activator complex as well as substrate HPG with which it is known to interact. Also, the SK molecule was getting cleaved between Lys257 and Ser258 that rendered the entire region disordered in the structure.

2.5.11 Crystal Structure of SK-β domain

Since the crystal structure of SK in complex with μPN was silent on the β domain, Wang and coworkers (1999b) determined the structure of the isolated β domain at 2.4 Å. The overall folding of SK β is of the β-grasp folding class. The X-ray diffraction studies show the presence of two loops, namely the 170-loop and the 250-loop. The 170-loop spanning residues 170-182, is located between strands β_1 and β_2. The fact that this loop contains three Asp residues and other charged residues and is positioned close to the presumed substrate-binding site indicates that this might be interacting with substrate HPG. This epitope has also been implicated in the immunogenicity of SK (Torrens *et al.*, 1999a). The 250-loop, encompassing residues 251-264 of SK and strands β_6' and β_6'', forms a hairpin structure and projects out into the solvent. It has three Glu residues at the stem and two Lys residues at the tip. The

loop faces away from the interface of SK β and μPN (SKβ) in the SK.μPN complex and is therefore unlikely to participate directly in 1:1 binding that has validated by biochemical studies (Lin *et al.*, 1996; Nihalani *et al.*, 1997). Two buried salt bridges Arg219-Glu272 and Arg248-Asp68, which are conserved in SK β among the SK family (Malke, 1993) are buried in the core and probably help to maintain structure stability.

Though the crystal structure provides deep insight into the interaction between the three domains of SK on one hand and partner μPN, it lacks accurate information regarding the sites in SK that interact with complementary epitopes in the substrate and there is a lot of ambiguity regarding the precise protein-protein interactions that play a cardinal role in substrate HPG recognition and activation.

In addition, it would also be intriguing to know whether the isolated α domain of SK that bears a high degree of structural homology with SAK (a single-domain HPG activator), displays cofactor activity or not, and even if it shows traces of activity, whether the activity could be further enhanced through a systematic protein engineering approach. This treatise was carried out with an objective to address these issues.

CHAPTER III

INVOLVEMENT OF A NINE-RESIDUE LOOP OF STREPTOKINASE IN THE GENERATION OF MACROMOLECULAR SUBSTRATE-SPECIFICITY BY THE ACTIVATOR COMPLEX THROUGH INTERACTION WITH SUBSTRATE KRINGLE DOMAINS

Abstract

Computer modeling studies of the three domains of SK superimposed on each other revealed a discrete surface-exposed epitope (residues 254-262; termed the 250-loop) in the β domain that is absent in the other two otherwise structurally homologous domains. The deletion of this nine-residue loop in SK led to significant decrease in the rates of substrate HPG activation by the mutant ($SK_{del254-262}$). A kinetic analysis of $SK_{del254-262}$ revealed that its low HPG activator activity arose primarily from a 5-6 fold increase in K_M for HPG as substrate, with little alteration in k_{cat} rates. Under these conditions, the k_{cat} for the small peptide substrate tosyl-glycyl-prolyl-lysine-4-nitranilide-acetate was essentially unchanged. Remarkably, the observed increase in the K_M for the macromolecular substrate was proportional to a similar decrease in the binding affinity for substrate HPG as observed in a new Resonant Mirror based assay for the real-time kinetic analysis of the docking of substrate HPG onto pre-formed binary complex, although under those conditions, the 1:1 affinity of $SK_{del254-262}$ for partner HPG was minimally changed. In contrast, kinetic studies on the interaction of the two proteins with μPG showed no difference between formation of ternary complex with μPG by preformed equimolar complexes of HPG with either SK or $SK_{del254-262}$, nor between the rates of activation of μPG to μPN under conditions where native HPG was activated differentially by SK and $SK_{del254-262}$. This clearly indicated a kringle-mediated mechanism for the role of the 250-loop of SK in substrate docking/recognition. The involvement of kringles was further established by a hyper-susceptibility of the $SK_{del254-262}$.HPN activator complex to EACA-mediated inhibition of substrate HPG activation in comparison to that of the native SK.HPN activator complex. Further, 'ternary' binding experiments on the Resonant Mirror showed that the binding affinity of kringles 1-5 of HPG to the preformed binary complex of the 250-loop deleted mutant and HPG was reduced by about 3-fold in comparison to that of SK.HPG. Overall, these observations identify the 250-loop of SK as an important structural determinant of the inordinately stringent substrate specificity of the SK.plasmin(ogen) activator complex and demonstrate that this structural epitope in the β domain promotes the binding of substrate HPG to the activator via the kringle/s during the HPG activation process.

3.1 INTRODUCTION

Streptokinase, a bacterial protein secreted by the Lancefield Group C β-hemolytic streptococci, is widely used as a thrombolytic agent in the treatment of various circulatory disorders, including myocardial infarction (ISIS-3, 1992). Biochemical and structural studies have revealed that SK is composed of three structurally similar domains (termed α, β and γ), separated by random coils and small, flexible regions at the amino and carboxyl termini (Parrado *et al.*, 1996; Conejero-Lara *et al.*, 1996; Wang *et al.*, 1998). The recently solved crystal structure of the catalytic domain of HPN complexed with SK strongly indicates how SK might modulate the substrate-specificity of HPN by providing a "valley" or cleft in which the macromolecular substrate can dock through protein-protein interactions, thus positioning the scissile peptide bond optimally for cleavage by the HPN active site, thereby conferring a narrow substrate preference onto an otherwise 'indiscriminate' active center. In this structure, SK does not appear to induce any significant conformational changes in the active site residues directly but, along with 'partner' HPG, seems to provide a template on which the substrate molecule can dock through protein-protein interactions, resulting in the optimized presentation of the HPG activation loop at the active center of the complex (Esmon and Mather, 1998; Wang, *et al.*, 1998). However, the identity of these interactions, and their contributions to the formation of the enzyme-substrate intermediate/s remains a mystery so far.

Besides the well-recognized "switch" in substrate preference (Markus and Werkheiser, 1964), the binding of SK to HPN results in a several-fold enhancement of the K_M for diverse small molecular weight (MW) chromogenic peptide substrates but relatively little alteration in their k_{cat} values as compared to free HPN indicating that the primary, covalent specificity characteristics of the active center of HPN upon SK binding are unchanged but result in steric hindrance/reduced accessibility for even the small molecular weight (MW) peptide substrates. Thus, the remarkable alteration of the macromolecular substrate specificity of HPN by SK is currently thought to be due to 'exosites' generated on the SK.HPN complex, as shown recently by the elegant use of active site-labeled fluorescent HPN derivatives (Boxrud *et al.*, 2000). 'Peptide Walking' studies in our laboratory had also indicated that short peptides based on the

primary structure of SK, particularly those derived from selected regions in the α and β domains, displayed competitive inhibition for HPG activation by the pre-formed SK.HPN complex under conditions where the 1:1 complexation of SK and HPN was essentially unaffected (Nihalani *et al.*, 1997; Nihalani *et al.*, 1998). However, the crystal structure of SK complexed with microplasmin(ogen) (Wang *et al.*, 1998), while providing a high degree of resolution of the residues involved in the SK.μPN complexation, yielded few unambiguous insights regarding the interactions engendered between the activator complex and 'substrate' HPG. This is likely due to the binary nature of the complex that is, an absence of a juxtaposed substrate molecule, large average thermal factors especially in the β domain, and a total absence, in both partner and substrate HPG, of the kringles which are known to be important in HPG activation (Lin *et al.*, 2000). Thus, despite a detailed and high-resolution exposition of the overall nature of protein-protein interactions in the SK.μPN binary complex, discrete structures/epitopes of SK, if any, that are directly involved in the exosite formation process by the full-length activator complex have not yet been identified.

Previously, charged side-chains, both in HPG, particularly around the active center (Dawson *et al.*, 1994) as well as in SK in the beta domain (Chaudhary *et al.*, 1999) have been shown to be important for HPG activation ability. However, a clear-cut identification of a structural epitope/element in conferring substrate HPG affinity onto the SK.HPG activator complex has not been demonstrated till now. Of the three domains of SK, the central β domain displays maximal affinity for HPG (Conejero-Lara *et al.*, 1998), the N-terminal α domain displays relatively lesser affinity, with much less affinity exhibited by the isolated γ domain for HPG. Solution and structural studies suggest that both α and β domains are involved in the substrate recognition phenomena (Nihalani *et al.*, 1998; Wang *et al.*, 1998). Although some mutagenesis studies have implicated positively charged residues in the β domain to be important (Chaudhary *et al.*, 1999), others failed to show that such residues are directly involved in substrate recognition by the binary complex (Lin *et al.*, 1996).

We undertook this study to probe more conclusively for epitopes in SK, if any, that may be involved in interaction with substrate PG, during the activation phenomenon and chose the β domain as the first 'target' for this investigation.

Accordingly, in the present study, we have identified a structural motif that is functionally an important component of the macromolecular substrate-specific exosite operative in the SK.HPN complex and interacts with substrate HPG via its kringle/s domains. This represents a very stimulating insight into the mechanism of operation of the SK.HPN activator complex since the substrate kringles are structurally far removed from the target of the enzyme complex, that is, they are distinct from the scissile peptide bond in the macromolecular substrate.

3.2 MATERIALS AND METHODS

3.2.1 Reagents

Glu-plasminogen was either purchased from Roche Diagnostics GmbH (Penzberg, Germany) or purified from human plasma by affinity chromatography (Deutsch and Mertz, 1970). Both commercially obtained PG as well as plasma-purified PG had trace contamination of free HPN (less than 0.01 %) and Lys-PG (less than 2 %). The T7 RNA polymerase promoter-based expression vector, pET-23d and *Escherichia coli* strain BL21 (DE3) were products of Novagen Inc. (Madison, WI). Thermostable DNA polymerase (*Pfu*) was obtained from Stratagene (La Jolla, CA), and restriction endonucleases, T4 DNA ligase and other DNA modifying enzymes were acquired from New England Biolabs (Beverly, MA). Oligonucleotide primers were supplied by Integrated DNA Technologies Inc. (Indianapolis, IN). Purifications of DNA and extraction of PCR amplified products from agarose gels were performed using kits available from Qiagen GmbH (Germany). Automated DNA sequencing using fluorescent dyes was done on Applied Biosystems DNA sequencing system Model 310. The N-terminal amino acid sequencing was done with Applied Biosystems sequencer, Model 476A. Plasmin was prepared by digesting Glu-HPG with UK covalently immobilized on agarose beads (Stults *et al.*, 1989) using a ratio of 300 Plough units/mg HPG in 50 mM Tris.Cl, pH 8.0, 25 % glycerol and 25 mM L-Lysine at 22 °C for 10 h (Chaudhary *et al.*, 1999). Urokinase, EACA, sodium cyanoborohydride and L-Lysine were purchased from Sigma Chemical Co., St. Louis, USA. Phenyl Agarose 6XL and DEAE Sepharose (Fast Flow) were procured from Pharmacia Biotech, Uppsala, Sweden. All other reagents were of the highest analytical grade available.

3.2.2 General methods

In general, the standard methods and techniques routinely used in recombinant DNA technology work were employed in this investigation. These are readily available from several protocol manuals of molecular biology and gene-cloning, for example, Sambrook and coworkers (1989), Sambrook and Russell (2001), and are not elucidated here in any detail. In all cases, all the fundamental protocols, for example, DNA quantitation, restriction endonuclease (RE) digestions, PCR, DNA ligation, transformation and measurement of transformation efficiencies were first validated and optimized using standard systems.

3.2.3 Genetic constructs

3.2.3.1 Cloning of recombinant SK in pET-23d vector (pET-23d-SK)

The design and construction of the pET vector containing the SK gene (pET-23d-SK) has been described in Yadav (1999). It involved the cloning of the SK gene from *Streptococcus equisimilis* H46A in pBR 322 (Pratap *et al.*, 1996), followed by subcloning into pET-23d, an expression vector containing a highly efficient ribosome binding site from the phage T7 major capsid protein (Studier and Moffatt, 1986) and further modification of the 5' end of the gene to minimize the propensity for formation of secondary structure. It had an in-frame juxtaposition of an initiation codon for Met at the beginning of the open reading frame encoding SK so as to express the protein as Met-SK. The circular map of pET-23d-SK has been depicted in Figure 3.1.

3.2.3.2 Cloning of the isolated β domain of SK in pET-23d vector (pET-23d-β)

The construction of the cDNA encoding the β domain (sequence encompassing residues 144-293 of SK, based on limited proteolysis data reported in Parrado *et al.*, 1996) has been described earlier (Vasudha, 2002). Briefly, it involved the PCR amplification of the selected region of the gene encoding for SK, using specific upstream and downstream primers. The amplified product was digested with REs, Nco I and BamH I, and cloned into pET-23d vector at corresponding sites. This approach allowed the ligation of the cDNA in-frame with the initiation codon at the Nco I site. The sequence of the construct was confirmed by automated DNA sequencing.

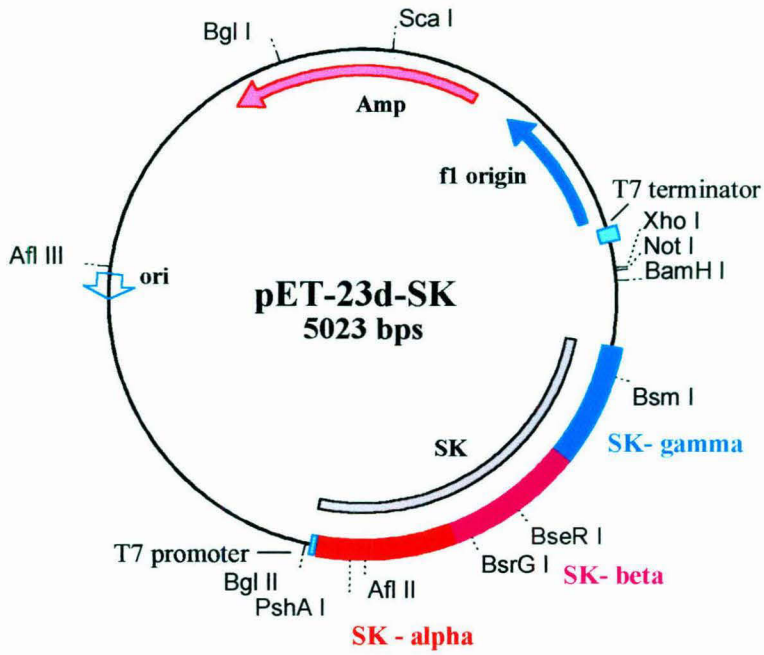

Figure 3.1 Circular map of pET-23d-SK. The circular map highlights a few selected, unique RE sites on the pET-23d vector, a T7-RNA polymerase promoter-based expression vector (Studier *et al.*, 1990) and the incorporated gene encoding for SK that was used for the construction and expression of mutants of full-length or truncated SK.

3.2.4 Site-directed mutagenesis using overlap-extension based polymerase chain reaction

The 250-loop deletion in the context of SK and β was carried out using the overlap-extension based polymerase chain reaction (Ho *et al.*, 1989). This approach involves the generation of DNA fragments that, by virtue of having incorporated complementary oligo primers in independent reactions, can be effectively 'fused' by combining them in a second primer extension reaction. The method is illustrated in Figure 3.2.

3.2.4.1 Design and construction of $SK_{del254-262}$ and $\beta_{del254-262}$

A set of mutagenic and either standard upstream or downstream primers corresponding to the ends of the gene, carrying unique restriction sites, were used in polymerase chain reactions to generate DNA fragments having overlapping ends. The sequences of the mutagenic and flanking primers used for the mutagenesis experiments are given in Table 3A. The diagnostic RE sites introduced in the primers by translational silent mutagenesis, used to screen clones have also been indicated in Table 3A.

The first two PCRs were carried out using *Pfu* thermostable DNA polymerase in a reaction volume of 100 µl containing 100 ng of template DNA, 1x polymerase buffer, 200 µM dNTPs and 20 pmol each of mutagenic and flanking primers. These were subjected to a 'hot start' (94°C, 5 min) followed by 30 cycles of denaturation (94°C, 45 sec), annealing (50°C, 1 min), extension (72°C, 1 min) and a final extension (72°C, 10 min). The PCR amplification products were purified from agarose gels, using the Qiagen gel extraction kit.

Thereafter, the purified PCR-generated DNA fragments from the initial set of reactions were mixed in equal molar ratios and subjected to overlap-extension PCR reactions (Ho *et al.*, 1989) using the two standard upstream and downstream flanking primers. The reaction conditions used for the fusion of the two PCR-generated fragments were identical to those used to generate the fragments. The resultant amplification products were digested with REs and ligated with pET-23d-SK (or pET-23d-β) digested with the same enzymes; and further transformed into chemical

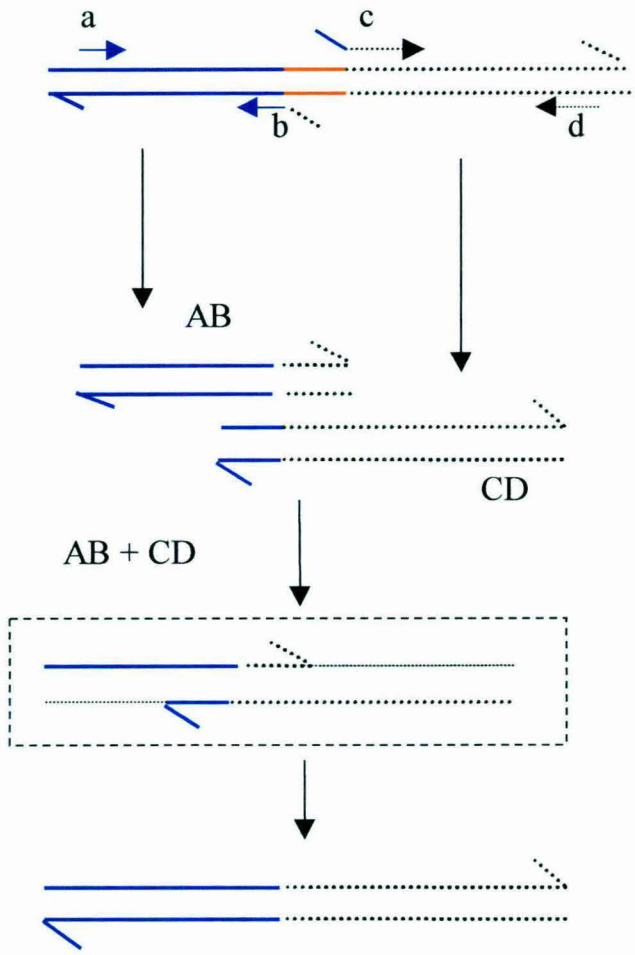

Figure 3.2 Schematic diagram showing how deletion mutation may be generated by the overlap extension method. The double stranded DNA and primers are indicated by lines with arrows indicating the 5′ to 3′ direction. The sequence to be deleted is depicted by the red lines. The blue and black lines indicate the template sequence on either side of the point of deletion. Primers 'b' and 'c' are designed such that their 3′ ends hybridize to template sequence on one side of the deletion, and the 5′ ends are complementary to template sequence on the other side of the deletion. Upstream primer, 'a' and downstream primer, 'd' flank the 5′ and 3′ ends of the gene respectively. The 'AB' and 'CD' products generated from the PCR reaction, using these primers are therefore overlapping across the deletion point. These denatured fragments then anneal at the overlap and are then extended 3′ to finally form the deletion product.

Table 3A Sequences of primers used for the construction of $SK_{del254-262}$ and $\beta_{del254-262}$[a]

Mutation	Sequence of primer	RE site[a]
mutagenic U* for the construction of $SK_{del254-262}$ *(soe2-us)*	5′AACAGGCTTATAGGGAAATAAAC-AACACTGACCTGATATCTGAGAAA 3′	EcoR V
mutagenic D for the construction of $SK_{del254-262}$ *(soe2-ds)*	5′ TGTTGTTTATTTCCCTATAAGCC-TGTTCCCGATTTTTAA 3′	
flanking U for the construction of $SK_{del254-262}$ *(krg 6)*	5′ ATTTATGAACGTGACTCCTCAA-TCGTC 3′	BseR I
flanking D for the construction of $SK_{del254-262}$ *(krg 7)*	5′ATAGGCTAAATGATAGCTAGCA-TTCTCTCC 3′	Bsm I
mutagenic U for the construction of $\beta_{del254-262}$ *(soe2-us)*	5′AACAGGCTTATAGGGAAATAAAC-AACACTGACCTGATATCTGAGAAA 3′	EcoR V
mutagenic D for the construction of $\beta_{del254-262}$ *(soe2-ds)*	5′TGTTGTTTATTTCCCTATAAGCCT-GTTCCCGATTTTTAA 3′	
flanking U for the construction of $\beta_{del254-262}$ *(216 dn)*	5′GTGGAATATACTGTACAGTTTACT-CC 3′	BsrG I
flanking D for the construction of $\beta_{del254-262}$ *(β-stop)*	5′ATCGGGATCCTATTTCAAGTGACT-GCGATCAAAGGG 3′	BamH I

[a] The diagnostic RE sites introduced in the primers by translational silent mutagenesis, used during the screening of clones have been underlined. The flanking primers also contained RE sites, unique in the SK or β cassette, to re-ligate the PCR cassette, containing the deletion mutation, with the expression vector.
*U represents upstream primer and D represents downstream primer.

competent cells of *Escherichia coli* XL1-Blue strain. The positive clones were selected by screening plasmid DNAs of clones for their respective diagnostic sites.

3.2.5 Purification of SK/$SK_{del254-262}$ from *Escherichi coli* BL21 (DE3) strain.

In order to purify SK/$SK_{del254-262}$, the seed culture (pre-inoculum) was developed by inoculating 10 ml of LB-Amp culture medium with pET-23d-SK/pET-23d-$SK_{del254-262}$ culture from a single colony on LB-Amp plate streaked with pET-23d-SK/pET-23d-$SK_{del254-262}$ that was retrieved from -70°C glycerol stock, and further incubating for 10 h at 37°C under shaking conditions (200 rpm).

This pre-inoculum was used to seed 500 ml of LB-Amp medium at 2 % v/v and allowed to grow at 37°C at 200 rpm to an $O.D_{600\ nm}$ of 0.5 - 0.6. At this stage, it was induced with IPTG (final concentration of 1 mM) and further grown for 12 h at 37°C. Cells were then harvested from the broth culture by centrifugation at 6000 xg for 10 min. The pellet was then washed twice with ice-cold STE buffer (final concentrations-100 mM NaCl, 10 mM Tris.Cl, pH 8.0,1 mM EDTA). The harvested cells were lyzed using Bug-buster® (5 ml reagent per gram wet weight of the cell pellet), a non-ionic detergent based commercial reagent for rapid bacterial cell lysis, procured from Novagen (Madison, WI), along with 'Benzonase' (a genetically engineered endonuclease that degrades different forms of DNA and RNA) at a ratio of 1 µl per ml of Bug-buster® for 30 min at room temperature under shaking conditions. Alternatively, the pellet was thoroughly suspended in ice-cold STE buffer and this was then subjected to sonication (Heat System, New York) at 4°C, under conditions of 30 sec sonic-pulses interspersed with equal periods of rest.

The cell lysate was centrifuged at 12,000 xg for 15 min at 4°C and the resultant supernatant was then subjected to ammonium sulphate precipitation, till a final concentration of 60 % was achieved. The precipitated protein was then separated by centrifugation and the pellet was then resuspended in 20 mM Tris.Cl buffer (pH 7.5). After centrifugation, the supernatant was subjected to chromatography on a Poros-D anion exchange column, fitted onto a Bio-Cad Sprint liquid chromatographic workstation (Perseptive Biosystems Inc., Framingham, MA). The bound SK/$SK_{del254-262}$ was eluted in fractions using a linear gradient of NaCl (0 to 0.5 M) in 20 mM Tris.Cl buffer (pH 7.5) and the amount of protein in each fraction was measured using

Bradford's method of protein estimation (1976). The eluted proteins were more than 95 % pure, as analyzed by SDS-PAGE.

3.2.6 N-terminal amino acid sequencing of SK

The purified recombinant SK/$SK_{del254-262}$ expressed in *Escherichia coli* was subjected to N-terminal amino acid sequencing in order to compare its sequence with that of natural SK from *Streptococcus equisimilis* H46A. The N-terminal amino acid sequence of SK was found to be identical with that of natural SK, except for the presence of an extra Met residue at the N-terminus (the sequencing was carried out for 25 cycles (using ABI, model 476A Protein Sequencer).

3.2.7 Expression and purification of $\beta/\beta_{del254-262}$

The $\beta/\beta_{del254-262}$ protein was expressed intracellularly in *Escherichia coli* BL21 (DE3) cells as inclusion bodies (IBs). The culture was raised, harvested and cells lysed using a procedure as described above. The pellet obtained after sonication was taken up in 8 M urea and placed under gentle shaking conditions for 30 min to effect dissolution. After a high-speed centrifugation step, the protein in the supernatant was refolded by 20-fold dilution with 20 mM Tris.Cl buffer, pH 7.5. Then it was then purified to more than 95 % homogeneity by chromatography (as analyzed by SDS-PAGE) on DEAE Sepharose (Fast Flow) (Pharmacia Biotech, Uppsala, Sweden) at 4°C, using a linear NaCl gradient (0-0.25 M NaCl in 20 mM Tris.Cl buffer, pH 7.5).

3.2.8 Preparation of human microplasminogen (μPG)

Microplasminogen (μPG), the catalytic domain of HPG (residues Lys530-Asn790) devoid of all kringles was prepared by cleavage of HPG by HPN under alkaline conditions (0.1 N glycine/ NaOH buffer, pH 10.5, 10:1 ratio of HPG and HPN) at 30°C for 24 h. It was purified from the reaction mixture by passing through a Lys-Sepharose column (Amersham Biosciences), followed by a Soybean-trypsin inhibitor-Sepharose 4B column to absorb HPN and μPN, as reported (Shi and Wu, 1988). The flow-through was then subjected to molecular sieve chromatography, after concentration by ultrafiltration, on a column (16 mm x 60 cm) of Superdex-75™ (Pharmacia Biotech). The purity of μPG formed was analyzed by SDS-PAGE which showed a single band moving at the position expected from its molecular size (Shi and

Wu, 1988). Digestion with UK, which is known to be a good activator of μPG irrespective of the presence of kringle domains (Shi and Wu, 1988), was used to establish that the activation of this preparation, when used as substrate, was comparable to that obtained when using SK.HPN as the activator species; thereby ensuring that the preparation of μPG was suitable for use in kinetic and binding assays.

3.2.9 Preparation of kringles 1-5 (K1-5)

The proteolytic fragment containing all of the HPG kringle domains was prepared by incubating HPG with urokinase-free HPN (5:1 ratio of HPG to HPN) un

under alkaline conditions (0.1 N glycine/ NaOH, pH 9.0) for 72 h at 25°C. Under these conditions, the proteolytic conversion of native HPG to K1-5 was found to be quantitative, with minimal residual HPG. HPN was removed from the reaction mixture by passing through a Soy bean-trypsin inhibitor-Sepharose column (1.6 mm x 3.6 cm). This was followed by gel filtration on Superdex-75, to obtain K1-5 free of HPG and μPG. The purity of this preparation was confirmed by SDS-PAGE analysis (Wu *et al.*, 1990).

3.2.10 One-stage HPG activation assay

The ability of SK/$SK_{del254-262}$ to activate HPG was examined using one-stage activation assays (Wohl *et al.*, 1980; Shi *et al.*, 1994). Native SK/$SK_{del254-262}$ (0.5-50 nM) was added to a 100 μl quartz assay cuvette containing HPG (2 μM) in assay buffer (50 mM Tris.Cl buffer, pH 7.5) containing 0.5 mM chromogenic substrate (Roche Diagnostics GmbH, Germany). The generation of activator activity was monitored at 22°C by measuring the change in absorbance at 405 nm as a function of time in a Shimadzu UV-160 model spectrophotometer. The activator activities were obtained from the slopes of the progress curves, which were plotted as change in absorbance/time against time (Wohl *et al.*, 1980).

3.2.11 Amidolytic activation of equimolar HPG.SK/$SK_{del254-262}$ complexes

An equimolar complex of HPG (5 μM) and SK/$SK_{del254-262}$ (5.5 μM) was made in 50 mM Tris.Cl, pH 7.5 containing 0.5 % BSA. Aliquots (50 nM) were

withdrawn from equimolar HPG.SK/$SK_{del254-262}$ complexes at regular periods and transferred to a 100 µl quartz cuvette containing 2 mM Chromozym® PL (Tosyl-glycyl-prolyl-lysine-4-nitranilide-acetate) and 50 mM Tris.Cl, pH 7.5 at 22°C. The change in absorbance at 405 nm was monitored to compute the kinetics of amidolytic activation (Nihalani *et al.*, 1998; Wohl *et al.*, 1980) by plotting slopes of the activation curves as a function of pre-incubation times.

3.2.12 Esterolytic activation of equimolar HPG.SK/$SK_{del254-262}$ complexes

Five µM HPG was added to an assay cuvette containing 5.5 µM SK/$SK_{del254-262}$, 100 µM NPGB and 10 mM sodium phosphate buffer, pH 7.5 and the 'burst' of p-nitrophenol release due to acylation of active center was monitored at 410 nm as a function of time at 22°C (McClintock and Bell, 1971; Chase and Shaw, 1969).

3.2.13 Determination of kinetic constants for HPG activator activity

Varying amounts of HPG (0.1 to 10 µM) were added to the assay cuvette containing fixed amounts of SK/$SK_{del254-262}$ (0.5 to 50 nM) and chromogenic substrate (0.5 mM) and the change in absorbance was monitored at 405 nm as a function of time at 22°C. Also, the kinetics of HPG activation by HPN.SK/$SK_{del254-262}$ complexes was measured by transferring suitable aliquots of preformed HPN.SK/$SK_{del254-262}$ complexes to the assay cuvette containing different concentrations of substrate HPG (Wohl *et al.*, 1980). The kinetic parameters for HPG activation were then calculated from inverse Lineweaver-Burke plots (Wohl *et al.*, 1980). To compute the k_{cat}, the number of HPN active sites was determined using the NPGB reaction (McClintock and Bell, 1971; Chase and Shaw, 1969; Wohl *et al.*, 1977).

To study the effect of EACA on substrate HPG activation, catalytic amounts of the pre-formed equimolar activator complexes between HPN and either SK or $SK_{del254-262}$ were added to obtain final concentrations of 0.25 nM and 3 nM, respectively in presence of varying concentrations of EACA (0-1 mM), along with substrate HPG and chromogenic substrate in 50 mM Tris.Cl buffer (pH 7.5) and the reaction was monitored at 405 nm at 22°C.

3.2.14 Determination of the steady-state kinetic constants for amidolytic activity of SK/SK $_{del254-262}$

SK/SK$_{del254-262}$ and HPN were pre-complexed at 4°C in equimolar ratios (100 nM each) for 1 min in 50 mM Tris.Cl, pH 7.5, containing 0.5 % BSA and an aliquot of the reaction mixture was transferred to a 100-µL assay cuvette containing 50 mM Tris.Cl buffer, pH 7.5, and varying concentrations of the chromogenic substrate (0.1-2 mM) to obtain a final concentration of 10 nM of the complex in the reaction. The reaction was monitored spectrophotometrically at 405 nm for 5 min at 22°C. The kinetic constants were calculated by standard methods (Chase and Shaw, 1969).

3.2.15 Kinetic analysis of protein-protein interactions using Resonant Mirror technology

a) Binary interaction analysis - Association and dissociation between HPG and the SK/SK$_{del254-262}$, called hereafter as binary interaction, were followed in real time by Resonant Mirror based detection using the IAsys Plus™ system (Cambridge, UK) (Cush *et al.*, 1993, Buckle *et al.*, 1993). In these experiments, streptavidin was captured on biotin cuvette according to the manufacturer's protocols (IAsys protocol 1.1). This was followed by the attachment of (mildly) biotinylated HPG to the streptavidin captured on the cuvette. Non-specifically bound HPG was then removed by repeated washing with PBS followed by three washes with 10 mM HCl. The net response chosen for the immobilized biotinylated HPG onto the cuvette was 700-800 arc sec in all experiments. Experiments were performed at 25°C in 10 mM PBS, pH 7.4 containing 0.05 % Tween 20 and 50 µM NPGB (binding buffer). The latter was included in order to prevent HPN-mediated proteolysis (Conejero-Lara *et al.*, 1998).

After equilibrating the cuvette with binding buffer, varying concentrations of either SK or SK$_{del254-262}$ were added and each binding response was monitored during the 'association' phase. Subsequently, the cuvette was washed with binding buffer and the 'dissociation' phase was recorded (Myszka, 1997). Following each cycle of analysis, the cuvette was regenerated by washing with 10 mM HCl, and baseline was re-established with binding buffer. In parallel, in the control cell of the dual channel cuvette, immobilized streptavidin alone was taken as a negative control for the binding studies. In experiments where EACA was used to examine its effect on SK.HPG interaction, the binary complex was formed between ligate SK/SK$_{del254-262}$

and immobilized HPG, in binding buffer (as described above). The dissociation of the binary complexes was done by washing the cuvette with EACA, instead of buffer alone.

The data were analyzed after substraction of the corresponding non-specific refractive index component(s), and the kinetic constants were calculated from the sensorgrams by non-linear fittings of association and dissociation curves using the software FASTfit^{TM}, supplied by the manufacturer. The dissociation rate constant (k_d) was calculated from the average of four dissociation curves obtained at saturating concentration of ligate. The equilibrium dissociation constant (K_D) was then calculated from the extent of association of monophasic curve. The k_a was calculated from the equation k_d/K_D. Values of K_D obtained using this relationship were in good approximation to those obtained by k_d/k_a obtained from the linear fit of k_{on} *versus* ligate concentration (Morton *et al.*, 1995).

b) Ternary interaction analysis - Resonant Mirror technology based biosensor was also used to measure the rate and equilibrium dissociation constants describing interactions between soluble ligate (HPG, μPG or K1-5) and SK/SK$_{del254-262}$ complexed with immobilized HPG, a situation simulating substrate binding to binary complex and hereafter called as ternary interaction. In binary interaction studies, it was evident that when soluble SK/SK$_{del254-262}$ was added to immobilized HPG, a rapid and avid SK.HPG binary complex formation occurs. The dissociation of this complex is very slow due to the high stability of the SK.HPG complex, as has been observed by others also (Conejero-Lara *et al.*, 1998). After allowing the complex to dissociate maximally (~20 min), the dissociation baseline becomes stable which remains unaffected even after washing with 2.5 mM EACA. It has been reported that when SK was pre-incubated with immobilized HPG, EACA was more than 100-fold less potent at dissociating the binary complex than it was at preventing binary complex formation when SK and EACA were added synchronously to immobilized HPG (Lin *et al.*, 2000). Thus this comparative resistance to dissociation of the SK.HPG binary complex by EACA permitted us to study ternary substrate interaction, under conditions that did not adversely affect the stability of the binary interaction. In contrast, EACA was found to be strongly inhibitory to ternary complex formation (given below).

In a typical ternary interaction experiment, a stable binary complex was formed by adding saturating amount of SK/$SK_{del254-262}$ onto HPG, immobilized on streptavidin captured on biotin cuvette. After maximally dissociating the binary complex with binding buffer and washing with 2.5 mM EACA, a stable dissociation baseline was obtained. Varying concentrations of either 'ternary' HPG (0.1 – 1.0 μM) or μPG (1-6 μM) or K1-5 (1-6 μM) were then added to monitor the binding by recording the association phase. Subsequently, the cuvette was washed with binding buffer three times and the dissociation phase was recorded. After each cycle of analysis, the original baseline was re-established by stripping off the undissociated 'ternary' ligate with 2.5 mM EACA followed by three washes with binding buffer. It was established that EACA, at this concentration, completely abolishes the interaction of ternary HPG with the binary complex, while the binary complex remains stable. The latter attribute was considered to be a necessary precondition to obtain reliable and reproducible values of the kinetic constants for ternary complex formation and dissociation. In order to test whether this was indeed so, control experiments were carried out in which the ternary complex formation and dissociation experiments were done at various time intervals after a stable baseline was attained subsequent to binary complex formation followed by buffer and EACA washes, as described above. It was observed that the rate constants so obtained did not differ significantly (within a margin of ± 5 %) as a function of time. In experiments where μPG was used as soluble ternary ligate, 1 mM EACA was found to be sufficient to strip off the undissociated μPG, while washing with binding buffer alone resulted in incomplete regeneration of baseline. Association and dissociation phases at varying ligate (HPG, μPG and K1-5) concentrations were fitted as described above and the equilibrium dissociation constant/s were calculated.

The effect of EACA on the binding of soluble 'ternary' HPG to SK/$SK_{del254-262}$ complexed with immobilized HPG was assessed by measuring the binding extents, measured in arc second units, at equilibrium at a fixed concentration of substrate HPG (0.4 μM) in the presence of varying EACA concentrations (0-2 mM). For the analysis of these data, binding extent in buffer alone was taken as 100 % and varying extents of formation of ternary complexes at equilibrium were plotted as a function of EACA concentration to obtain EACA-dependant binding isotherms for SK and $SK_{del254-262}$.

As controls, the effect of EACA was similarly examined for dissociation of preformed complexes between HPG and either SK or $SK_{del254-262}$ in the absence of substrate HPG.

3.2.16 Circular dichroic analysis of SK/$SK_{del254-262}$

Far-UV CD spectra of proteins (concentration 0.15 mg/ml in PBS, pH 7.2) were recorded on a Jasco-720 spectropolarimeter to assess the secondary structures of SK, $SK_{del254-262}$, β and $\beta_{del254-262}$. Measurements were carried out from 200 to 250 nm in a 0.1 cm path length cell and the appropriate buffer baseline was subtracted from the protein spectra. The final spectrum analyzed was an average of 10 scans (Radek and Castellino, 1989). The percentages of various secondary structural features (α-helix, β-sheet, β-turn and unstructured region) were then calculated using a reference algorithm provided by the manufacturers (Yang *et al.*, 1986).

3.2.17 Modeling studies

Cartesian coordinates of the kringle 5 domain of HPG (used as a prototypical representative structure of HPG kringle domains) and those of SK β domain, and SK.μPN complex were retrieved from the Protein Data Bank (codes - 5HPG, 1C4P and 1BML, respectively). The β domain in SK.μPN complex reveals several disordered loops, including the 250-loop (Wang *et al.*, 1998). The coordinates in this complex were hence replaced with those of the isolated β domain (Wang *et al.*, 1999b). The isolated β domain was superimposed on the β domain of the complex, and the corresponding set of coordinates was simply replaced. The isolated β domain has the 250-loop clearly defined, and hence it is more suitable for docking analysis.

Molecular surface for a typical HPG kringle domain was generated using the kringle 5 co-ordinates (taken as a prototype) with the aid of GRASP (Nicholls *et al.*, 1991) with standard atomic radii, and the probe radius of 1.4 Å. Electrostatic potential was then mapped onto the molecular surface. There were two distinct regions of negative charges on the surface. The negatively charged surface of kringles was likely to interact with the positively charged loop of the SK structure, and therefore these regions were of particular interest in generating the SK β.μPN.kringle docked complex. One of the negatively charged regions was at the interface of the dimeric

kringle structure. This region was therefore not considered appropriate for docking. The other negatively charged region was then manually brought into close proximity of the '250 loop' of SK β domain.

3.3 RESULTS

3.3.1 Construction, purification and functional characterization of SK/$SK_{del254-262}$ and β/$β_{del254-262}$

An examination of the crystal structure of the free β domain (Wang *et al.*, 1999b) and its comparison with the other two SK domains possessing closely similar (but not identical) structures revealed the presence of a distinct flexible loop in the β domain (the 250-loop) that protrudes into the solvent (Figure 3.3). In order to investigate the functional role of the 250-loop (comprising of residues, Ile254-Asn255 -Lys256-Lys257-Ser258-Gly259-Leu260-Asn261-Glu262) *viz.* its involvement in the modulation of substrate specificity of HPN by SK, a deletion mutant (termed $SK_{del254-262}$) was constructed employing the overlap-extension based PCR method (Ho *et al.*, 1989). The desired deletion mutation was confirmed by sequencing of both strands of the cloned DNA. This was followed by sub-cloning of the PCR amplification product in pET-23d, a T7 RNA polymerase promoter-based expression vector (Studier *et al.*, 1990). With the nine-residue deletion, we expected that a minimal perturbation of the underlying β sheet would occur (Figure 3.3), since the two residues flanking the loop (Tyr252 and Glu263) had a distance of 4 Å between the C^{α} atoms (Wang *et al.*, 1999b).

The *Escherichia. coli* BL21 (DE3) cells carrying the plasmid were grown in shake-flasks to mid log phase and the expression of the protein of interest was then induced by addition of IPTG. $SK_{del254-262}$ was subsequently purified using a rapid purification protocol (details given in Materials and Methods). The protein so obtained was generally more than 95 % pure, as analyzed by SDS-PAGE (Figure 3.4).

To observe the effect of deletion in the β domain alone, we carried out the deletion at the same site in a truncated gene encoding for the isolated β domain. The cDNAs encoding for the β domain alone and $β_{del254-262}$ were then expressed in

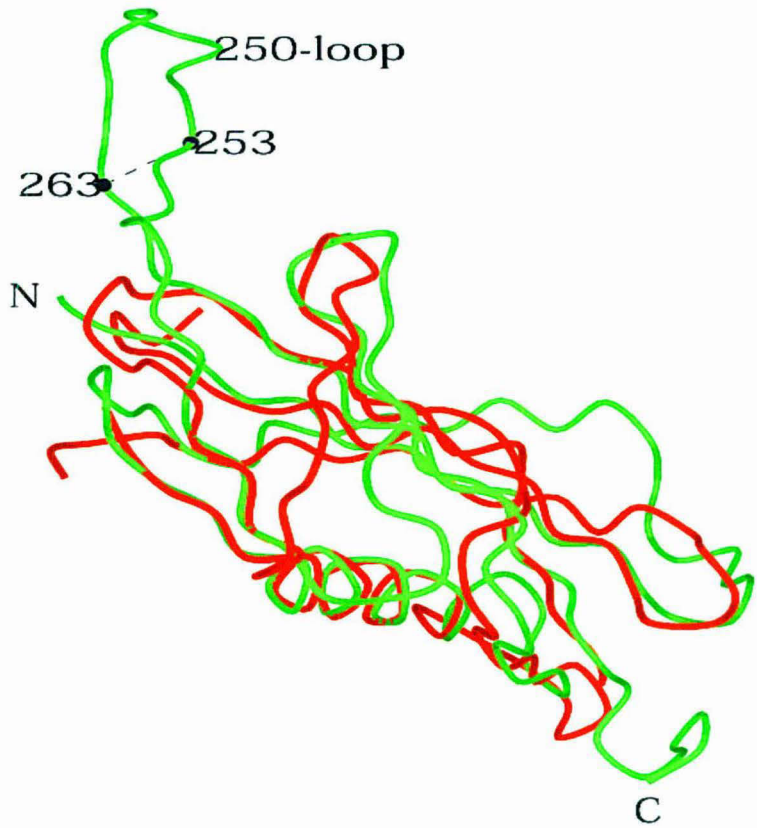

Figure 3.3 Superposition of α and β domains of SK. The α domain of SK is shown in red and the β domain is shown in green. The 250-loop is a distinct feature of the β domain, while the rest of the structure between the two domains overlaps extensively. The residues 253 and 263, where the loop was truncated, are indicated. The superposition with the γ domain of SK showed similar results (not shown).

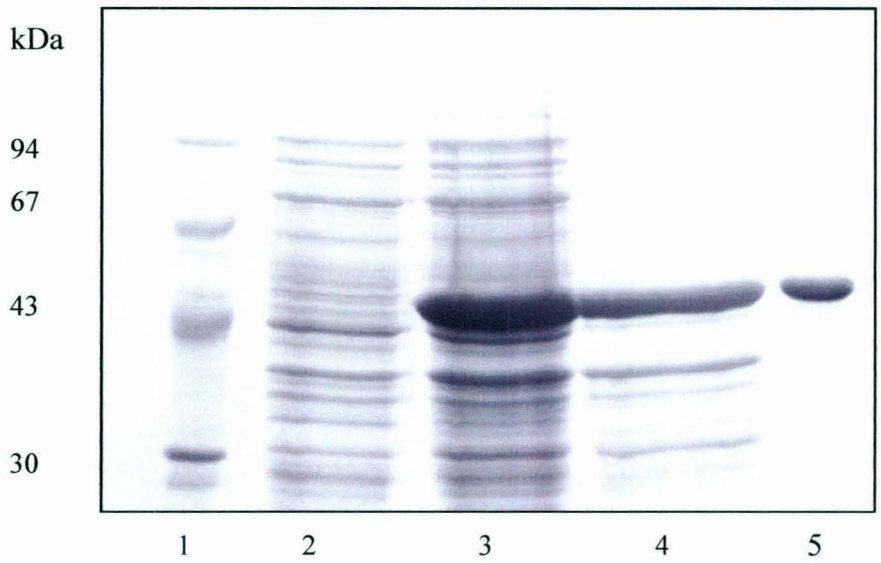

Figure 3.4 Purification of SK expressed in *Escherichia coli.* Streptokinase was over-expressed in *E. coli* cells as soluble protein. The induced cells were lyzed and the proteins in the supernatants were precipitated with ammonium sulphate and then subjected to rapid ion-exchange chromatography on Poros-D matrix, as described under Materials and Methods. The samples, drawn at various stages of purification, were analyzed by SDS-PAGE on 10 % acrylamide gel. Lanes represent: 1- standard MW markers, 2- whole cell lysate of uninduced cells, 3- whole cell lysate of induced cells, 4- pellet obtained after precipitation with 60 % ammonium sulphate, 5- ion-exchange purified SK.

Escherichia coli and purified to more than 95 % (Figure 3.5) as explained under Materials and Methods.

When purified $SK_{del254-262}$ was examined for its ability to activate substrate HPG (2 μM) using the one-stage activation assay (described under Materials and Methods), it showed a specific activity that was only about 20 % that of SK, similarly expressed and purified using the same expression plasmid and host system. On the other hand, β domain alone and $\beta_{del254-262}$ however, showed only traces of activator activity with substrate HPG (less than 0.0005 % activity, compared to that of full-length SK).

3.3.2 Physico-chemical characterization of SK/$SK_{del254-262}$

3.3.2.1 N-terminal amino acid sequencing analysis

When purified SK and the mutant ($SK_{del254-262}$) prepared similarly from *Escherichia coli*, employing the same expression vector, were subjected to N-terminal amino acid sequencing, both the proteins were found to have their N-terminal Met removed at a 50 % level.

3.3.2.2 Circular dichroism studies

In order to assess whether the deletion of the 250-loop resulted in changes in the overall folding characteristics of SK, the secondary structure/s of SK/$SK_{del254-262}$ were monitored using CD. The far-UV CD spectra of SK and the mutant ($SK_{del254-262}$), however, did not show any significant discernable differences (Figure 3.6).

However, since a native-like CD spectrum of the mutant could still result if relatively small, local conformational changes occurred in and around the site of the deletion in the β domain that might get 'averaged out' in the presence of the CD contributions from rest of the two domains of SK in the full-length molecule, the far-UV CD spectra of β domain alone and $\beta_{del254-262}$ were recorded. Interestingly, no noticeable changes were observed in the secondary structure of $\beta_{del254-262}$ with respect to β similarly expressed in *Escherichia coli* also (Figure 3.6), indicating that neither the overall secondary structure of SK nor that of the β domain alone had been perturbed by the deletion of the nine-residue loop.

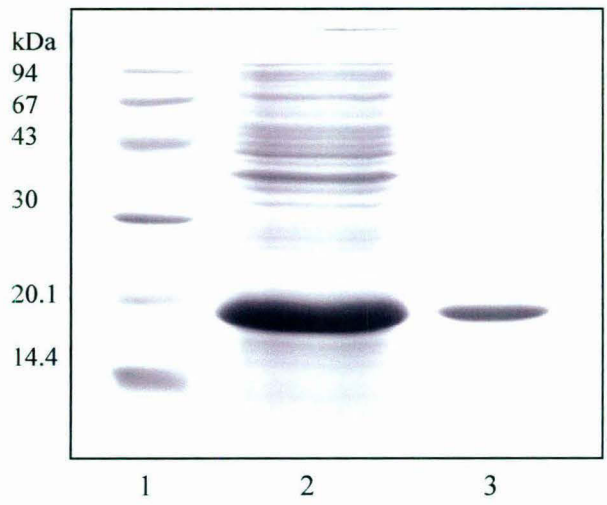

Figure 3.5 Purification of the β domain of SK from *Escherichia coli.* The β domain was intracellularly over-expressed and purified from the lysate of *E. coli* cells. The β domain was purified by chromatography on DEAE-Sepharose. The lanes of the 15 % SDS-PAGE represent: 1- standard MW markers, 2- whole cell lysate of induced cells, 3- purified β domain.

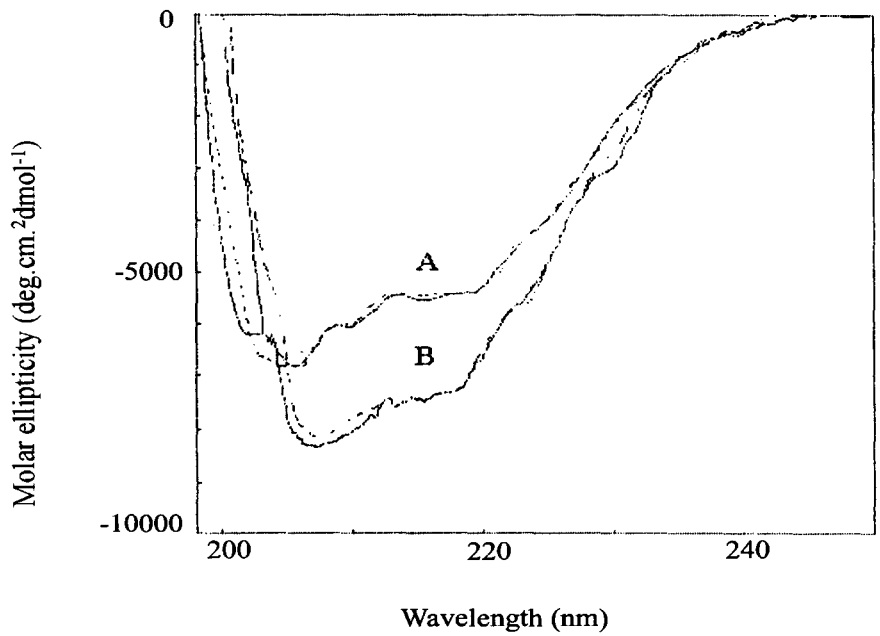

Figure 3.6 Far UV-CD spectra of SK/SK$_{del\ 254\text{-}262}$ and β/β $_{del\ 254\text{-}262}$. Far UV-CD spectra of proteins (concentration 0.15 mg/ml in PBS, pH 7.2) were recorded on a Jasco-720 spectropolarimeter to assess the secondary structures of (curves marked A) SK (solid line), SK$_{del254\text{-}262}$ (dotted line); (curves marked B) β (solid line) and β$_{del254\text{-}262}$ (dotted line). Measurements were carried out from 200 to 250 nm in a 0.1 cm path length cell and the appropriate buffer baseline was subtracted from the protein spectra. The final spectrum analyzed was an average of 10 scans.

3.3.2.3 Binding interactions between SK/$SK_{del254-262}$, and HPG

In order to explore whether the loss in HPG activator activity was a result of alteration in the affinity of the mutant with partner HPG, the kinetics of interaction between immobilized HPG and SK were compared with that of $SK_{del254-262}$ by the Resonant Mirror approach using a semi-automated instrument for measuring protein-protein interactions in real time (IAsys, Cambridge UK). Preliminary experiments were performed by immobilizing SK or $SK_{del254-262}$ onto carboxy-methyl dextran cuvettes, using an amino-coupling protocol recommended by the manufacturers, to examine the effect of immobilization chemistry on the values of kinetic constants. The kinetics of association and dissociation of HPG with immobilized SK/$SK_{del254-262}$ were then measured as described in Materials and Methods. In another approach, biotinylated HPG was immobilized on streptavidin captured on biotin cuvette and the binding kinetics with SK were studied as described. For these assays, SK/$SK_{del254-262}$ was added at concentrations ranging between 5-80 nM. Relatively fast association kinetics was observed for the binding of both proteins, which is consistent with a monophasic pattern of association (Figure 3.7). When the association data for the interaction were fitted to a single exponential curve, a linear relationship was observed between k_{on} and added ligate concentration, according to the equation $k_{on} = k_d + k_a$ [ligate] (see Figure 3.7, inset). The results show that the mutant exhibited an affinity that was not significantly different from that of SK (Table 3B).

Interestingly, experiments performed by immobilizing SK/$SK_{del254-262}$ on carboxy-methyl dextran cuvettes using standard amino-coupling procedures, as shown by other groups also (Conejero-Lara *et al.*, 1998; Loy *et al.*, 2001) yielded similar binding constants for SK and $SK_{del254-262}$, indicating that the coupling procedure *per se* does not interfere in the binding interaction between SK and HPG significantly.

3.3.2.4 Active site exposure in HPG by SK/$SK_{del254-262}$

To further explore the underlying reason for partial loss of activator activity of the loop-deletion mutant, we examined if, like the native protein, it could expose the active site in 'partner' HPG. For this purpose, we employed the active site acylating agent, NPGB, to test whether the characteristic 'burst' that occurs upon mixing equimolar SK and HPG (McClintock and Bell, 1971; Chase and Shaw, 1969)

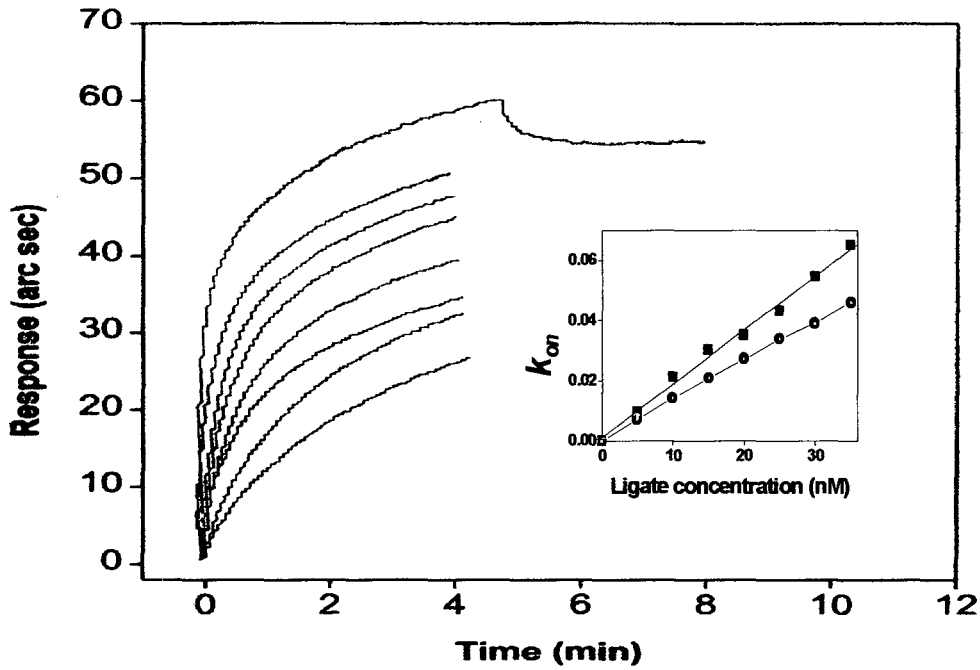

Figure 3.7 Diagrammatic representation of optical biosensor determination of binding constants for the interaction of SK/SK$_{del254-262}$ with immobilized HPG. Overlay plots representing the binding and dissociation of SK to the immobilized HPG are depicted. Human PG was biotinylated and immobilized on streptavidin surfaces of IAsys planar cuvettes, as described under Materials and Methods. For each individual concentration of ligate (only data for SK is shown), the association or binding to immobilized HPG was monitored. Subsequently, the cuvette was washed with binding buffer and the dissociation phase was monitored. For the sake of clarity, only dissociation at saturating ligate concentration is shown. The value of k_{on} for the binding curves for each ligate concentration was determined using FASTfit^{TM} program, supplied by IAsys Ltd., U.K. and each value was plotted against the corresponding concentration of the ligate. **Inset:** The plot of k_{on} against ligate concentration for SK (squares) or SK$_{del254-262}$ (circles), which gives a straight line. The kinetic constants were calculated as described under Materials and Methods.

Table 3B Association and dissociation rate constants and apparent equilibrium dissociation constants for the binding of immobilized HPG to the derivatives of SK [a]

Ligate	k_a (x 10^6) ($M^{-1} s^{-1}$)	k_d (x 10^{-3}) (s^{-1})	K_D (x 10^{-9}) (M)
SK	1.98 ± 0.08	1.81 ± 0.21	0.91 ± 0.34
$SK_{del254-262}$	1.43 ± 0.07	2.27 ± 0.15	1.58 ± 0.79

[a] Biotinylated HPG was immobilized on streptavidin captured onto biotin cuvette. Different concentrations of the SK/$SK_{del254-262}$ were then titrated, as described under Materials and Methods. The pseudo-first order rate constant (k_{on}) was determined using the FASTfit™ program. The dissociation rate constant (k_d) value was calculated from the average of four dissociation curves obtained at saturating concentration of ligate. The equilibrium dissociation constant (K_D) was than calculated from the extent of association of monophasic curve. The k_a was calculated from the equation k_d/K_D. Values of K_D obtained using this relationship were in good approximation to those obtained by k_d/k_a obtained from the linear fit of k_{on} versus ligate concentration.

was also observed with the mutant. Neither SK nor HPG alone give the burst, but only once the two are mixed in equimolar proportions is this burst, characteristically associated with a rapid NPGB hydrolysis, observed due to the formation of a 'virgin' SK.HPG complex and consequent acylation at the cryptic active site of HPG with NPGB (McClintock and Bell, 1971). When the recombinant SK (used as a control) was tested with this reagent in the presence of equimolar HPG, the characteristic colorimetrically detectable burst was indeed observed. A similar response was evident in the case of $SK_{del254-262}$ as well (Figure 3.8, inset).

The mutant ($SK_{del254-262}$) was then further verified for its ability to activate partner HPG by carrying out amidolytic assays of its equimolar mixtures with HPG. In this case too, it exhibited a similar, though slightly delayed time-course of generation of amidolytic activity with respect to SK (Figure 3.8) suggesting that it could open the active site in partner HPG. Thus, these results demonstrated that the observed lower HPG activator activity of $SK_{del254-262}$ was not due to any major effect on its ability to activate partner HPG at the binary complex formation stage.

3.3.2.5 Steady-state kinetics of HPG activation and amidolysis by SK/$SK_{del254-262}$

In order to obtain a glimpse of the functional characteristics of the active site, the kinetic constants associated with the substrate binding and processing of both macromolecular substrate, HPG and the small molecular weight (MW) amidolytic, peptide substrate, tosyl-glycyl-prolyl-lysine-4-nitranilide acetate were measured by the equimolar complexes of HPN with either SK or $SK_{del254-262}$. Remarkably, the results for the steady-state kinetic analysis of the activation of substrate HPG by the equimolar $SK_{del254-262}$.HPN complex revealed a 5-6 fold increase in the K_M for HPG when compared to that of SK.HPN, with relatively little alteration in the k_{cat} values (Table 3C). This clearly indicated that the loop-deleted mutant formed an activator complex with HPN that had an apparent decreased affinity for the macromolecular substrate as compared to that of the native SK.

On the other hand, the k_{cat} values exhibited either by SK.HPN or $SK_{del254-262}$.HPN for the small MW peptide substrate were essentially unaltered as compared to that of 'free' HPN (suggesting that the primary covalent specificity characteristics of the active site in HPN remained unchanged), but, revealingly, the K_M for this substrate was decreased as compared to that of SK.HPN.

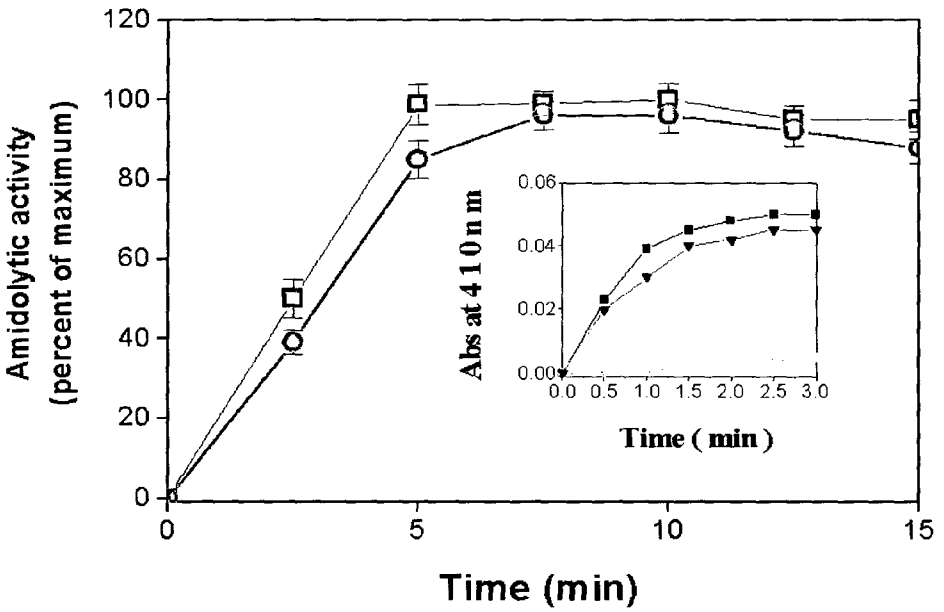

Figure 3.8 Time-course of the generation of amidolytic activity of SK and $SK_{del254-262}$. Equimolar SK.HPG and $SK_{del254-262}$.HPG complexes were made and aliquots were withdrawn at regular periods and transferred into a micro-cuvette containing 2 mM chromogenic substrate. The generation of amidolytic activity was monitored at 405 nm at 22°C, as described under Materials and Methods. The % of maximum amidolytic activity as a function of pre-incubation time by SK.HPG complex (blue squares) and $SK_{del254-262}$.HPG complex (magenta circles) are plotted. **Inset:** Active site titration of HPG on complexing with SK or $SK_{del254-262}$ using the active site acylating agent, NPGB. The figure shows progress curves of NPGB hydrolysis by SK.HPG (black squares), $SK_{del254-262}$.HPG (red, inverted triangles) and control reaction (grey circles).

Table 3C Steady-state kinetic parameters for HPG activation by equimolar complexes of HPN and SK/$SK_{del254-262}$ [a]

Activator protein	K_M (μM)	k_{cat} (min^{-1})	k_{cat}/K_M (min^{-1}/μM)
SK.HPN	0.5 ± 0.05	11 ± 0.5	22.0
$SK_{del254-262}$.HPN	2.5 ± 0.3	9.7 ± 0.52	3.9

[a] Fixed, catalytic amounts of the respective pre-formed activator complexes of each protein with HPN were added to the cuvette containing HPG as the substrate and Chromozym® PL in 50 mM Tris.Cl buffer, pH 7.5, and the reactions were monitored at 405 nm at 22°C. The kinetic parameters for substrate HPG activation were determined, as described under Materials and Methods. The data represent the mean of three independent determinations.

The present results on the abolishment of the 'K_M shift' (Table 3D) in $SK_{del254-262}$ suggest that the 250-loop interacts with a region in partner plasmin(ogen) that is situated close to the active center, a surmise that is entirely consistent with its proposed role in sequestering substrate HPG to the activator complex and with peptide inhibition experiments reported earlier (Nihalani *et al.*, 1997). Noticeably, the k_{cat} for the hydrolysis of the low-molecular weight peptide substrate by the 1:1 HPN complex of the deletion mutant remained unchanged (Table 3D). These results clearly demonstrate that the affinity for macromolecular substrate (HPG) was selectively decreased in the case of $SK_{del254-262}$.HPN, without a concomitant alteration in the processivity of the small MW peptide substrate.

3.3.2.6 Ternary interactions between the activator complex and substrate HPG on the Resonant Mirror

The foregoing results on increased K_M for HPG in case of $SK_{del254-262}$, prompted us to explore the comparative affinities of activator complexes of SK.HPG, on one hand and $SK_{del254-262}$.HPG on the other, for substrate HPG using a more direct physico-chemical approach. For this purpose, a new 'docking' assay for ternary complex formation between SK and two molecules of HPG, one in the binary mode, and the other docked as a substrate was devised based on a real-time approach utilizing Resonant Mirror based biosensor equipment. Earlier, a 'static' analysis of the formation of such a ternary complex with radioactively labeled substrate HPG bound onto the binary complex of immobilized HPG and SK on plastic surfaces has been reported (Young *et al.*, 1998). Though such an assay can provide a clear estimate of affinity in terms of equilibrium dissociation constants (K_D), it fails to give insight into the dynamics of the interaction of the activator complex with the macromolecular substrate. In order to establish the authenticity of ternary complex formation with substrate HPG onto the preformed binary SK.HPG complex on Resonant Mirror cuvettes, two criteria were used: (a) sensitivity of the ternary complex, and comparative refractoriness of the preformed binary complex, to EACA, and (b) distinctive concentration range-dependence of binary (low nM) and ternary complex/es (high nM range) to HPG binding (see Materials and Methods for detailed protocols). It has been well-established that the pre-formed SK.HPG complex is highly refractory to EACA whereas the action of the activator complex on the substrate is

Table 3D Steady-state kinetic parameters for amidase activity of equimolar complexes of HPN and SK/$SK_{del254-262}$ [a]

Protein	K_M (mM)	k_{cat} (min^{-1})	k_{cat}/K_M (min^{-1}/mM)
HPN	0.17 ± 0.03	310 ± 18	1823.53
SK.HPN	0.6 ± 0.02	370 ± 15	616.67
$SK_{del254-262}$.HPN	0.2 ± 0.07	320 ± 14	1600

[a] For the determination of the amidolytic parameters, SK/$SK_{del254-262}$ and HPN were pre-complexed in equimolar ratio and an aliquot of this mixture was assayed for amidolysis at varying concentrations of Chromozym® PL, as detailed under Materials and Methods. The data represent the mean of three independent determinations.

susceptible to inhibition in the low millimolar range (Lin *et al.*, 2000), a fact which we also observed, while the same concentration of EACA potently inhibited the interaction of substrate HPG with preformed SK.HPG complex. This comparative resistance of the pre-formed binary complex, and susceptibility of the ternary complex to EACA allowed us to selectively examine the interaction of 'ternary' HPG with SK.HPG binary complex. Similarly, due to the comparatively low affinity of the substrate HPG towards the SK.HPG binary complex (Wohl *et al.*, 1980), higher concentration of substrate HPG was required, while the SK.HPG binary interaction, due to its intrinsically high affinity, could easily be monitored at the sub- and low-nanomolar ranges of concentration (Tables 3B and 3E). A composite picture of IAsys^{TM} Resonant Mirror-based real-time kinetic analysis to explore the ternary interactions between substrate HPG and equimolar binary complex of SK and immobilized HPG has been shown in Figure 3.9. The results obtained for the interaction of substrate HPG, μPG and K1-5 with either SK or $SK_{del254-262}$ complexed with immobilized HPG are given in Table 3E. It is clear that substrate HPG interacts with $SK_{del254-262}$.HPG binary complex with a 5-fold lower affinity (K_D ~ 0.75 μM) as compared with SK.HPG binary complex (K_D ~ 0.15 μM). This decrease in affinity is remarkably proportionate to the increase in the K_M for substrate HPG (5-6 fold) using enzymatic activity as the criterion for discrimination between SK and mutant. These results clearly indicate the importance of the 250-loop in 'capturing' substrate HPG molecules by the activator complex.

3.3.2.7 Effect of EACA on substrate HPG activation with binary complexes of SK.HPN and $SK_{del254-262}$.HPN

To understand the role of kringles in substrate affinity, the HPG activator activities of SK and the mutant were compared in the presence of varying concentrations of EACA, a lysine analogue that is well known to inhibit HPG activation by SK as well as disrupt ternary complex formation through kringle-mediated mechanism (Castellino, 1981; Lin *et al.*, 2000; Young *et al.*, 1998). Kinetic studies to check the effect of varying concentrations of EACA on substrate HPG activation by SK.HPN and $SK_{del254-262}$.HPN showed that the mutant exhibited a greater susceptibility to EACA-mediated inhibition of substrate HPG activation than SK (Figure 3.10), in a concentration range that did not affect the activity of the two binary

Table 3E Association and dissociation rate constants and apparent equilibrium dissociation constants for the interaction of substrate HPG, μPG and K1-5 with SK/$SK_{del254-262}$ complexed with immobilized HPG [a]

[Ligand]	[Ligate]	k_a (x 10^5) (M^{-1} s^{-1})	k_d (x 10^{-1}) (s^{-1})	K_D (x 10^{-6}) (M)
SK.HPG	HPG	10.70 ± 1.30	1.76 ± 0.23	0.16 ± 0.04
SK.HPG	μPG	0.75 ± 0.02	1.29 ± 0.74	1.72 ± 0.91
SK.HPG	K1-5	0.29 ± 0.06	1.19 ± 0.17	4.10 ± 0.62
$SK_{del254-262}$.HPG	HPG	4.62 ± 0.51	3.35 ± 0.13	0.72 ± 0.09
$SK_{del254-262}$.HPG	μPG	0.90 ± 0.03	1.33 ± 0.12	1.48 ± 0.20
$SK_{del254-262}$.HPG	K1-5	0.28 ± 0.12	3.41 ± 0.21	12.18 ± 2.08

[a] Kinetic constants for the interactions of substrate HPG, μPG and K1-5 with SK.HPG or $SK_{del254-262}$.HPG binary complex were determined by applying the FASTfit™ program to the binding data obtained using IAsys biosensor, as described under Materials and Methods. A stable binary complex between SK/$SK_{del254-262}$ and HPG immobilized onto the cuvette was made and then the binding of varying concentrations of either substrate HPG (0.1-1 μM), μPG (1-6 μM) or K1-5 (1-6 μM) was monitored, as described in the legend of Figure 3.9.

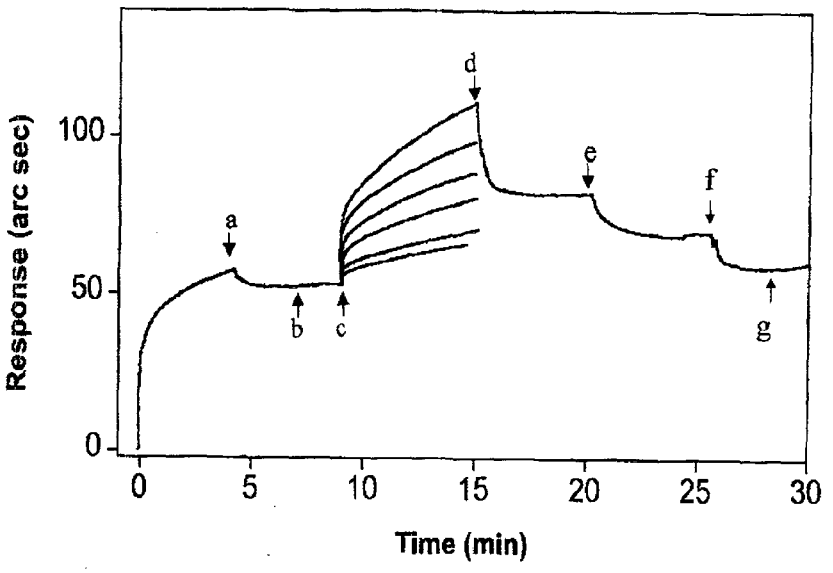

Figure 3.9 Tracings from the IAsys^{TM} Resonant Mirror based system to quantitate the interactions between substrate HPG and the equimolar binary complex of SK and immobilized HPG. The experiment was carried out at 25°C in binding buffer as described under Materials and Methods. Human PG was biotinylated and immobilized on streptavidin captured onto the biotin cuvette. A stable binary complex was formed by adding saturating concentration of SK onto immobilized HPG. After washing with binding buffer (point of addition of binding buffer, as depicted by arrow marked 'a'), a stable dissociation baseline (arrow marked 'b') was obtained due to high affinity and stability of the SK.HPG binary complex, which remained unaffected even after washing with 2.5 mM EACA (data not shown). Thereafter, varying concentrations of substrate HPG (0.1-1 μM) were then added (point of addition of substrate, as depicted by arrow marked 'c') to monitor the association phase and subsequently, the cuvette was washed with binding buffer thrice (point of addition depicted by arrow marked 'd'), and thereafter, the dissociation phase was recorded. After each cycle of analysis, the undissociated substrate HPG was stripped off with 2.5 mM EACA (point of addition of EACA, as shown by arrow marked 'e'), followed by re-equilibrating the cuvette with binding buffer (depicted by arrow marked 'f') that re-established the original baseline (arrow marked 'g'). The immobilized streptavidin alone was taken as the negative control and it was subjected to the same kind of treatments as given to the test cell containing immobilized HPG. No significant non-specific binding was observed (data not shown).

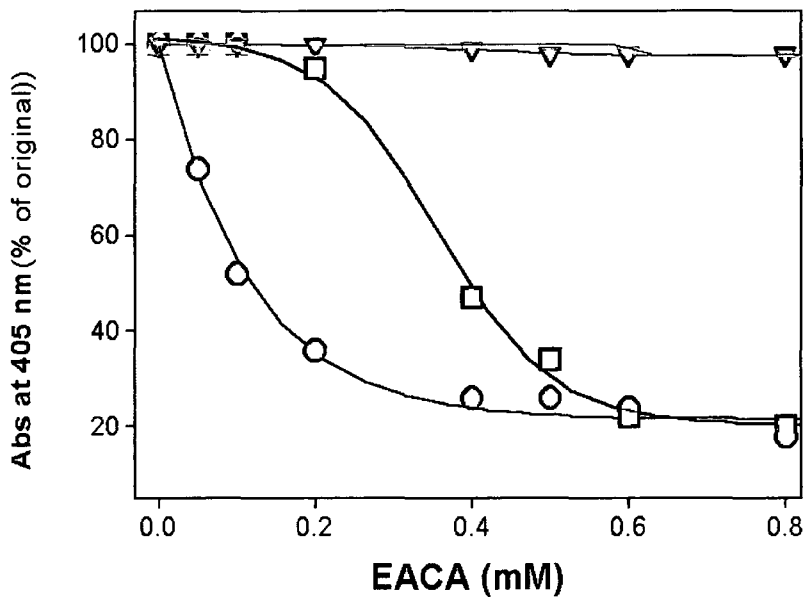

Figure 3.10 Differential susceptibility to EACA of substrate activation by SK and $SK_{del254-262}$. The effect of different concentrations of EACA (0-1 mM) on the substrate HPG activation by SK (blue squares) and $SK_{del254-262}$ (magenta circles) was examined. Controls containing 10 nM each of SK and HPN (light grey triangles), or HPN alone (dark grey, inverted triangles) are also shown. The HPG activator activity of constant, catalytic amounts of the pre-formed equimolar activator complexes between HPN and either SK or $SK_{del254-262}$ to obtain final concentrations of 0.25 nM and 3 nM, respectively in presence of varying concentrations of EACA, along with substrate HPG and chromogenic substrate in 50 mM Tris.Cl buffer, pH 7.5, was monitored at 405 nm at 22°C. The initial velocities in different concentrations of EACA are expressed relative to the controls not containing any EACA (taken as 100 %). Similar differential effects between SK and $SK_{del254-262}$ were observed at HPG concentrations of 0.5 μM, 2 μM and 4 μM, though the IC_{50} values were different (data not shown).

complexes or the activity of free HPN. It has been shown earlier (Lin *et al.*, 2000; Young *et al.*, 1998), using sandwich-binding assay that EACA completely abolishes the docking of substrate HPG onto SK.HPG binary complex formed on plastic surface. However, this does not allow the measurement of the rates of binding and dissociation of substrate HPG with the high affinity binary complex.

3.3.2.8 Effect of EACA on ternary interactions on the Resonant Mirror

Experiments were also carried out to see the effect of EACA on the ternary complexation of substrate HPG to SK/$SK_{del254-262}$ pre-complexed with immobilized HPG on Resonant Mirror cuvettes, as described earlier. With $SK_{del254-262}$.HPG binary complex, an IC_{50} of 0.3 mM was obtained which is approximately 3-fold less than the IC_{50} (1 mM) obtained with SK.HPG binary complex (Figure 3.11). These data clearly support the conclusion that the binary complex of the mutant, with the 250-loop deleted, interacted with substrate in a manner that is more vulnerable, as compared to SK.plasmin(ogen), to disruption with the lysine-binding site competitive ligand, EACA.

3.3.2.9 Kinetic and physico-chemical studies of ternary interactions with substrate microplasminogen

Interestingly, kinetic studies using μPG as the substrate showed no discernable difference between SK and $SK_{del254-262}$ with respect to initial velocities of substrate μPG activation ($K_M \sim 2$ μM), under conditions where the activator activities of the two complexes (SK.HPN and $SK_{del254-262}$.HPN) showed a remarkable difference when the substrate (native HPG) contained the kringle domains (Figure 3.12).

To further establish that kringles are involved in activator-substrate interactions, ternary binding experiments on the Resonant Mirror where the binding of the substrates, μPG and K1-5 of HPG, to the binary complex pre-formed between either SK or the mutant with immobilized HPG were carried out (Table 3E). Remarkably, in consonance with kinetic data, μPG showed the same affinities for both SK and $SK_{del254-262}$ complexed with HPG. When K1-5 was used as the docking 'substrate' during ternary complex formation, the SK.HPG binary complex showed an affinity of 4.1 μM for K1-5, while that of $SK_{del254-262}$.HPG complex was determined to

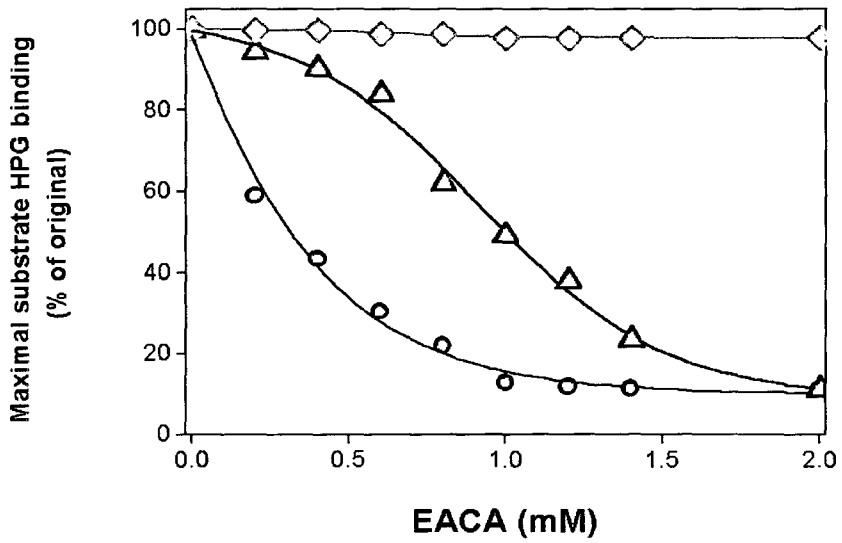

Figure 3.11 Effect of EACA on the physical binding of substrate HPG to SK.HPG or $SK_{del254-262}$.HPG binary complex examined by Resonant Mirror technique. Binding of substrate HPG (0.4 μM) to either SK.HPG (blue triangles) or $SK_{del254-262}$.HPG (magenta circles) binary complex was measured at various concentrations of EACA (0-2 mM) using IAsys^{TM} system, as described under Materials and Methods. The maximal extent of binding under varying concentrations of EACA was quantitated and the maximal binding in buffer alone was used to normalize the extent of binding under different experimental conditions. The extent of substrate HPG binding is plotted as a function of EACA concentration. The effect of respective EACA concentrations on the binary SK/$SK_{del254-262}$.HPG complex was checked, that was taken as control (represented by grey diamonds).

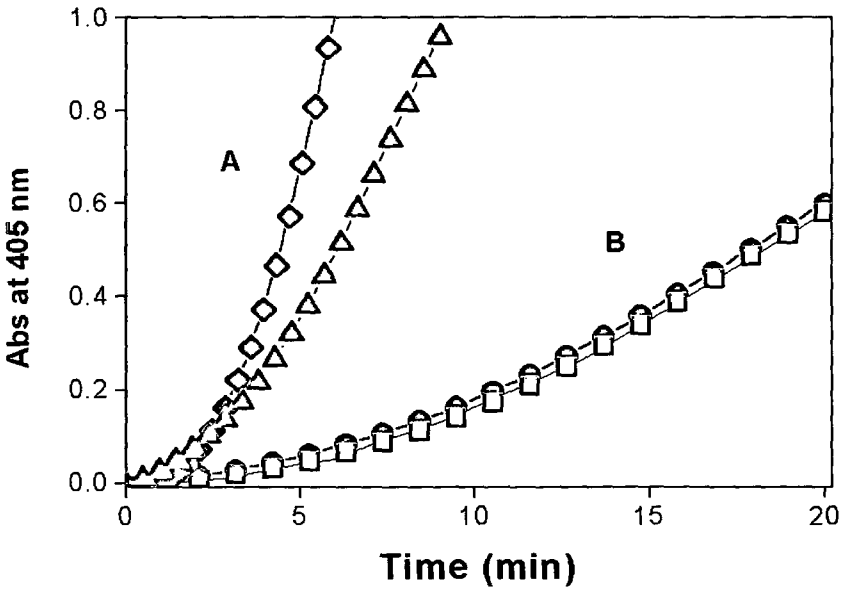

Figure 3.12 Abolishment of the differential substrate activation phenomenon by SK and $SK_{del254-262}$ by using substrate μPG. Fixed, catalytic amounts of the respective pre-formed activator complexes of each protein with HPN were added to the cuvette containing HPG or μPG as the substrate and Chromozym® PL in 50 mM Tris.Cl buffer, pH 7.5, and the reactions were monitored at 405 nm at 22°C. The figure shows progress curves of activation of (A) HPG by SK (blue diamonds) and $SK_{del254-262}$ (magenta triangles) and of (B) μPG by SK (black circles) and $SK_{del254-262}$ (red squares).

be 12 μM, indicating approximately a 3-fold higher affinity for SK (Table 3E). Again, these results strongly argue that the 250-loop of the β domain of SK interacts with substrate HPG via the latter's kringle domains.

3.3.2.10 Modeling studies

Molecular modeling studies wherein the intermolecular surfaces between the β domain of SK and the isolated kringle 5 (which was used as a typical representative structure of the five HPG kringles, and does not necessarily indicate any preferred role in the substrate-activator complex interplay; however, see below) were explored for mutual complementarities (see under Materials and Methods for details) indicate that a kringle structure can indeed dock the 250-loop in a remarkably optimal fashion. The best-docked complex is shown in Figure 3.13. Remarkably, the surface of the kringle showed nearly perfect complementarity to the surface of the SK.μPN complex. The mode of docking also revealed that the C-terminal of the kringle domain is within connecting distance of the N-terminal of the μPN moiety, as would be expected in the physiological situation. Thus, the close complementarities of kringle and SK.μPN surfaces, the perfect electrostatic match among the two structures, and the proximity between connecting peptide units suggest that indeed, the kringle might dock onto SK.μPN in the mode shown in Figure 3.13.

3.4 DISCUSSION

It is well-known that SK indirectly activates HPG through a unique three-step mechanism that involves (i) a high affinity binding of SK with HPG, followed by (ii) structural rearrangement of the zymogen to generate an active site in the complex and (iii) finally, binding of substrate PG by the activator and catalysis (Summaria and Robbins, 1976; Summaria *et al.*, 1968; Reddy and Markus, 1972; Schick and Castellino, 1974). A truly intriguing aspect of this system which has been a subject for many active investigations is the structural basis of conversion of the broadly specific serine protease, HPN to a highly substrate (HPG)-specific protease, virtually with exclusive propensity for acting on the target scissile peptide bond in HPG once complexed with 'cofactor' SK (Parrado *et al.*, 1996; Esmon and Mather, 1998; Conejero-Lara *et al.*, 1996; Wang *et al.*, 1998; Parry *et al.*, 2000; Boxrud *et al.*, 2000;

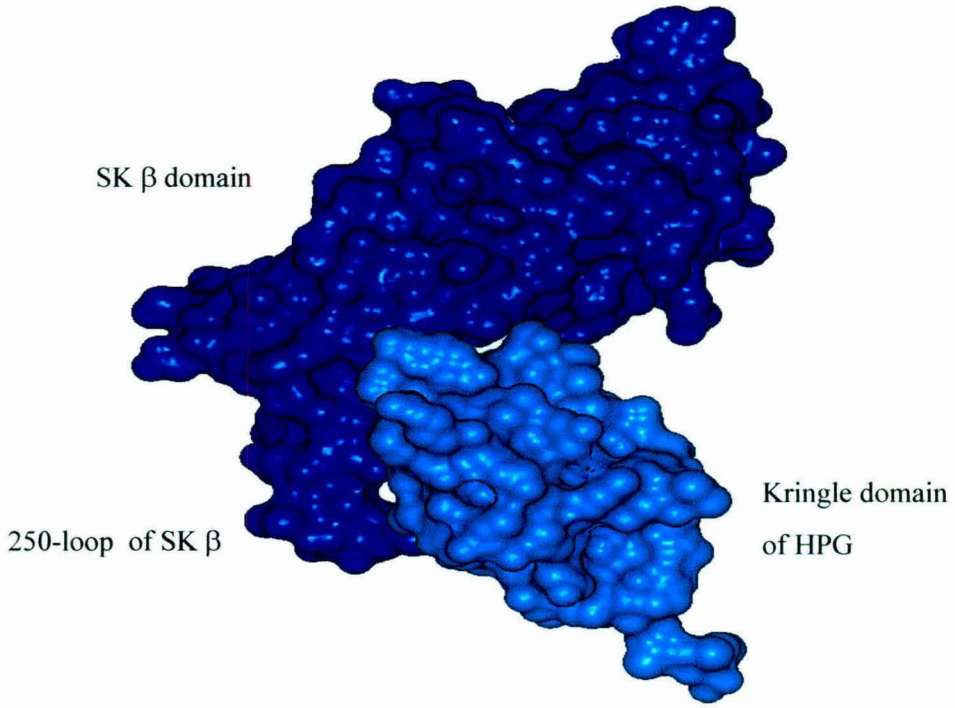

Figure 3.13 Docking of kringle 5 of HPG with the β domain of SK. Connolly surfaces of the β domain (shown in blue) and kringle 5 of HPG (depicted in cyan) were calculated by using the GRASP program. Kringle 5 has been used here as a typical representative structure of the five HPG kringles. In order to generate the molecular surface, the radius of a water molecule was considered to be 1.4 Å. Electrostatic potentials were mapped onto the surfaces with GRASP. The β domain showed a distinct patch of positive charges in the 250-loop. Similarly, the kringle domain also showed a distinct patch of negative charges. The two patches were brought in close proximity by manual docking, which showed close surface and electrostatic complementarities (see Materials and Methods for details).

Nihalani *et al.*, 1997; Nihalani *et al.*, 1998). Though modeling studies based on the X-ray data of SK.μPN (Wang *et al.*, 1998) has highlighted several potential contacts in SK between the activator complex and the substrate, it is silent on the precise points of interaction between SK and HPG that could be important for substrate docking and catalysis.

In this present study, we have endeavored to identify and establish that an epitope in the central β domain of SK *viz.* the 250-loop is involved in substrate HPG activation phenomenon. Deletion of this 250-loop adversely affected the substrate HPG activation properties of the molecule. A similar effect has been previously observed when the two Lys residues (Lys256, Lys257) in the core region of the β domain of SK were subjected to site-specific mutagenesis (Lin *et al.*, 1996; Chaudhary *et al.*, 1999). Far-UV CD studies were carried out which ruled out the possibility that the deletion of the loop resulted in destabilization of the entire structure of SK or β *per se*, that could possibly explain the low rates of HPG activation. Further on, to check whether the reduction in activation rates was due to decrease in 1:1 affinity for partner HPG or not, a highly sensitive Resonant Mirror-based approach to measure real-time kinetics of interaction between molecules was used and it was found that the 1:1 affinity for HPG in the mutant was not adversely affected.

Also, $SK_{del254\text{-}262}$ when combined with HPG, displayed esterolytic activity similar to that of the SK.HPG activator complex, in presence of NPGB. However, the maximal level of these bursts was approximately half of that observed with natural SK prepared from *Streptococcus equisimilis*. It has been demonstrated recently that a free N-terminal (Ile) is required for the NPGB reaction of native SK due to the participation of the α-amino group of the N-terminal residue (Wang *et al.*, 1999a), as also some flanking residues (Boxrud *et al.*, 2001), in the auto-activation of HPG by SK. However, the positive NPGB reaction of SK, albeit less than that of natural SK, was easily explained when N-terminal sequence analysis of the purified SK and $SK_{del254\text{-}262}$ showed that approximately 50 % of the purified protein fractions had (like natural SK) a free Ile at the N-terminus, probably due to partial processing by host methionyl aminopeptidase (Hirel *et al.*, 1989). The mutant could also amidolytically activate partner HPG in as facile a manner as SK, indicating that the loss in activity in the mutant was not because if its inability to activate partner HPG.

To critically look at the characteristics of the active site *per se*, the kinetics of amidolysis of small molecular-weight chromogenic substrates was carried out. It is known that the complexation of SK with free HPN leads to an overall reduced accessibility of the HPN active site by small molecular weight substrates and inhibitors probably due to steric hindrance brought about by SK binding in the vicinity of the active site; this phenomenon is manifested, for example, in a significant increase in the K_M for the amidolysis of chromogenic substrates by SK.HPN complex compared with that of HPN alone (Wang *et al.*, 1998; Robbins *et al.*, 1981; Wohl, 1984). The characteristic increase in K_M of HPN for amidolytic substrates has also been observed with the isolated β domain (Nihalani *et al.*, 1997). The present results on the abolishment of the 'K_M shift' in $SK_{del254-262}$ suggest that the 250-loop interacts with a region in partner plasmin(ogen) that is situated close to the active center, a surmise that is entirely consistent with its proposed role in sequestering substrate HPG to the activator complex and with peptide inhibition experiments reported earlier (Nihalani *et al.*, 1997). Noticeably, the k_{cat} for the hydrolysis of the low-molecular weight peptide substrate by the 1:1 HPN complex of the deletion mutant remained unchanged.

However, when the steady-state kinetics of $SK_{del254-262}$ with fully opened active site (HPN as partner) was carried out, they revealed that the affinity for interaction with substrate HPG has reduced 5-fold compared to that of SK. This alludes to the idea that this nine-residue loop is giving crucial anchorage to substrate HPG during the activation process. These results clearly demonstrate that the affinity for macromolecular substrate (HPG) was selectively decreased in the case of $SK_{del254-262}$.HPN, without a concomitant alteration in the processivity of the small-molecular weight peptide substrate.

The increase of K_M for activation of substrate HPG encouraged us to look at ternary interaction studies of HPG with SK/$SK_{del254-262}$.HPG binary complex using Resonant Mirror based approach. Similar studies have been reported earlier using solid phase assay (Young *et al.*, 1998). Though such an assay can provide a clear estimate of affinity in terms of equilibrium dissociation constants (K_D), it fails to give insight into the dynamics of the interaction of the activator complex with the macromolecular substrate. Real-time based kinetics indicated a 5-fold increase in K_D in the ternary interaction of $SK_{del254-262}$.HPG with substrate HPG as compared with

SK.HPG binary complex. This decrease in affinity is remarkably proportionate to the increase in the K_M for substrate HPG (5-6 fold) using enzymatic activity as the criterion for discrimination between SK and mutant. In addition, no such difference in affinity for binding was observed in case when μPG (kringle-less catalytic domain of HPG) was used as the substrate whereas a 3-fold decrease in affinity in case of the mutant was observed when K1-5 was used as 'docked' substrate onto binary complex on the IAsys. These results clearly specify the importance of the 250-loop in 'capturing' substrate HPG molecules by the activator complex.

Recent biochemical studies suggest that an 'exosite' mediated substrate HPG binding, independent of the primary covalent specificity of the HPN active site, represents the major mechanism of SK-induced changes in the macromolecular substrate specificity of HPN (Boxrud *et al.*, 2000; Nihalani *et al.*, 1998). The structural basis whereby such an exosite contributes towards the change in substrate specificity of the HPN active site consequent to SK binding has, however, remained essentially unknown so far. The data presented here clearly implicate the 250-loop of the β domain as an important determinant of the macromolecular substrate specificity of the SK.HPG activator complex.

The presence of two tandem lysine residues at the tip of the 250-loop suggests that interactions with the kringle domain/s in substrate HPG may be the operative mechanism behind this interaction. To validate this point, both kinetic studies as well as ternary interaction studies on the Resonant Mirror to check the effect of varying concentrations of EACA (the lysine-binding site competitive ligand) on substrate HPG activation by SK.HPN and $SK_{del254\text{-}262}$.HPN were carried out that showed that the mutant exhibited a greater vulnerability to EACA-mediated inhibition of substrate HPG activation than SK, in a concentration range that did not affect the activity of the two binary complexes or the activity of free HPN. It has been shown earlier (Lin *et al.*, 2000; Young *et al.*, 1998), using sandwich-binding assay that EACA completely abolishes the docking of substrate HPG onto SK.HPG binary complex formed on plastic surface. However, this does not allow the measurement of the rates of binding and dissociation of substrate HPG with the high affinity binary complex. However, it is worth noting that if all of the kringle mediated interactions between activator and substrate had been abolished by the deletion of the loop, the mutant should have been completely resistant to inhibition by EACA. The fact that the mutant is susceptible to

lower concentrations of EACA suggests that other EACA-sensitive, kringle-dependant interactions are still operative, but at least one of the critical interactions has been abolished by the selective deletion of the 250-loop.

If the observed difference in substrate affinities between SK.HPG and $SK_{del254-262}$.HPG activator complexes is indeed kringle-mediated, it is reasonable to assume that the rates of activation of substrate μPG, which is devoid of all five HPG kringles, by SK and $SK_{del254-262}$ should not substantially differ from each other. Microplasminogen is known to be a poor substrate for the preformed SK.PG activator complex (Shi and Wu, 1988). Interestingly, kinetic studies using μPG as the substrate failed to show any stark difference between SK and $SK_{del254-262}$ with respect to substrate μPG activation, under conditions where the activator activities of the two complexes (SK.HPN and $SK_{del254-262}$.HPN) with substrate HPG (containing all the kringle domains) showed a remarkable difference. These observations prove convincingly that interactions involving lysine binding site/s in the kringle domains are intimately involved in the mechanism of operation of the macromolecular substrate-specific exosite in the SK.plasmin(ogen) activator complex.

Although whether kringle 5 *per se* or any other kringle is involved in this interaction cannot be judged at this stage, during the course of this work, another report was published which demonstrates the involvement of kringle 5 in the 1:1 binding with the β domain of SK (Loy *et al.*, 2001). Although speculative at this stage, this offers a tantalizing possibility that this kringle-mediated interaction at the levels of both binary and ternary complex formation, operate through kringle 5. If this scenario is correct, the loop might "switch" its binding specificity towards partner or substrate depending on the temporal stage in the catalytic cycle, a possibility that is strengthened by a previous observation (Nihalani *et al.*, 1997) that a synthetic peptide encompassing the 250-loop exhibits bifunctional behaviour by competitively inhibiting both SK.HPG binding as well as HPG activation by preformed SK.HPN activator complex. On the other hand, the current evidence does not rule out that the different kringles in substrate and partner HPG are directed to different sites in SK. Whatever the exact mechanism, this study provides unmistakable evidence of the direct involvement of a discrete epitope in SK in substrate recognition and binding via the kringle/s of HPG. Undoubtedly, further studies are needed to identify the relative contributions of the kringle/s *versus* the catalytic domain of the substrate towards the

latter's recognition, docking and turnover in the 'valley' formed by the activator complex. This would aid in a better understanding of this enigmatic interaction at the molecular level.

It needs to be realized, however, that the observation that even after the excision of the 250-loop, the HPG activation reaction still survived (albeit with increased K_M), indicates that this loop is not the sole determinant of the SK.HPN exosite property. Indeed, earlier studies had suggested that the α domain as well as the β domain, together, contribute to the generation of HPG specificity in the activator complex (Nihalani *et al.*, 1998). The potential of the α domain to interact with substrate HPG is also evident from the SK.μPN crystal structure (Wang *et al.*, 1998), although whether it does so by interacting with kringle/s of substrate is still unclear. It is also established from recent work that the β domain contributes a major share towards SK's affinity for partner HPG as well (Nihalani *et al.*, 1998). However, the fact that mutagenesis of several residues in the β domain that, without altering the overall folding of the protein or its affinity for partner HPG, resulted in appreciable diminution in the k_{cat} for activator activity with little change in the K_M for HPG *per se* (Chaudhary *et al.*, 1999), suggests that regions other than the 250-loop in this domain are also intimately involved in the modulation of the substrate specificity of the activator complex. We have observed that mutations of residues immediately flanking the 250-loop (e.g., $SK_{Y252A,\ E263G}$) lead to further increase in the molecule's K_M for substrate HPG (to about 15-fold that of SK) with only minimal alteration in the k_{cat} of its complex with HPN, suggesting that the regions immediately flanking the loop are somehow related to catalysis. We believe that the loop is most probably, making decisive and direct contact with substrate kringle/s, juxtaposing it in the right orientation, during the cycle of catalysis, but it is the molecular motion/flexibility of the contours of the loop that determine the decoupling phenomenon *viz.* the dissociation of the substrate and release of product and thereby, the rate of turnover. What is essentially occurring in these 'sizzling' areas still remains to be uncovered.

It is quite intriguing that the β domain provides a major portion of the intermolecular affinity of SK for HPG necessary for the formation of the tightly held equimolar activator complex (Conejero-Lara *et al.*, 1998), and at least some of the affinity required for the (transient) interaction of the latter with substrate HPG, as the

present study indicates. This arouses curiosity whether this domain would, by itself, possess HPG activator activity, however compromised at a quantitative level, since two seemingly fundamental requirements for a single-domain HPG activator protein *viz.* ability to bind with partner plasmin(ogen) and to then interact with substrate, are present in this domain. This question assumes significance because SAK, a single-domain bacterial HPG activator, is also known to work as a 'protein co-factor' in a fashion akin to that of SK (Esmon and Mather, 1998), and has both these distinctive HPG interacting properties. The ternary structure of μPN.SAK.μPN suggests that SAK appears not to modify the active site conformation of the enzyme, but creates new exosites that indirectly alter the substrate specificity of μPN (Parry *et al.*, 1998). Identification of such functional 'hotspots' in PG activators in general, and SK in particular, that help in exosite mediated modulation of substrate specificity may greatly aid the future *de novo* design of improved HPG activators.

CHAPTER IV

RESUSCITATION OF COFACTOR ACTIVITY IN THE INTRINSICALLY INACTIVE ALPHA DOMAIN OF STREPTOKINASE THROUGH PROTEIN ENGINEERING

Abstract

Although the isolated α domain of SK shares remarkable structural homology with SAK, it displays virtually negligible cofactor activity (Loy *et al.*, 2001; Vasudha *et al.*, 2003), whereas SAK (also a single-domain molecule) displays high cofactor activity. Nevertheless, the fact that a low but genuine, *intrinsic* cofactor activity survives in the isolated α domain indicates that it might be possible to enhance this activity to higher levels, perhaps even to that of SAK, if critical features of the α domain that might have been lost during the evolutionary divergence of a common prototypic domain into the single-domain SAK structure and the three-domain SK molecule, are "grafted"sucessfully onto the deficient α domain. In order to possibly engineer such changes, we first compared the structures of α domain with that of SAK. This exercise identified a small loop present in SAK, but one that is completely absent in SK α. However, before setting out on a loop-grafting approach, preliminary studies on the HPN-mediated susceptibility of $\alpha_{wild\text{-}type}$ were carried out, which revealed that the $\alpha_{wild\text{-}type}$ was highly susceptible to proteolysis at a single peptide bond, *viz.* Lys59-Ser60. When the Lys59 was mutated to Ala, a dramatic stability in proteolysis was observed, with a concurrent 8-fold increase in cofactor activity over $\alpha_{wild\text{-}type}$. However, a greater than 100-fold increase in catalytic efficiency was obtained over that of $\alpha_{wild\text{-}type}$ when the SAK loop was grafted into α_{K59E}, followed by improving the 'sequence-context' of the heterologous loop by random mutagenesis of the flanks of the loop. A detailed kinetic analysis revealed that improvements in substrate affinity as well as the catalytic turnover rate contributed to this observed overall enhancement accrued through this protein engineering approach. Mechanistic studies using μPG *versus* full-length HPG, used as substrate, established that the observed increase in the catalytic efficiencies largely emanated from improved interactions between the combinatorial mutant and the kringle domains of substrate HPG.

4.1 INTRODUCTION

Streptokinase is composed of three structurally similar domains, α, β and γ, that are separated by coiled coils (Wang *et al.*, 1998). Unlike other well-known thrombolytic proteins like UK and t-PA, SK does not possess intrinsic proteolytic activity. It forms an equimolar complex with 'partner' HPG or HPN that then activates 'substrate' molecules of HPG by the cleavage of scissile peptide bond and then transforms them into HPN. Plasmin alone is essentially a serine protease with broad substrate specificity, but once combined with its protein cofactor SK, it becomes highly specific for the target Arg561-Val562 scissile peptide bond in HPG (Markus and Werkheiser, 1964). An understanding of the molecular basis of this enhanced specificity of HPN consequent to complexation with SK has important fundamental as well as application implications especially in the design of better clot-dissolver protein drugs.

The crystal structure of SK complexed with the μPN, the catalytic domain of HPN, devoid of the kringle domains has provided initial insights regarding the molecular mechanism by which SK switches the substrate specificity of the active center of HPN by forming a three-sided valley around μPN (Wang *et al.*, 1998). It has also shed light on the fact that out of all the three domains of SK, the maximum area of contact with μPN is that of the α domain of SK. This raises a pertinent question whether the isolated α domain of SK possesses any HPG activator or cofactor activity, even if highly compromised. This is relevant also because of the fact that another 'indirect' HPG activator, SAK that has only a single domain and shares high structural homology with each of the three domains of SK (see Figure 4.1). A recent study had attempted to address this issue, but found very low activator activities associated with individual SK domains; of all the three domains of SK, α exhibited the maximum activity, but one that was barely 0.002 % of the native activity of SK (Loy *et al.*, 2001). Previous studies in our laboratory on the cofactor activities of the individual domains of SK have shown that none of the isolated domains of SK was found to have significant cofactor activity (Vasudha, 2002). However, the absence of cofactor activity at a level comparable to native SK, or even SAK (which possesses relatively lower cofactor activity compared to SK) may be due to loss of critical structural

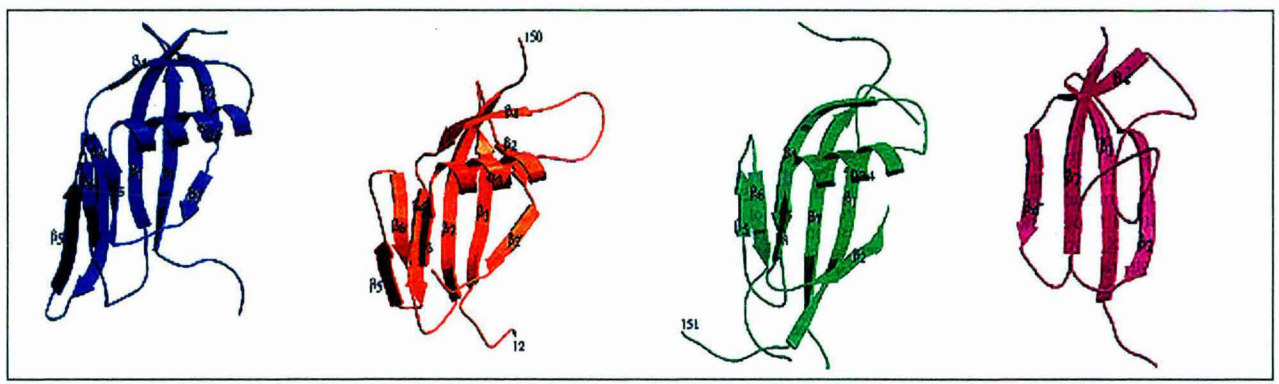

Figure 4.1 Ribbon plot representation of SAK and the three domains of SK. The three domains of SK are structurally homologous to each other and also to the single-domain PG activator, SAK (adapted from Parry *et al.*, 2000).

features during the evolution of the prototypic single domain into the three-domain structure of SK and/or increased vulnerability of the isolated domain to HPN-mediated proteolysis. These considerations prompted us to re-examine the structural differences between the SAK and the α domain of SK more carefully so as to possibly account for the observed vast disparity between the cofactor activities of SAK, and the nearly inactive isolated α domain of SK. Also, we reasoned that if a native-like activity could be engineered into the α domain, it would validate the assumption that the same prototypic fold has been utilized through evolution to develop the three-domain SK, two-domain SUPA and the single domain SAK. It is possible that through this exercise, meaningful insights may be gleaned that would allow the re-design of a PG activator based on the α domain alone through the resuscitation of its 'latent' biological activity by subtly manipulating its structural features. In the present study, we show that a dramatic enhancement of the catalytic efficiency of the intrinsically, nearly inactive, α domain of SK to nearly that of SAK could be accomplished through a loop grafting and combinatorial (semi-random) mutagenesis strategy. The results of the study are presented below.

4.2 MATERIALS AND METHODS

4.2.1 Reagents and chemicals

Glu-plasminogen (human) was purchased from Roche Diagnostics GmbH, Germany. The T7 RNA polymerase promoter-based expression vector, pET-23d and *Escherichia coli* strain BL21 (DE3) were obtained from Novagen Inc. (Madison, WI). Thermostable DNA polymerase (*Pfu*) was acquired from Stratagene Inc. (La Jolla, CA), and restriction endonucleases, T4 DNA ligase and other DNA modifying enzymes were products of New England Biolabs (Beverly, MA). Oligonucleotide primers were obtained from Integrated DNA Technologies Inc. (Indianapolis, IN) and BioBasic Inc. (Canada). Purifications of plasmid DNA and extraction of PCR amplified products from agarose gels were performed using kits available from Qiagen, GmbH (Germany). Automated DNA sequencing using fluorescent dyes was done on an Applied Biosystems DNA sequencing system Model 310. The N-terminal protein sequencing was carried out on an Applied Biosystems Protein sequencer, Model 476A. Phenyl Agarose 6XL, DEAE Sepharose (Fast Flow) and Chelating

Sepharose® (Fast Flow) were procured from Pharmacia Biotech, Uppsala, Sweden. All other reagents were of the highest analytical grade available.

4.2.2 Genetic constructs

4.2.2.1 Expression plasmid containing the cDNA encoding for the α domain of SK (pET-23d-α)

The construction of the intracellular expression plasmid for the α domain of SK has been described in detail elsewhere (Vasudha, 2002). Briefly, it involved the PCR-amplification of the α domain of SK using specific primers, followed by the double-digestion of the PCR product with suitable REs and further cloning of this DNA fragment into the pET-23d vector, at corresponding sites. The circular map of pET-23d-α is shown in Figure 4.2.

4.2.2.2 Plasmid vector pBluescript containing the SK gene (pBS-SK)

The cloning of the gene encoding SK in pBluescript II KS (-) vector has been illustrated in detail in Yadav, 1999. The plasmid contains the SK gene downstream of an *ompA* (outer membrane protein A of *Escherichia coli*) signal under the *lac* promoter. The presence of *ompA* signal facilitates the secretion of SK into the culture medium, as tested by Western blotting using anti-SK antiserum (data not shown). It also contains the gene for resistance to ampicillin for drug selection of bacterial clones containing the plasmid.

4.2.3 Construction of mutants of α

4.2.3.1 Site-directed mutagenesis using overlap-extension based polymerase chain reaction

The insertion of the eight-amino acid residue SAK loop in the α domain of SK was carried out using the overlap-extension based PCR (Ho *et al.*, 1989) that has been described earlier in Chapter III, under Materials and Methods. To construct the loop-grafted α (α_{loop}), mutagenic upstream primer (a3soe-us, carrying a unique restriction site, BseR I) and a flanking downstream primer (T7 Term-mod) were first used in PCR I reaction. Thereafter, mutagenic downstream primer (a3soe-ds) and flanking upstream primer (T7 Pro-mod) were used in PCR II reaction. These reactions

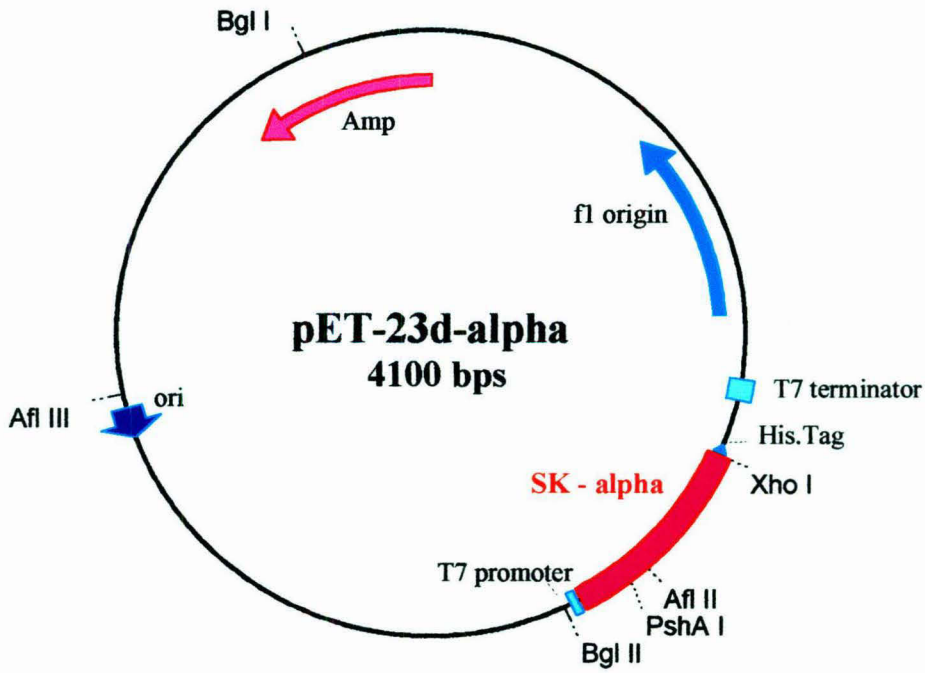

Figure 4.2 Circular map of pET-23d-α. This figure shows a few selected RE sites that were used to construct site-directed mutants of SK α. It also indicates the presence of His_6-tag at the C-terminus of the α gene to facilitate single-step affinity purification of the protein, after refolding from inclusion bodies.

generated DNA fragments having overlapping ends (sequences of the primers have been enlisted in Table 4A). Thereafter, overlap-extension PCR reaction (Ho *et al.*, 1989) was done, resulting in the amplification of the α gene carrying the insertion sequence, which was cloned into the pET-23d vector. The positive clones were confirmed by automated DNA sequencing.

4.2.3.2 Construction of site-directed mutants in the α domain of SK by 'megaprimer' PCR-based method

Site-directed mutation in the α domain of SK was also carried out using the 'megaprimer' PCR based method that was introduced by Kammann and coworkers (1989) and later modified (Sarkar and Sommer, 1990; Sarkar and Sommer, 1992) and Landt and coworkers (1990). This method involved two rounds of PCR that utilize two 'flanking' primers and one internal mutagenic primer, containing the desired base substitution(s). The schematic representation of the construction of site-directed mutants by this method has been shown in Figure 4.3. The sequences of the mutagenic primer and the upstream and downstream flanking primers used to make site-directed mutations are listed in Table 4B. The first PCR is performed using the mutagenic internal primer and the first flanking primer. The product of this first PCR, the 'megaprimer' is purified and is used, along with the second flanking primer, as a primer for a second PCR. The final PCR product contains the desired mutation in a particular DNA sequence. In the first PCR, 100 ng of DNA template (pET-23d-α, as the case may be), 200 μM dNTPs, 20 pmol each of forward and reverse primers, 1 unit of *Pfu* polymerase and 1x of *Pfu* polymerase buffer were taken in a total volume of 100 μl. After a 'hot-start' of 5 min at 95°C, 30 amplification cycles of 94°C for 45 sec, 50°C for 1 min and 72°C for 1 min were performed. This was followed by a final extension of partially completed daughter strands at 72°C for 10 min. Then the PCR amplification product was purified by gel-extraction using the Qiagen gel-extraction kit. The amplified DNA was then used as the megaprimer for the second PCR reaction. The second PCR-premix contained template DNA and megaprimer in the weight-to-molar ratios of 1:400 (5 ng of template DNA and approximately 150 ng of megaprimer), 200 μM dNTPs, 20 pmol of forward primer, 1 unit of *Pfu* polymerase and 1x of *Pfu* polymerase buffer in a total volume of 100 μl. The PCR-premix was

Table 4A Sequences of primers used for the transposition of the SAK loop into the α domain of SK

Mutation	Sequence of primer	RE site[a]
mutagenic U *(a3soe-us)*	5′CGATATGACAAGAATAAGAAGAAGGAG-GAGAACGGCAAGGTCTACTTCGCTGA 3′	BseR I
mutagenic D *(a3soe-ds)*	5′ CTCCTTCTTCTTATTCTTGTCATATCGG-TCAGTAATGGTTGCATCGCTTG 3′	
flanking U *(T7 Pro-mod)*	5′ GAAATTAATACGACTCACTATAGGGGA-ATTGTG 3′	
flanking D *(T7 Term-mod)*	5′ CCAAGGGGTTATGCTAGTTATTGCTCA3′	

[a] The diagnostic RE sites introduced in the primers by translationally silent mutagenesis, used during the screening of clones, have been underlined.
U* represents upstream primer and D represents down stream primer.
Parentheses describe the names of the primers.

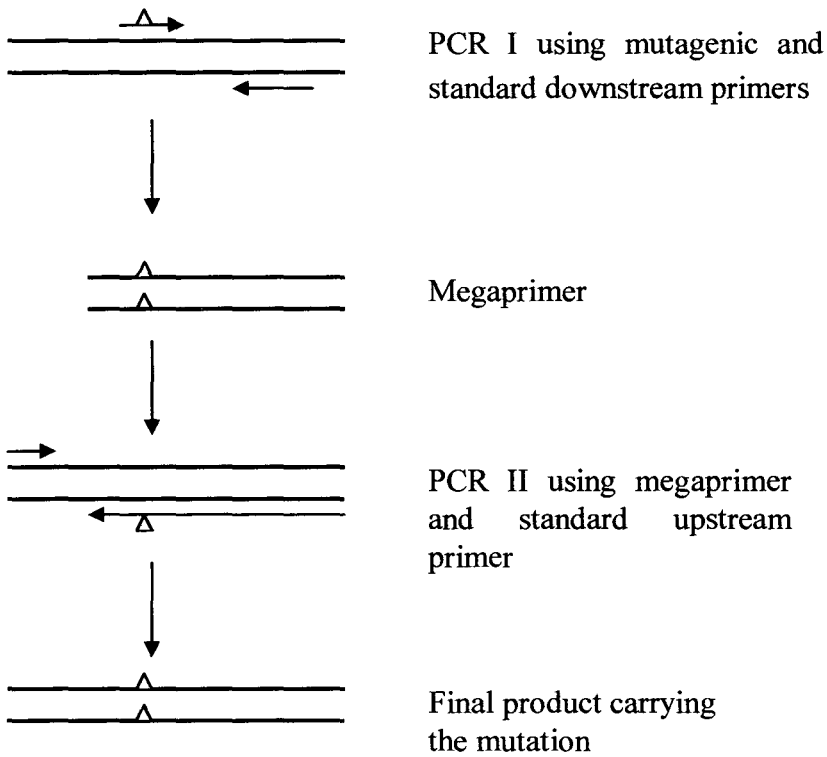

Figure 4.3 Diagrammatic representation of the 'megaprimer-extension' based PCR method used for the construction of site-directed mutants of SK α. The double-stranded DNA and primers are indicated by lines, with arrows indicating the 5′ to 3′ direction. The first round of PCR (PCR I) uses a 'mutagenic' primer (one carrying a predefined mutation) and the downstream primer to generate a fragment with the desired mutation. The resulting product is used subsequently in a second round of PCR (PCR II) alongwith the upstream primer, and the extended final fragment is then purified and subjected to digestion with REs prior to cloning into the appropriate vector.

Table 4B Sequences of primers used for the construction of site-directed mutant of SK α, in order to minimize HPN-mediated proteolysis

Mutation	Sequence of primer	RE site[a]
mutagenic U* *(K59E)*	5′ AGGCTTAAGTCCCGAGTCAAAACC-ATTT 3′	Ava I
flanking U *(T7 Pro-mod)*	5′ GAAATTAATACGACTCACTATAGG-GGAATTGTG 3′	
flanking D *(T7 Termmod)*	5′ CCAAGGGGTTATGCTAGTTATTGC-TCA 3′	

[a] The diagnostic RE sites introduced in the primers by translationally silent mutagenesis, used during the screening of clones, have been underlined.
U* represents upstream primer and D represents down stream primer.
Parentheses describe the names of the primers.

first subjected to a 'hot-start' of 5 min at 95°C, which was followed by 25 amplification cycles of denaturation (94°C for 45 sec), annealing (50°C for 2 min) and extension (72°C for 1 min) and a final extension at 72°C for 10 min. Then the PCR amplification product was purified on agarose gel and was subjected to digestion with REs, PshA I and Xho I. The insert obtained from RE digestion of the PCR product and the vector sequence obtained after digestion of the pET-23d-α construct with PshA I and Xho I, were purified from agarose gel, ligated with each other and transformed into *Escherichia coli* chemical competent cells. The positive clones were selected by restriction analyses of the mini-preps, using RE diagnostic sites that have been introduced in the mutagenic primers (see Table 4B). The sequences of the positive clones were confirmed by automated DNA sequencing.

4.2.4 Cloning of open reading frame encoding the α domain of SK into pBluescript vector (pBS-α)

The PCR-amplification product of pET-23d-α, using primers 'apmg-up' and 'apmg-dp-Not I' (sequences depicted in Table 4C) was gel-extracted using Qiagen Gel Extraction Kit and further subjected to digestion with REs, PshA I and Not I. The digested PCR product (insert) was again gel-extracted and ligated with the vector comprising of pBS-SK plasmid, digested with the same two REs (the site for PshA I is present at the N-terminal region in SKα, while site for Not I is present C-terminal to the SK gene, in the vector pBS). The ligation mixture was then transformed into chemical competent cells of XL1-Blue host strain. The sequences of positive clones were confirmed by automated DNA sequencing. The circular map of pBS-α is given in Figure 4.4. The gene encoding the α_{loop} was also sub-cloned into pBS-SK vector, by a procedure similar to one mentioned above.

4.2.5 Localized random mutagenesis, cloning and screening for improved function

As described above, the α_{loop} construct was cloned in pBluescript KS II (-) containing an *ompA* signal sequence upstream of the α sequence that directs the secretion of low levels of α_{loop} into the culture medium. The region immediately flanking the loop in the α domain of SK was subjected to random mutagenesis

Table 4C Sequences of primers used for combinatorial mutagenesis

Mutation	Sequence of primer	RE site[a]
mutagenic U* *(rdmlp-fp)*	5'ATTGATTTTGCAAGCGATGCAACCNNNNNNNNN-NNNTATGACGCGAATGCGAATGCGAAGAAGGAG 3'	Bsm I
mutagenic U *(rdmlp-dp)*	5' TACCGATCCATCTTTGTCAGCAAAGTANNN-NNNNNNNNNCTCCTTCTTCTTATTCTTGTCATA 3'	
flanking U *(apmg-up)*	5'TGTTGAGGGGACGAATCAAGACATTAGTCTTAA-ATTTTTTGAAA 3'	PshA I
flanking D *(apmg-dp-NotI)*	5' TTCCTTTTGCGGCCGCTTAAACGCGCACATGTC-CGTTAGAACAAA3'	Not I
flanking D *(143XhoI)*	5'ATCTTGCTCGAGAACGCGCACATGTCCGCTTA-GCAA3'	Xho I
flanking U *(T7 Pro-mod)*	5'GAAATTAATACGACTCACTATAGGGGAATTGTG 3'	
flanking D *(T7 Term-mod)*	5' CCAAGGGGTTATGCTAGTTATTGCTCA 3'	

[a] The diagnostic RE sites introduced in the primers by translationally silent mutagenesis, used during the screening of clones, have been underlined.
U* represents upstream primer and D represents down stream primer.
Parentheses describe the names of the primers.

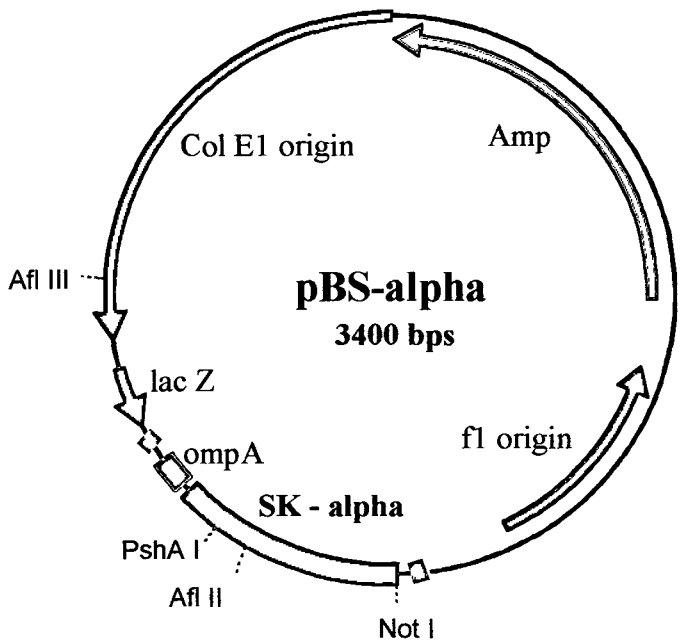

Figure 4.4 Circular map of pBS-α. This figure shows the gene encoding SK α in the pBluescript II KS (-) vector. The RE sites, PshA I and Not I, which were used to clone SK α gene in the vector are also indicated. The map also shows the presence of the *ompA* signal upstream to the α gene to facilitate the secretion of the protein out of the plasma membrane.

(localized to four amino acid residues on both sides of the SAK loop in α) using overlap-extension PCR (Ho *et al.*, 1989). The sequences of mutagenic primers (rdmlp-fp and rdmlp-dp) and the upstream (apmg-up) and downstream (apmg-dp-Not I) flanking primers have been listed in Table 4C. The randomly mutagenised amplification product was double-digested with REs, PshA I and Not I, gel-purified and ligated with similarly digested pBS-α, generating a plasmid library of α_{loop} mutants. The library containing the PCR-mutagenized gene was used to transform XL10-Gold® Ultracompetent cells of *Escherichia coli* (Stratagene Inc.). The resulting transformants were initially screened for higher plasminogenolytic ability, indicated by larger zones of clearance when compared to the zone formed by the parent plasmid, using the casein-HPG-agarose overlay method (Malke and Ferretti, 1984). The schematic representation of the procedure followed for random mutagenesis has been given in Figure 4.5.

This was followed by purification of α from the open reading frames corresponding to the clones with bigger haloes, followed by their detailed functional analyses after expression under the T7 RNA polymerase promoter in pET-23d vector. To transfer each mutein cassette from pBluescript vector to pET-23d vector, PCR amplification of the gene using primers, apmg-up and 143XhoI was carried out. The PCR product was then digested with PshA I and Xho I; and the digested product was then ligated with the similarly cut pET-23d-α. After transformation, clones were screened and the sequences of positive clones confirmed by automated DNA sequencing.

4.2.6 Casein-HPG overlay assay for detection of SK activity

Bacterial colonies producing SK were detected by overlay of casein and HPG in soft agar (Malke and Ferretti, 1984). After spread-plating the LB-Amp agarose plate with IPTG (final concentration of 50 mM), each clone corresponding to a random mutant was picked up and pitch-patched on the plate, taking care such that cross-contamination was minimized. The plate was then incubated at 37°C for 10 h; thereafter, casein-HPG-agarose plate was prepared by gently pouring the mixture of solutions A and B on top of the plate containing the colonies. Solution A was prepared by heating 0.52 g of skim milk (7 %) in 7.5 ml of 50 mM Tris.Cl (pH 7.5),

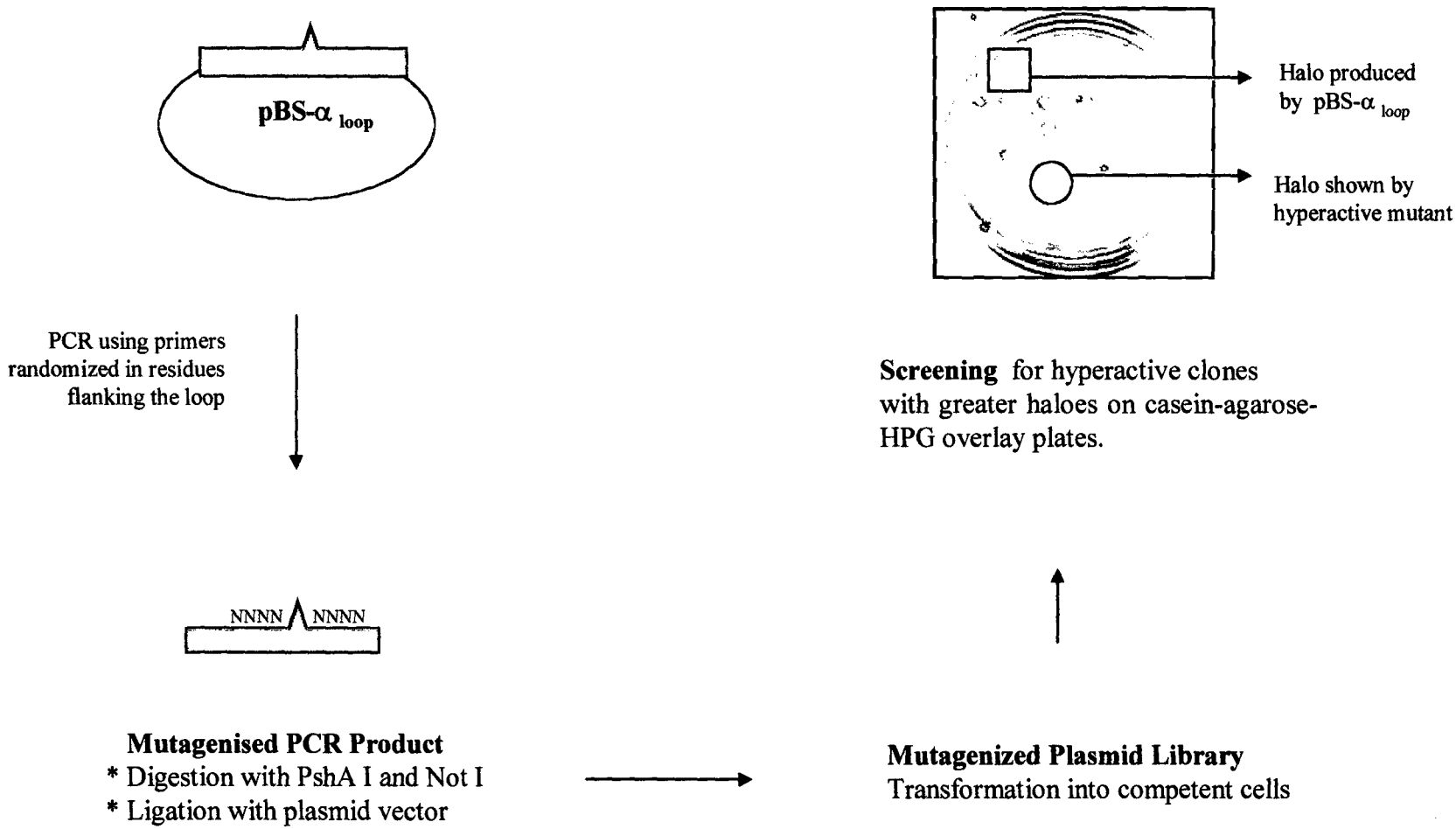

Figure 4.5 Schematic representation of the strategy of localized random mutagenesis and screening for 'hyperactive clones'. PCR mutagenesis was localized to the region of pBS-α_{loop}, in the immediate vicinity of the SAK loop inserted into the α domain of SK (as described under Materials and Methods). The amplification product was digested with restriction enzymes PshA I and Not I, extracted and ligated with the vector, generating a mutant library that was transformed into competent cells. Thereafter, screening was done to select 'hyperactive' clones, using the *in situ* radial caseinolysis plate assay.

after which it was maintained at 37°C in a water-bath till further use. Solution B was prepared by heating 0.19 g of agarose in 7.5 ml of 50 mM Tris.Cl (pH 7.5) at 50 °C. After tempering the solution to 37°C, 3 µl of TritonX-100 (0.04 % v/v) and 100 µg HPG was added. The plate was then incubated at 37°C and observed for the generation of zones of clearance due to casein hydrolysis, following HPG activation.

4.2.7 Expression and purification of different constructs of α domain

The single-domain construct α and all its mutants were expressed as proteins with His_6-tag extensions at their C-termini to aid their purification by affinity chromatography on Ni^{2+}-immobilized metal affinity chromatography (IMAC) (Porath *et al.*, 1975). A detailed description of the method of purification has been given in Vasudha (2002). Briefly, the *Escherichia coli* cells containing the pelleted IBs were first lyzed with Bug buster reagent (Novagen), and then the IBs were dissolved in 8 M urea and diluted fifteen-fold in 50 mM sodium phosphate buffer (pH 7.5) containing 10 mM imidazole and 250 mM NaCl. The mixture was then loaded on a Ni^{+2}-chelating Sepharose (Fast Flow) matrix-containing column, pre-equilibrated with 50 mM sodium phosphate buffer (pH 7.5) containing 10 mM imidazole and 250 mM NaCl. Successive washes with 50 mM sodium phosphate buffer (pH 7.5) containing 60 mM imidazole and 250 mM NaCl were given to remove unwanted, loosely bound proteins, and the His-tagged protein was finally eluted with 50 mM sodium phosphate buffer (pH 7.5) containing 250 mM imidazole and 250 mM NaCl. The protein eluted from Ni^{+2}-IMAC column was then subjected to DEAE-ion exchange chromatography. The protein from the IMAC column was diluted fifteen-fold with Tris.Cl buffer (pH 7.5) such that the final concentration became 20 mM Tris.Cl (pH 7.5), after which it was loaded onto a column packed with DEAE-Sepharose (Fast Flow) pre-equilibrated with 20 mM Tris.Cl (pH 7.5). After washes with buffer containing 20 mM Tris.Cl (pH 7.5), the protein was eluted with buffer containing 20 mM Tris.Cl (pH 7.5) containing 0.4 M NaCl. This process yielded imidazole-free α/α mutant preparations that were routinely more than 95 % pure as analyzed by SDS-PAGE.

With a view to rapidly purify several proteins simultaneously, a strategy was devised. The IBs of different α derivatives were prepared by the procedure discussed above, that were then resuspended in 8 M urea, further diluted ten-fold and then loaded onto syringes containing Ni^{+2}-chelating Sepharose (Fast Flow) matrices whose

tips had already been inserted into a vacuum manifold (Promega's Vac-Man), attached to a vacuum source. The rate of loading was adjusted using the stopcock, taking care that the resins did not dry. Further washes were given with 50 mM sodium phosphate buffer (pH 7.5) containing 60 mM imidazole and 250 mM NaCl and finally, the protein was eluted manually with 50 mM sodium phosphate buffer (pH 7.5) containing 250 mM imidazole and 250 mM NaCl. This yielded homogeneous α/α derivative with an overall purity of more than 95 %. This model was used for a number of α mutants and they showed very consistent results. Thus this method can be used to rapidly purify many proteins at a single time, during the screening process.

4.2.8 Preparation of microplasminogen

Microplasminogen (μPG) was prepared by cleavage of HPG by HPN (10:1 molar ratio of HPG and HPN) under alkaline conditions (0.1 N glycine/NaOH buffer, pH 10.5) at 30°C, as described in Chapter III, under Materials and Methods (Shi and Wu, 1988). The purity of μPG formed was analyzed by SDS-PAGE and the identity of the protein was confirmed by N-terminal protein sequencing.

4.2.9 Assay for measurement of very low intrinsic cofactor activities

Catalytic amounts of α/α mutant were added to the assay buffer (100 mM phosphate buffer, pH 7.5) containing 2 μM of HPG and chromogenic substrate (0.5 mM) and the change in absorbance was monitored spectrophotometrically at 405 nm as a function of time at 22°C. In order to detect intrinsically low HPG activation capability that may otherwise not be detected due to inability to activate partner HPG unless provided with a preformed HPN active site, equimolar complexes of HPN and α/mutant were prepared, and catalytic amounts (5 nM) were withdrawn and added into assay cuvettes containing 2 μM HPG and chromogenic peptide substrate (0.5 mM) in the assay buffer, 100 mM phosphate buffer, pH 7.5. The reactions were recorded spectrophotometrically at 405 nm and the progress curves obtained from corresponding control reactions (containing HPG and same amounts of HPN, but no α domain) were subtracted from the test reactions. The resultant curves so obtained were used to determine the rate of HPG activation, which was then expressed as % activity, relative to SAK.

In order to explore whether $\alpha_{wild\text{-}type}$ or its mutants had genuine activator activities over and above that associated with the 'background' of the host cells, *Escherichia coli* BL21 cultures transformed with the pET-23d vector but not containing α, after induction with IPTG, were harvested and lyzed similarly as ones prepared for purifying α. These cell lysates were subjected to exactly the same treatments as the ones prepared from cultures harbouring plasmids for α, including IMAC and desalting steps. The fractions from 'control' columns (on which the lysates containing just the expression plasmids without α were processed) identical in volume to the corresponding eluted protein fractions from the 'test' columns (from which the domain was being purified) were collected in parallel and these were then used for assessing cofactor activities, as described above. Thus, the 'control' fractions served to measure the background *Escherichia coli* cell-associated HPG activator activity (Lundrigan and Webb, 1992; Mangel *et al.*, 1994), if any, present in the 'test' fractions.

4.2.10 Determination of kinetic constants for cofactor activity

Varying amounts of HPG (0.5-7 μM) were added to the assay cuvette containing fixed amounts of preformed complexes of HPN and α/α mutant (5 nM) and chromogenic substrate (0.5 mM) and the change in absorbance was monitored at 405 nm as a function of time at 22°C. To compute the k_{cat}, the number of functional HPN active sites was determined by titration with an active-site acylating reagent, NPGB (McClintock and Bell, 1971; Chase and Shaw, 1969).

4.2.11 Kinetic Analysis of Protein-Protein Interactions using Resonant Mirror Technology

Binary interaction analysis- Association and dissociation between HPG and α/α mutants were followed in real time by resonant mirror-based detection using IAsys Plus™ system (Cambridge, UK) (Cush *et al.*, 1993; Buckle *et al.*, 1993). In these experiments, biotinylated HPG was allowed to bind to the streptavidin captured on the biotin cuvette. Nonspecifically bound HPG was then removed by repeated washing with phosphate-buffered saline followed by three washes with 10 mM HCl. Experiments were performed at 25°C in 50 mM phosphate buffered saline, pH 7.5 containing 0.1 %

Tween 20, 250 mM NaCl, and 50 μM NPGB (binding buffer). The latter was included in order to prevent HPN-mediated proteolysis. Thereafter, varying concentrations of either α/ α derivatives were added, and each binding response was monitored during the 'association' phase. The cuvette was then washed with the binding buffer, and the 'dissociation' phase was then monitored (Myszka, 1997). The cuvette was washed with 10 mM HCl, after each cycle, and base line was re-established with the binding buffer. In parallel, in the control cell in the dual channel cuvette, immobilized streptavidin alone was taken as a negative control for the binding studies. The data were analyzed and the binding constants were than calculated as mentioned in Chapter III, under Materials and Methods.

Ternary interaction analyses were also carried out to measure the rate and equilibrium dissociation constants describing interactions between HPG and α/α derivatives complexed with immobilized HPG. Varying concentrations of 'ternary' HPG (0.1-1.0 μM) were then added to monitor the binding by recording the association phase. Subsequently, the dissociation phase was recorded after washing the cuvette with the binding buffer. After each cycle of analysis, the original base line was re-established by stripping off the undissociated ternary ligate with 2.5 mM EACA followed by wash with binding buffer. It was earlier established that EACA, at this concentration, completely abolishes the interaction of ternary HPG with the binary SK.HPG complex, while the binary complex remains stable. Equilibrium dissociation constant/s were determined by analysis of the extent of association as well as from k_d/k_a. Dissociation and association constants were calculated by the procedure similar to the one followed in case of binary interaction analysis.

4.2.12 Proteolytic stability of α/α derivatives

Purified α/α mutants were pre-incubated with HPN at 22°C in the assay buffer, for varying time periods (0, 60, 180 and 300 sec). Samples were withdrawn after each time point, and the reactions stopped by addition of 100 μM NPGB (to stop HPN-mediated proteolysis; Chase and Shaw, 1969; Conejero-Lara *et al.*, 1998) followed by 5x SDS-PAGE sample buffer. These were then analyzed for extent of proteolytic degradation on a 15 % polyacrylamide gel.

4.2.13 N-terminal amino acid sequencing of α/ α mutants

The purified recombinant α/α mutants expressed in *Escherichia coli* were subjected to N-terminal amino acid sequencing in order to compare their sequences with that of natural SK from *Streptococcus equisimilis* H46A. The N-terminal amino acid sequences of the degradation products obtained from the proteolysis studies were also determined (the sequencing was carried out for 25 cycles using an ABI-PE model 476A Protein Sequencer).

4.2.14 Fibrin clot lysis study

Fibrin clot lysis in microtiter plates was carried out with minor modifications of the method suggested by Wu and co-workers (2003). Fibrin clots were formed by adding human thrombin (final concentration of 0.6 NIH units/ml) and $CaCl_2$ (final concentration of 2 mM) to human fibrinogen (1 mg/ml, final concentration) in HEPES-buffered saline (0.01 M HEPES, 0.13 M NaCl, pH 7.5). Aliquots of 100 µl each of the polymerizing fibrin solution were pipetted into the wells of micro-titer plates (Falcon 3912 flat-bottom polyvinyl chloride plates, Becton Dickinson Labware, New Jersey, USA), immediately after mixing, and clot formation was allowed to proceed for 1-2 h at 37°C. A 100 µl solution containing HPG (final concentration of 2 µM) and SAK/SK/α/α derivatives (3 µM, final concentration) in HBS was then layered onto each clot. Thereafter, the changes in clot turbidity with time were monitored by measuring changes in the absorbance at 405 nm at 25°C, using an Emax precision microplate reader (Molecular Devices, U.S.A.) till the absorbance reached a value that was observed in a control well in which no thrombolytic agent had been added. Duplicate wells were prepared for each concentration and the experiment was repeated three times.

4.3 RESULTS

4.3.1 Expression and purification of the α domain of SK

In order to successfully consign meaningful structure-function correlations in any array of mutants, it becomes crucial to evolve simple and rapid screening and/or purification methods that would yield proteins of adequate purity that can be utilized

directly for binding and kinetic studies. The α domain of SK was first cloned after PCR amplification of the desired sequence using specific upstream and downstream primers which not only contained pre-selected restriction enzyme sites to allow for facile, directional docking of the amplified fragment into pET-23d, but also contained additional codons for six His residues at the C-terminal end for facile Ni^{+2}-affinity chromatography. In *Escherichia coli*, this modified open reading frame was expressed primarily in the form of IBs. These were harvested, washed and refolded (see Materials and Methods), and then purified to near-homogeneity (see Figure 4.6) through Ni^{+2}-affinity chromatography procedure, followed by ion-exchange chromatography. This method was also amenable to medium-throughput purification using a vacuum manifold system (described in Materials and Methods).

4.3.2 Cofactor activity of wild-type α domain of SK

After purification, the $\alpha_{wild\text{-}type}$ was checked for its functional ability to activate substrate HPG using assay procedures sensitive enough to detect specific activity for HPG activation as low as 0.0001 % that of native SK (see Materials and Methods). Substrate HPG activation by SK is known to proceed along two pathways (Wang *et al.*, 1999a). In Pathway I, a high-affinity complexation occurs between SK and partner HPG molecule, after which a virgin active site is formed in the zymogen even before any proteolytic cleavage has taken place (McClintock and Bell, 1971; Reddy and Markus, 1972). However, this complex rapidly converts to SK.HPN, the activator species that catalytically activates molecules of substrate HPG, after the partner HPG has been proteolytically converted to HPN. A functional SK.HPN activator complex can also be formed directly (Pathway II), wherein SK complexes with the active protease, HPN, which then can activate substrate HPG. Thus, generation of HPG activator activity is accomplished via two distinct, yet partially overlapping pathways, one through an intramolecular activation of zymogen, and second, via formation of activator complex between SK and preformed HPN (Castellino, 1981).

Apparent activities observed with purified $\alpha_{wild\text{-}type}$ using human Glu-PG (Pathway I), were not more than 0.002 % when compared to that of SK, measured under similar conditions. This observation supports the report of Loy and coworkers (2001) that the isolated α domain displays extremely low, virtually negligible, HPG activator activity. However, such meager levels of activator activity in these

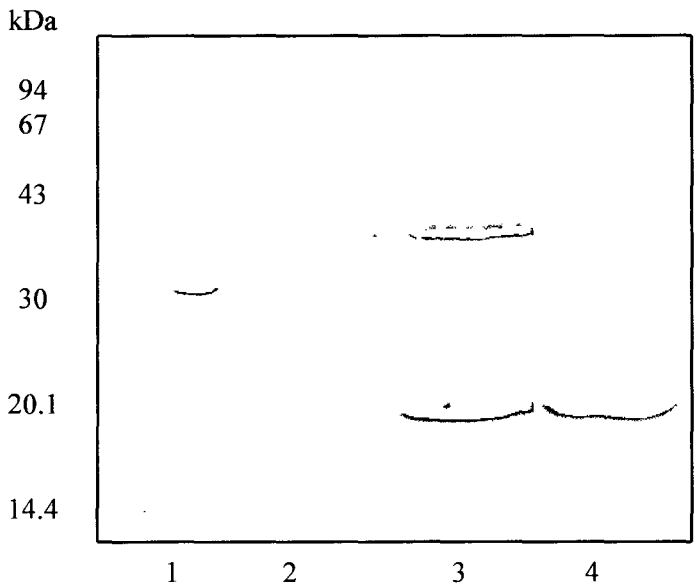

Figure 4.6 Purification of α/α mutants expressed in *Escherichia coli*. The α/α mutants were expressed as inclusion bodies and purified using Ni^{+2}-affinity chromatography. The lanes of the 15 % polyacrylamide gel represent: 1-standard MW markers, 2-whole cell lysate of uninduced cells, 3- whole cell lysate of induced cells, 4-purified protein.

constructs prompted us to investigate further whether this is 'true' activity or not since it is known that an outer membrane protein, termed omptin, present in certain strains of *Escherichia coli* also possesses HPG activator activity (Lundrigan and Webb, 1992; Mangel *et al.*, 1994). Indeed, in our experiments as well, crude cell-free lysates from *Escherichia coli* BL21 host cells transfected with expression plasmids without the α domain of SK, revealed a low, but easily measurable, HPG activator activity despite the fact that the host strain employed was *ompT* negative. This could be probably because several other genes closely homologous to *ompT* are also known to be present in *Escherichia coli* (Mangel *et al.*, 1994), thus raising the possibility that the *Escherichia coli* BL21 cells could be responsible for the low cofactor activity observed in the purified α domain of SK.

In order to explore whether the isolated α domain had genuine activator activities over and above that possibly associated with the 'background' cells, we subjected the lysates obtained from *Escherichia coli* BL21 cultures transformed with the pET-23d vector, but without the α domain-encoding cDNA insert, to exactly similar procedures of lysis and purification including the various purification steps viz. Ni^{+2}-affinity chromatography followed by DEAE-Sepharose ion-exchange chromatography (see Materials and Methods). The fractions from 'control' columns (on which the lysate containing just the expression plasmid without the gene encoding α domain was processed) were collected in 'parallel' to the ones eluted from the 'test' columns (from which the α domain was being purified), and these were then used for assessing HPG activator activity. Interestingly, although a distinct, concentration-dependent HPG activation activity was detected even in the 'mock' purified fractions, the purified α domain showed an activity distinctly higher that of the background BL21 (DE3) cells, establishing that the low activity associated with $\alpha_{wild\text{-}type}$ was indeed genuine.

4.3.3 Cofactor activity of the α.HPN activator complex against substrate HPG

Since the cofactor activity with substrate HPG (Pathway I) was very low, we examined the cofactor activity of $\alpha_{wild\text{-}type}$, after pre-mixing with equimolar amounts of HPN (Pathway II) to ascertain if the zymogen activation of partner HPG could be a rate-limiting step in expression of significant HPG activator activity in $\alpha_{wild\text{-}type}$.

Remarkably, the activity associated with that of $\alpha_{wild\text{-}type}$ was found to be highly dependent on HPN since a 25-fold increase in activity (0.05 % when compared to that of SK) was observed compared to the activity measured with HPG alone (0.002 % when compared to SK) (see Figure 4.7). However, though a genuine activator activity of the SAK type (that is, one that required preformed active site, in the form of HPN) existed in the α domain of SK, it still represented, at best, a very small fraction of that engendered by native SK.

4.3.4 Susceptibility of $\alpha_{wild\text{-}type}$ to HPN-mediated proteolysis

In order to assess if the activity associated with the α domain of SK was not under-estimation due to possible HPN-mediated proteolysis *during* the assay, $\alpha_{wild\text{-}type}$ was examined for stability by SDS-PAGE after exposure to conditions similar to those employed for our HPG activation assays (see Materials and Methods). Indeed, SDS-PAGE analysis by observing the time-dependent proteolysis profile showed signs of degradation of $\alpha_{wild\text{-}type}$ after initiation of the reaction, indicating that it was very labile to proteolytic scission (Figure 4.8). When the degradation band/s were subjected to N-terminal amino acid sequencing, the results revealed that the principal target of scission of $\alpha_{wild\text{-}type}$ by HPN was at the Lys59-Ser60 peptide bond.

4.3.5 Construction, expression, purification and characterization of α_{K59E}

With a view to possibly decrease the highly pronounced susceptibility of the Lys59-Ser60 peptide bond in SK to proteolysis mediated by HPN (which is like trypsin, specified for the C-terminal side of Arg and Lys residues), a single-point mutation (K59E) was introduced in the α domain, using the 'megaprimer' PCR-based method (see Table 4B, for sequences of primers used). In the past also, it has been shown that the mutation of this peptide bond results in stabilization of native SK and survival of cofactor activity in presence of HPN (Wu *et al.*, 1998; Shi *et al.*, 1998). The resultant construct, $\alpha_{K59E,}$ was then purified in a manner similar to that of $\alpha_{wild\text{-}type}$ and thereafter analyzed for proteolytic susceptibility to HPN, as well as cofactor activity. This analysis showed that α_{K59E} was considerably stabilized against HPN-mediated proteolysis when compared to $\alpha_{wild\text{-}type}$ (Figure 4.8), showing little signs of degradation even after 15 min of incubation with HPN under conditions where $\alpha_{wild\text{-}}$

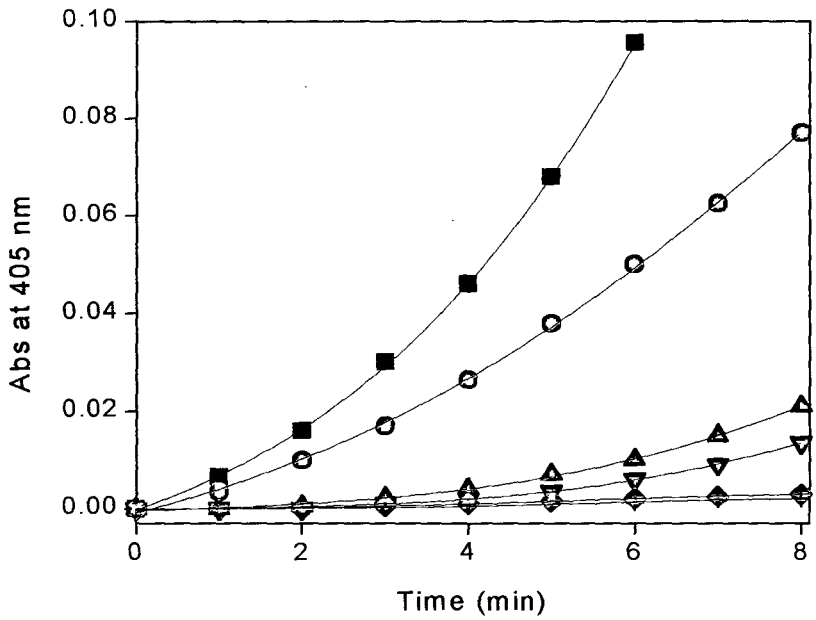

Figure 4.7 Activation of substrate HPG by $\alpha_{wild\text{-}type}$ and α_{K59E}. An equimolar mixture of either $\alpha_{wild\text{-}type}$ or α_{K59E} was prepared with HPN (0.5 μM each) and catalytic amounts of the complexes were added to the assay cuvette, already containing HPG (2 μM) and chromogenic substrate (0.5 mM) in assay buffer. The reaction was then monitored spectrophotometrically at 405 nm. The figure shows progress curves of HPG activation by varying concentrations (2 and 5 nM) of α_{K59E}.HPN complexes (black squares and red circles, respectively) and $\alpha_{wild\text{-}type}$.HPN complexes (green triangles and blue inverted triangles, respectively). Also shown are the basal activation (cyan diamonds) with a 'control' protein (from cells transfected with plasmid not containing the gene for α) that was purified from IBs by IMAC, using a protocol identical to that for α domain, and control HPN (magenta 'plus' symbols).

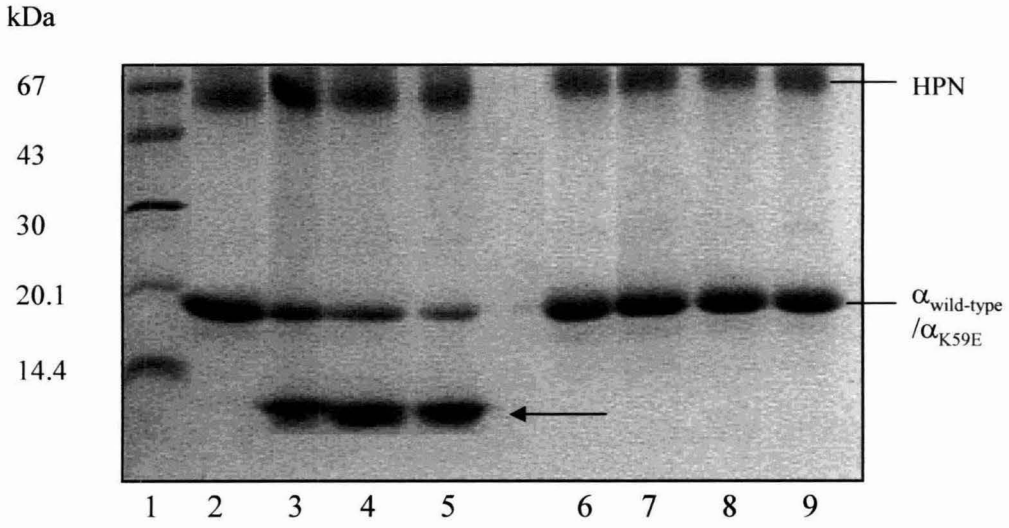

Figure 4.8 Composite picture of 15 % SDS-PAGE gel showing HPN-mediated proteolysis of $\alpha_{wild-type}$ and α_{K59E}. An equimolar mixture of $\alpha_{wild-type}$/α_{K59E} and HPN was made and aliquots were withdrawn after requisite time-intervals (0 s, 60 s, 180 s and 300 s) in case of $\alpha_{wild-type}$ (lanes 2-5, respectively) and α_{K59E} (lanes 6-9, respectively). The reactions were rapidly quenched using NPGB (100 μM) followed by addition of 5x sample buffer. The arrow indicates the degradation band observed in case of $\alpha_{wild-type}$ that was N-terminally sequenced to examine the principal site of HPN-mediated cleavage of SK α.

$_{type}$ was completely degraded to small-MW products. Also, when α_{K59E} was assessed for its ability to activate HPG, under similar conditions of assay as employed for $\alpha_{wild\text{-}type}$ (that is, using HPN as partner), there was a remarkable increase in cofactor activity, nearly an order of magnitude compared to that of $\alpha_{wild\text{-}type}$ (Figure 4.7). Thus the low activity of $\alpha_{wild\text{-}type}$ became strikingly enhanced when its intrinsic proteolytic vulnerability towards HPN-mediated degradation was decreased through the mutation of one of the key sites (Lys59-Ser60 peptide bond) that is highly susceptible to HPN-mediated proteolysis.

Thus, these results reveal that there certainly exists a potential for relatively high cofactor activity in the isolated α domain of SK, and which was overlooked earlier (Loy *et al.*, 2001) since HPN-mediated proteolysis was not examined as one of the causes for rapid decay of biological function of the isolated $\alpha_{wild\text{-}type}$ domain. However, our results clearly establish that once the proteolysis is minimized by mutation, the potential capability of this domain to activate HPG becomes increasingly manifest. The steady-state kinetic parameters associated with substrate HPG processing for SK α and SAK were then compared in order to compare the relative capabilities of the respective proteins. The kinetic data reveal that despite the addition of preformed HPN and minimizing the HPN-mediated proteolysis, the catalytic efficiency of α_{K59E} was still considerably lower (approximately 28-fold) than that of SAK.

4.3.6 Transposition of an eight-residue SAK loop into the α domain of SK dramatically enhances catalytic efficiency

In view of the fact that cofactor activity of the isolated α domain of SK was low as compared to that of SAK despite proteolytic stabilization, a question arises whether there are certain epitopes/ microstructures that are present in SAK, but absent in α, whose inclusion and correct juxtaposition into the 'deficient' α domain of SK might lead to enhanced catalytic efficiency. With this in mind, we carried out an analysis of the sequence homology between the different domains of SK and SAK and an examination of these crystal structures (Wang *et al.*, 1998; Parry *et al.*, 1998; Parry *et al.*, 2000). This exercise strongly suggested the presence of an eight-residue loop in SAK (Tyr-Asp-Lys-Asn-Lys-Lys-Lys-Glu) that is absent in SK α (see Figure

4.9). In the recent past, mutations in this region of SAK have been shown to affect the K_M of SAK with HPG (Rajamohan *et al.*, 2002). Therefore, with the premise that this loop in SAK might be involved in substrate sequestering and/or recognition in a manner demonstrated in case of the 250-loop in the β domain of SK (Dhar *et al.*, 2002), an insertion mutant (termed α_{loop}) with the SAK loop grafted between the Arg112 and Asn113 amino acid residues of the α domain of SK was constructed, employing the overlap-extension PCR method (see Table 4A and Materials and Methods for details). When expressed in pET-23d, fairly good expression levels for this 'hybrid' were observed. It was then purified by a one-step Ni^{+2}-IMAC chromatography, followed by an ion-exchange step to remove the imidazole in the purified preparation, and then subjected to kinetic assays with HPG.

When the 'loop-grafted' mutant (termed α_{loop}) was assayed for HPG cofactor specific activity after mixing with equimolar HPN, the construct showed a nearly two-fold higher cofactor-activity than α_{K59E}. To obtain an insight into the increased catalysis of α_{loop} for processing substrate HPG, analysis of its steady-state kinetic constants with HPG as substrate was then carried out. This showed a dramatic, nearly 6-fold decrease in K_M for HPG (0.33 μM for α_{loop} versus ~ 2 μM for α_{K59E}), thereby strongly indicating that besides a nearly 2-fold improved k_{cat}, the α_{loop} had an appreciably increased affinity for macromolecular substrate as compared to that of either $\alpha_{wild\text{-}type}$ or α_{K59E}.

4.3.7 Random mutagenesis of the flanking residues of the transposed SAK loop in α leads to further dramatic enhancement of catalytic efficiency

Since the cofactor activity of α_{loop} was considerably lower than that of SAK, one could reason that the presence of the SAK-derived loop in α domain, though structurally advantageous, was perhaps still not optimized with respect to its heterologous 'background' sequence (that is, SK derived) in this domain. It may be mentioned here that SAK and the α domain of SK, though structurally similar, display very little sequence homology between each other (Parry *et al.*, 1998). In other words, although grafting of the SAK loop into the α domain of SK did result in perceptible improvement in biological functioning, it might still not be optimally suited with respect to critical variables such as its contacts with the side-chains of the flanking

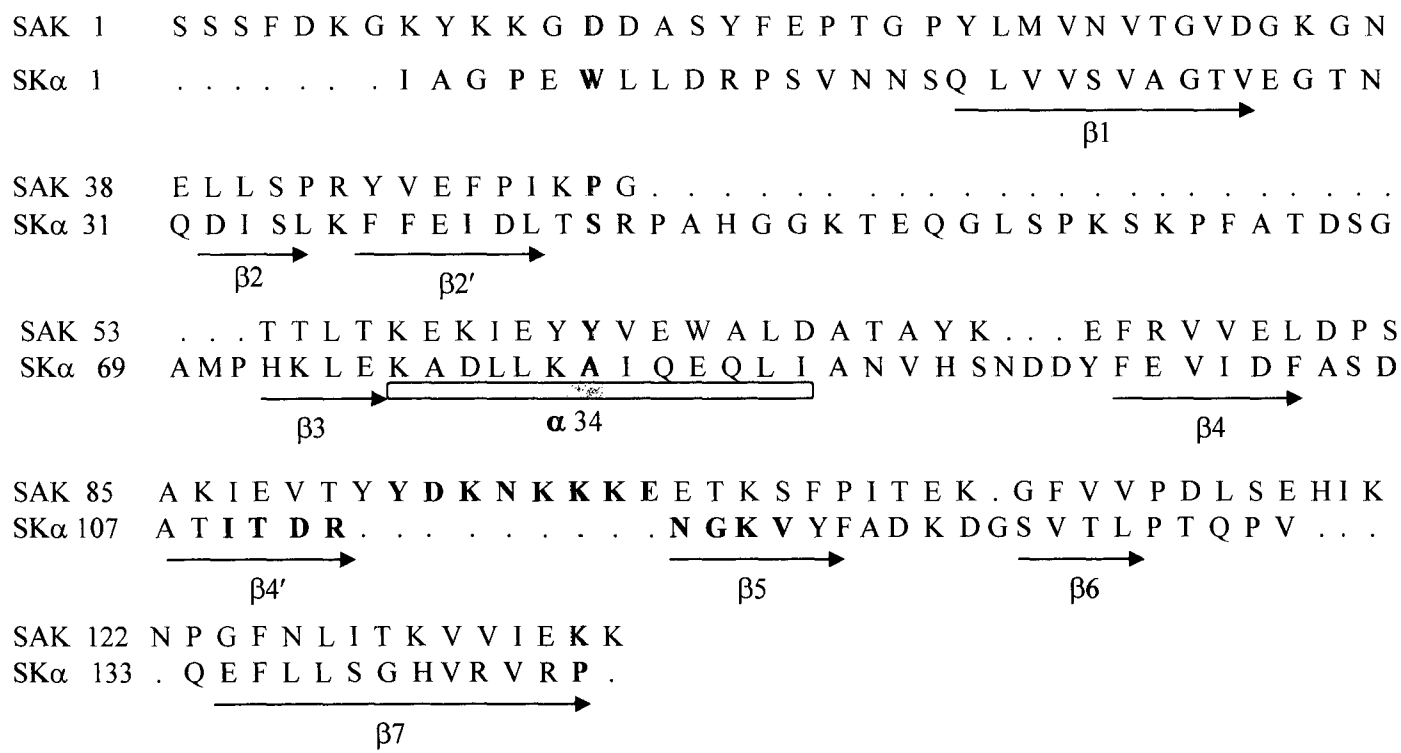

Figure 4.9 Sequence alignment of SAK and SK α. The alignment is based on the homology of their three-dimensional structures. Residue numbers are indicated at the beginning of each line. The secondary structure elements of SAK and SK α are shown at the bottom; β strands as arrows, and α helices as cylinders (adapted from Parry *et al.*, 2000). The amino acid residues in SK α, which are marked in black, are the flanks of the SAK loop in α, that were subjected to random mutagenesis.

residues, flexibility characteristics etc. thereby resulting in less-than optimal cofactor activity in the derivative that is less than its optimal capacity to induce.

Therefore, with a view to possibly optimize the stereo-chemical positioning and/or side-chain compatibility of the SAK loop in the α domain, localized random PCR- mutagenesis was carried out for the flanking residues on either side of the loop. Accordingly, oligonucleotides were synthesized in which twelve bases coding for four amino acid residues on each side of the SAK loop were randomized, and these were subsequently employed in overlap-extension PCR reactions to generate a library of mutant-PCR products with randomization of four residues on both flanks of the SAK loop (see Figure 4.5). The resultant amplification product was ligated with a suitably digested pBS-α vector to generate a repertoire of mutants (the sequences of primers used for this 'randomization' are depicted in Table 4C and the schematic representation has been given in Figure 4.5). If the assumptions implicit in carrying out this exercise were valid, the 'correct' primary structure/s that allow a more efficient functioning of the loop in the SK α context may be selected out in an *in situ* plate assay. Therefore, the library was expressed from the secretory plasmid in *E. coli*, and the screening for clones with bigger haloes on the casein-HPG plates was carried out (Malke and Ferretti, 1984). The *in situ* radial caseinolysis plate assay was adapted such that it allowed facile screening of hundreds of PG activator secreting clones at the same time, thereby bypassing laborious and time-consuming assay-based evaluation methods (see Materials and Methods for details). Approximately 10,000 clones were screened using the overlay assay and around five hundred clones showed 'bigger haloes' on the plates.

After this screening, minipreps of plasmid DNA from several of the clones exhibiting larger zones of casein clearance as compared to α_{loop} were then made and subjected to automated DNA sequencing. The sequencing data revealed a pool of loop sequences with random mutations in the four amino acid residues immediately flanking the two sides (see Table 4D). Remarkably, all the clones selected for hyperactivity were found to have mutations in the amino acid residues only on one side of the loop and none had mutations on both flanks simultaneously. Though a ready answer is not available at this stage for this observed 'bias', it is possible that alteration on both sides of the loop simultaneously adversely affects either the stability of the genetic construct or the secretion process, or it may be that mutations on both flanks at the same time are not conducive to higher functionality. To explore whether in the gamut of clones, clones

Table 4D Amino acid sequences of some of the combinatorial mutants constructed by limited random mutagenesis and selected based on the results of their larger zones of clearance on casein-HPG-agarose overlay plates.

Combinatorial mutant variant	Amino acid sequence
α_{loop}	5′- ITDR- loop -NGKV -3′
CM	5′- ITDR-loop- SAST -3′
CM1	5′-AGVR-loop -NGKV -3′
CM2	5′- ITDR-loop -QMTT -3′
CM3	5′- ITDR-loop-RKLV -3′
CM4	5′- ITDR-loop-YAQF -3′
CM5	5′- ITDR-loop-QRTS -3′

having mutations in both flanks exist or not, forty clones were randomly selected (but not on the basis of a larger zone of clearance/ but ones which were like the wild-type controls) and subjected to automated sequencing. In this case, ~ 3 % of the clones sequenced were indeed found to contain mutations in *all eight residues*, four each on either side of the loop (see Table 4E) suggesting that mutations in all eight residues are 'tolerated' at the genetic level (although the frequency is low) but are not apparently consistent with improved functioning.

4.3.8 Characterization of the combinatorial mutants

To investigate whether the greater zones of clearance on the casein overlay plates observed with some clones were actually representative of greater HPG activator activities (and not, say, just a result of improved secretion), six 'best hyperclones' were selected based on the plate assay, and each of these was then transferred to pET-23d expression vector by a single-step PCR-based sub-cloning procedure using specific primers (apmg-up and 143XhoI) for docking the α mutein cassette back into the pET vector (see Materials and Methods, and Table 4C). The DNA sequences of each of these mutants in pET vector were then reconfirmed by automated DNA sequencing.

Since all the α mutants carried His-tags at their C-termini, this process enabled rapid and facile purification of the mutants after expression in *E. coli* BL21 (DE3) by Ni^{+2}-IMAC affinity chromatography (see Materials and Methods for details). All six purified mutant proteins were then assayed for co-factor activities. These combinatorial mutants displayed specific activities that were 3-6 fold higher than α_{K59E}. One of the combinatorial mutants exhibited cofactor-activity that was ~ 6-fold higher than α_{K59E}. Remarkably, the steady-state kinetic analyses of this 'best' combinatorial mutant (designated as α_{CM}) showed a catalytic efficiency for HPG activation nearly that of SAK (see Table 4F and Figure 4.10).

4.3.9 Interaction of α/ α mutants with HPG

The successful resuscitation of a significantly enhanced catalytic activity in α domain of SK by protein engineering prompted us to examine the mechanistic basis of this effect, in order to derive beneficial structure-function insights. For this

Table 4E Variation in the amino acid sequences of twenty combinatorial mutants[a] to explore for the presence of simultaneous mutations on both sides of the SAK loop

S.No.	Combinatorial mutant variant	Deduced amino acid sequences of the residues flanking the loop that were subjected to random mutagenesis
1	CM a	5′-ITDR-loop -APPG-3′
2	CM b	5′-ITDR-loop-RGQQ-3′
3	CM c	5′-ITDR-loop-PKDV-3′
4	CM d	5′-ITDR-loop-QKSP-3′
5	CM e	5′-ITDR-loop-PAPD-3′
6	CM f	5′-WSRG-loop-NGKV-3′
7	CM g	5′-ITDR-loop-ASRP-3′
8	CM h	5′-ITDR-loop-SAPV-3′
9	CM i	5′-ITDR-loop-APPG-3′
10	CM j	5′-LGHG-loop-NGKV-3′
11	CM k	5′-GVVY-loop-NGKV-3′
12	CM l	5′-GRSK-loop-NGKV-3′
13	CM m	5′-GVPR-loop-NGKV-3′
14	CM n	5′-RHVG-loop-NGKV-3′
15	CM q	5′-ITDR-loop-NPNQ- 3′
16	CM r	5′-ITDR- loop-ARTQ-3′
17	CM s	5′-ITDR- loop-PREA-3′
18	CM t	5′-GNGV-loop-SAAR-3′
19	CM u	5′-ITDR- loop-PAGN-3′
20	CM v	5′-ITDR-loop-PLCL-3′

[a] These mutants were not associated with a greater zone of HPG-casein clearance, but were selected to examine whether simultaneous eight-residue mutations across the transposed loop of SAK were indeed generated in the ensemble of mutants or not.

Table 4F Steady-state kinetic parameters for HPG activation by equimolar mixtures of HPN and α/α mutants [a]

Activator species	K_M (μM)	k_{cat} (min^{-1})	k_{cat}/K_M (min^{-1} / μM)
SAK.HPN	2.5 ± 0.5	2.0 ± 0.3	0.8
α_{CM}.HPN	0.4 ± 0.2	0.28 ± 0.1	0.7
α_{loop}.HPN	0.33 ± 0.1	0.1 ± 0.03	0.3
α_{K59E}.HPN	1.8 ± 0.5	0.05 ± 0.2	0.028
$\alpha_{wild\text{-}type}$.HPN	1.7 ± 0.5	0.0063 ± 0.2	0.0037

[a] The kinetic parameters for co-factor activity against macromolecular substrate HPG were measured at 22°C, as described under Materials and Methods. The data represent the mean of three independent determinations.

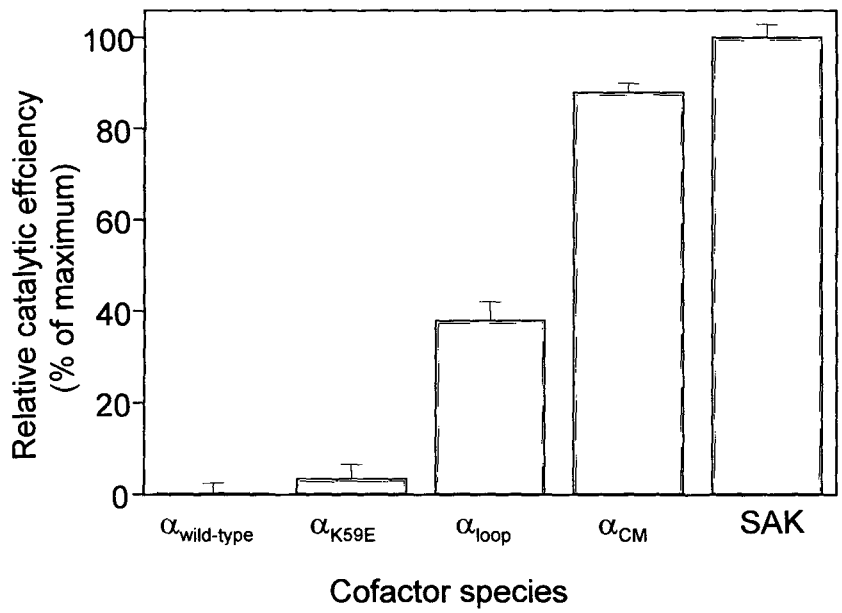

Figure 4.10 Relative catalytic efficiencies of SAK, $\alpha_{wild\text{-}type}$ and different derivatives of α, prepared by site-directed and localized-random mutagenesis. The histogram depicts the comparison of the relative catalytic efficiencies of SAK, $\alpha_{wild\text{-}type}$, α_{K59E}, α_{loop}, α_{CM}; in all cases, activity was measured along with equimolar HPN, for the activation of the macromolecular substrate, HPG. The catalytic efficiencies of the respective activator complexes were then calculated as % values in comparison to the catalytic efficiency of SAK.HPN (taken to be 100 %).

purpose, first various real-time binding parameters such as association and dissociation rate constants and equilibrium dissociation constants for binary interactions between immobilized biotinylated-HPG, and the α on one hand, and its various mutated constructs, on the other, were compared by the Resonant Mirror approach using a real-time semi-automatic molecular interaction system (IAsys Ltd., U.K.). The kinetic parameters so obtained for the binary interaction between immobilized HPG and α/α mutants are presented in Table 4G. These observations indicate that 'partner' HPG binds to α_{K59E} and α_{CM} with nearly the same affinity (K_D ~114 nM for α_{K59E} as against ~116 nM for α_{CM}). It may be noted that this is much weaker than SAK, which has a K_D ~ 1 nM (like SK). Since the binary complex of α or any of its mutants is much weaker as compared to SAK, this provides the first rational 'weakness' in this system, that is, full SAK-like activity may not be just achievable by virtue of this weakness. However, the fact that binding constants are still in the nanomolar range (in contrast to the micromolar range used during the assay conditions) some association (even if transient) must be occurring to generate a stable binary complex. Thus this aspect of activator.HPG interaction is most likely not the reason for the enhanced activity observed in α_{CM}. The K_D of binding to partner HPG in case of α_{loop} (~ 142 nM) was also in the range of that was observed for α_{CM}.

After examining the 1:1 interaction between $\alpha_{wild\text{-}type}$ and the α mutants with HPG, ternary interactions between 'substrate' HPG and $\alpha_{K59E}/\alpha_{loop}/\alpha_{CM}$ pre-complexed with immobilized HPG were examined using an approach also based on the Resonant Mirror technique. The application of the Resonant Mirror technique to studying ternary interactions in the SK.HPG system has been described earlier in Chapter III, in which biotinylated HPG was first immobilized onto the surface of a Resonant Mirror biotin-cuvette onto which a thin film of streptavidin had earlier been layered ('sandwiched'), followed by washing with buffer to remove excess unbound HPG. According to this procedure (see Materials and Methods) the immobilized HPG is then allowed to interact with α domain to form equimolar α.HPG complex. The binary complex so formed is washed with buffer, followed by the addition of different concentrations of excess 'substrate' HPG. This yields additional 'ternary signals' over and above that obtained earlier at the binary complexation stage, and thus the kinetics of formation of a ternary HPG.α.HPG complex can be observed and studied in real

Table 4G Association and dissociation rate constants and apparent equilibrium dissociation constants of 'partner' HPG with α/ α mutants [a]

Activator protein	k_a ($M^{-1} s^{-1}$)	k_d (s^{-1})	K_D (M)
α_{K59E}.HPN	$0.14 \pm 0.05 \times 10^{7}$	$1.6 \pm 2.0 \times 10^{-1}$	$114 \pm 10 \times 10^{-9}$
α_{loop}.HPN	$0.14 \pm 0.04 \times 10^{7}$	$2 \pm 1.9 \times 10^{-1}$	$142 \pm 15 \times 10^{-9}$
α_{CM}.HPN	$0.18 \pm 0.05 \times 10^{7}$	$2.1 \pm 1.7 \times 10^{-1}$	$116 \pm 9 \times 10^{-9}$

[a] The kinetic constants for the binary interaction between immobilized biotinylated-HPG and α/α mutants were determined by applying the FASTfit™ program (IAsys Ltd., U. K.) to the binding data obtained using the IAsys plus biosensor system, as described under Materials and Methods.

Figure 4.11 Composite pictures of IAsys™ Resonant Mirror-based real-time kinetic analysis to explore the ternary interactions between substrate HPG and equimolar binary complex of α/α derivatives and immobilized HPG. The experiment was carried out at 25°C in binding buffer as described under Materials and Methods. Human PG was biotinylated and immobilized onto a layer of streptavidin captured on the biotin cuvette surface. Stable binary complexes were then formed by adding saturating concentration of either α_{K59E} (1 μM, panel A), α_{loop} (1 μM, panel B), and α_{CM} (1 μM, panel C) onto the immobilized HPG. The point of addition of α/α derivatives (*viz.* α, panel A; α_{loop}, panel B; α_{CM}, panel C) in the top three panels (A-C) is depicted by vertical arrows, all marked 1. After washing with binding buffer (point of addition of binding buffer depicted by arrow marked 2), a stable dissociation baseline (except in case of α domain, panel A) was rapidly obtained due to the high affinity and stability of the binary complexes. Thereafter, various concentrations of substrate HPG (0.1-1μM) were added onto the binary complexes. However, for clarity in the figure, only a single (saturating) concentration of HPG (1 μM) is depicted (shown in panels A and B by arrows, marked 3). The association phases were monitored for ~5 min and subsequently the cuvettes were washed with the binding buffer (point of addition depicted in panels A and B by vertical arrows marked 4). After each cycle of analysis in A and B, the undissociated substrate HPG was stripped off with 2.5 mM EACA, followed by re-equilibrating the cuvette with binding buffer, which re-established the original baseline (data not shown). The non-specific binding interaction between added substrate HPG with the HPG immobilized onto the cuvette in the absence of any α/α derivatives is depicted in panel D (arrow 1 depicts the addition of protein, arrow 2 depicts the addition of binding buffer, arrow 3 depicts the addition of HPG and arrow 4 depicts the dissociation of non-specific HPG with the binding buffer). Note that the non-specific signal was found to be less then 20% of the ternary signal in case of α/α derivatives. In a separate experiment, the immobilized streptavidin alone was also taken as a negative control, and it was subjected to the same kind of treatments as given to the test cell containing immobilized HPG. Under these conditions no significant non-specific binding was observed (data not shown).

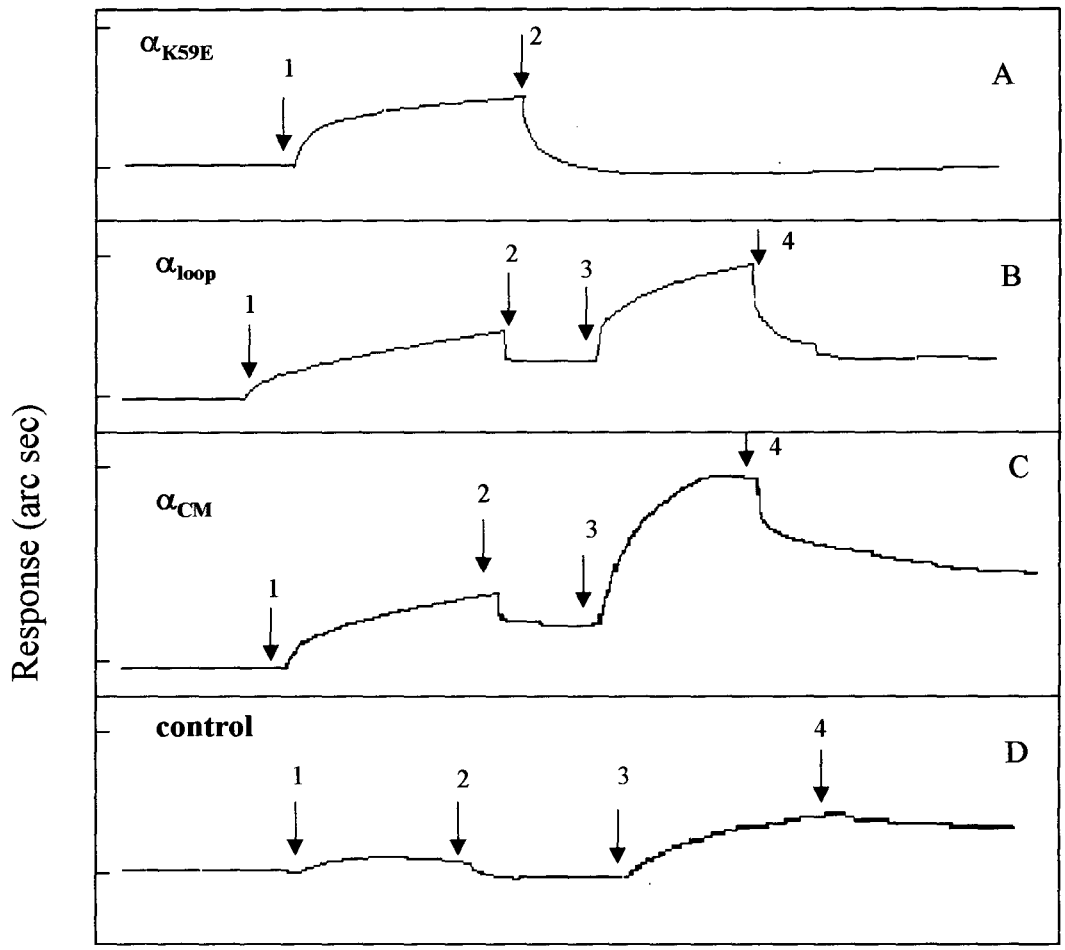
α_{K59E}
1
2
A
α_{loop}
1
2
3
4
B
α_{CM}
1
2
3
4
C
control
1
2
3
4
D
Response (arc sec)
Time (min)

Figure 4.11

Table 4H Association and dissociation rate constants and apparent equilibrium dissociation constants of 'substrate' HPG with α/α mutants [a]

Activator protein	k_a ($M^{-1} s^{-1}$)	k_d (s^{-1})	K_D (M)
SAK.HPN	$1.0 \pm 0.4 \times 10^{5}$	$4 \pm 0.3 \times 10^{-2}$	$0.4 \pm 0.1 \times 10^{-6}$
α_{K59E}.HPN	n.d.*	n.d.	n.d.
α_{loop}.HPN	$6.1 \pm 0.5 \times 10^{5}$	$9.7 \pm 0.2 \times 10^{-2}$	$0.16 \pm 0.01 \times 10^{-6}$
α_{CM}.HPN	$4.5 \pm 0.4 \times 10^{5}$	$4.5 \pm 0.5 \times 10^{-2}$	$0.1 \pm 0.005 \times 10^{-6}$

[a] The kinetic constants for the binary interaction between immobilized biotinylated-HPG and α/α mutants and thereafter, those of the ternary interaction of substrate HPG with α/α mutants were determined, as mentioned under Materials and Methods. A stable binary complex between α/α mutant and HPG immobilized onto the cuvette was first made, and then the binding of varying concentrations of HPG (0.1-1 μM) was monitored. The kinetic constants were determined by applying the FASTfit™ program to the binding data obtained using the IAsys plus biosensor system, as described under Materials and Methods.

* n.d.: could not be determined (see text for details)

time, as depicted in Figure 4.11. Thus, altered substrate-interacting capability, if exhibited by a given α mutant, can be potentially observed using this procedure of 'docking' substrate HPG onto a pre-formed binary complex, provided the latter is stable on the time-scale of such an experiment. Earlier, we have seen that this approach works well with SK. When this assay was carried out with α/α mutants, it was observed that real-time kinetic constants for ternary complexation, in case of either $\alpha_{\text{wild-type}}/\alpha_{\text{K59E}}$ could not be determined with reliability (Figure 4.11, panel A), due to the intrinsically weak affinity of this protein for binary complex formation with HPG even at the highest possible concentration of substrate HPG employed (1 μM). Under the same conditions, however, ternary complexation by SK.HPG as well as SAK.HPG, were clearly detectable. In contrast to $\alpha_{\text{wild-type}}/\alpha_{\text{K59E}}$, however, whose binary complex with immobilized HPG dissociated rapidly even by moderate buffer washing conditions, the respective binary complexes of α_{loop} and α_{CM} with HPG were relatively more stable to washing (see Figure 4.11, panels B and C) and hence, ternary interactions with substrate HPG could be measured (see Table 4H). The K_D of the ternary interaction of substrate HPG with α_{CM} (~ 0.1 μM) was found to be slightly lower when compared to that of α_{loop} (~ 0.2 μM) (see Table 4H). Also, the dissociation rate constant (k_d) in case of α_{loop} was observed to be twice that of α_{CM}, these enhanced off-rates (lesser residence time) could be indicative of the observed biological properties of α_{loop} and α_{CM}. These results clearly demonstrate that α_{CM} is capable of docking macromolecular substrate, a property that α lacks virtually completely. In contrast to the α mutants, when the 'ternary' interaction of the binary complex of SAK and HPG was analyzed, the equilibrium dissociation constant was found to be approximately 4-fold higher than that of α_{CM} which is not inconsistent with the differences observed in their K_M parameters for HPG activation viz. 2.5 μM for SAK and 0.4 μM for α_{CM} (see Table 4E). Under these conditions, the non-specific signal resulting from binding interactions between added substrate HPG with the HPG immobilized on the cuvette, in absence of α/α derivatives, was found to be considerably less than the ternary signal in case of α/α derivatives (Figure 4.11, panel D). The foregoing results indicate that atleast one of the principal mechanistic reasons for enhancement in the cofactor activity associated with α_{CM} over that of α_{loop} was via

an increased affinity of the ternary complex between binary complex for substrate HPG.

4.3.10 Interaction of α/α derivatives with microplasminogen (μPG)

If the difference in substrate affinities between activator complexes of $\alpha_{K59E}/\alpha_{loop}/\alpha_{CM}$ is arbitrated by the kringle domains of HPG, it is logical to presume that the rates of activation of substrate μPG, which is devoid of all five HPG kringles, by respective HPN complexes of $\alpha_{K59E}/\alpha_{loop}/\alpha_{CM}$ should not substantially differ from each other. Microplasminogen was prepared by HPN-mediated enzymatic cleavage of HPG. Activator assays using μPG as the substrate and the activator complexes formed between HPN and different α/α mutants were carried out. Interestingly, all of them showed an activity of ~ 1 %, when μPG was used as the substrate; in other words, no discernable difference was observed between α_{K59E}.HPN, α_{loop}.HPN and α_{CM}.HPN with respect to initial velocities of substrate μPG activation, under conditions where the activator activities of the activator complexes (α_{K59E}.HPN, α_{loop}.HPN and α_{CM}.HPN) had shown substantial differences when native HPG was used as substrate. These observations strongly point out that the kringle domains of substrate might be involved in the latter's recognition by the activator complex of α_{loop}.HPN or α_{CM}.HPN.

To further establish that kringles are indeed involved in improving activator-substrate interactions in α_{CM}, ternary binding experiments on the Resonant Mirror where the binding of substrate μPG onto the preformed binary complexes of α/α derivatives with immobilized HPG were carried out. As shown previously with HPG, in case of α_{K59E}, real-time kinetic constants for ternary complexation could not be determined due to the weak affinity between α and immobilized HPG, as a result of which the complex dissociated rapidly even with moderate washing with buffer. However, the binary complexes of α_{loop} and α_{CM} with biotinylated HPG were stable enough to 'capture' the ternary interactions with μPG. Remarkably, α_{loop} and α_{CM} showed very similar affinities for substrate μPG in the ternary interaction mode (K_D ~ 0.28 μM).

The above-described results give credence to the premise that the loop of SAK, once juxtaposed in the α domain of SK helps to recognize the kringle domains of substrate HPG during the catalytic cycle, resulting in an appreciable increase in the affinity of the activated complex for the macromolecular substrate. Localized random mutagenesis in the flanks of the loop led to further optimization of the turnover rates for HPG activation with the loop-inclusive derivative, probably via either an improvement of the stereochemistry of the interaction with substrate HPG, or via a favourable alteration in the flexibility of the loop, thereby leading to a catalytic enhancement in the 'hybrid' molecule over the one in which the SAK loop had been placed in the SK sequence context without an alteration in sequence.

4.3.11 Fibrin clot-lysis

It was of interest to investigate whether the higher levels of HPG cofactor activity engendered into the various α derivatives compared to that of $\alpha_{wild\text{-}type}$ were also actually translated into an increased ability to lyse fibrin clots. For this purpose, fibrin clot lysis assays were carried out using an ELISA plate protocol (Wu *et al.*, 2003) in which the various constructs as well as SAK were allowed to act upon preformed fibrin clots, prepared *in vitro* by the action of thrombin on human fibrinogen. The loss in turbidity on the ELISA plate was then continuously monitored over time at 405 nm. Interestingly, like SAK and SK that are well known to dissolve clots, α_{CM} was also able to mediate clot-lysis with nearly a similar efficacy, a fact that supports its action in being able to sustain clot lysis *in vivo* as well. This capability was in contrast compared with $\alpha_{wild\text{-}type}$ which failed to show effective clot lysis even after prolonged duration (Figure 4.12). This indicated that that the observed increase in cofactor activity employing HPG activator assays did actually translate into improved clot-dissolving ability as well, and not merely an artifact of the chromogenic peptide/*in vitro* HPG activation assays.

4.4 Discussion

The design of 'miniaturized' proteins, that is, small polypeptides that have acquired novel properties or that have retained significant activities of their original 'parent' polypeptides, is a daunting task. In the recent past, several attempts have been made to design functional 'mini-proteins' with mixed success (Vita *et al.*, 1995;

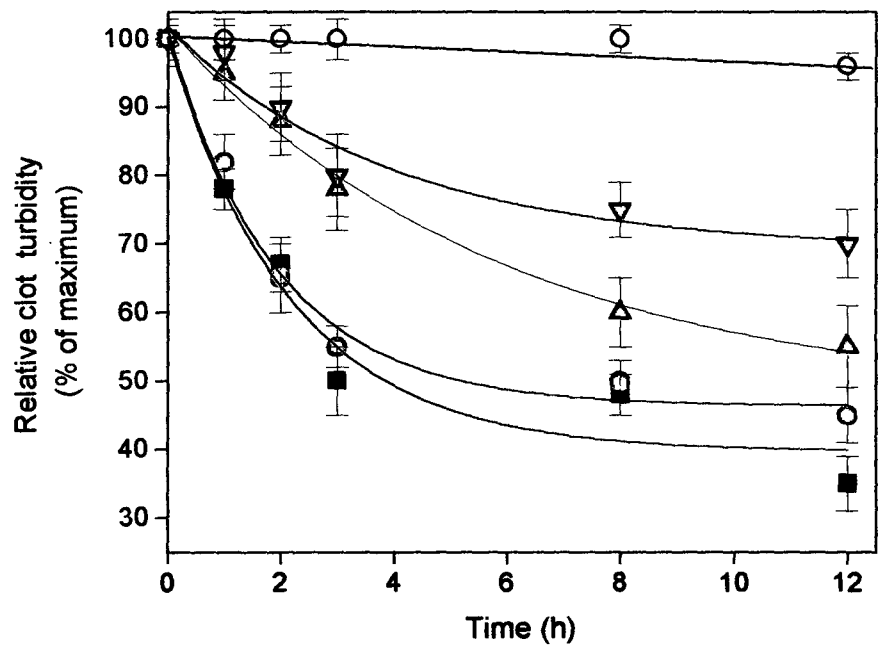

Figure 4.12 Representative curves showing time course of fibrin clot lysis. Fibrin clots were prepared on the wells of an ELISA plate and then incubated with SAK (red circles), SK (black squares), α_{CM} (green triangles), α_{loop} (blue, inverted triangles) and $\alpha_{wild\text{-}type}$ (black, hollow circles). The decrease in absorbance at 405 nm with time was used to calculate % relative clot turbidity after different time intervals (as mentioned under Materials and Methods). Control clots treated with buffer only (data not shown) indicated that the readings were stable during the incubation period.

Braisted and Wells, 1996; Cunningham and Wells, 1997; McColl *et al.*, 1999; Domingues *et al.*, 1999; Segal and Barbas, 2000). In this regard, three-dimensional structural information has proved to be an invaluable aid to protein engineering (Kast and Hilvert, 1997).

With a view to design a 'miniaturized' SK-based HPG activator, the crystal structures of SK and SAK were examined; this revealed that of all the three structurally similar domains of SK, the α domain is structurally the closest to SAK, particularly given the fact that its orientation during the interaction of SK with partner HPG whilst in the SK.μPN activator complex is closely comparable to that of SAK in the SAK.μPN complex (Parry *et al.*, 1998; Wang *et al.*, 1998). An exciting corollary of this proposal, if correct, is that the α domain, on its own, should mimic the functional attributes of SAK, particularly HPG activator activity, as well. If true, this would help to validate the intriguing proposal that a single prototypic module, or domain, has been utilized to evolve to form all of the present-day indirect PG activators found in the bacterial kingdom, viz. SK, SAK and perhaps the two-domain SUPA. Although attractive, this interesting hypothesis has never actually been experimentally validated and, indeed, actually been somewhat relegated in status with the recent demonstration of almost negligible cofactor activity in the isolated α domain (Loy *et al.*, 2001). However, given that considerable evolutionary divergence between α and SAK proteins may have already occurred due to the former being part of a three-domain structure (and hence, by implication, one in which, an enhanced adaptation to a greater inter-domain co-operative mode of action may have evolved), the presence of an intrinsically low cofactor activity in α once 'taken out' from the SK molecule probably can also be argued to be equally probable. In this light, a critical test of the validity, or otherwise, of this hypothesis would not only be the presence of a 'convincing' degree of independent activator activity in the isolated α domain, but also one that could be further enhanced, possibly to SAK-like levels, if 'appropriate' modifications could be introduced that thwart or overcome the 'weak spots' left over from the single-domain to three-domain divergence phenomenon.

In the past, investigations along this line have been pursued in our as well as other laboratories that suggested that a low HPG activator activity was indeed associated with some of the SK domains (Nihalani *et al.*, 1998; Rodriguez *et al.*,

1995; Shi *et al.*, 1994; Conejero-Lara *et al.*, 1998). In all cases, however, the domains of SK were prepared by proteolytic scission of native SK through limited proteolysis. Therefore, there existed a finite possibility of contamination with traces of native SK in preparations of the domains, giving rise to the low activity. Therefore, in the present study, in order to carefully measure the HPG activator activities of the single isolated α domain and its mutants, the constructs were prepared by recombinant DNA methods in which the respective cDNAs encoding were amplified and cloned in pET-23d, a T7 phage RNA polymerase promoter-based vector (Studier *et al.*, 1990). Purification of α and its derivatives using Ni^{+2}-IMAC chromatography yielded purified proteins, observed as single bands on SDS-PAGE. Measurement of the cofactor activity of $\alpha_{wild\text{-}type}$ showed that it exhibits distinct biological activity over and above a small background associated with the host cells.

The fact that the purified α domain is capable of exhibiting measurable cofactor activity independently even in the wild-type state indicates that the evolution of a three-domain organization in SK has not brought about a complete suppression of the intrinsic capability of the basic prototypic SK domain to engender a functional macromolecular substrate-specific exosite, provided a functional HPN active center is present in the reaction milieu. However, since the activity engendered is so low, the enigma persists as to why the α domain of SK, despite sharing high structural homology with the single-domain HPG activator, SAK, displays a co-factor activity only 0.25 % of that of SAK. Studies on the HPN-mediated proteolytic susceptibility of native α provided unmistakable evidence that $\alpha_{wild\text{-}type}$ was highly vulnerable to proteolysis, with the site of cleavage being the Lys59 in the domain. Once this residue was mutated to Ala, the resultant construct's cofactor activity jumped by an order of magnitude.

To further explore strategies to enhance the cofactor activity of α, computer-modeling studies were carried out, in which the α domain of SK and SAK were superimposed on each other. This exercise pointed out the presence of a loop unique to SAK and absent in the α domain. Protein grafting, that involves installing a functional epitope (comprising of residues critical for recognition in their native context) onto an existing stable scaffold, is emerging as a powerful technique to create ligands with improved biological function (Domingues *et al.*, 1999; Zondlo and Schepartz, 1999;

Vita *et al.*, 1999; Chin and Schepartz, 2001; Montclare and Schepartz, 2003), while minimally altering protein conformation, thereby retaining the stable native fold of the template protein (Sia and Kim, 2003). Therefore, we employed a strategy involving grafting of the SAK loop into the loop-deficient α domain of SK, and then studied the functional consequences. Indeed, such a transposition of the loop into the α domain of SK resulted in a remarkable reduction (~ 5-fold) in K_M for macromolecular substrate, but only a relatively moderate (~2-fold) increase in catalytic turnover rates. The enhancement of substrate affinities by steady-state kinetics was further validated by a more direct physico-chemical approach, in which the ternary interaction of substrate HPG with the binary complex of α_{loop} and biotinylated HPG could be monitored on the Resonant Mirror, wherein in contrast to a highly unstable $\alpha_{wild\text{-}type}$.HPG binary complex that failed to show any ternary interaction with substrate HPG, the α_{loop} showed a 3-fold increase in affinity for the macromolecular substrate.

Thus the eight-residue long SAK loop, once incorporated into the α domain of SK, allowed an improved interaction of the activator with the kringle domain/s of substrate HPG, thereby helping to enhance the intrinsically low cofactor activity of α domain. However, the exact manner whereby catalytic rates are enhanced is presently unclear, although what is undeniable is that the loop provides additional substrate affinity. The catalytic enhancement rates, however do suggest that events that are important post-substrate docking are also being positively accentuated once the loop sequence is 'corrected' in its new context viz. in the backdrop of the SK sequence. Presumably, not only is the formation of the enzyme-macromolecular substrate adduct formation critical for catalysis, subsequent steps whereby the scissile peptide bond in PG is cleaved, and the nascently formed product (HPN) expunged from the active site, are also likely equally important for bringing the catalytic process to completion.

It is worth noting that despite a distinct increase in substrate affinity, the catalytic efficiency of α_{loop} was still lower when compared to that of SAK. Large-scale random mutagenesis of moderate-sized polypeptides is laborious and time-consuming since the number of mutants that have to be screened becomes nearly astronomical (Zhao and Arnold, 1997; Miyazaki *et al.*, 1999; Sroga and Dordick, 2001; Cohen *et al.*, 2001). Therefore, as a compromise, in order to further augment the catalytic efficiency of the SK α-based miniaturized HPG activator, a 'limited site' but essentially

combinatorial protein engineering approach was employed in which the residues flanking the loop in the α domain were subjected to random mutagenesis, and hyperactive mutants were selected using an *in situ* screening assay. This strategy was based on the premise that such a limited site random mutagenesis followed by screening would allow the selection of mutants with optimized contacts of the loop with its neighboring residues that might favour enhanced interactions with the macromolecular substrate (as apparent in reduced K_M values). Alternatively, this process may as well facilitate selection of sequences that are more conducive to better substrate turnover due to an optimized flexibility of the loop or its substrate interaction sites; this effect should be manifest in an improved catalytic turn-over rates. This strategy, therefore, allowed the generation, screening and selection of mutants with specifically improved k_{cat} and K_M properties.

The fact that the combinatorial approach of site-directed mutagenesis to minimize proteolysis, 'loop-grafting' followed by random mutagenesis allowed us to transform a molecule with virtually negligible activity into one that was capable of reasonably high HPG activation as well as clot-dissolution properties offers new approaches for protein re-design, particularly for miniaturization of 'old' proteins. Also, such a truncated derivative of SK is expected to result in activation with lower immunogenicity, thus helping to overcome a problem that limits therapeutic use of SK to one or two administrations.

The present study also unveils the critical function played by a small solvent-exposed, flexible and 'mobile' loop structure that is present in SAK, but 'jettisoned' by the evolutionary process in SK. Clearly, thus it appears that nature has adopted two different design plans for evolving the two different PG activator proteins, SK and SAK, from a common structural motif, wherein a single basic unit is utilized to drive catalysis successfully in case of SAK, but three such units are harnessed for the same function of SK. It has been recently shown that the three domains of SK co-operate closely together to engender high native-like catalytic rates by exploiting long-range protein-protein interactions specifically with substrate kringles (Sundram *et al.*, 2003), which might be considered as 'levers' for optimization of the catalytic efficiency of SK. On the other hand, SAK, although it has catalytic efficiencies that are much lower than that of SK (Robbins *et al.*, 1981) (which might perhaps indeed be in consonance with its survival requirements in its *in vivo* niches) utilizes the eight-residue loop to

'substitute' for the functionalities provided by the other two (that is, β and γ) domains of SK in terms of kringle-mediated enzyme-substrate interactions. Even though this phenomenological aspect has been brought out by this work, it is an altogether different and practical challenge to design a functional module that begins to attain native-like catalytic efficiency (that is, with respect to SAK), starting from a hitherto inactive α domain. The fact that loop-grafting followed by sequence-optimization using 'localized'-random mutagenesis has allowed the selection of a molecule with substantial superior qualities when compared to the native wild-type domain, clearly indicates the strengths of a combinatorial approach.

Also, understanding the mechanistic details of protein-protein interactions via these microstructures and their manipulation provide deep practical insight into the mode of action bacterial PG activator proteins, and also paves a way for the development of newer HPG activators with improved therapeutic value.

SUMMARY

Acute coronary ischemic syndromes and strokes are caused by thrombosis in arteries where obstruction leads to ischemia of the heart or brain, respectively. Thrombolytic therapy has become a cornerstone of treatment for acute myocardial infarction and the development of SK as a thrombolytic agent in the developed world earlier, and now in India, has given a fresh lease to life, especially because of its low cost and high potency as a HPG activator. However, it is imperative to have a detailed insight into the structure-function aspects of SK and its mechanism of action in order to design and develop more efficacious molecules or molecules with novel properties.

Although named as a 'kinase', SK is an inert molecule by itself, but becomes active once it binds to HPG in a 1:1 stoichiometric complex, thereby forming the 'activator complex'. This activator complex then further acts on other 'substrate' HPG molecules to convert them into HPN. Unlike free HPN, however, which is essentially a trypsin-like protease with broad substrate-preference, the SK.HPN complex displays an extremely narrow substrate specificity. This remarkable modification of the macromolecular substrate specificity of HPN by SK is currently believed to be due to 'exosites' generated on the SK.HPN complex (Nihalani *et al.*, 1998; Boxrud *et al.*, 2000). However, although solution and structural studies have suggested that SK along with partner HPG, seems to provide a template on which the substrate molecule can dock through protein-protein interactions, resulting in the optimized presentation of the HPG activation loop at the active center of the complex, the identity of these interactions, and their exact contributions to the formation of the enzyme-substrate intermediate/s still remain largely an ambiguity.

In order to clearly identify a structural epitope/element that has a role in conferring substrate HPG affinity onto the SK.HPG activator complex, the three-dimensional structures of the isolated three domains of SK were superimposed through computer modeling studies that revealed the presence of a distinct, solvent-exposed flexible loop in the β domain (residues 254-262; 250-loop) of SK that is absent in the other two otherwise structurally homologous domains. A deletion mutant, $SK_{del254-262}$ was constructed, using overlap extension-PCR reaction that was cloned in the pET-23d expression vector. Both $SK_{del254-262}$ as well as native SK proteins were expressed intracellularly in *Escherichia coli* BL21 (DE3) cells after induction with IPTG and purified using a rapid purification method. The eluted proteins were more than 95 %

pure, as analyzed by SDS-PAGE. To check whether the deletion of the 250-loop resulted in changes in secondary structure, the far-UV CD spectra of SK and the mutant ($SK_{del254-262}$) were studied. No significant differences were observed. In addition, the far-UV CD spectra of the β domain alone and β domain containing the deletion ($\beta_{del254-262}$) were also checked to obviate any 'averaging' effect of local changes due to the CD contributions from rest of the two domains of SK in the full-length molecule. For this, the isolated β domain with the deletion at the same site was constructed. The cDNAs encoding for the β domain alone and $\beta_{del254-262}$ were then expressed in *Escherichia coli* and purified from IBs to more than 95 % homogeneity by ion-exchange chromatography. Interestingly, no discernable changes were observed in the secondary structure of $\beta_{del254-262}$ with respect to $\beta_{wild-type}$, indicating that neither the overall secondary structure of SK nor that of the β domain alone had been perturbed by the deletion of the nine-residue loop from the protein.

When the mutant was checked for HPG activator activity, significant decrease in the rates of substrate HPG activation by the mutant ($SK_{del254-262}$) were observed. In order to explore whether the deletion of the 250-loop resulted in any significant alteration in the affinity of the mutant with partner HPG, the kinetics of interaction between immobilized HPG and SK were compared with that of $SK_{del254-262}$ by the Resonant Mirror approach using a semi-automated instrument for measuring protein-protein interactions in real time. To examine the effect of immobilization chemistry on the values of kinetic constants, preliminary experiments were performed by immobilizing SK/$SK_{del254-262}$ onto both carboxy-methyl dextran cuvettes (using a amino-coupling protocol recommended by the manufacturers) and onto biotin cuvettes in which biotinylated HPG was immobilized on streptavidin captured on this cuvette. The kinetics of association and dissociation of HPG with immobilized SK/$SK_{del254-262}$ indicated that the mutant exhibited an affinity that was not significantly different from that of SK. Remarkably, both immobilization techniques yielded similar binding constants for SK and $SK_{del254-262}$, indicating that the coupling procedure *per se* does not significantly interfere in the binding interaction between SK and HPG.

In order to find out the principal cause of fractional loss in activity, the mutant was checked whether it could open the active site in partner HPG. It was found that $SK_{del254-262}$ could indeed open the active site and generate amidolytic activity,

suggesting that the lower activity was not due to any significant effect on the ability to activate partner HPG at the binary complexation stage.

A steady-state kinetic analysis of $SK_{del254-262}$ revealed that its low HPG activator activity arose primarily from a 5-6 fold increase in K_M for HPG as substrate, with little alteration in k_{cat} rates. Under these conditions, the k_{cat} for the small peptide substrate tosyl-glycyl-prolyl-lysine-4-nitranilide-acetate was essentially unchanged indicating that the primary characteristics of the active site remained unaltered.

A new Resonant Mirror based assay was devised for the real-time kinetic analysis of the docking of substrate HPG onto pre-formed binary complex of biotinylated HPG and SK/$SK_{del254-262}$. Remarkably, the observed increase in the K_M for the macromolecular substrate was proportional to a similar decrease in the binding affinity for substrate HPG, as obtained in case of $SK_{del254-262}$, although under those conditions the 1:1 affinity of $SK_{del254-262}$ for partner HPG was minimally changed.

In contrast, kinetic studies on the interaction of the two proteins with μPG (having just the catalytic domain of HPG without any of the five kringles) showed no difference between formation of ternary complex with μPG by preformed equimolar complexes of HPG with either SK or $SK_{del254-262}$, nor between the rates of activation of μPG into μPN under conditions where native HPG was activated differentially by SK and $SK_{del254-262}$, clearly indicating a kringle-mediated mechanism for the role of the 250-loop of SK in substrate docking/recognition.

The involvement of kringles was further indicated by a hyper-susceptibility of the $SK_{del254-262}$.HPN activator complex to EACA inhibition of substrate HPG activation in comparison to that of the native SK.HPN activator complex. Further, 'ternary' binding experiments on the Resonant Mirror showed that the binding affinity of K1-5 of HPG to the preformed binary complex of the 250-loop deleted mutant and HPG was reduced by about 3-fold in comparison to that of SK.HPG. Overall, these observations identify the 250-loop of SK as an important structural determinant of the inordinately stringent substrate specificity of the SK.plasmin(ogen) activator complex and demonstrate that this structural epitope in the β domain promotes the binding of substrate HPG to the activator via the kringle/s during the HPG activation process.

The elucidation of the crystal structures of SAK and SK has highlighted the remarkable structural homology between SAK on one hand, and each of the three domains of SK, especially the α domain of SK, on the other. In order to find out

whether the α domain of SK displays cofactor activity similar to that of SAK, $\alpha_{wild\text{-}type}$ was purified to near-homogeneity using two chromatographic steps, *viz.* Ni^{+2}-IMAC followed by ion-exchange chromatography and then checked for its ability to activate substrate HPG. The wild-type α domain was found to exhibit only 0.002 % activity when compared to that of SK. To explore whether this meager activity was genuine activity or was due to the known proteins in *Escherichia coli* that have been shown to possess HPG activation ability, lysates of *Escherichia coli* cultures transformed with the pET-23d vector alone, without SK α gene, were subjected to exactly the same purification procedure employed for $\alpha_{wild\text{-}type}$. The purified $\alpha_{wild\text{-}type}$ protein showed higher cofactor activity than the 'mock' purified proteins.

When the cofactor activity of $\alpha_{wild\text{-}type}$ generated after mixing with equimolar amounts of HPN was examined, a 25-fold increase in activity was observed compared to the activity measured with HPG alone, indicating that the activity was HPN-dependent. In order to investigate whether the cofactor activity of $\alpha_{wild\text{-}type}$ was an under-estimation because of HPN-mediated proteolysis, the susceptibility of $\alpha_{wild\text{-}type}$ to HPN-mediated proteolysis, if any, was checked; this showed that $\alpha_{wild\text{-}type}$ was highly prone to proteolysis. The principal target of scission was found to be Lys59-Ser60 peptide bond in SK α, by N-terminal amino acid sequencing. With a view to minimize the proteolysis, Lys59 was mutated to an Ala residue. This construct (α_{K59E}) was found to be highly stabilized against HPN-mediated proteolysis and interestingly, showed a 8-fold increase in cofactor activity, compared to that of $\alpha_{wild\text{-}type}$. However, the cofactor activity measured was still much lower than that of SAK.

With a view to further enhance the cofactor activity of α_{K59E}, the structures of the α domain of SK and SAK were compared; this revealed the presence of an eight-residue loop in SAK, which was absent in SK α. The loop was then grafted into SK α (α_{loop}) by the overlap extension PCR-based method. The resultant construct, termed α_{loop}, showed a 2-fold higher cofactor activity than α_{K59E}. A detailed kinetic analysis showed a 5-fold decrease in K_M over that of α_{K59E}. In order to optimize the stereo-chemical contacts of the SAK loop with the rest of the α domain, random PCR-mutagenesis in the flanks encompassing four amino acid residues on either side of the loop in α, was carried out. The library of these mutants was expressed in a secretory vector, and nearly ten thousand clones were screened, using the *in situ* radial

caseinolysis plate assay (Malke and Ferretti, 1984). Five hundred 'hyperactive' clones were selected on the basis of larger zones of clearance on the agarose plates layered with casein and HPG. The best of these 'hyperactive' mutants were then transferred from the secretory vector to pET-23d, a T7 RNA polymerase promoter-based expression vector, and the proteins were purified by Ni^{+2}-IMAC followed by ion-exchange chromatography. When these combinatorial mutants were assayed for their cofactor activities, they were found to exhibit ~ 3-6 fold higher activity than α_{K59E}. One of the combinatorial mutants (termed α_{CM}), which showed ~ 6-fold higher activity than that of α_{K59E} was then analyzed further. The steady-state kinetics of α_{CM} indicated that α_{CM} displayed overall catalytic efficiencies nearly that of SAK.

The HPG-binding interactions of $\alpha_{wild\text{-}type}/\alpha_{K59E}$ and α derivatives were then checked using the Resonant Mirror based approach, in which each of these proteins was allowed to interact with biotinylated HPG. It was found that the interactions at the binary level were not greatly altered for these constructs. However, when attempts were made to study ternary interactions between substrate HPG and $\alpha_{wild\text{-}type}/\alpha_{K59E}/\alpha$ derivatives/SAK pre-complexed with immobilized HPG, reliable binding constants could not be determined in case of α_{K59E} because of the weak nature of the binary complex formed between α_{K59E} and HPG. On the other hand, the binary complex of α_{CM} and HPG was stable even after washing with buffer, and therefore, binding constants for its ternary interactions with substrate HPG could be determined. The equilibrium dissociation constant of the ternary interaction in case of SAK was found to be 4-fold higher than that of α_{CM}, an effect that was also observed in a corresponding increase in affinity (K_M) for substrate HPG in case of the combinatorial mutant.

When cofactor assays and Resonant Mirror-based ternary interaction studies were carried out with μPG as substrate, no discernable differences were detected in case of $\alpha_{wild\text{-}type}/\alpha_{K59E}$ and α_{CM}, under conditions where substantial differences were observed, when HPG was used as the substrate. These observations strongly point out the role of kringles in substrate recognition and overall catalytic enhancement.

To explore whether the higher levels of cofactor activity observed in the α derivatives over that of $\alpha_{wild\text{-}type}$ were translated into an increased ability to dissolve fibrin clots, fibrin-clot lysis assays were carried out, using these proteins.

Remarkably, this miniaturized SK α-based HPG activator was capable of *in vitro* fibrin clot lysis, thereby making it a possible candidate for *in vivo* therapeutic use.

These results clearly point out the critical role played by the eight-residue loop in SAK, which, upon transposition into the α domain of SK, and, further optimization by localized random mutagenesis, promotes substrate recognition and turn-over via the kringle domains of HPG. The fact that protein-grafting followed by random mutagenesis successfully transformed an *intrinsically inactive α domain* into a module that exhibited catalytic efficiency nearing that of SAK, and also carried out clot-dissolution *in vitro* provides new insight into the evolutionary process associated with the bacterial PG activators, and paves the way for the design and development of miniaturized clot-buster proteins with greater therapeutic value.

BIBLIOGRAPHY

Aoki N, Harpel PC (1984). Inhibitors of the fibrinolytic enzyme system. *Semin Thromb Hemost* **10,** 24-41.

Atkinson RA, Williams RJ (1990). Solution structure of the kringle 4 domain from human plasminogen by 1H nuclear magnetic resonance spectroscopy and distance geometry. *J Mol Biol* **212,** 541-552.

Bajaj AP, Castellino FJ (1977). Activation of human plasminogen by equimolar levels of streptokinase. *J Biol Chem* **252,** 492-498.

Barlow GH (1976). Urinary and kidney cell plasminogen activator (urokinase). *Methods Enzymol* **45,** 239-244.

Barlow GH, Francis CW, Marder VJ (1981). On the conversion of high molecular weight urokinase to the low molecular weight form by plasmin. *Thromb Res* **23,** 541-547.

Barrett AJ, Starkey PM (1973). The interaction of alpha 2-macroglobulin with proteinases. Characteristics and specificity of the reaction, and a hypothesis concerning its molecular mechanism. *Biochem J* **133,** 709-724.

Barrett AJ (1981). Alpha 2-macroglobulin. *Methods Enzymol* **80 Pt C,** 737-754.

Behnke D, Gerlach D (1987). Cloning and expression in *Escherichia coli, Bacillus subtilis,* and *Streptococcus sanguis* of a gene for staphylokinase-a bacterial plasminogen activator. *Mol Gen Genet* **210,** 528-534.

Blomback B, Blomback M (1972). The molecular structure of fibrinogen. *Ann N Y Acad Sci* **202,** 77-97.

Bode W, Huber R (1976). Induction of the bovine trypsinogen-trypsin transition by peptides sequentially similar to the N-terminus of trypsin. *FEBS Lett* **68,** 231-236.

Booyse FM, Scheinbuks J, Radek J, Osikowicz G, Feder S, Quarfoot AJ (1981). Immunological identification and comparison of plasminogen activator forms in cultured normal human endothelial cells and smooth muscle cells. *Thromb Res* **24,** 495-504.

Boxrud PD, Fay WP, Bock PE (2000). Streptokinase binds to human plasmin with high affinity, perturbs the plasmin active site, and induces expression of a substrate recognition exosite for plasminogen. *J Biol Chem* **275,** 14579-14589.

Boxrud PD, Verhamme IM, Fay WP, Bock PE (2001). Streptokinase triggers conformational activation of plasminogen through specific interactions of the amino-terminal sequence and stabilizes the active zymogen conformation. *J Biol Chem* **276,** 26084-26089.

Bradford MM (1976). A rapid and sensitive method for the quantitation of microgram quantities of protein utilizing the principle of protein-dye binding. *Anal Biochem* **72,** 248-254.

Braisted AC, Wells JA (1996). Minimizing a binding domain from protein A. *Proc Natl Acad Sci U S A* **93,** 5688-5692.

Brockway WJ, Castellino FJ (1974). A characterization of native streptokinase and altered streptokinase isolated from a human plasminogen activator complex. *Biochemistry* **13,** 2063-2070.

Bruserud O, Elsayed S, Pawelec G (1992). At least five antigenic epitopes on the streptokinase molecule are recognized by human CD4+ TCR alpha beta+ T cells. *Mol Immunol* **29,** 1097-1104.

Buck FF, Hummel BC, De Renzo EC (1968). Interaction of streptokinase and human plasminogen. V. Studies on the nature and mechanism of formation of the enzymatic site of the activator complex. *J Biol Chem* **243,** 3648-3654.

Buckle PE, Davies RJ, Kinning T, Yeung D, Edwards PR, Pollard-Knight D, Lowe CR (1993). The resonant mirror: a novel optical biosensor for direct sensing of biomolecular interactions Part II: applications. *Biosensors & Bioelectronics* **8,** 365-370.

Cannon CP, Gibson CM, McCabe CH, Adgey AA, Schweiger MJ, Sequeira RF, Grollier G, Giugliano RP, Frey M, Mueller HS, Steingart RM, Weaver WD, Van de Werf F, Braunwald E (1998). TNK-tissue plasminogen activator compared with front-loaded alteplase in acute myocardial infarction: results of the TIMI 10B trial. Thrombolysis in Myocardial Infarction (TIMI) 10B Investigators. *Circulation* **98,** 2805-2814.

Cannon CP, McCabe CH, Gibson CM, Ghali M, Sequeira RF, McKendall GR, Breed J, Modi NB, Fox NL, Tracy RP, Love TW, Braunwald E (1997). TNK-tissue plasminogen activator in acute myocardial infarction. Results of the Thrombolysis in Myocardial Infarction (TIMI) 10A dose-ranging trial. *Circulation* **95,** 351-356.

Castellino FJ (1979). A unique enzyme-protein substrate modifier reaction: plasmin/streptokinase interaction. *Trends Biochem Sci* **4,** 1-5.

Castellino FJ (1981). Recent advances in the chemistry of the fibrinolytic system. *Chem Rev* **81,** 431-446.

Castellino FJ (1984). Biochemistry of human plasminogen. *Semin Thromb Hemost* **10,** 18-23.

Castellino FJ, Sodetz JM, Brockway WJ, Siefring GE Jr (1976). Streptokinase. *Methods Enzymol* **45,** 244-257.

Castellino FJ, Powell JR (1981). Human plasminogen. *Methods Enzymol* **80 Pt C,** 365-378.

Chang Y, Mochalkin I, McCance SG, Cheng B, Tulinsky A, Castellino FJ (1998). Structure and ligand binding determinants of the recombinant kringle 5 domain of human plasminogen. *Biochemistry* **37,** 3258-3271.

Chase T Jr, Shaw E (1969). Comparison of the esterase activities of trypsin, plasmin, and thrombin on guanidinobenzoate esters. Titration of the enzymes. *Biochemistry* **8,** 2212-2224.

Chaudhary A, Vasudha S, Rajagopal K, Komath SS, Garg N, Yadav M, Mande SC, Sahni G (1999). Function of the central domain of streptokinase in substrate plasminogen docking and processing revealed by site-directed mutagenesis. *Protein Sci* **8,** 2791-2805.

Chin JW, Schepartz A (2001). Concerted evolution of structure and function in a miniature protein. *J Am Chem Soc* **123,** 2929-2930.

Christensen U, Clemmensen I (1977). Kinetic properties of the primary inhibitor of plasmin from human plasma. *Biochem J* **163,** 389-391.

Christensen U, Sottrup-Jensen L, Magnusson S, Petersen TE, Clemmensen I (1979). Enzymic properties of the neo-plasmin-Val-422 (miniplasmin). *Biochim Biophys Acta* **567,** 472-481.

Christie R, Wilson H (1941). A test of staphylococcal fibrinolysin. *Aust J Exp Biol Med Sci* **19,** 329.

Coffey JA, Jennings KR, Dalton H (2001). New antigenic regions of streptokinase are identified by affinity-directed mass spectrometry. *Eur J Biochem* **268,** 5215-5221.

Cohen N, Abramov S, Dror Y, Freeman A (2001). In vitro enzyme evolution: the screening challenge of isolating the one in a million. *Trends Biotechnol* **19,** 507-510.

Cole ER, Bachmann FW (1977). Purification and properties of a plasminogen activator from pig heart. *J Biol Chem* **252,** 3729-3737.

Collen D (1976). Identification and some properties of a new fast-reacting plasmin inhibitor in human plasma. *Eur J Biochem* **69,** 209-216.

Collen D, de Maeyer L (1975). Molecular biology of human plasminogen. I. Physiochemical properties and microheterogeneity. *Thromb Diath Haemorrh* **34,** 396-402.

Collen D, Stump DC, Gold HK (1988). Thrombolytic therapy. *Annu Rev Med* **39,** 405-423.

Collen D, Lijnen HR (1995). Molecular basis of fibrinolysis, as relevant for thrombolytic therapy. *Thromb Haemostasis* **74,** 167-171.

Conejero-Lara F, Parrado J, Azuaga AI, Dobson CM, Ponting CP (1998). Analysis of the interactions between streptokinase domains and human plasminogen. *Protein Sci* **7,** 2190-2199.

Conejero-Lara F, Parrado J, Azuaga AI, Smith RA, Ponting CP, Dobson CM (1996). Thermal stability of the three domains of streptokinase studied by circular dichroism and nuclear magnetic resonance. *Protein Sci* **5,** 2583-2591.

Cunningham BC, Wells JA (1997). Minimized proteins. *Curr Opin Struct Biol* **7,** 457-462.

Cush R, Cronin JM, Stewart WJ, Maule CH, Molloy J, Goddard NJ (1993). The resonant mirror: a novel optical biosensor for direct sensing of biomolecular interactions Part I: Principle of operation and associated instrumentation. *Biosensors & Bioelectronics* **8**, 347-354.

Damaschun G, Damaschun H, Gast K, Gerlach D, Misselwitz R, Welfle H, Zirwer D (1992). Streptokinase is a flexible multi-domain protein. *Eur Biophys J* **20,** 355-361.

Damaschun G, Damaschun H, Gast K, Misselwitz R, Zirwer D, Guhrs KH, Hartmann M, Schlott B, Triebel H, Behnke D (1993). Physical and conformational properties of staphylokinase in solution. *Biochim Biophys Acta* **1161,** 244-248.

Dawson KM, Marshall JM, Raper RH, Gilbert RJ, Ponting CP (1994). Substitution of arginine 719 for glutamic acid in human plasminogen substantially reduces its affinity for streptokinase. *Biochemistry* **33,** 12042-12047.

De Renzo EC, Boggiano E, Barg WF Jr, Buck FF (1967). Interaction of streptokinase and human plasminogen. IV. Further gel electrophoretic studies on the combination of streptokinase with human plasminogen or human plasmin. *J Biol Chem* **242,** 2428-2434.

Degen SJ, Bell SM, Schaefer LA, Elliott RW (1990). Characterization of the cDNA coding for mouse plasminogen and localization of the gene to mouse chromosome 17. *Genomics* **8,** 49-61.

den Heijer P, Vermeer F, Ambrosioni E, Sadowski Z, Lopez-Sendon JL, von Essen R, Beaufils P, Thadani U, Adgey J, Pierard L, Brinker J, Davies RF, Smalling RW, Wallentin L, Caspi A, Pangerl A, Trickett L, Hauck C, Henry D, Chew P (1998). Evaluation of a weight-adjusted single-bolus plasminogen activator in patients with myocardial infarction: a double-blind, randomized angiographic trial of lanoteplase versus alteplase. *Circulation* **98,** 2117-2125.

Deutsch DG, Mertz ET (1970). Plasminogen: purification from human plasma by affinity chromatography. *Science* **170,** 1095-1096.

Dhar J, Pande AH, Sundram V, Nanda JS, Mande SC, Sahni G (2002). Involvement of a nine-residue loop of streptokinase in the generation of macromolecular substrate specificity by the activator complex through interaction with substrate kringle domains. *J Biol Chem* **277,** 13257-13267.

Domingues H, Cregut D, Sebald W, Oschkinat H, Serrano L (1999). Rational design of a GCN4-derived mimetic of interleukin-4. *Nat Struct Biol* **6,** 652-656.

Doolittle RF (1984). Fibrinogen and fibrin. *Annu Rev Biochem* **53,** 195-229.

Einarsson M, Skoog B, Forsberg B, Einarsson R (1979). Characterization of highly purified native streptokinase and altered streptokinase after alkaline treatment. *Biochim Biophys Acta* **568,** 19-29.

Esmon CT, Mather T (1998). Switching serine protease specificity. *Nat Struct Biol* **5,** 933-937.

Fabian H, Naumann D, Misselwitz R, Ristau O, Gerlach D, Welfle H (1992). Secondary structure of streptokinase in aqueous solution: a Fourier transform infrared spectroscopic study. *Biochemistry* **31,** 6532-6538.

Fay WP, Bokka LV (1998). Functional analysis of the amino- and carboxyl-termini of streptokinase. *Thromb Haemost* **79,** 985-991.

Francis CW, Marder VJ (1994). Physiologic Regulation and Pathologic Disorders. In: Colman RW, Hirsh J, Marder VJ, Salzman EW, eds. *Haemostasis and Thrombosis: Basic Principles and Clinical Practice*, 3rd edition, J. B. Lippincott Company, Philadelphia, USA. pp 1076-1103.

Folk JE, Finlayson JS (1977). The epsilon-(gamma-glutamyl) lysine crosslink and the catalytic role of transglutaminases. *Adv Protein Chem* **31,** 1-133.

Gardell SJ, Duong LT, Diehl RE, York JD, Hare TR, Register RB, Jacobs JW, Dixon RA, Friedman PA (1989). Isolation, characterization, and cDNA cloning of a vampire bat salivary plasminogen activator. *J Biol Chem* **264,** 17947-17952.

Gardell SJ, Friedman PA (1993). Vampire bat salivary plasminogen activator. *Methods Enzymol* **223,** 233-249.

Gardell SJ, Hare TR, Bergum PW, Cuca GC, O'Neill-Palladino L, Zavodny SM (1990). Vampire bat salivary plasminogen activator is quiescent in human plasma in the absence of fibrin unlike human tissue plasminogen activator. *Blood* **76,** 2560-2564.

Gardell SJ, Ramjit DR, Stabilito II, Fujita T, Lynch JJ, Cuca GC, Jain D, Wang SP, Tung JS, Mark GE (1991). Effective thrombolysis without marked plasminemia after bolus intravenous administration of vampire bat salivary plasminogen activator in rabbits. *Circulation* **84,** 244-253.

Gething MJ, Adler B, Boose JA, Gerard RD, Madison EL, McGookey D, Meidell RS, Roman LM, Sambrook J (1988). Variants of human tissue-type plasminogen activator that lack specific structural domains of the heavy chain. *EMBO J* **7,** 2731-2740.

Gladysheva IP, Sazonova IY, Chowdhry SA, Liu L, Turner RB, Reed GL (2002). Chimerism reveals a role for the streptokinase beta-domain in nonproteolytic active site formation, substrate, and inhibitor interactions. *J Biol Chem* **277,** 26846-26851.

Gonias SL, Reynolds JA, Pizzo SV (1982a). Physical properties of human alpha 2-macroglobulin following reaction with methylamine and trypsin. *Biochim Biophys Acta* **705,** 306-314.

Gonias SL, Einarsson M, Pizzo SV (1982b). Catabolic pathways for streptokinase, plasmin, and streptokinase activator complex in mice. In vivo reaction of plasminogen activator with alpha 2-macroglobulin. *J Clin Invest* **70,** 412-423.

Gonzalez-Gronow M, Grenett HE, Fuller GM, Pizzo SV (1990). The role of carbohydrate in the function of human plasminogen: comparison of the protein obtained from molecular cloning and expression in *Escherichia coli* and COS cells. *Biochim Biophys Acta* **1039,** 269-276.

Gonzalez-Gronow M, Siefring GE Jr, Castellino FJ (1978). Mechanism of activation of human plasminogen by the activator complex, streptokinase-plasmin. *J Biol Chem* **253,** 1090-1094.

Grant PG, Colman RW (1988). Purification of cAMP phosphodiesterase from platelets. *Methods Enzymol* **159,** 772-777.

Gunzler WA, Steffens GJ, Otting F, Kim SM, Frankus E, Flohe L (1982). The primary structure of high molecular mass urokinase from human urine. The complete amino acid sequence of the A chain. *Hoppe Seylers Z Physiol Chem* **363,** 1155-1165.

Gurewich V, Pannell R (1987). Inactivation of single-chain urokinase (pro-urokinase) by thrombin and thrombin-like enzymes: relevance of the findings to the interpretation of fibrin-binding experiments. *Blood* **69,** 769-772.

Gusto III (1997). A comparison of reteplase with alteplase for acute myocardial infarction. The global use of strategies to open occluded arteries (GUSTO III) investigators. *N Engl J Med* **337,** 1118-1123.

Hagenson MJ, Holden KA, Parker KA, Wood PJ, Cruze JA, Fuke M, Hopkins TR, Stroman DW (1989). Expression of streptokinase in *Pichia pastoris* yeast. *Enzyme Microb Technol* **11,** 650-656.

Harpel PC (1973). Studies on human plasma alpha 2-macroglobulin-enzyme interactions. Evidence for proteolytic modification of the subunit chain structure. *J Exp Med* **138,** 508-521.

Haslam RJ, Davidson MM, Fox JE, Lynham JA (1978). Cyclic nucleotides in platelet function. *Thromb Haemost* **40,** 232-240.

Hauptmann J, Glusa E (1995). Differential effects of staphylokinase, streptokinase and tissue-type plasminogen activator on the lysis of retracted human plasma clots and fibrinolytic plasma parameters in vitro. *Blood Coagul Fibrinolysis* **6,** 579-583.

Hayes ML, Castellino FJ (1979a). Carbohydrate of the human plasminogen variants. I. Carbohydrate composition, glycopeptide isolation, and characterization. *J Biol Chem* **254,** 8768-8771.

Hayes ML, Castellino FJ (1979b). Carbohydrate of the human plasminogen variants. II. Structure of the asparagine-linked oligosaccharide unit. *J Biol Chem* **254,** 8772-8776.

Hayes ML, Castellino FJ (1979c). Carbohydrate of the human plasminogen variants. III. Structure of the O-glycosidically linked oligosaccharide unit. *J Biol Chem* **254,** 8777-8780.

Hermans J, McDonagh J (1982). Fibrin: structure and interactions. *Semin Thromb Hemost* **8,** 11-24.

Highsmith RF, Kline DL (1971). Kidney: primary source of plasminogen after acute depletion in the cat. *Science* **174,** 141-142.

Hirel PH, Schmitter MJ, Dessen P, Fayat G, Blanquet S (1989). Extent of N-terminal methionine excision from *Escherichia coli* proteins is governed by the side-chain length of the penultimate amino acid. *Proc Natl Acad Sci USA* **86,** 8247-8251.

Hirosawa S, Nakamura Y, Miura O, Sumi Y, Aoki N (1988). Organization of the human alpha 2-plasmin inhibitor gene. *Proc Natl Acad Sci U S A* **85,** 6836-6840.

Ho SN, Hunt HD, Horton RM, Pullen JK, Pease LR (1989). Site-directed mutagenesis by overlap extension using the polymerase chain reaction. *Gene* **77,** 51-59.

Hoeprich PD Jr, Doolittle RF (1983). Dimeric half-molecules of human fibrinogen are joined through disulfide bonds in an antiparallel orientation. *Biochemistry* **22,** 2049-2055.

Holmes WE, Nelles L, Lijnen HR, Collen D (1987). Primary structure of human alpha 2-antiplasmin, a serine protease inhibitor (serpin). *J Biol Chem* **262,** 1659-1664.

Horrevoets AJ, Smilde AE, Fredenburgh JC, Pannekoek H, Nesheim ME (1995). The activation-resistant conformation of recombinant human plasminogen is stabilized by basic residues in the amino-terminal hinge region. *J Biol Chem* **270,** 15770-15776.

Hortin GL, Gibson BL, Fok KF (1988). Alpha 2-antiplasmin's carboxy-terminal lysine residue is a major site of interaction with plasmin. *Biochem Biophys Res Commun* **155,** 591-596.

Hoylaerts M, Rijken DC, Lijnen HR, Collen D (1982). Kinetics of the activation of plasminogen by human tissue plasminogen activator. Role of fibrin. *J Biol Chem* **257,** 2912-2919.

Hu CK, Kohnert U, Wilhelm O, Fischer S, Llinas M (1994). Tissue-type plasminogen activator domain-deletion mutant BM 06.022: modular stability, inhibitor binding, and activation cleavage. *Biochemistry* **33,** 11760-11766.

Husain SS (1991). Single-chain urokinase-type plasminogen activator does not possess measurable intrinsic amidolytic or plasminogen activator activities. *Biochemistry* **30,** 5797-5805.

Husain SS, Gurewich V, Lipinski B (1983). Purification and partial characterization of a single-chain high-molecular-weight form of urokinase from human urine. *Arch Biochem Biophys* **220,** 31-38.

Hutchinson EG, Thornton JM (1996). PROMOTIF-a program to identify and analyze structural motifs in proteins. *Protein Sci* **5,** 212-220.

Ichinose A, Fujikawa K, Suyama T (1986). The activation of pro-urokinase by plasma kallikrein and its inactivation by thrombin. *J Biol Chem* **261,** 3486-3489.

Ichinose A, Kisiel W, Fujikawa K (1984). Proteolytic activation of tissue plasminogen activator by plasma and tissue enzymes. *FEBS Lett* **175,** 412-418.

ISIS-3 (Third International Study of Infarct Survival) Collaborative Group (1992). A randomized comparison of streptokinase vs tissue plasminogen activator vs anistreplase and of aspirin plus heparin vs aspirin alone among 41229 cases of suspected acute myocardial infarction. *Lancet* **339,** 753-770.

Jackson CM, Nemerson Y (1980). Blood coagulation. *Annu Rev Biochem* **49,** 765-811.

Jackson KW, Malke H, Gerlach D, Ferretti JJ, Tang J (1986). Active streptokinase from the cloned gene in *Streptococcus sanguis* is without the carboxyl-terminal 32 residues. *Biochemistry* **25,** 108-114.

Jackson KW, Tang J (1978). The amino-terminal sequence of streptokinase and its functional implications in plasminogen activation. *Thromb Res* **13,** 693-699.

Jackson KW, Tang J (1982). Complete amino acid sequence of streptokinase and its homology with serine proteases. *Biochemistry* **21,** 6620-6625.

Jalihal S, Morris GK (1990). Antistreptokinase titres after intravenous streptokinase. *Lancet* **335,** 184-185.

Johnsen LB, Poulsen K, Kilian M, Petersen TE (1999). Purification and cloning of a streptokinase from *Streptococcus uberis*. *Infect Immun* **67,** 1072-1078.

Johnsen LB, Rasmussen L, Petersen T, Etzerodt M, Fedosov S (2000). Kinetic and structural characterization of a two-domain streptokinase: Dissection of domain functionality. *Biochemistry* **39,** 6440-6448.

Johnson WC Jr (1986). Extending circular dichroism spectra into the vacuum UV and its application to proteins. *Photochem Photobiol* **44,** 307-313.

Kast P, Hilvert D (1997). 3D structural information as a guide to protein engineering using genetic selection. *Curr Opin Struct Biol* **7,** 470-479.

Kammann M, Laufs J, Schell J, Gronenborn B (1989). Rapid insertional mutagenesis of DNA by polymerase chain reaction (PCR). *Nucleic Acids Res* **17,** 5404.

Keyt BA, Paoni NF, Refino CJ, Berleau L, Nguyen H, Chow A, Lai J, Pena L, Pater C, Ogez J (1994). A faster-acting and more potent form of tissue plasminogen activator. *Proc Natl Acad Sci U S A* **91,** 3670-3674.

Kim DM, Lee SJ, Kim IC, Kim ST, Byun SM (2000). Asp41-His48 region of streptokinase is important in binding to a substrate plasminogen. *Thromb Res* **99,** 93-98.

Kim DM, Lee SJ, Yoon SK, Byun SM (2002). Specificity role of the streptokinase C-terminal domain in plasminogen activation. *Biochem Biophys Res Commun* **290,** 585-588.

Kim IC, Kim JS, Lee SH, Byun SM (1996). C-terminal peptide of streptokinase, Met369-Pro373, is important in plasminogen activation. *Biochem Mol Biol Int* **40,** 939-945.

Kitt AJ, Leigh JA (1997). The auxotrophic nature of *Streptococcus uberis*. The acquisition of essential acids from plasmin derived casein peptides. *Adv Exp Med Biol* **418,** 647-560.

Klessen C, Malke H (1986). Expression of the streptokinase gene from *Streptococcus equisimilis* in *Bacillus subtilis*. *J Basic Microbiol* **26,** 75-81.

Kohnert U, Rudolph R, Verheijen JH, Weening-Verhoeff EJ, Stern A, Opitz U, Martin U, Lill H, Prinz H, Lechner M (1992). Biochemical properties of the kringle 2 and protease domains are maintained in the refolded t-PA deletion variant BM 06.022. *Protein Eng* **5,** 93-100.

Kosow DP (1975). Kinetic mechanism of the activation of human plasminogen by streptokinase. *Biochemistry* **14,** 4459-4465.

Kruithof EK, Gudinchet A, Bachmann F (1988). Plasminogen activator inhibitor 1 and plasminogen activator inhibitor 2 in various disease states. *Thromb Haemost* **59,** 7-12.

Lack CH (1948). Staphylokinase: an activator of plasma protease. *Nature* **161,** 559-561.

Lähteenmäki K, Kuusela P, Korhonen TK (2001). Bacterial plasminogen activators and receptors. *FEMS Microbiol Rev* **25,** 531-552.

Lamba D, Bauer M, Huber R, Fischer S, Rudolph R, Kohnert U, Bode W (1996). The 2.3 Å crystal structure of the catalytic domain of recombinant two-chain human tissue-type plasminogen activator. *J Mol Biol* **258,** 117-135.

Landt O, Grunert HP, Hahn U (1990). A general method for rapid site-directed mutagenesis using the polymerase chain reaction. *Gene* **96,** 125-128.

Laplace F, Muller J, Gumpert J, Malke H (1989). Novel shuttle vectors for improved streptokinase expression in streptococci and bacterial L-forms. *FEMS Microbiol Lett* **53,** 89-94.

Larsen GR, Timony GA, Horgan PG, Barone KM, Henson KS, Angus LB, Stoudemire JB (1991). Protein engineering of novel plasminogen activators with increased thrombolytic potency in rabbits relative to activase. *J Biol Chem* **266,** 8156-8161.

Lee BR, Park SK, Kim JH, Byun SM (1989). Site-specific alteration of Gly-24 in streptokinase: its effect on plasminogen activation. *Biochem Biophys Res Commun* **165,** 1085-1090.

Lee HS, Cross S, Davidson R, Reid T, Jennings K (1993). Raised levels of antistreptokinase antibody and neutralization titres from 4 days to 54 months after administration of streptokinase or anistreplase. *Eur Heart J* **14,** 84-89.

Lee SH, Jeong ST, Kim IC, Byun SM (1997). Identification of the functional importance of valine-19 residue in streptokinase by N-terminal deletion and site-directed mutagenesis. *Biochem Mol Biol Int* **41,** 199-207.

Leigh JA, Lincoln RA (1997). *Streptococcus uberis* acquires plasmin activity following growth in the presence of bovine plasminogen through the action of its specific plasminogen activator. *FEMS Microbiol Lett* **154,** 123-129.

Leigh JA (1993). Activation of bovine plasminogen by *Streptococcus uberis*. *FEMS Microbiol Lett* **114,** 67-71.

Lerch PG, Rickli EE, Lergier W, Gillessen D (1980). Localization of individual lysine-binding regions in human plasminogen and investigations on their complex-forming properties. *Eur J Biochem* **107,** 7-13.

Levin EG, Loskutoff DJ (1982). Cultured bovine endothelial cells produce both urokinase and tissue-type plasminogen activators. *J Cell Biol* **94,** 631-636.

Levitt M, Chothia C (1976). Structural patterns in globular proteins. *Nature* **261,** 552-558.

Lewis JH, Ferguson JH (1951). A proteolytic enzyme system of the blood. III. Activation of dog serum profibrinolysin by staphylokinase. *Am J Physiol* **166,** 594-603.

Lijnen HR, Van Hoef B, De Cock F, Okada K, Ueshima S, Matsuo O, Collen D (1991). On the mechanism of fibrin-specific plasminogen activation by staphylokinase. *J Biol Chem* **266,** 11826-11832.

Lin LF, Oeun S, Houng A, Reed GL (1996). Mutation of lysines in a plasminogen binding region of streptokinase identifies residues important for generating a functional activator complex. *Biochemistry* **35,** 16879-16885.

Lin LF, Houng A, Reed GL (2000). Epsilon amino caproic acid inhibits streptokinase-plasminogen activator complex formation and substrate binding through kringle-dependent mechanisms. *Biochemistry* **39,** 4740-4745.

Liu L, Sazonova IY, Turner RB, Chowdhry SA, Tsai J, Houng AK, Reed GL (2000). Leucine 42 in the fibronectin motif of streptokinase plays a critical role in fibrin-independent plasminogen activation. *J Biol Chem* **275,** 37686-37691.

Loskutoff DJ, Schleef RR (1988). Plasminogen activators and their inhibitors. *Methods Enzymol* **163,** 293-302.

Loy JA, Lin X, Schenone M, Castellino FJ, Zhang XC, Tang J (2001). Domain interactions between streptokinase and human plasminogen. *Biochemistry* **40,** 14686-14695.

Lundrigan MD, Webb RM (1992). Prevalence of ompT among *Escherichia coli* isolates of human origin. *FEMS Microbiol Lett* **76,** 51-56.

Madison EL (1994). Probing structure-function relationships of tissue-type plasminogen activator by site-specific mutagenesis. *Fibrinolysis* **8,** 221-236.

Malke H, Ferretti JJ (1984). Streptokinase: cloning, expression, and excretion by *Escherichia coli. Proc Natl Acad Sci USA* **81,** 3557-3561.

Malke H, Gerlach D, Kohler W, Ferretti JJ (1984). Expression of a streptokinase gene from *Streptococcus equisimilis* in *Streptococcus sanguis. Mol Gen Genet* **196,** 360-363.

Malke H, Roe B, Ferretti JJ (1985). Nucleotide sequence of the streptokinase gene from *Streptococcus equisimilis* H46A. *Gene* **34,** 357-362.

Malke H. (1993). Polymorphism of the streptokinase gene: implications for the pathogenesis of post-streptococcal glomerulonephritis. *Zentralbl Bakteriol* **278,** 246-257.

Mangel WF, Toledo DL, Brown MT, Worzalla K, Lee M, Dunn JJ (1994). Omptin: an *Escherichia coli* outer membrane proteinase that activates plasminogen. *Methods Enzymol* **244,** 384-399.

Marder VJ, Sherry S (1988). Thrombolytic therapy: current status (1). *N Engl J Med* **318,** 1512-1520.

Markus G, Evers JL, Hobika GH (1976). Activator activities of the transient forms of the human plasminogen-streptokinase complex during its proteolytic conversion to the stable activator complex. *J Biol Chem* **251,** 6495-6504.

Markus G, Werkheiser WC (1964). The interaction of streptokinase with plasminogen. Functional properties of the activated enzyme. *J Biol Chem* **239,** 2637-2643.

Marti D, Schaller J, Ochensberger B, Rickli EE (1994). Expression, purification and characterization of the recombinant kringle 2 and kringle 3 domains of human plasminogen and analysis of their binding affinity for omega-aminocarboxylic acids. *Eur J Biochem* **219,** 455-462.

Mathews II, Vanderhoff-Hanaver P, Castellino FJ, Tulinsky A (1996). Crystal structures of the recombinant kringle 1 domain of human plasminogen in complexes with the ligands epsilon-aminocaproic acid and trans-4-(aminomethyl)cyclohexane-1-carboxylic Acid. *Biochemistry* **35,** 2567-2576.

Matsuo O, Okada K, Fukao H, Tomioka Y, Ueshima S, Watanuki M, Sakai M (1990). Thrombolytic properties of staphylokinase. *Blood* **76,** 925-929.

McCance SG, Menhart N, Castellino FJ (1994). Amino acid residues of the kringle-4 and kringle-5 domains of human plasminogen that stabilize their interactions with omega-amino acid ligands. *J Biol Chem* **269,** 32405-32410.

McClintock DK, Bell PH (1971). The mechanism of activation of human plasminogen by streptokinase. *Biochem Biophys Res Commun* **43,** 694-702.

McColl DJ, Honchell CD, Frankel AD (1999). Structure-based design of an RNA-binding zinc finger. *Proc Natl Acad Sci U S A* **96,** 9521-9526.

McGrath KG, Patterson R (1984). Anaphylactic reactivity to streptokinase. *JAMA* **252,** 1314-1317.

McGrath KG, Zeffren B, Alexander J, Kaplan K, Patterson R (1985). Allergic reactions to streptokinase consistent with anaphylactic or antigen-antibody complex-mediated damage. *J Allergy Clin Immunol* **76,** 453-457.

Menhart N, Sehl LC, Kelley RF, Castellino FJ (1991). Construction, expression, and purification of recombinant kringle 1 of human plasminogen and analysis of its interaction with omega-amino acids. *Biochemistry* **30,** 1948-1957.

Misselwitz R, Kraft R, Kostka S, Fabian H, Welfle K, Pfeil W, Welfle H, Gerlach D (1992). Limited proteolysis of streptokinase and properties of some fragments. *Int J Biol Macromol* **14,** 107-116.

Miyazaki C, Iba Y, Yamada Y, Takahashi H, Sawada J, Kurosawa Y (1999). Changes in the specificity of antibodies by site-specific mutagenesis followed by random mutagenesis. *Protein Eng* **12,** 407-415.

Montclare JK, Schepartz A (2003). Miniature homeodomains: high specificity without an N-terminal arm. *J Am Chem Soc* **125,** 3416-3417.

Moroi M, Aoki N (1976). Isolation and characterization of alpha2-plasmin inhibitor from human plasma. A novel proteinase inhibitor which inhibits activator-induced clot lysis. *J Biol Chem* **251,** 5956-5965.

Mortensen SB, Sottrup-Jensen L, Hansen HF, Petersen TE, Magnusson S (1981). Primary and secondary cleavage sites in the bait region of alpha 2-macroglobulin. *FEBS Lett* **135,** 295-300.

Morton TA, Myszka DG, Chaiken IM (1995). Interpreting complex binding kinetics from optical biosensors: a comparison of analysis by linearization, the integrated rate equation, and numerical integration. *Anal Biochem* **227,** 176-185.

Motta A, Laursen RA, Llinas M, Tulinsky A, Park CH (1987). Complete assignment of the aromatic proton magnetic resonance spectrum of the kringle 1 domain from human plasminogen: structure of the ligand-binding site. *Biochemistry* **26,** 3827-3836.

Mulichak AM, Tulinsky A, Ravichandran KG (1991). Crystal and molecular structure of human plasminogen kringle 4 refined at 1.9-A resolution. *Biochemistry* **30,** 10576-10588.

Mundada LV, Prorok M, DeFord ME, Figuera M, Castellino FJ, Fay WP (2003). Structure-function analysis of the streptokinase amino terminus (residues 1-59). *J Biol Chem* **278,** 24421-24427.

Murzin AG, Brenner SE, Hubbard T, Chothia C (1995). SCOP: a structural classification of proteins database for the investigation of sequences and structures. *J Mol Biol* **247,** 536-540.

Myszka DG (1997). Kinetic analysis of macromolecular interactions using surface plasmon resonance biosensors. *Curr Opin Biotechnol* **8,** 50-57.

Nakashima A, Okada T, Sugie I (1990). Fibrin-dependent activation of plasminogen by a proteolytic digest of streptokinase. *Blood Coagul Fibrinolysis* **1,** 279-284.

Nemerson Y, Nossel HL (1982). The biology of thrombosis. *Annu Rev Med* **33,** 479-488.

Neurath H (1989). Proteolytic processing and physiological regulation. *Trends Biochem Sci* **14,** 268-271.

Nicholls A, Sharp KA, Honig B (1991). Protein folding and association: insights from the interfacial and thermodynamic properties of hydrocarbons. *Proteins* **11,** 281-296.

Nienaber VL, Young SL, Birktoft JJ, Higgins DL, Berliner LJ (1992). Conformational similarities between one-chain and two-chain tissue plasminogen activator (t-PA): implications to the activation mechanism on one-chain t-PA. *Biochemistry* **31,** 3852-3861.

Nihalani D (1997). Structural and functional studies of streptokinase. PhD thesis (Science). Panjab University.

Nihalani D, Kumar R, Rajagopal K, Sahni G (1998). Role of the amino-terminal region of streptokinase in the generation of a fully functional plasminogen activator complex probed with synthetic peptides. *Protein Sci* **7,** 637-648.

Nihalani D, Raghava GP, Sahni G (1997). Mapping of the plasminogen binding site of streptokinase with short synthetic peptides. *Protein Sci* **6,** 1284-1292.

Nihalani D, Sahni G (1995). Streptokinase contains two independent plasminogen-binding sites. *Biochem Biophys Res Commun* **217,** 1245-1254.

Novokhatny VV, Ingham KC, Medved LV (1991). Domain structure and domain-domain interactions of recombinant tissue plasminogen activator. *J Biol Chem* **266,** 12994-13002.

Novokhatny VV, Matsuka YuV, Kudinov SA (1989). Analysis of ligand binding to kringles 4 and 5 fragments from human plasminogen. *Thromb Res* **53,** 243-252.

Ogata N, Ogata Y, Hokamaki J, Araki H, Morikami Y, Numata Y (1996). Serial changes of plasminogen activator inhibitor activity in thrombolytic therapy for acute myocardial infarction: Comparison between thrombolytic therapies with mutant TPA (lanoteplase/BMS-200980) and recombinant TPA (alteplase). *Circulation* **94 suppl I,** I-89.

Pannell R, Gurewich V (1987). Activation of plasminogen by single-chain urokinase or by two-chain urokinase-a demonstration that single-chain urokinase has a low catalytic activity (pro-urokinase). *Blood* **69,** 22-26.

Parhami-Seren B, Keel T, Reed GL (1996). Structural characterization of immunodominant regions of streptokinase recognized by murine monoclonal antibodies. *Hybridoma* **15,** 169-176.

Parhami-Seren B, Keel T, Reed GL (1997). Sequences of antigenic epitopes of streptokinase identified via random peptide libraries displayed on phage. *J Mol Biol* **271,** 333-341.

Parrado J, Conejero-Lara F, Smith RA, Marshall JM, Ponting CP, Dobson CM (1996). The domain organization of streptokinase: nuclear magnetic resonance, circular dichroism, and functional characterization of proteolytic fragments. *Protein Sci* **5,** 693-704.

Parry MA, Fernandez-Catalan C, Bergner A, Huber R, Hopfner KP, Schlott B, Guhrs KH, Bode W (1998). The ternary microplasmin-staphylokinase-microplasmin complex is a proteinase-cofactor-substrate complex in action. *Nat Struct Biol* **5,** 917-923.

Parry MA, Zhang XC, Bode I (2000). Molecular mechanisms of plasminogen activation: bacterial cofactors provide clues. *Trends Biochem Sci* **25,** 53-59.

Peisach E, Wang J, de los Santos T, Reich E, Ringe D (1999). Crystal structure of the proenzyme domain of plasminogen. *Biochemistry* **38,** 11180-11188.

Pennica D, Holmes WE, Kohr WJ, Harkins RN, Vehar GA, Ward CA, Bennett WF, Yelverton E, Seeburg PH, Heyneker HL, Goeddel DV, Collen D (1983). Cloning and expression of human tissue-type plasminogen activator cDNA in *E. coli*. *Nature* **301,** 214-221.

Petersen LC, Lund LR, Nielsen LS, Dano K, Skriver L (1988). One-chain urokinase-type plasminogen activator from human sarcoma cells is a proenzyme with little or no intrinsic activity. *J Biol Chem* **263,** 11189-11195.

Pirie-Shepherd SR, Stevens RD, Andon NL, Enghild JJ, Pizzo SV (1997). Evidence for a novel O-linked sialylated trisaccharide on Ser-248 of human plasminogen 2. *J Biol Chem* **272,** 7408-7411.

Pisano JJ, Finlayson JS, Peyton MP (1968). Cross-link in fibrin polymerized by factor 13: epsilon-(gamma-glutamyl) lysine. *Science* **160,** 892-893.

Ponting CP, Holland SK, Cederholm-Williams SA, Marshall JM, Brown AJ, Spraggon G, Blake CC (1992a). The compact domain conformation of human Glu-plasminogen in solution. *Biochim Biophys Acta* **1159,** 155-161.

Ponting CP, Marshall JM, Cederholm-Williams SA (1992b). Plasminogen: a structural review. *Blood Coagul Fibrinolysis* **3,** 605-614.

Porath J, Carlsson J, Olsson I, Belfrage G (1975). Metal chelate affinity chromatography, a new approach to protein fractionation. *Nature* **258,** 598-599.

Pratap J, Kaur J, RajaMohan G, Singh D, Dikshit KL (1996). Role of N-terminal domain of streptokinase in protein transport. *Biochem Biophys Res Commun* **227,** 303-310.

Pytela R, Pierschbacher MD, Ginsberg MH, Plow EF, Ruoslahti E (1986). Platelet membrane glycoprotein IIb/IIIa: member of a family of Arg-Gly-Asp-specific adhesion receptors. *Science* **231,** 1559-1562.

Rabijns A, De Bondt HL, De Ranter C (1997). Three-dimentional structure of staphylokinase, a plasminogen activator with therapeutic potential. *Nat Struct Biol* **4,** 357-360.

Radek JT, Castellino FJ (1989). Conformational properties of streptokinase. *J Biol Chem* **264,** 9915-9922.

Rajagopalan S, Gonias SL, Pizzo SV (1985). A nonantigenic covalent streptokinase-polyethylene glycol complex with plasminogen activator function. *J Clin Invest* **75,** 413-419.

Rajamohan G, Dahiya M, Mande SC, Dikshit KL (2002). Function of the 90-loop (Thr90-Glu100) region of staphylokinase in plasminogen activation probed through site-directed mutagenesis and loop deletion. *Biochem J* **365,** 379-389.

Ranby M, Bergsdorf N, Nilsson T (1982). Enzymatic properties of the one- and two-chain form of tissue plasminogen activator. *Thromb Res* **27,** 175-183.

Raum D, Marcus D, Alper CA, Levey R, Taylor PD, Starzl TE (1980). Synthesis of human plasminogen by the liver. *Science* **208,** 1036-1037.

Reddy KN, Markus G (1972). Mechanism of activation of human plasminogen by streptokinase. Presence of active center in streptokinase-plasminogen complex. *J Biol Chem* **247,** 1683-16891.

Reed GL, Kussie P, Parhami-Seren B (1993). A functional analysis of the antigenicity of streptokinase using monoclonal antibody mapping and recombinant streptokinase fragments. *J Immunol* **150,** 4407-4415.

Reed GL, Lin LF, Parhami-Seren B, Kussie P (1995). Identification of a plasminogen binding region in streptokinase that is necessary for the creation of a functional streptokinase-plasminogen activator complex. *Biochemistry* **34,** 10266-10271.

Refino CJ, Paoni NF, Keyt BA, Pater CS, Badillo JM, Wurm FM, Ogez J, Bennett WF (1993). A variant of t-PA (T103N, KHRR 296-299 AAAA) that, by bolus, has increased potency and decreased systemic activation of plasminogen. *Thromb Haemost* **70,** 313-319.

Rejante MR, Llinas M (1994a). 1H-NMR assignments and secondary structure of human plasminogen kringle 1. *Eur J Biochem* **221,** 927-937.

Rejante MR, Llinas M (1994b). Solution structure of the epsilon-aminohexanoic acid complex of human plasminogen kringle 1. *Eur J Biochem* **221,** 939-949.

Renatus M, Engh RA, Stubbs MT, Huber R, Fischer S, Kohnert U, Bode W (1997). Lysine 156 promotes the anomalous proenzyme activity of tPA: X-ray crystal structure of single-chain human tPA. *EMBO J* **16,** 4797-4805.

Rickli EE, Otavsky WI (1973). Release of an N-terminal peptide from human plasminogen during activation with urokinase. *Biochim Biophys Acta* **295,** 381-384.

Robbins KC, Summaria L, Hsieh B, Shah RJ (1967). The peptide chains of human plasmin. Mechanism of activation of human plasminogen to plasmin. *J Biol Chem* **242,** 2333-2342.

Robbins KC, Summaria L, Wohl RC (1981). Human plasmin. *Methods Enzymol* **80 Pt C,** 379-387.

Rodriguez P, Fuentes D, Munoz E, Rivero D, Orta D, Alburquerque S, Perez S, Besada V, Herrera L (1994). The streptokinase domain responsible for plasminogen binding. *Fibrinolysis* **8,** 276-281.

Rodriguez P, Fuentes P, Barro M, Alvarez JG, Munoz E, Collen D, Lijnen HR (1995). Structural domains of streptokinase involved in the interaction with plasminogen. *Eur J Biochem* **229,** 83-90.

Rodriguez P, Hernandez L, Munoz E, Castro A, de la Fuente J, Herrera L (1992). Purification of streptokinase by affinity chromatography on immobilized acylated human plasminogen. *Biotechniques* **12,** 424-429.

Rosey EL, Lincoln RA, Ward PN, Yancey RJ Jr, Leigh JA (1999). PauA: a novel plasminogen activator from *Streptococcus uberis. FEMS Microbiol Lett* **178,** 27-33.

Ross AM (1999). New plasminogen activators: a clinical review. *Clin Cardiol* **22,** 165-171.

Saito H, Hamilton SM, Tavill AS, Louis L, Ratnoff OD (1980). Production and release of plasminogen by isolated perfused rat liver. *Proc Natl Acad Sci U S A* **77,** 6837-6840.

Sako T, Sawaki S, Sakurai T, Ito S, Yoshizawa Y, Kondo I (1983). Cloning and expression of the staphylokinase gene of *Staphylococcus aureus* in *Escherichia coli. Mol Gen Genet* **190,** 271-277.

Sako T, Tsuchida N (1983). Nucleotide sequence of the staphylokinase gene from *Staphylococcus aureus. Nucleic Acids Res* **11,** 7679-7693.

Sako T (1985). Overproduction of staphylokinase in *Escherichia coli* and its characterization. *Eur J Biochem* **149,** 557-563.

Sambrook J, Fritsch EF, Maniatis T (1989). *Molecular Cloning: a Laboratory Manual.* Cold Spring Harbor Laboratory Press, Cold Spring Harbor, New York, USA.

Sambrook J, Russell D (2001). *Molecular Cloning: a Laboratory Manual.* Cold Spring Harbor Laboratory Press, Cold Spring Harbor, New York, USA.

Sarkar G, Sommer SS (1990). The "megaprimer" method of site-directed mutagenesis. *Biotechniques* **8,** 404-407.

Sarkar G, Sommer SS (1992). Double-stranded DNA segments can efficiently prime the amplification of human genomic DNA. *Nucleic Acids Res* **20,** 4937-4938.

Sazonova IY, Houng AK, Chowdhry SA, Robinson BR, Hedstrom L, Reed GL (2001). The mechanism of a bacterial plasminogen activator intermediate between streptokinase and staphylokinase. *J Biol Chem* **276,** 12609-12613.

Schaller J, Rickli EE (1988). Structural aspects of the plasminogen of various species. *Enzyme* **40,** 63-69.

Schick LA, Castellino FJ (1974). Direct evidence for the generation of an active site in the plasminogen moiety of the streptokinase-human plasminogen activator complex. *Biochem Biophys Res Commun* **57,** 47-54.

Schwartz ML, Pizzo SV, Hill RL, McKee PA (1973). Human Factor XIII from plasma and platelets. Molecular weights, subunit structures, proteolytic activation, and cross-linking of fibrinogen and fibrin. *J Biol Chem* **248,** 1395-1407.

Schweitzer DH, van der Wall EE, Bosker HA, Scheffer E, Macfarlane JD (1991). Serum-sickness-like illness as a complication after streptokinase therapy for acute myocardial infarction. *Cardiology* **78,** 68-71.

Segal DJ, Barbas CF 3rd (2000). Design of novel sequence-specific DNA-binding proteins. *Curr Opin Chem Biol* **4,** 34-39.

Sehl LC, Castellino FJ (1990). Thermodynamic properties of the binding of alpha-, omega-amino acids to the isolated kringle 4 region of human plasminogen as determined by high sensitivity titration calorimetry. *J Biol Chem* **265,** 5482-5486.

Shen LL, Hermans J, McDonagh J, McDonagh RP, Carr M (1975). Effects of calcium ion and covalent crosslinking on formation and elasticity of fibrin cells. *Thromb Res* **6,** 255-265.

Shen LL, McDonagh RP, McDonagh J, Hermans J (1977). Early events in the plasmin digestion of fibrinogen and fibrin. Effects of plasmin on fibrin polymerization. J Biol Chem **252,** 6184-6189.

Shi GY, Chang BI, Chen SM, Wu DH, Wu HL (1994). Function of streptokinase fragments in plasminogen activation. *Biochem J* **304,** 235-241.

Shi GY, Chang BI, Su SW, Young KC, Wu DH, Chang LC, Tsai YS, Wu HL (1998). Preparation of a novel streptokinase mutant with improved stability. *Thromb Haemost* **79,** 992-997.

Shi GY, Wu HL (1988). Isolation and characterization of microplasminogen. A low molecular weight form of plasminogen. *J Biol Chem* **263,** 17071-17075.

Shotton DM, Watson HC (1970). Three-dimensional structure of tosyl-elastase. *Nature* **225,** 811-816.

Sia SK, Kim PS (2003). Protein grafting of an HIV-1-inhibiting epitope. *Proc Natl Acad Sci U S A* **100,** 9756-9761.

Smalling RW, Bode C, Kalbfleisch J, Sen S, Limbourg P, Forycki F, Habib G, Feldman R, Hohnloser S, Seals A (1995). More rapid, complete, and stable coronary thrombolysis with bolus administration of reteplase compared with alteplase infusion in acute myocardial infarction. RAPID Investigators. *Circulation* **91,** 2725-2732.

Smalling RW (1997). Pharmacological and clinical impact of the unique molecular structure of a new plasminogen activator. *Eur Heart J* **18 suppl F,** F11-16.

Smith RA, Dupe RJ, English PD, Green J (1981). Fibrinolysis with acyl-enzymes: a new approach to thrombolytic therapy. *Nature* **290,** 505-508.

Soberano ME, Ong EB, Johnson AJ, Levy M, Schoellmann G (1976). Purification and characterization of two forms of urokinase. *Biochim Biophys Acta* **445,** 763-773.

Sodetz JM, Brockway WJ, Castellino FJ (1972). Multiplicity of rabbit plasminogen. Physical characterization. *Biochemistry* **11,** 4451-4458.

Sottrup-Jensen L, Claeys H, Zajdal M, Petersen TE, Magnusson S (1978). The primary structure of human plasminogen: Isolation of two lysine binding fragments and one "mini" plasminogen (MW, 38,000) by elastase-catalyzed-specific limited proteolysis. In: Davidson JF, Rowan RM, Samama MM, Desnoyers PC, eds. *Progress in chemical fibrinolysis and thrombolysis, vol 3,* Raven Press, New York. pp 191-209.

Sottrup-Jensen L, Stepanik TM, Kristensen T, Wierzbicki DM, Jones CM, Lonblad PB, Magnusson S, Petersen TE (1984). Primary structure of human alpha 2-macroglobulin. V. The complete structure. *J Biol Chem* **259,** 8318-8327.

Sroga GE, Dordick JS (2001). Generation of a broad esterolytic subtilisin using combined molecular evolution and periplasmic expression. *Protein Eng* **14,** 929-937.

Steffens GJ, Gunzler WA, Otting F, Frankus E, Flohe L (1982). The complete amino acid sequence of low molecular mass urokinase from human urine. *Hoppe Seylers Z Physiol Chem* **363,** 1043-1058.

Studier FW, Moffatt BA (1986). Use of bacteriophage T7 RNA polymerase to direct selective high-level expression of cloned genes. *J Mol Biol* **189,** 113-130.

Studier FW, Rosenberg AH, Dunn JJ, Dubendorff JW (1990). Use of T7 RNA polymerase to direct expression of cloned genes. *Methods Enzymol* **185,** 60-89.

Stults NL, Asta LM, Lee YC (1989). Immobilization of proteins on oxidized crosslinked sepharose preparations by reductive amination. *Anal Biochem* **180,** 114-119.

Stump DC, Lijnen HR, Collen D (1986a). Purification and characterization of single-chain urokinase-type plasminogen activator from human cell cultures. *J Biol Chem* **261,** 1274-1278.

Stump DC, Thienpont M, Collen D (1986b). Urokinase-related proteins in human urine. Isolation and characterization of single-chain urokinase (pro-urokinase) and urokinase-inhibitor complex. *J Biol Chem* **261,** 1267-1273.

Summaria L, Robbins KC (1976). Isolation of a human plasmin-derived, functionally active, light (B) chain capable of forming with streptokinase an equimolar light (B) chain-streptokinase complex with plasminogen activator activity. *J Biol Chem* **251,** 5810-5813.

Summaria L, Arzadon L, Bernabe P, Robbins KC (1974). The interaction of streptokinase with human, cat, dog, and rabbit plasminogens. The fragmentation of streptokinase in the equimolar plasminogen-streptokinase complexes. *J Biol Chem* **249,** 4760-4769.

Summaria L, Boreisha I, Wohl RC, Robbins KC (1979). Recombinant human Lys-plasmin and the Lys-plasmin.streptokinase complex. *J Biol Chem* **254,** 6811-6814.

Summaria L, Hsieh B, Robbins KC (1967). The specific mechanism of activation of human plasminogen to plasmin. *J Biol Chem* **242,** 4279-4283.

Summaria L, Ling CM, Groskopf WR, Robbins KC (1968). The active site of bovine plasminogen activator. Interaction of streptokinase with human plasminogen and plasmin. *J Biol Chem* **243,** 144-150.

Sundram V, Nanda JS, Rajagopal K, Dhar J, Chaudhary A, Sahni G (2003). Domain truncation studies reveal that the streptokinase-plasmin activator complex utilizes long range protein-protein interactions with macromolecular substrate to maximize catalytic turnover. *J Biol Chem* **278,** 30569-30577.

Taylor FB Jr, Beisswenger JG (1973). Identification of modified streptokinase as the activator of bovine and human plasminogen. *J Biol Chem* **248,** 1127-1134.

Taylor FB Jr, Botts J (1968). Purification and characterization of streptokinase with studies of streptokinase activation of plasminogen. *Biochemistry* **7,** 232-242.

Teuten AJ, Broadhurst RW, Smith RA, Dobson CM (1993). Characterization of structural and folding properties of streptokinase by NMR spectroscopy. *Biochem J* **290 (Pt 2),** 313-319.

Thewes T, Constantine K, Byeon IJ, Llinas M (1990). Ligand interactions with the kringle 5 domain of plasminogen. A study by 1H NMR spectroscopy. *J Biol Chem* **265,** 3906-3915.

Tillet WS, Garner RL (1933). The fibrinolytic activity of hemolytic streptococci. *J Exp Med* **68,** 485-488.

Torrens I, Ojalvo AG, Seralena A, Hayes O, de la Fuente J (1999b). A mutant streptokinase lacking the C-terminal 42 amino acids is less immunogenic. *Immunol Lett* **70,** 213-218.

Torrens I, Ojalvo AG, Seralena A, Pupo E, Lugo V, Paez R (1999c). A mutant streptokinase lacking the C-terminal 42 amino acids is less reactive with preexisting antibodies in patient sera. *Biochem Biophys Res Commun* **266,** 230-236.

Torrens I, Reyes O, Ojalvo AG, Seralena A, Chinea G, Cruz LJ, de la Fuente J (1999a). Mapping of the antigenic regions of streptokinase in humans after streptokinase therapy. *Biochem Biophys Res Commun* **259,** 162-168.

Travis J, Salvesen GS (1983). Human plasma proteinase inhibitors. *Annu Rev Biochem* **52,** 655-709.

Urano T, de Serrano VS, Gaffney PJ, Castellino FJ (1988). The activation of human [Glu1] plasminogen by human single-chain urokinase. *Arch Biochem Biophys* **264,** 222-230.

van Zonneveld AJ, Veerman H, Pannekoek H (1986). On the interaction of the finger and the kringle-2 domain of tissue-type plasminogen activator with fibrin. Inhibition of kringle-2 binding to fibrin by epsilon-amino caproic acid. *J Biol Chem* **261,** 14214-14218.

Vasudha S (2002). Structure-function studies of streptokinase. PhD thesis (Science). Jawaharlal Nehru University.

Verheijen JH, Caspers MP, Chang GT, de Munk GA, Pouwels PH, Enger-Valk BE (1986). Involvement of finger domain and kringle 2 domain of tissue-type plasminogen activator in fibrin binding and stimulation of activity by fibrin. *EMBO J* **5,** 3525-3530.

Verstraete M (2000). Third-generation thrombolytic drugs. *Am J Med* **109,** 52-58.

Violand BN, Castellino FJ (1976). Mechanism of the urokinase-catalyzed activation of human plasminogen. *J Biol Chem* **251,** 3906-3912.

Vita C, Drakopoulou E, Vizzavona J, Rochette S, Martin L, Menez A, Roumestand C, Yang YS, Ylisastigui L, Benjouad A, Gluckman JC (1999). Rational engineering of a miniprotein that reproduces the core of the CD4 site interacting with HIV-1 envelope glycoprotein. *Proc Natl Acad Sci U S A* **96,** 13091-13096.

Vita C, Roumestand C, Toma F, Menez A (1995). Scorpion toxins as natural scaffolds for protein engineering. *Proc Natl Acad Sci U S A* **92,** 6404-6408.

Wakeham N, Terzyan S, Zhai P, Loy JA, Tang J, Zhang XC (2002). Effects of deletion of streptokinase residues 48-59 on plasminogen activation. *Protein Eng* **15,** 753-761.

Wallen P, Wiman B (1972). Characterization of human plasminogen. II. Separation and partial characterization of different molecular forms of human plasminogen. *Biochim Biophys Acta* **257,** 122-134.

Wang X, Lin X, Loy JA, Tang J, Zhang XC (1998). Crystal structure of the catalytic domain of human plasmin complexed with streptokinase. *Science* **281,** 1662-1665.

Wang S, Reed GL, Hedstrom L (1999a). Deletion of Ile1 changes the mechanism of streptokinase: evidence for the molecular sexuality hypothesis. *Biochemistry* **38,** 5232-5240.

Wang X, Tang J, Hunter B, Zhang XC (1999b). Crystal structure of streptokinase beta-domain. *FEBS Lett* **459,** 85-89.

Wang X, Terzyan S, Tang J, Loy JA, Lin X, Zhang XC (2000a). Human plasminogen catalytic domain undergoes an unusual conformational change upon activation. *J Mol Biol* **295,** 903-914.

Wang S, Reed GL, Hedstrom L (2000b). Zymogen activation in the streptokinase-plasminogen complex. Ile1 is required for the formation of a functional active site. *Eur J Biochem* **267,** 3994-4001.

Weinstein MJ, Doolittle RF (1972). The effect of some synthetic arginyl and lysyl compounds on clotting and fibrinolysis. *Thromb Diath Haemorrh* **28,** 289-297.

Weitz JI, Stewart RJ, Fredenburgh JC (1999). Mechanism of action of plasminogen activators. *Thromb Haemost* **82,** 974-982.

Welfle K, Pfeil W, Misselwitz R, Welfle H, Gerlach D (1992). Conformational properties of streptokinase-differential scanning calorimetric investigations. *Int J Biol Macromol* **14,** 19-22.

White WF, Barlow GH, Mozen MM (1966). The isolation and characterization of plasminogen activators (urokinase) from human urine. *Biochemistry* **5,** 2160-2169.

Wiman B, Collen D (1977). Purification and characterization of human antiplasmin, the fast-acting plasmin inhibitor in plasma. *Eur J Biochem* **78,** 19-26.

Wiman B, Collen D (1978a). Molecular mechanism of physiological fibrinolysis. *Nature* **272,** 549-550.

Wiman B, Collen D (1978b). On the kinetics of the reaction between human antiplasmin and plasmin. *Eur J Biochem* **84,** 573-578.

Wiman B, Collen D (1979). On the mechanism of the reaction between human alpha 2-antiplasmin and plasmin. *J Biol Chem* **254,** 9291-9297.

Wiman B, Lijnen HR, Collen D (1979). On the specific interaction between the lysine-binding sites in plasmin and complementary sites in alpha2-antiplasmin and in fibrinogen. *Biochim Biophys Acta* **579,** 142-154.

Wiman B, Wallen P (1973). Activation of human plasminogen by an insoluble derivative of urokinase. Structural changes of plasminogen in the course of activation to plasmin and demonstration of a possible intermediate compound. *Eur J Biochem* **36,** 25-31.

Wiman B, Wallen P (1977). The specific interaction between plasminogen and fibrin. A physiological role of the lysine binding site in plasminogen. *Thromb Res* **10,** 213-222.

Wohl RC (1984). Interference of active site specific reagents in plasminogen-streptokinase active site formation. *Biochemistry* **23,** 3799-3804.

Wohl RC, Arzadon L, Summaria L, Robbins KC (1977). Comparison of the esterase and human plasminogen activator activities of various activated forms of human plasminogen and their equimolar streptokinase complexes. *J Biol Chem* **252,** 1141-1147.

Wohl RC, Summaria L, Arzadon L, Robbins KC (1978). Steady state kinetics of activation of human and bovine plasminogens by streptokinase and its equimolar complexes with various activated forms of human plasminogen. *J Biol Chem* **253,** 1402-1407.

Wohl RC, Summaria L, Robbins KC (1980). Kinetics of activation of human plasminogen by different activator species at pH 7.4 and 37 degrees C. *J Biol Chem* **255,** 2005-2013.

Wong SL, Ye R, Nathoo S (1994). Engineering and production of streptokinase in a *Bacillus subtilis* expression-secretion system. *Appl Environ Microbiol* **60,** 517-523.

Wu SC, Castellino FJ, Wong SL (2003). A fast-acting, modular-structured staphylokinase fusion with kringle-1 from human plasminogen as the fibrin-targeting domain offers improved clot lysis efficacy. *J Biol Chem* **278,** 18199-18206.

Wu DH, Shi GY, Chuang WJ, Hsu JM, Young KC, Chang CW, Wu HL (2001). Coiled coil region of streptokinase gamma-domain is essential for plasminogen activation. *J Biol Chem* **276,** 15025-15033.

Wu HL, Chang BI, Wu DH, Chang LC, Gong CC, Lou KL, Shi GY (1990). Interaction of plasminogen and fibrin in plasminogen activation. *J Biol Chem* **265,** 19658-19664.

Wu TP, Padmanabhan K, Tulinsky A, Mulichak AM (1991). The refined structure of the epsilon-aminocaproic acid complex of human plasminogen kringle 4. *Biochemistry* **30,** 10589-10594.

Wu XC, Ye R, Duan Y, Wong SL (1998). Engineering of plasmin-resistant forms of streptokinase and their production in Bacillus subtilis: streptokinase with longer functional half-life. *Appl Environ Microbiol* **64,** 824-829.

Wulf RJ, Mertz ET (1969). Studies on plasminogen. 8. Species specificity of streptokinase. *Can J Biochem* **47,** 927-931.

Yadav M (1999). Construction of novel streptokinase derivatives with enhanced fibrin specificity. PhD thesis (Science). Panjab University.

Yang JT, Wu C-SC, Martinez HM (1986). Calculation of protein conformation from circular dichroism. *Methods Enzymol* **130,** 208-269.

Young KC, Shi GY, Chang YF, Chang BI, Chang LC, Lai MD, Chuang WJ, Wu HL (1995). Interaction of streptokinase and plasminogen. Studied with truncated streptokinase peptides. *J Biol Chem* **270,** 29601-29606.

Young KC, Shi GY, Wu DH, Chang LC, Chang BI, Ou CP, Wu HL (1998). Plasminogen activation by streptokinase via a unique mechanism. *J Biol Chem* **273,** 3110-3116.

Zamarron C, Lijnen HR, Van Hoef B, Collen D (1984). Biological and thrombolytic properties of proenzyme and active forms of human urokinase-I. Fibrinolytic and fibrinogenolytic properties in human plasma in vitro of urokinases obtained from human urine or by recombinant DNA technology. *Thromb Haemost* **52,** 19-23.

Zondlo NJ, Schepartz A (1999). Highly specific DNA recognition by a designed miniature protein. *J Am Chem Soc* **121,** 6938-6939.

Zhai P, Wakeham N, Loy JA, Zhang XC (2003). Functional roles of streptokinase C-terminal flexible peptide in active site formation and substrate recognition in plasminogen activation. *Biochemistry* **42,** 114-120.

Zhao H, Arnold FH (1997). Combinatorial protein design: strategies for screening protein libraries. *Curr Opin Struct Biol* **7,** 480-485.

APPENDIX

THE JOURNAL OF BIOLOGICAL CHEMISTRY
Vol. 277, No. 15, Issue of April 12, pp. 13257–13267, 2002
Printed in U.S.A.

Involvement of a Nine-residue Loop of Streptokinase in the Generation of Macromolecular Substrate Specificity by the Activator Complex through Interaction with Substrate Kringle Domains*

Received for publication, August 31, 2001, and in revised form, January 28, 2002
Published, JBC Papers in Press, January 30, 2002, DOI 10.1074/jbc.M108422200

Jayeeta Dhar‡, Abhay H. Pande‡, Vasudha Sundram, Jagpreet S. Nanda, Shekhar C. Mande, and Girish Sahni§

From the Institute of Microbial Technology, Sector 39-A, Chandigarh-160036, India

The selective deletion of a discrete surface-exposed epitope (residues 254–262; 250-loop) in the β domain of streptokinase (SK) significantly decreased the rates of substrate human plasminogen (HPG) activation by the mutant ($SK_{del254-262}$). A kinetic analysis of $SK_{del254-262}$ revealed that its low HPG activator activity arose from a 5–6-fold increase in K_m for HPG as substrate, with little alteration in k_{cat} rates. This increase in the K_m for the macromolecular substrate was proportional to a similar decrease in the binding affinity for substrate HPG as observed in a new resonant mirror-based assay for the real-time kinetic analysis of the docking of substrate HPG onto preformed binary complex. In contrast, studies on the interaction of the two proteins with microplasminogen showed no difference between the rates of activation of microplasminogen under conditions where HPG was activated differentially by nSK and $SK_{del254-262}$. The involvement of kringles was further indicated by a hypersusceptibility of the $SK_{del254-262}$·plasmin activator complex to ε-aminocaproic acid-mediated inhibition of substrate HPG activation in comparison with that of the nSK·plasmin activator complex. Further, ternary binding experiments on the resonant mirror showed that the binding affinity of kringles 1–5 of HPG to $SK_{del254-262}$·HPG was reduced by about 3-fold in comparison with that of nSK·HPG. Overall, these observations identify the 250 loop in the β domain of SK as an important structural determinant of the inordinately stringent substrate specificity of the SK·HPG activator complex and demonstrate that it promotes the binding of substrate HPG to the activator via the kringle(s) during the HPG activation process.

Streptokinase (SK),[1] a bacterial protein secreted by the Lancefield Group C β-hemolytic streptococci, is widely used as a thrombolytic agent in the treatment of various circulatory disorders, including myocardial infarction (1). Unlike other human plasminogen (HPG) activators, like tissue plasminogen activator and urokinase, SK does not possess any intrinsic enzymatic activity. Instead, SK forms an equimolar, stoichiometric complex with "partner" HPG or plasmin (HPN), which then catalytically activates free "substrate" molecules of HPG to HPN by selective cleavage of the Arg^{561}-Val^{562} peptide bond (2, 3). It is believed that consequent to the initial SK·HPG complexation, there is a structural rearrangement within the complex, and even before any proteolytic cleavage takes place, an active center within the HPG moiety capable of undergoing acylation is formed (3). This activated complex is rapidly transformed into an SK·HPN complex and develops an HPG activator activity. Unlike free HPN, however, which is essentially a trypsin-like protease with broad substrate preference, SK·HPN displays a very narrow substrate specificity (4). The structural basis of the conversion of the broadly specific serine protease HPN to a highly substrate-specific protease, once complexed with the "cofactor" SK, with exclusive propensity for acting on the target scissile peptide bond in HPG has been the subject of active investigations with both fundamental and applied implications (5–12).

SK has been shown to be composed of three structurally similar domains (termed α, β, and γ), separated by random coils and small, flexible regions at the amino and carboxyl termini (5, 7, 8). The recently solved crystal structure of the catalytic domain of HPN complexed with SK strongly indicates how SK might modulate the substrate specificity of HPN by providing a "valley" or cleft in which the macromolecular substrate can dock through protein-protein interactions, thus positioning the scissile peptide bond optimally for cleavage by the HPN active site, thereby conferring a narrow substrate preference onto an otherwise "indiscriminate" active center. In this structure, SK does not appear to induce any significant conformational changes in the active site residues directly but, along with partner HPG, seems to provide a template on which the substrate molecule can dock through protein-protein interactions, resulting in the optimized presentation of the HPG activation loop at the active center of the complex (6, 8). However, the identity of these interactions and their contributions to the formation of the enzyme-substrate intermediate(s) remains a mystery so far.

Besides the well recognized "switch" in substrate preference (4), the binding of SK to HPN results in a severalfold enhancement of the K_m for diverse small molecular weight chromogenic peptide substrates but relatively little alteration in their k_{cat} values as compared with free HPN, indicating that the pri-

* This work was supported by grants from the Department of Biotechnology and the Council of Scientific and Industrial Research, Government of India. The costs of publication of this article were defrayed in part by the payment of page charges. This article must therefore be hereby marked "*advertisement*" in accordance with 18 U.S.C. Section 1734 solely to indicate this fact.

‡ These two authors have contributed equally to this work.

§ To whom correspondence should be addressed: Inst. of Microbial Technology, Sector 39-A, Chandigarh-160036, India. Tel.: 91-172-695215; Fax: 91-172-690585; E-mail: sahni@imtech.res.in.

[1] The abbreviations used are: SK, streptokinase; PG, plasminogen (irrespective of source); HPG, human plasminogen; HPN, human plasmin; μPN, microplasmin; μPG, microplasminogen; K1–5, kringles 1–5 of plasminogen; NPGB, *p*-nitrophenyl *p*-guanidinobenzoate; SOE, splicing-overlap-extension; EACA, ε-amino caproic acid; nSK, native-like SK.

mary, covalent specificity characteristics of the active center of HPN upon SK binding are unchanged but result in steric hindrance/reduced accessibility for even the small molecular weight peptide substrates. Thus, the remarkable alteration of the macromolecular substrate specificity of HPN by SK is currently thought to be due to "exosites" generated on the SK·HPN complex, as shown recently by the elegant use of active site-labeled fluorescent HPN derivatives (10). Peptide walking studies in our laboratory had also indicated that short peptides based on the primary structure of SK, particularly those derived from selected regions in the α and β domains, displayed competitive inhibition for HPG activation by the preformed SK·HPN complex under conditions where the 1:1 complexation of SK and HPN was essentially unaffected (11, 12) However, the crystal structure of SK complexed with microplasmin(ogen) (8), while providing a high degree of resolution of the residues involved in the SK·μPN complexation, yielded few unambiguous insights regarding the interactions engendered between the activator complex and substrate HPG. This is probably due to the binary nature of the complex (*i.e.* an absence of a juxtaposed substrate molecule, large average thermal factors especially in the β domain, and a total absence, in both partner and substrate HPG, of the kringles that are known to be important in HPG activation) (13). Thus, despite a detailed and high resolution exposition of the overall nature of protein-protein interactions in the SK·μPN binary complex, discrete structures/epitopes of SK, if any, that are directly involved in the exosite formation process by the full-length activator complex have not yet been identified.

Previously, charged side chains, both in HPG, particularly around the active center (14), and in SK in the β domain (16, 17), have been shown to be important for HPG activation ability. However, a clear cut identification of a structural epitope/element in conferring substrate HPG affinity onto the SK·PG activator complex has not been demonstrated until now. Of the three domains of SK, the central β domain displays maximal affinity for HPG (15), the N-terminal α domain displays relatively lesser affinity for HPG with the γ domain showing much less affinity of for HPG.[2] Solution and structural studies suggest that both α and β domains are involved in the substrate recognition phenomenon (8, 12). Mutagenesis studies have also implicated positively charged residues in the β domain to be important but have failed to show that these residues are directly involved in substrate recognition by the binary complex (17). An examination of the crystal structure of the free β domain (18) and its comparison with the other two SK domains possessing closely similar (but not identical) structures revealed the presence of a distinct flexible loop in the β domain (the 250-loop) that protrudes into the solvent (Fig. 1).

In the present study, we chose to delete this loop based on the premise that if this structural motif is involved in substrate recognition, discrete deletion of this loop would lead to a selective increase in K_m of the activator complex. The results obtained provide clear cut evidence of the role played by this nine-residue loop in substrate recognition and thus identify a functionally important component of the macromolecular substrate-specific exosite operative in the SK·HPN complex, which interacts via the kringle(s) in HPG.

EXPERIMENTAL PROCEDURES

Reagents

Glu-plasminogen was either purchased from Roche Diagnostics Inc. or purified from human plasma by affinity chromatography (19). The RNA polymerase promoter-based expression vector, pET23(d) and *Escherichia coli* strain BL21 (DE3) were products of Novagen Inc. (Madison, WI). Thermostable DNA polymerase (*pfu*) was obtained from Stratagene Inc. (La Jolla, CA), and restriction endonucleases, T4 DNA ligase, and other DNA-modifying enzymes were acquired from New England Biolabs (Beverly, MA). Oligonucleotide primers were supplied by Integrated DNA Technologies Inc., (Indianapolis, IN). HPN was prepared by digesting Glu-HPG with urokinase covalently immobilized on agarose beads using a ratio of 300 Plough units/mg HPG in 50 mM Tris-Cl, pH 8.0, 25% glycerol, and 25 mM L-lysine at 22 °C for 10 h (15, 16). All other reagents were of the highest analytical grade available.

Design and Construction of $SK_{del254-262}$ and $\beta_{wild\ type}/\beta_{del254-262}$

A set of mutagenic and flanking primers, carrying unique restriction sites, were used in polymerase chain reactions to generate DNA fragments having overlapping ends. Thereafter, splicing-overlap-extension PCR (SOE-PCR) reactions (20) were carried out, resulting in amplification products, which were cloned in the pET23(d) expression vector (16, 21).

Oligonucleotide primers for SOE-PCR for the construction of $SK_{del254-262}$ were as follows. The mutagenic primers were as follows: upstream primer, 5′-AACAGGCTTATAGGGAAATAAACAACACTGACCTGATATCTGAGAAA-3′; downstream primer, 5′ TGTTGTTTATTTCCCTATAAGCCTGTTCCCGATTTTTAA 3′. The flanking primers were as follows: upstream primer, 5′-ATTTATGAACGTGACTCCTCAATCGTC-3′; downstream primer, 5′-ATAGGCTAAATGATAGCTAGCATTCTCTCC-3′.

Oligonucleotide primers for SOE-PCR for the construction of $\beta_{wild\ type}$ and $\beta_{del254-262}$ were as follows. Sequences of the mutagenic primers were as follows: upstream primer, 5′-AACAGGCTTATAGGGAAATAAACAACACTGACCTGATATCTGAGAAA-3′; downstream primer, 5′-TGTTGTTTATTTCCCTATAAGCCTGTTCCCGATTTTTAA-3′. Sequences of the flanking primers were as follows: upstream primer, 5′-GTGGAATATACTGTACAGTTTACTCC-3′; downstream primer, 5′-ATCGGGATCCTATTTCAAGTGACTGCGATCAAAGGG-3′.

Expression and Purification of nSK/$SK_{del254-262}$

Both proteins were expressed intracellularly in *E. coli* BL21 (DE3) cells after induction with isopropyl-1-thio-β-D-galactopyranoside essentially according to the instructions of the supplier (Novagen Inc.). The host-vector system for the expression of the cDNA corresponding to mature SK from *Streptococcus equisimilis* H46A after in-frame juxtaposition of an initiator methionine codon (so as to express the protein as Met-SK) has been described earlier (16). However, protein sequence analysis of the purified SK expressed intracellularly in *E. coli* (referred to as nSK hereafter) was found to have its N-terminal Met removed at a 50% level. The same case was seen in the mutant ($SK_{del254-262}$) prepared similarly from *E. coli* employing the same expression vector. The pelleted cells were sonicated, and the proteins in the supernatants were precipitated with ammonium sulfate (16). This fraction, after dissolution in 20 mM Tris-Cl buffer, pH 7.5, was then chromatographed on a Poros-D anion exchange column fitted onto a Bio-Cad Sprint liquid chromatographic workstation (Perseptive Biosystems Inc., Framingham, MA). nSK/$SK_{del254-262}$ were eluted using a linear gradient of NaCl (0–0.5 M) in 20 mM Tris-Cl buffer, pH 7.5. The eluted proteins were more than 95% pure, as analyzed by SDS-PAGE.

Expression and Purification of $\beta_{wild\ type}/\beta_{del254-262}$

Both proteins were expressed intracellularly in *E. coli* BL21 (DE3) cells as inclusion bodies. The pellet obtained after sonication was taken up in 8 M urea and placed under gentle shaking conditions for 30 min to effect dissolution. After a high speed centrifugation step, the protein in the supernatant was refolded by 20-fold dilution with 20 mM Tris-Cl buffer, pH 7.5. The β domain was then purified to more than 95% homogeneity by chromatography on DEAE-Sepharose Fast-flow (Amersham Biosciences) at 4 °C using a linear NaCl gradient (0–0.25 M NaCl in 20 mM Tris-Cl buffer, pH 7.5).

Preparation of μPG and K1–5

Microplasminogen, the catalytic domain of plasminogen (residues Lys^{530}–Asn^{790}) devoid of all kringles was prepared by cleavage of HPG by HPN under alkaline conditions (0.1 N glycine/NaOH buffer, pH 10.5) at 25 °C. Microplasminogen was purified from the reaction mixture by passing through a Lys-Sepharose column (Amersham Biosciences), followed by a soybean-trypsin inhibitor-Sepharose 4B column to absorb HPN and μPN, as reported (22). The flow-through

[2] V. Sundram, K. Rajagopal, A. Chaudhary, S. S. Komath, and G. Sahni, unpublished observations.

was then subjected to molecular sieve chromatography, after concentration by ultrafiltration, on a column (16 × 60 cm) of Superdex-75™ (Amersham Biosciences). The purity of μPG formed was analyzed by SDS-PAGE, which showed a single band moving at the position expected from its molecular size (22). The proteolytic fragment containing all of the HPG kringle domains (K1–5) was prepared by incubating HPG with urokinase-free HPN (5:1 ratio of HPG and HPN) under alkaline conditions (0.1 N glycine/NaOH, pH 9.0) for 72 h at 25 °C. Under these conditions, the proteolytic conversion of native HPG to K1–5 was found to be quantitative, with minimal residual HPG. HPN was removed from the reaction mixture by passing through a soybean trypsin inhibitor-Sepharose column (1.6 × 3.6 cm). This was followed by gel filtration on Superdex-75, to obtain HPG- and μPG-free K1–5. The purity of this preparation was confirmed by SDS-PAGE analysis (23). Activation with urokinase, which is known to be a good activator of μPG irrespective of the presence of kringle domains (22), was used to establish that the activation of this preparation, when used as substrate, was comparable with that obtained when using SK·HPN as the activator species.

Characterization of $SK_{del254-262}$

Amidolytic Activation of Equimolar HPG·nSK/$SK^{del254-262}$ Complexes—Aliquots (50 nM) were withdrawn from equimolar HPG·nSK/$SK_{del254-262}$ complexes at regular periods and transferred to a 100-μl quartz microcuvette containing 2 mM tosyl-glycyl-prolyl-lysine-4-nitranilide-acetate (Chromozym® PL) and 50 mM Tris-Cl, pH 7.5, at 22 °C. The change in absorbance at 405 nm was monitored to compute the kinetics of amidolytic activation (12, 24).

Esterolytic Activation of Equimolar HPG·nSK/$SK_{del254-262}$ Complexes—Five μM HPG was added to an assay cuvette containing 5.5 μM nSK/$SK_{del254-262}$, 100 μM NPGB, and 10 mM phosphate buffer, pH 7.5, and the "burst" of *p*-nitrophenol release was monitored at 410 nm as a function of time at 22 °C (3, 25).

Determination of Kinetic Constants for HPG Activator Activity of nSK/$SK_{del254-262}$—Varying amounts of HPG were added to the assay cuvette containing fixed amounts of nSK/$SK_{del254-262}$ and chromogenic substrate (1 mM), and the change in absorbance was monitored at 405 nm as a function of time at 22 °C. Also, the kinetics of HPG activation by HPN·nSK/$SK_{del254-262}$ complexes were measured by transferring suitable aliquots of preformed HPN·nSK/$SK_{del254-262}$ complexes to the assay cuvette containing different concentrations of substrate HPG (24). To compute the k_{cat}, the number of HPN active sites was determined using the NPGB reaction (3, 25, 26).

Assay for the Determination of the Steady-state Kinetic Constants for Amidolytic Activity of nSK/$SK_{del254-262}$—nSK/$SK_{del254-262}$ and HPN were precomplexed at 4 °C in equimolar ratios (100 nM each) for 1 min in 50 mM Tris-Cl, pH 7.5, containing 0.5% bovine serum albumin, and an aliquot of the reaction mixture was transferred to a 100-μl assay cuvette containing 50 mM Tris-Cl buffer, pH 7.5, and varying concentrations of the chromogenic substrate (0.1–2 mM) to obtain a final concentration of 10 nM complex in the reaction. The reaction was monitored spectrophotometrically at 405 nm for 5 min at 22 °C. The kinetic constants were calculated by standard methods (25).

Kinetic Analysis of Protein-Protein Interactions Using Resonant Mirror Technology

Binary Interaction Analysis—Association and dissociation between HPG and the nSK/$SK_{del254-262}$, referred to hereafter as binary interaction, were followed in real time by resonant mirror-based detection using the IAsys Plus™ system (Cambridge, UK) (27, 28). In these experiments, streptavidin was captured on biotin cuvette according to the manufacturer's protocols (IAsys protocol 1.1). This was followed by the attachment of (mildly) biotinylated HPG to the streptavidin captured on the cuvette. Nonspecifically bound HPG was then removed by repeated washing with phosphate-buffered saline followed by three washes with 10 mM HCl. The net response chosen for the immobilized biotinylated HPG onto the cuvette was 700–800 arc seconds in all experiments. Experiments were performed at 25 °C in 10 mM phosphate-buffered saline, pH 7.4, containing 0.05% Tween 20 and 5×10^{-3} M NPGB (binding buffer). The latter was included in order to prevent plasmin-mediated proteolysis.

After equilibrating the cuvette with binding buffer, varying concentrations of either nSK or $SK_{del254-262}$ were added, and each binding response was monitored during the "association" phase. Subsequently, the cuvette was washed with binding buffer, and the "dissociation" phase was recorded (29). Following each cycle of analysis, the cuvette was regenerated by washing with 10 mM HCl, and base line was reestablished with binding buffer. In parallel, in the control cell in the dual channel cuvette, immobilized streptavidin alone was taken as a negative control for the binding studies. In experiments where EACA was used to examine its effect on SK-HPG interaction, the binary complex was formed between ligate nSK/$SK_{del254-262}$ and immobilized HPG in binding buffer (as described above). The dissociation of the binary complexes was done by washing the cuvette with EACA instead of buffer alone.

The data were analyzed after subtraction of the corresponding nonspecific refractive index component(s), and the kinetic constants were calculated from the sensorgrams by nonlinear fitting of the association and dissociation curves according to 1:1 model $A + B = AB$ using the software FASTfit™, supplied by the manufacturers. Briefly, the association curves at each concentration of ligate were fitted to the pseudo-first order equation to calculate the observed rate constant (k_{on}). Then the concentration dependence of k_{on} was fitted using linear regression to find the association rate constant (k_a) from the slope of the linear fit (30). The dissociation rate constant (k_d) was calculated from the average of four dissociation curves obtained at saturating concentration of ligate. The equilibrium dissociation constant (K_D) was then calculated as k_d/k_a. Values of K_D obtained using this relationship were in good approximation to those obtained by Scatchard analysis of the extent of association (data not shown).

Ternary Interaction Analysis—Resonant mirror technology-based biosensor was also used to measure the rate and equilibrium dissociation constants describing interactions between soluble ligate (PG, μPG, or K1–5) and nSK/SKdel$_{254-262}$ complexed with immobilized HPG, a situation simulating substrate binding to binary complex and hereafter referred to as ternary interaction. In binary interaction studies, it was evident that when soluble nSK/$SK_{del254-262}$ was added to immobilized HPG, a rapid and avid SK·HPG binary complex formation occurs. The dissociation of this complex is very slow due to the high stability of the SK·HPG complex, as has been observed by others also (15). After allowing the complex to dissociate maximally (~20 min), the dissociation base line becomes stable, which remains unaffected even after washing with 2.5 mM EACA. It has been reported that when SK was preincubated with immobilized HPG, EACA was >100-fold less potent at dissociating the binary complex than it was at preventing binary complex formation when SK and EACA were added synchronously to immobilized HPG (13). Thus, this comparative resistance to dissociation of the SK·HPG binary complex by EACA permitted us to study ternary substrate interaction under conditions that did not adversely affect the stability of the binary interaction. In contrast, EACA was found to be strongly inhibitory to ternary complex formation (see below).

In a typical ternary interaction experiment, a stable binary complex was formed by adding a saturating amount of either nSK or $SK_{del254-262}$ onto HPG, immobilized on streptavidin captured on biotin cuvette. After maximally dissociating the binary complex with binding buffer and washing with 2.5 mM EACA, a stable dissociation base line was obtained. Varying concentrations of either "ternary" HPG (0.1–1.0 μM), μPG (1–6 μM), or K1–5 (1–6 μM) were then added to monitor the binding by recording the association phase. Subsequently, the cuvette was washed with binding buffer three times, and the dissociation phase was recorded. After each cycle of analysis, the original base line was reestablished by stripping off the undissociated ternary ligate with 2.5 mM EACA followed by three washes with binding buffer. It was established that EACA, at this concentration, completely abolishes the interaction of ternary HPG with the binary complex, while the binary complex remains stable. The latter attribute was considered to be a necessary precondition to obtain reliable and reproducible values of the kinetic constants for ternary complex formation and dissociation. In order to test whether this was indeed so, control experiments were carried out in which the ternary complex formation and dissociation experiments were done at various time intervals after a stable base line was attained subsequent to binary complex formation followed by buffer and EACA washes, as described above. It was observed that the rate constants so obtained did not differ significantly (within a margin of ±5%) as a function of time. In experiments where μPG was used as soluble ternary ligate, 1 mM EACA was found to be sufficient to strip off the undissociated μPG, whereas washing with binding buffer alone resulted in incomplete regeneration of base line. Association and dissociation phases at varying ligate (HPG, μPG and K1–5) concentrations were fitted as described above, and the equilibrium dissociation constant/s were calculated as k_d/k_a.

The effect of EACA on the binding of soluble ternary HPG to nSK/$SK_{del254-262}$ complexed with immobilized HPG was assessed by measuring the binding extents, measured in arc second units, at equilibrium at a fixed concentration of substrate HPG (0.4 μM) in the

presence of varying EACA concentrations (0–2 mM). For the analysis of these data, the binding extent in buffer alone was taken as 100%, and varying extents of formation of ternary complexes at equilibrium were plotted as a function of EACA concentration to obtain EACA-dependent binding isotherms for nSK and $SK_{del254-262}$. As controls, the effect of EACA was similarly examined for dissociation of preformed complexes between HPG and either nSK or $SK_{del254-262}$ in the absence of substrate HPG.

Circular Dichroic Analysis of nSK/$SK_{del254-262}$

Far-UV CD spectra of proteins (concentration 0.15 mg/ml in phosphate-buffered saline, pH 7.2) were recorded on a Jasco-720 spectropolarimeter. Measurements were carried out from 200 to 250 nm in a 0.1-cm path length cell, and the appropriate buffer base line was subtracted from the protein spectra. The final spectrum analyzed was an average of 10 scans (31).

Modeling Studies

Cartesian coordinates of the kringle 5 domain of HPG (used as a prototypical representative structure of HPG kringle domains) and those of SK β domain and the SK-μPN complex were retrieved from the Protein Data Bank (codes 5HPG, 1C4P, and 1BML, respectively). The β domain in SK-μPN reveals several disordered loops, including the 250-loop (8). The coordinates in this complex were hence replaced with those of the isolated β domain (18). The isolated β domain was superimposed on the β domain of the complex, and the corresponding set of coordinates was simply replaced. The isolated β domain has the 250-loop clearly defined; hence, it is more suitable for docking analysis.

Molecular surface for a typical HPG kringle domain was generated using the kringle 5 coordinates (taken as a prototype) with the aid of GRASP (32) with standard atomic radii, and the probe radius of 1.4 Å. Electrostatic potential was then mapped onto the molecular surface. There are two distinct regions of negative charges on the surface. The negatively charged surface of kringles is likely to interact with the positively charged loop of the SK structure, and therefore these regions were of particular interest in generating the SK β-μPN-kringle docked complex. One of the negatively charged regions is at the interface of the dimeric kringle structure. This region was therefore not considered appropriate for docking. The other negatively charged region was then manually brought into close proximity of the 250-loop of SK β domain. The best docked complex is shown in Fig. 7. Remarkably, the surface of the kringle showed nearly perfect complementarity to the surface of the SK-μPN complex. The mode of docking also revealed that the C terminus of the kringle domain is within connecting distance of the N terminus of the μPN moiety, as would be expected in the physiological situation. Thus, the close complementarity of kringle and SK-μPN surfaces, the perfect electrostatic match among the two structures, and the proximity between connecting peptide units suggest that indeed the kringle might dock onto SK-μPN in the mode shown in Fig. 7.

RESULTS AND DISCUSSION

To investigate the functional role of the 250-loop (*viz.* its involvement in the modulation of substrate specificity of HPN by SK), we prepared a deletion mutant ($SK_{del254-262}$) employing the SOE-PCR method (20). The desired deletion mutation was confirmed by sequencing of both strands of the cloned DNA (see "Experimental Procedures" for other details). This was followed by subcloning of the PCR amplification product in a T7 RNA polymerase promoter-based expression vector (21). With the nine-residue deletion, we expected that a minimal perturbation of the underlying β sheet would occur (Fig. 1), since the two residues flanking the loop (Tyr^{252} and Glu^{263}) had a distance of 4 Å between the C^{α} atoms (18). The *E. coli* BL21 (DE3) cells carrying the plasmid were grown in shake flasks to midlog phase, and the expression of the protein of interest was then induced by the addition of isopropyl-1-thio-β-D-galactopyranoside. $SK_{del254-262}$ was then purified from the intracellular milieu to homogeneity using a rapid, two-step protocol (16). When purified $SK_{del254-262}$ was examined for its ability to activate substrate HPG, it showed a specific activity that was only about 20% that of native-like SK (termed nSK) similarly expressed and purified using the same expression plasmid and host system.

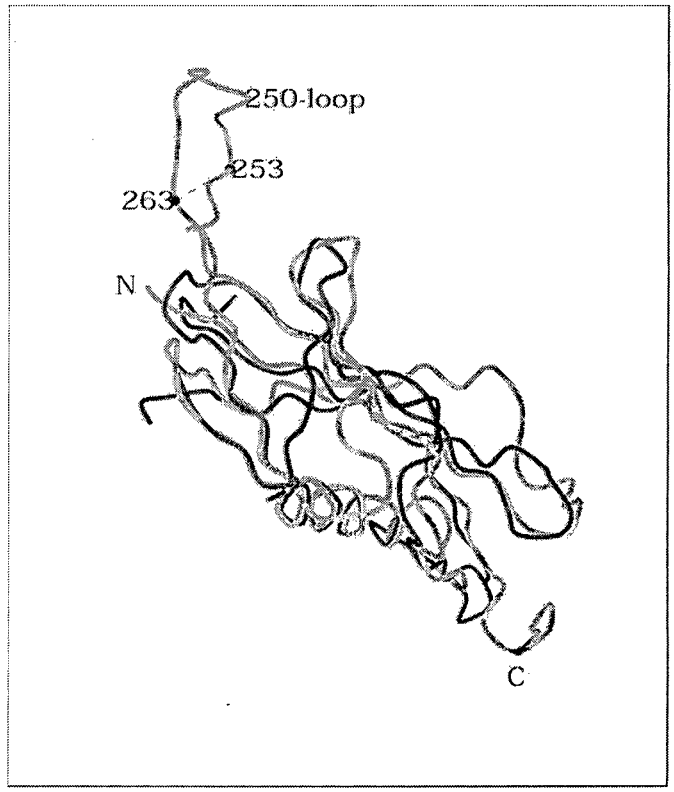

FIG. 1. **Superposition of α and β domains of streptokinase.** The β domain is shown in *green*, and the α domain is in *red*. The 250-loop is a distinct feature of the β domain, while the rest of the structure between the two domains overlaps extensively. The superposition with the γ domain of SK showed similar results (not shown). The residues 253 and 263, where the loop was truncated, are indicated.

We checked whether the deletion of the 250-loop resulted in changes in the overall folding characteristics of SK as judged by its secondary structure analyzed by CD. The far-UV CD spectra of nSK and the mutant ($SK_{del254-262}$), however, did not show any significant discernible differences (data not shown). However, since a native-like CD spectrum of the mutant could still result if relatively small, local conformational changes occurred in and around the site of the deletion in the β domain that might get "averaged out" in the presence of the CD contributions from rest of the two domains of SK in the full-length molecule, we carried out a deletion at the same site in a truncated gene encoding for the isolated β domain. The cDNAs encoding for the β domain alone and $\beta_{del254-262}$ were then expressed in *E. coli* and purified (see "Experimental Procedures" for details), and their far-UV CD spectra were recorded. Interestingly, no noticeable changes were observed in the secondary structure of $\beta_{del254-262}$ with respect to $\beta_{wild\ type}$ similarly expressed in *E. coli* also (data not shown), indicating that neither the overall secondary structure of SK nor that of the β domain alone had been perturbed by the deletion of the nine-residue loop from the protein.

To explore whether the deletion of the 250-loop resulted in any significant alteration in the affinity of the mutant with partner HPG, the kinetics of interaction between immobilized HPG and nSK were compared with those of $SK_{del254-262}$ by the resonant mirror approach using a semiautomated instrument for measuring protein-protein interactions in real time (IAsys, Cambridge UK). To examine the effect of immobilization chemistry on the values of kinetic constants, preliminary experiments were performed by immobilizing either nSK or $SK_{del254-262}$ onto carboxymethyldextran cuvettes, using an

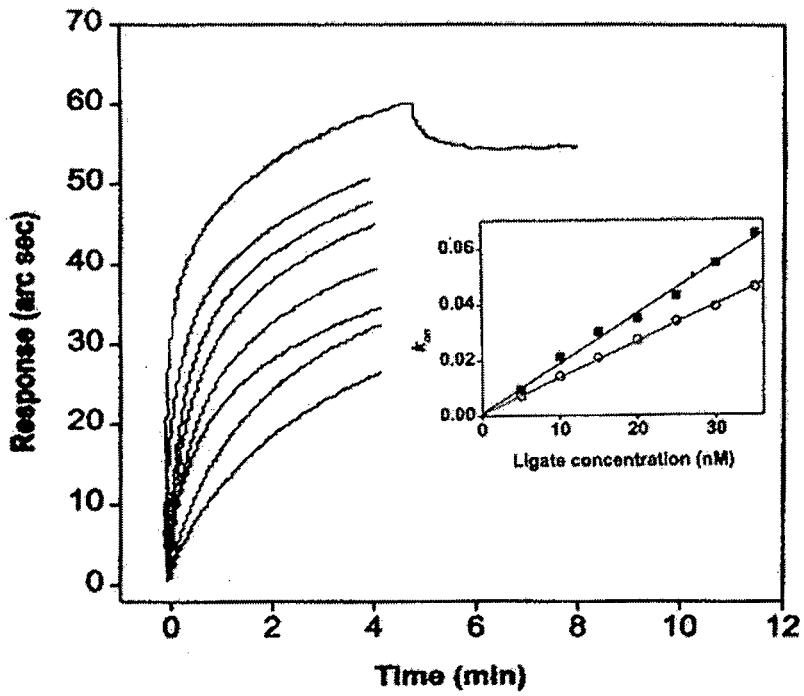

FIG. 2. **Optical biosensor determination of binding constants for the interaction of nSK/$SK_{del254-262}$ with immobilized HPG.** Overlay plots representing the binding and dissociation of nSK to the immobilized HPG are depicted. Human PG was biotinylated and immobilized on streptavidin surfaces of IAsys cuvettes, as described under "Experimental Procedures." For each individual concentration of ligate (only data for nSK is shown), the association or binding to immobilized HPG was monitored. Subsequently, the cuvette was washed with binding buffer, and the dissociation phase was monitored (see "Experimental Procedures" for details). For the sake of clarity, only dissociation at saturating ligate concentration is shown. The value of k_{on} for the binding curves for each ligate concentration was determined using the FASTfit™ program, and each value was plotted against the corresponding concentration of the ligate. *Inset*, the plot of k_{on} against ligate concentration for nSK (*filled squares*) or $SK_{del254-262}$ (*open circles*), which gives a *straight line*. The k_a values were obtained from the slope of the *straight line*, and k_d values were calculated from the average of four dissociation curves obtained at saturating ligate concentrations, as described under "Experimental Procedures."

amino-coupling protocol recommended by the manufacturers. The kinetics of association and dissociation of HPG with immobilized nSK/$SK_{del254-262}$ were then measured as described under "Experimental Procedures." In another approach, biotinylated HPG was immobilized on streptavidin captured on a biotin cuvette, and the binding kinetics with SK were studied as described. For these assays, nSK/$SK_{del254-262}$ were added at concentrations ranging between 5 and 80 nM. Relatively fast association kinetics were observed for the binding of both proteins, which is consistent with a monophasic pattern of association (Fig. 2). When the association data for the interaction were fitted to a single exponential curve, a linear relationship was observed between k_{on} and added ligate concentration, according to the equation $k_{on} = k_d + k_a$ (ligate). The results show that the mutant exhibited an affinity that was not significantly different from that of nSK (Table I).

Interestingly, experiments performed by immobilizing nSK/$SK_{del254-262}$ on carboxymethyldextran cuvettes using standard amino-coupling procedures, as shown by other groups also (15, 33), yielded similar binding constants for nSK and $SK_{del254-262}$ (data not shown), indicating that the coupling procedure *per se* does not interfere significantly in the binding interaction between SK and HPG.

To further explore the underlying reason for partial loss of activator activity of the loop deletion mutant, we examined whether, like the native protein, it could expose the active site in partner HPG. For this purpose, we employed the active site acylating agent, NPGB, to test whether the characteristic burst that occurs upon mixing equimolar SK and HPG (3, 25) was also observed with the mutant. Neither SK nor HPG alone give the burst, but only once the two are mixed in equimolar proportions is this burst, characteristically associated with a rapid NPGB hydrolysis, observed due to the formation of a "virgin"

TABLE I

Association and dissociation rate constants and apparent equilibrium dissociation constants for the binding of immobilized HPG to the derivatives of SK

Biotinylated HPG was immobilized on streptavidin captured onto a biotin cuvette. Different concentrations of the nSK/$SK_{del254-262}$ were then titrated as outlined under "Experimental Procedures." The pseudo-first order rate constant (k_{on}) was determined using the FASTfit™ program. The concentration dependence of k_{on} was fitted using linear regression to find the association rate constant (k_a) from the slope of linear fit. The dissociation rate constant (k_d) value was calculated from the average of four dissociation curves obtained at saturating concentration of ligate. The K_D was estimated from the ratio of kinetic constants as k_d/k_a.

Ligate	k_a ($\times 10^6$)	k_d ($\times 10^{-3}$)	K_D ($\times 10^{-9}$)
	$M^{-1}\,s^{-1}$	s^{-1}	M
nSK	1.98 ± 0.08	1.81 ± 0.21	0.91 ± 0.34
$SK_{del254-262}$	1.43 ± 0.07	2.27 ± 0.15	1.58 ± 0.79

SK·HPG complex and consequent acylation at the cryptic active site of HPG with NPGB (3). When the recombinant nSK (used as a control) was tested with this reagent in the presence of equimolar HPG, the characteristic colorimetrically detectable burst was indeed observed. A similar response was evident in the case of $SK_{del254-262}$ as well (Fig. 3, *inset*). However, the maximal level of these bursts was approximately half of that observed with natural SK prepared from *S. equisimilis* (data not shown). It has been demonstrated recently that a free N-terminal residue (Ile) (34) and some flanking residues (35) are required for the auto-activation of HPG by SK. However, the positive NPGB reaction of nSK, albeit less than that of natural SK, was easily explained when N-terminal sequence analysis of

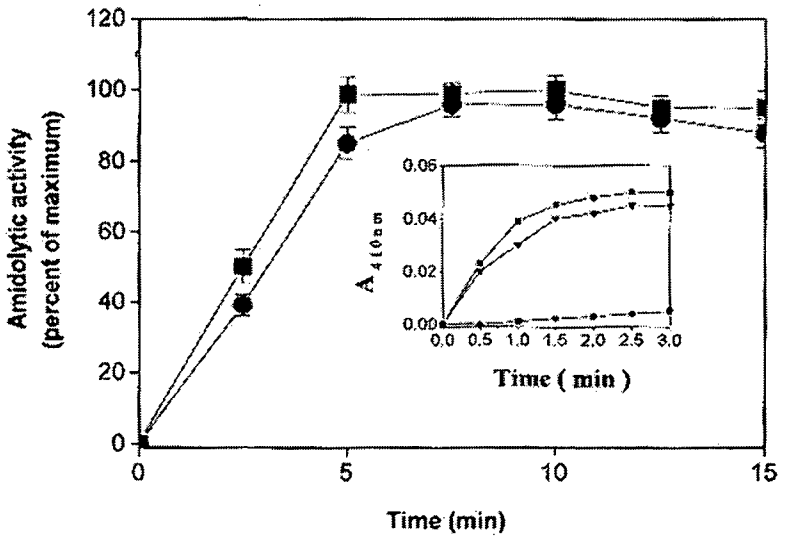

FIG. 3. **Time course of the generation of amidolytic activity of nSK and $SK_{del254-262}$.** Equimolar nSK·HPG and $SK_{del254-262}$·HPG complexes were made, and aliquots were withdrawn at regular periods and transferred into a microcuvette containing 2 mM chromogenic substrate. The generation of amidolytic activity was monitored at 405 nm at 22 °C, as described under "Experimental Procedures." The percentage of maximum amidolytic activity as a function of preincubation time by nSK·HPG complex (*filled squares*) and $SK_{del254-262}$·HPG complex (*filled circles*) is plotted. *Inset*, active site titration of HPG on complexing with nSK or $SK_{del254-262}$ using the active site acylating agent, NPGB. The *figure* shows progress curves of NPGB hydrolysis by nSK·HPG (*filled squares*), $SK_{del254-262}$·HPG (*filled inverted triangles*), and a control reaction (*filled circles*).

the purified nSK and $SK_{del254-262}$ showed that ~50% of the purified protein fractions had (like natural SK) a free Ile at the N terminus, probably due to partial processing by host methionyl aminopeptidase (36). The mutant ($SK_{del254-262}$) was then further verified for its ability to activate partner HPG by carrying out amidolytic assays of its equimolar mixtures with HPG. In this case too, it exhibited a similar, although slightly delayed, time course of generation of amidolytic activity with respect to nSK (Fig. 3), suggesting that it could open the active site in partner HPG. Thus, these results demonstrated that the observed lower HPG activator activity of $SK_{del254-262}$ was not due to any major effect on its ability to activate partner HPG at the binary complex formation stage.

To obtain a glimpse of the functional characteristics of the active site, the kinetic constants associated with the substrate binding and processing of both macromolecular substrate (HPG) and the low molecular weight amidolytic peptide substrate tosyl-glycyl-prolyl-lysine-4-nitranilide acetate were measured by the equimolar complexes of HPN with either nSK or $SK_{del254-262}$. Remarkably, the results for the steady-state kinetic analysis of the activation of substrate HPG by the equimolar $SK_{del254-262}$·HPN complex revealed a 5–6-fold increase in the K_m for HPG when compared with that of nSK·HPN, with relatively little alteration in the k_{cat} values (Table III). This clearly indicated that the loop-deleted mutant formed an activator complex with HPN that had an apparent decreased affinity for the macromolecular substrate as compared with that of the native SK. On the other hand, the k_{cat} values exhibited either by nSK·HPN or $SK_{del254-262}$·HPN for the small MW peptide substrate were essentially unaltered as compared with that of "free" HPN (suggesting that the primary covalent specificity characteristics of the active site in HPN remained unchanged), but, revealingly, the K_m for this substrate was decreased as compared with that of nSK·HPN.

It is known that the complexation of SK with free HPN leads to an overall reduced accessibility of the HPN active site by small molecular weight substrates and inhibitors probably due to steric hindrance brought about by SK binding in the vicinity of the active site; this phenomenon is manifested, for example, in a significant increase in the K_m for the amidolysis of chromogenic substrates by SK·HPN complex compared with that of HPN alone (8, 37, 38). The characteristic increase in K_m of HPN for amidolytic substrates has also been observed with the isolated β domain (11). The present results on the abolition of the "K_m shift" (Table II) in $SK_{del254-262}$ suggest that the 250-loop interacts with a region in partner plasmin(ogen) that is situated close to the active center, a surmise that is entirely consistent with its proposed role in sequestering substrate HPG to the activator complex and with peptide inhibition experiments reported earlier (11). Noticeably, the k_{cat} for the hydrolysis of the low molecular weight peptide substrate by the 1:1 HPN complex of the deletion mutant remained unchanged (Table II). These results clearly demonstrate that the affinity for macromolecular substrate (HPG) was selectively decreased in the case of $SK_{del254-262}$·HPN, without a concomitant alteration in the processivity of the low molecular weight peptide substrate.

The foregoing results on increased K_m for HPG prompted us to explore the comparative affinity of substrate HPG with activator complexes between HPG and nSK, on the one hand, and HPG with $SK_{del254-262}$ on the other, using a more direct physico-chemical approach. For this purpose, a new "docking" assay for ternary complex formation between SK and two mol-

TABLE II
Steady-state kinetic parameters for amidase activity of equimolar complexes of HPN and nSK/$SK_{del254-262}$

For the determination of the amidolytic parameters, nSK/$SK_{del254-262}$ and HPN were precomplexed in an equimolar ratio, and an aliquot of this mixture was assayed for amidolysis at varying concentrations of Chromozym® PL as detailed under "Experimental Procedures." The data represent the mean of three independent determinations.

Protein	K_m	k_{cat}	k_{cat}/K_m
	mM	min^{-1}	min^{-1}/mM
HPN	0.17 ± 0.03	310 ± 18	1823.53
nSK · HPN	0.6 ± 0.02	370 ± 15	616.67
$SK_{del254-262}$ · HPN	0.2 ± 0.07	320 ± 14	1600

TABLE III
Steady-state kinetic parameters for HPG activation by equimolar complexes of HPN and nSK/$SK_{del254-262}$

The kinetic parameters for substrate HPG activation were determined at 22 °C as described under "Experimental Procedures." The data represent the mean of three independent determinations. Closely similar values were obtained for the direct activation of substrate HPG by $SK_{del254-262}$ (data not shown).

Activator protein	K_m	k_{cat}	k_{cat}/K_m
	μM	min^{-1}	$min^{-1}/\mu M$
nSK · HPN	0.5 ± 0.05	11 ± 0.5	22.0
$SK_{del254-262}$ · HPN	2.5 ± 0.3	9.7 ± 0.52	3.9

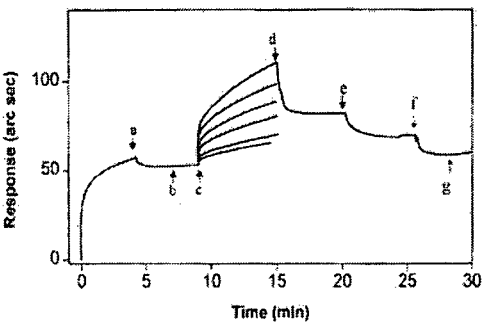

FIG. 4. **Tracings from the IAsys™ resonant mirror-based system to quantitate the interactions between substrate HPG and the equimolar binary complex of nSK and immobilized HPG.** The experiment was carried out at 25 °C in binding buffer as described under "Experimental Procedures." Human PG was biotinylated and immobilized on streptavidin captured onto the biotin cuvette. A stable binary complex was formed by adding saturating concentration of nSK onto immobilized HPG. After washing with binding buffer (point of addition of binding buffer as depicted by *a*), a stable dissociation base line (*b*) was obtained due to high affinity and stability of the SK·HPG binary complex, which remained unaffected even after washing with 2.5 mM EACA (data not shown). Thereafter, varying concentrations of substrate HPG (0.1–1 μM) were then added (point of addition of substrate as depicted by *c* to monitor the association phase (6 min), and subsequently, the cuvette was washed with binding buffer three times (point of addition as depicted by *d*), and the dissociation phase was recorded for the next 6 min. After each cycle of analysis, the undissociated substrate HPG was stripped off with 2.5 mM EACA (point of addition of EACA as shown by *e*), followed by reequilibrating the cuvette with binding buffer (*f*), which reestablished the original base line (*g*). The immobilized streptavidin alone was taken as the negative control, and it was subjected to the same kind of treatments as given to the test cell containing immobilized HPG. No significant nonspecific binding was observed (data not shown).

ecules of HPG, one in the binary mode and the other docked as a substrate, was devised based on a real time approach utilizing resonant mirror-based biosensor equipment (Fig. 4). Earlier, a "static" analysis of the formation of such a ternary complex with radioactively labeled substrate HPG bound onto the binary complex of immobilized HPG and nSK on plastic surfaces has been reported (39). In order to establish the authenticity of ternary complex formation with substrate HPG onto the preformed binary SK·HPG complex on resonant mirror cuvettes, we have used two criteria: (*a*) sensitivity of the ternary complex, and comparative refractoriness of the preformed binary complex, to EACA, and (*b*) distinctive concentration range dependence of binary (low nanomolar range) and ternary complex(es) (high nanomolar range) to HPG binding (see "Experimental Procedures" for detailed protocols). It has been well established that the preformed SK·HPG complex is highly refractory to EACA, whereas the action of the activator complex on the substrate is susceptible to inhibition in the low millimolar range (13), a fact that we also observed, while the same concentration of EACA potently inhibited the interaction of substrate HPG with preformed SK·HPG complex. This comparative resistance of the preformed binary complex and susceptibility of the ternary complex to EACA allowed us to selectively examine the interaction of ternary HPG with the SK·HPG binary complex. Similarly, due to the comparatively low affinity of the substrate HPG toward the SK·HPG binary complex (24), a higher concentration of substrate HPG was required, while the SK·HPG binary interaction, due to its intrinsically high affinity, could easily be monitored at the subnanomolar and low nanomolar ranges of concentration (Tables I and IV).

Ternary interaction studies of HPG with SK·HPG binary complex have been reported earlier using solid phase assay (39). Although such an assay can provide a clear estimate of affinity in terms of equilibrium dissociation constants (K_D), it fails to give insight into the dynamics of the interaction of the activator complex with the macromolecular substrate. The results obtained for the interaction of substrate HPG, μPG, and K1–5 with either nSK or $SK_{del254-262}$ complexed with immobilized HPG are given in Table IV. It is clear that substrate HPG interacts with the $SK_{del254-262}$·HPG binary complex with a 5-fold lower affinity (K_D ~0.75 μM) as compared with nSK·HPG binary complex (K_D ~0.15 μM). This decrease in affinity is remarkably proportionate to the increase in the K_m for substrate HPG (5–6-fold) using enzymatic activity as the criterion for discrimination between nSK and mutant. These results clearly indicate the importance of the 250-loop in "capturing" substrate HPG molecules by the activator complex.

Recent biochemical studies suggest that an exosite-mediated substrate HPG binding, independent of the primary covalent specificity of the HPN active site, represents the major mechanism of SK-induced changes in the macromolecular substrate specificity of HPN (10, 12). The structural basis whereby such an exosite contributes toward the change in substrate specificity of the HPN active site consequent to SK binding has, however, remained essentially unknown so far. The data presented in this paper clearly implicate the 250-loop of the β domain as an important determinant of the macromolecular substrate specificity of the SK·HPG activator complex. The presence of two tandem lysine residues at the tip of the 250-loop suggests that interactions with the kringle domain(s) in substrate HPG may be the operative mechanism behind this interaction. To understand the role of kringles in substrate affinity, the activities of nSK and the mutant were compared in the presence of varying concentrations of EACA, a lysine analogue that is well known to inhibit HPG activation by SK as well as disrupt ternary complex formation through a kringle-mediated mechanism (2, 13, 39). Kinetic studies to check the effect of varying concentrations of EACA on substrate HPG activation by nSK·HPN and $SK_{del254-262}$·HPN showed that the mutant exhibited a greater susceptibility to EACA-mediated inhibition of substrate HPG activation than nSK (Fig. 5*A*) in a concentration range that did not affect the activity of the two binary complexes or the activity of free HPN. It has been shown earlier (13, 39), using a sandwich binding assay, that EACA completely abolishes the docking of substrate HPG onto SK·HPG binary complex formed on a plastic surface. However, this does not allow the measurement of the rates of binding and dissociation of substrate HPG with the high affinity binary complex. Experiments were carried out to see the effect of EACA on the ternary complexation of substrate HPG to nSK/$SK_{del254-262}$ precomplexed with immobilized PG on resonant mirror cuvettes, as described earlier. With $SK_{del254-262}$·HPG binary complex, an IC_{50} of 0.3 mM was obtained, which is ~3-fold less than the IC_{50} (1 mM) obtained with nSK·HPG binary complex (Fig.

TABLE IV

Association and dissociation rate constants and apparent equilibrium dissociation constants for the interaction of substrate HPG, μPG, and K1–5 with nSK/$SK_{del254-262}$ complexed with immobilized HPG

Kinetic constants for the interactions of substrate HPG, μPG, and K1–5 with nSK · HPG or $SK_{del254-262}$ · HPG binary complex were determined by applying the FASTfit™ program to the binding data obtained using IAsys biosensor, as described under "Experimental Procedures." A stable binary complex between nSK/$SK_{del254-262}$ and HPG immobilized onto the cuvette was made, and then the binding of varying concentrations of substrate HPG (0.1–1 μM), μPG (1–6 μM), or K1–5 (1–6 μM) was monitored.

Ligand	Ligate	k_a (× 10^5)	k_d (× 10^{-1})	K_D (× 10^{-6})
		$M^{-1}\ s^{-1}$	s^{-1}	M
nSK · HPG	HPG	10.70 ± 1.30	1.76 ± 0.23	0.16 ± 0.04
nSK · HPG	μPG	0.75 ± 0.02	1.29 ± 0.74	1.72 ± 0.91
nSK · HPG	K1–5	0.29 ± 0.06	1.19 ± 0.17	4.11 ± 0.62
$SK_{del254-262}$ · HPG	HPG	4.62 ± 0.51	3.35 ± 0.13	0.72 ± 0.09
$SK_{del254-262}$ · HPG	μPG	0.90 ± 0.03	1.33 ± 0.12	1.48 ± 0.20
$SK_{del254-262}$ · HPG	K1–5	0.28 ± 0.12	3.41 ± 0.21	12.02 ± 2.08

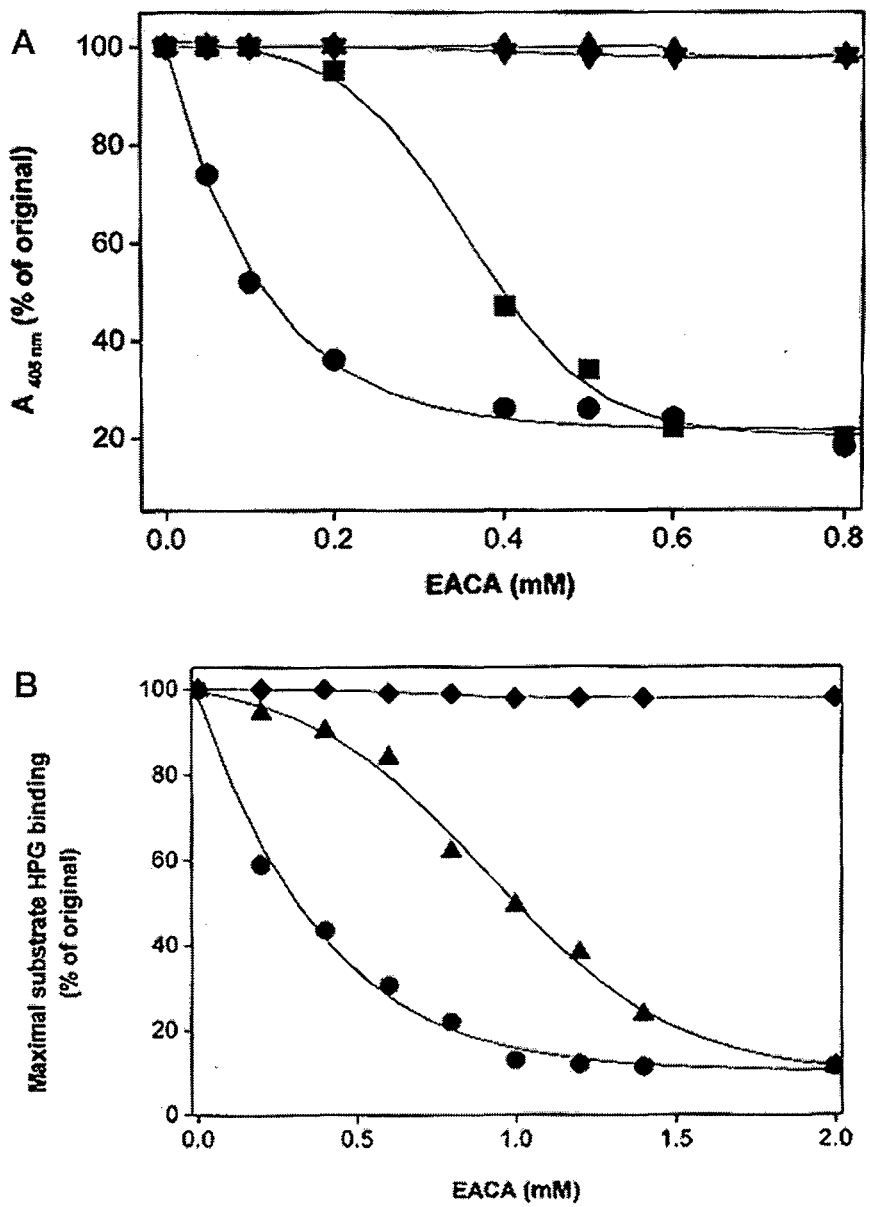

FIG. 5. **Differential susceptibility to EACA of the substrate with binary complexes of nSK and $SK_{del254-262}$-HPG.** *A*, differential susceptibility to EACA of substrate activation by nSK and $SK_{del254-262}$. The effect of different concentrations of EACA (0–1 mM) on the substrate HPG activation by nSK (*filled squares*) and $SK_{del254-262}$ (*filled circles*) was examined. Controls containing a 10 nM concentration each of SK and HPN (*filled triangles*), or HPN alone (*filled inverted triangles*) are also shown. The HPG activator activity of constant, catalytic amounts of the preformed equimolar activator complexes between HPN and either nSK or $SK_{del254-262}$ to obtain final concentrations of 0.25 and 3 nM, respectively in the presence of varying concentrations of EACA, along with substrate HPG and chromogenic substrate in 50 mM Tris-Cl buffer, pH 7.5, was monitored at 405 nm at 22 °C. The initial velocities in different concentrations of EACA are expressed relative to the controls not containing any EACA (taken as 100%). Similar differential effects between nSK and the mutant were observed at HPG concentrations of 0.5, 2, and 4 μM, although the IC_{50} values were different (data not shown). *B*, effect of EACA on the physical binding of substrate HPG to nSK·HPG or $SK_{del254-262}$·HPG binary complex examined by the resonant mirror technique. Binding of substrate HPG (0.4 μM) to either nSK·HPG (*filled triangles*) or $SK_{del254-262}$·HPG

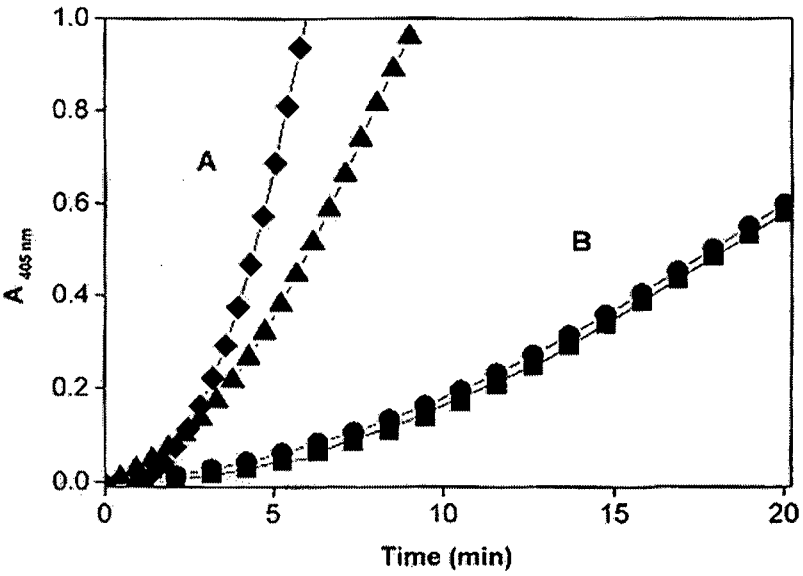

FIG. 6. **Abolishment of the differential substrate activation phenomenon by nSK and $SK_{del254-262}$ by using substrate μPG.** Fixed, catalytic amounts of the respective preformed activator complexes of each protein with HPN were added to the cuvette containing subsaturating concentrations of HPG or μPG as the substrate and Chromozym® PL in 50 mM Tris-Cl buffer, pH 7.5, and the reactions were monitored at 405 nm at 22 °C. The *figure* shows *progress curves* of activation of HPG by nSK (*filled diamonds*) and $SK_{del254-262}$ (*filled triangles*) (*A*) and of μPG by nSK (*filled circles*) and $SK_{del254-262}$ (*filled squares*) (*B*).

5*B*). These data clearly support the conclusion that the binary complex of the mutant, with the 250-loop deleted, interacted with substrate in a manner that is more vulnerable, as compared with nSK-plasmin(ogen), to disruption with the lysine-binding site competitive ligand, EACA. However, it is worth noting that if all of the kringle-mediated interactions between activator and substrate had been abolished by the deletion of the loop, the mutant should have been completely resistant to inhibition by EACA. The fact that the mutant is susceptible to lower concentrations of EACA suggests that other EACA-sensitive kringle-dependent interactions are still operative, but at least one of the critical interactions has been abolished by the selective deletion of the 250-loop.

If the observed difference in substrate affinities between nSK·HPG and $SK_{del254-262}$·HPG activator complexes is indeed kringle-mediated, it is reasonable to assume that the rates of activation of substrate μPG, which is devoid of all five HPG kringles, by nSK and $SK_{del254-262}$ should not substantially differ from each other. This, indeed, was found to be the case (Fig. 6). Microplasminogen is known to be a poor substrate for the preformed SK-PG activator complex (22). Interestingly, kinetic studies using μPG as the substrate showed no discernible difference between nSK and $SK_{del254-262}$ with respect to initial velocities of substrate μPG activation at subsaturating concentrations ($K_m \sim 6 \pm 2$ μM), under conditions where the activator activities of the two complexes (nSK·HPN and $SK_{del254-262}$·HPN) showed a remarkable difference when the substrate (native HPG) contained the kringle domains. These observations prove convincingly that interactions involving lysine binding site(s) in the kringle domains are intimately involved in the mechanism of operation of the macromolecular substrate-specific exosite in the SK-plasmin(ogen) activator complex. To further establish that kringles are involved in activator-substrate interactions, ternary binding experiments on the resonant mirror, where the binding of the substrates, μPG and kringles 1–5 of HPG, to the binary complex preformed between either nSK or the mutant with immobilized HPG, were carried out (Table IV). Remarkably, in consonance with kinetic data, μPG showed the same affinities for both nSK and $SK_{del254-262}$ complexed with HPG. When K1–5 was used as the docking substrate during ternary complex formation, the nSK·HPG binary complex showed an affinity of 4.1 μM for K1–5, while that of the $SK_{del254-262}$·HPG complex was determined to be 12 μM, indicating approximately a 3-fold higher affinity for nSK (Table IV). Again, these results strongly argue that the 250-loop of the β domain of SK interacts with substrate HPG via the latter's kringle domains.

Molecular modeling studies wherein the intermolecular surfaces between the β domain of SK and the isolated kringle 5 (which was used as a typical representative structure of the five HPG kringles and does not necessarily indicate any preferred role in the substrate-activator complex interplay; however, see below) were explored for mutual complementarity (see "Experimental Procedures" for details) indicate that a kringle structure can indeed dock the 250-loop in a remarkably optimal fashion (Fig. 7). Although whether kringle 5 *per se* or any other kringle is involved in this interaction cannot be judged at this stage, during the course of revision of this manuscript, another report was published that demonstrates the involvement of kringle 5 in the 1:1 binding with the β domain of SK (33). Although speculative at this stage, this offers a tantalizing possibility that this kringle-mediated interaction at the levels of both binary and ternary complex formation operates through kringle 5. If this scenario is correct, the loop might switch its binding specificity toward partner or substrate depending on the temporal stage in the catalytic cycle, a possibility that is strengthened by a previous observation (11) that a synthetic peptide encompassing the 250-loop exhibits bifunctional behavior by competitively inhibiting both SK·HPG binding and HPG activation by preformed SK·HPN activator complex. On the other hand, the current evidence does not rule out the possibility that the different kringles in substrate and partner HPG are directed to different sites in SK. Whatever the exact mechanism, this

(*filled circles*) binary complex was measured at various concentrations of EACA (0–2 mM) using the IAsys™ system, as described under "Experimental Procedures." The maximal extent of binding under varying concentrations of EACA was quantitated, and the maximal binding in buffer alone was used to normalize the extent of binding under different experimental conditions. The extent of substrate HPG binding is plotted as a function of EACA concentration. The effect of respective EACA concentrations on the binary nSK/$SK_{del254-262}$·HPG complex is represented by *filled diamonds* (control).

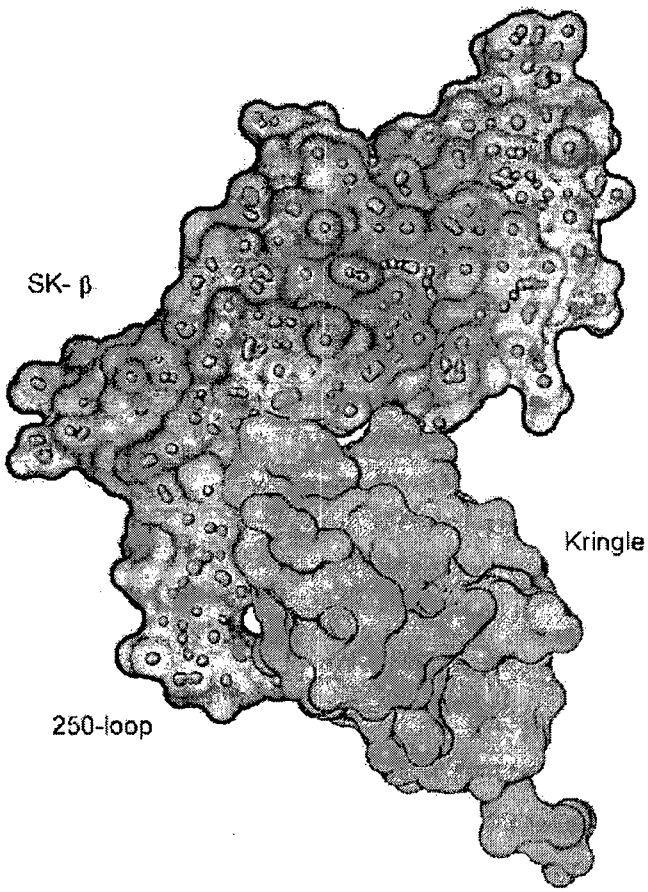

FIG. 7. **Docking of kringle 5 of HPG with the β domain of SK.** Connolly surfaces of the β domain and kringle 5 of HPG were calculated by using the GRASP program. Kringle 5 has been used here as a typical representative structure of the five HPG kringles. In order to generate the molecular surface, the radius of a water molecule was considered to be 1.4 Å. Electrostatic potentials were mapped onto the surfaces with GRASP. The β domain showed a distinct patch of positive charges in the 250-loop. Similarly, the kringle domain also showed a distinct patch of negative charges. The two patches were brought in close proximity by manual docking, which showed close surface and electrostatic complementarities (see "Experimental Procedures" for details).

study provides unmistakable evidence of the direct involvement of a discrete epitope in SK in substrate recognition and binding via the kringle(s) of HPG. Undoubtedly, further studies are needed to identify the relative contributions of the kringle(s) *versus* the catalytic domain of the substrate toward the latter's recognition, docking, and turnover in the "valley" formed by the activator complex. This would aid in a better understanding of this enigmatic interaction at the molecular level.

It must be realized, however, that the observation that, even after the excision of the 250-loop, the HPG activation reaction still survived (albeit with increased K_m) indicates that this loop is not the sole determinant of the SK-HPN exosite property. Indeed, earlier studies had suggested that the α domain as well as the β domain, together, contribute to the generation of HPG specificity in the activator complex (12, 16). The potential of the α domain to interact with substrate HPG is also evident from the SK-μPN crystal structure (8), although whether it does so by interacting with kringle(s) of substrate is still unclear. It is also established from recent work that the β domain contributes a major share toward SK's affinity for partner HPG as well (12). However, the fact that mutagenesis of several residues in the β domain resulted in appreciable diminution in the k_{cat} for activator activity with little change in the K_m for HPG *per se* (16) suggests that regions other than the 250-loop in this domain are also intimately involved in the modulation of the substrate specificity of the activator complex. We have observed[3] that mutations of residues immediately flanking the 250-loop (*e.g.* $SK_{Y252A,E263G}$) lead to further increase in the molecule's K_m for substrate HPG (to about 15-fold that of nSK) with only minimal alteration in the k_{cat} of its complex with HPN.

It is quite intriguing that the β domain provides a major portion of the intermolecular affinity of SK for HPG necessary for the formation of the tightly held equimolar activator complex (15) and at least some of the affinity required for the (transient) interaction of the latter with substrate HPG, as the present study indicates. This arouses curiosity as to whether this domain would, by itself, possess HPG activator activity, however compromised at a quantitative level, since two seemingly fundamental requirements for a single-domain HPG activator protein (*viz.* ability to bind with partner plasmin(ogen) and to then interact with substrate) are present in this domain. This question assumes significance because staphylokinase, a single-domain bacterial HPG activator, is also known to work as a "protein co-factor" in a fashion akin to that of SK (6) and has both of these distinctive HPG interacting properties. The ternary structure of μPN-staphylokinase-μPN suggests that staphylokinase appears not to modify the active site conformation of the enzyme but creates new exosites that indirectly alter the substrate specificity of μPN (40). Identification of such functional "hot spots" in PG activators in general, and SK in particular, that help in exosite-mediated modulation of substrate specificity may greatly aid the future *de novo* design of improved HPG activators.

Acknowledgments—We thank Dr. Amit Ghosh for the facilities provided and support, and Paramjit Kaur for expert technical assistance. We express our gratitude to K. Rajagopal for providing the plasmid construct for the expression of SK $\beta_{wild\ type}$ domain. Automated DNA sequencing was carried out with the unstinted help of Drs. Jagmohan Singh and K. Ganesan. We express our gratitude to Dr. Rajendra P. Roy (National Institute of Immunology, New Delhi) for the use of CD facilities.

REFERENCES

1. International Study of Infarct Survival-3 (1992) *Lancet* **339,** 753–781
2. Castellino, F. J. (1981) *Chem. Rev.* **81,** 431–446
3. McClintock, D. K., and Bell, P. H. (1971) *Biochem. Biophys. Res. Commun.* **43,** 694–702
4. Markus, G., and Werkheiser, W. C. (1964) *J. Biol. Chem.* **239,** 2637–2643
5. Parrado, J., Conejero-Lara, F., Smith, R. A. G., Marshall, J. M., Ponting, C. P., and Dobson, C. M. (1996) *Protein Sci.* **5,** 693–704
6. Esmon, C. T., and Mather, T. (1998) *Nat. Struct. Biol.* **5,** 933–937
7. Conejero-Lara, F., Parrado, J., Azuaga, A. I., Smith, R. A. G., Ponting, C. P., and Dobson, C. M. (1996) *Protein Sci.* **5,** 2583–2591
8. Wang, X., Lin, X., Loy, J. A., Tang, J., and Zhang, X. C. (1998) *Science* **281,** 1662–1665
9. Parry, M. A., Zhang, X. C., and Bode, W. (2000) *Trends Biochem. Sci.* **25,** 53–59
10. Boxrud, P. D., Fay, W. P., and Bock, P. E. (2000) *J. Biol. Chem.* **275,** 14579–14589
11. Nihalani, D., Raghava, G. P. S., and Sahni, G. (1997) *Protein Sci.* **6,** 1284–1292
12. Nihalani, D., Kumar, R., Rajagopal, K., and Sahni, G. (1998) *Protein Sci.* **7,** 637–648
13. Lin, L-F., Houng, A., and Reed, G. L. (2000) *Biochemistry* **39,** 4740–4745
14. Dawson, K. M., Marshall, J. M., Raper, R. H., Gilbert, R. J., and Ponting, C. P. (1994) *Biochemistry* **33,** 12042–12047
15. Conejero-Lara, F. C., Parrado, J., Azuaga, A. I., Dobson, C. M., and Ponting, C. P. (1998) *Protein Sci.* **7,** 2190–2199
16. Chaudhary, A., Vasudha, S., Rajagopal, K., Komath, S. S., Garg, N., Yadav, M., Mande, S. C., and Sahni, G. (1999) *Protein Sci.* **8,** 2791–2805
17. Lin, L-F., Oeun, S., Houng, A., and Reed, G. L. (1996) *Biochemistry* **35,** 16879–16885
18. Wang, X., Tang, J., Hunter, B., and Zhang, X. C. (1999) *FEBS Lett.* **459,** 85–89
19. Deutsch, D. G., and Mertz, E. T. (1970) *Science* **170,** 1095–1096
20. Ho, S. N., Hunt, H. D., Horton, R. M., Pullen, J. K., and Pease, L. R. (1989) *Gene (Amst.)* **77,** 51–59
21. Studier, F. W., Rosenberg, A. H., Dunn, J. J., and Dubendorff, J. W. (1990) *Methods Enzymol.* **185,** 60–89
22. Shi, G-Y., and Wu, H-L. (1988) *J. Biol. Chem.* **263,** 17071–17075

[3] J. Dhar and G. Sahni, unpublished observations.

23. Wu, H.-L., Chang, B.-I., Wu, D.-H., Chang, L.-C., Gong, G.-C., Lou, K.-L., and Shi, G.-Y. (1990) *J. Biol. Chem.* **265,** 19658–19664
24. Wohl, R. C., Summaria, L., and Robbins, K. C. (1980) *J. Biol. Chem.* **255,** 2005–2013
25. Chase, T., Jr., and Shaw, E. (1969) *Biochemistry* **8,** 2212–2224
26. Wohl, R. C., Arzadon, L., Summaria, L., and Robbins, K. C. (1977) *J. Biol. Chem.* **252,** 1141–1147
27. Cush, R., Cronin, J. M., Stewart, W. J., Maule, C. H., Molloy, J., and Goddard, N. J. (1993) *Biosensors Bioelectronics* **8,** 347–354
28. Buckle, P. E., Davies, R. J., Kinning, T., Yeung, D., Edwards, P. R., Pollard-Knight, D., and Lowe, C. R. (1993) *Biosensors Bioelectronics* **8,** 355–363
29. Myszka, D. G. (1997) *Curr. Opin. Biotechnol.* **8,** 50–57
30. Morton, T. A., Myszka, D. G., and Chaiken, I. M. (1995) *Anal. Biochem.* **227,** 176–185
31. Radek, J. T., and Castellino, F. J. (1989) *J. Biol. Chem.* **264,** 9915–9922
32. Nicholls, A., Sharp, K. A., and Honig, B. (1991) *Proteins* **11,** 281–296
33. Loy, J. A., Lin, X., Schenone, M., Castellino, F. J., Zhang, X. C., and Tang, J. (2001) *Biochemistry* **40,** 14686–14695
34. Wang, S., Reed, G. L., and Hedstrom, L. (1999) *Biochemistry* **38,** 5232–5240
35. Boxrud, P. D., Verhamme, I. M. A., Fay, W. P., and Bock, P. E. (2001) *J. Biol. Chem.* **276,** 26084–26089
36. Hirel, P. H., Schmitter, J-M., Dessen, P., Fayat, G., and Blanquet, S. (1989) *Proc. Natl. Acad. Sci. U. S. A.* **86,** 8247–8251
37. Robbins, K. C., Summaria, L., and Wohl, R. C. (1981) *Methods Enzymol.* **80,** 379–387
38. Wohl, R. C. (1984) *Biochemistry* **23,** 3799–3804
39. Young, K-C., Shi, G-Y., Wu, D-H., Chang, L-C., Chang, B-I., Ou, C-P., and Wu, H-L. (1998) *J. Biol. Chem.* **273,** 3110–3116
40. Parry, M. A. A., Fernandez-Catala, C., Bergner, A., Huber, R., Hopfner, K-P., Schlott, B., Gührs, K-H., and Bode, W. (1998) *Nature* **5,** 917–923